

CRANFIELD UNIVERSITY

Susanna Kirk

The vitreous materials from the 2nd millennium BC city of Nuzi: their preservation,
technology and distribution

CRANFIELD DEFENCE AND SECURITY

Phd THESIS

CRANFIELD UNIVERSITY

CRANFIELD DEFENCE AND SECURITY

DEPARTMENT OF APPLIED SCIENCE, SECURITY AND RESILIENCE

Phd THESIS

Academic Year 2009-2010

Susanna Kirk

The vitreous materials from the 2nd millennium BC city of Nuzi: their preservation,
technology and distribution

Supervisors: Dr A Shortland and Dr Eva Valsami-Jones

October 2009

© Cranfield University 2009. All rights reserved. No part of this publication may be reproduced without the written permission of the copyright owner.

Abstract

This project presents the first large-scale study of the preservation and alteration of Late Bronze Age vitreous materials from the Near East. An understanding of the processes that affect buried glasses is of importance both in the conservation of ancient artefacts and as analogues for the disposal of vitrified nuclear waste. This project has focused on the vitreous material from Nuzi, a mid 2nd millennium BC site in Iraq, held at the Semitic Museum at Harvard University. This is one of the largest assemblages of vitreous material known from the Late Bronze Age, containing a wide range of objects. A survey was made of the assemblage and the distribution of vitreous materials across the site was established. It was found that the majority of these materials are associated with high-status and religious areas of the city. Over 150 samples of vitreous material, including 90 LBA glasses, were characterised in detail, using a variety of analytical techniques including, SEM-EDS, SEM-WDS, LA-ICPMS and XRD. Compositional analysis suggested that the antimony-opacified glasses may have been manufactured at a higher temperature than the translucent glasses; supported by a series of experiments replicating the opaque glasses. The results also showed that the alteration of the glasses was highly variable, both in the degree of alteration and the composition and morphology of the alteration layers. This variability could not be correlated with the original location of the objects on the site, including objects from the same room, and it was concluded that small microenvironmental changes were responsible for producing the large range of variation seen. In addition, a distinction was noted between the alteration of translucent and opaque glasses, which was found to be repeated in the dissolution experiments with the opaque glass having a much higher dissolution rate. The alteration experiments have established a dissolution rate for LBA composition glasses and indicated that replica glasses are a good analogue for archaeological glasses of the same type. It is suggested that the dependence on the burial environment of archaeological glasses, an open system, compared to the closed system of nuclear waste glasses means that the use of data from archaeological glasses in looking at the effects of long-term burial on nuclear waste glasses has to be carefully applied.

Acknowledgements

My great thanks go to my supervisors, Andrew Shortland at Cranfield University and Eva Valsami-Jones at the Natural History Museum for all of their help and support with my thesis. My thanks also go to Katherine Eremin at the Harvard Arts Museums for organising access to the collection, for a place to stay while working at the museum, and for an immeasurable amount of help, support and ideas throughout the project. I would also like to thank the Semitic Museum at Harvard University for allowing me access to the collection and to take the necessary samples, and in particular Joseph Greene, the Assistant Director. My special thanks must go to James Armstrong, former curator at the Semitic Museum, for his limitless patience with my work, his helpful comments and discussion, and his enthusiasm and knowledge which has encouraged the whole team working on the Nuzi material. I would also like to thank John Spratt and Anton Kearsley of the EMMA division, Department of Mineralogy, Natural History Museum, for their immense help in carrying out the analytical work and lending me their expertise and knowledge in the techniques used. Also from the Natural History Museum I would like to thank Terry Williams, Catherine Unsworth and Tony Wightman for their help and support with the project. At Cranfield University my thanks must go to Keith Rogers, Mike Edwards, Sophie Beckett, Jon Painter, Adrian Mustey, Joe Rogers, Nicola Attard-Montalto, Melanie Sapsford, Rebecca Scott, Rachel Cochrane and Annaig Lecomte for their help and support with the analytical and experimental work of the project. Finally I would like to warmly thank Elinor Kirk for proofreading the thesis itself and Ian Kirk for all his support, and helpful discussions, in the final stages of the process.

Contents

| | | |
|----------|--|-----------|
| 1 | Introduction | 9 |
| 1.1 | Background | 9 |
| 1.2 | Project Aims and objectives | 10 |
| 1.3 | Why study the alteration of the glasses from Nuzi? | 11 |
| 2 | Literature survey | 12 |
| 2.1 | Introduction | 12 |
| 2.2 | Glass | 12 |
| 2.3 | Alteration processes of buried glasses | 13 |
| 2.4 | Nuzi | 22 |
| 2.5 | Late Bronze Age vitreous materials | 33 |
| 2.6 | Summary | 35 |
| 3 | Methodology | 36 |
| 3.1 | Introduction | 36 |
| 3.2 | Sampling | 36 |
| 3.3 | Analytical techniques | 40 |
| 3.4 | Sample preparation | 50 |
| 3.5 | Dissolution experiments | 52 |
| 3.6 | Experimental replication of antimonate glasses | 54 |
| 4 | Results 1: Typology and distribution | 56 |
| 4.1 | Introduction | 56 |
| 4.2 | Survey of the vitreous assemblage | 56 |
| 4.3 | Survey of vitreous materials recorded in finds notebooks | 66 |
| 4.4 | Assignment of find locations to objects | 70 |
| 4.5 | Distribution of vitreous materials | 71 |
| 4.6 | Intrusion into Stratum II | 76 |
| 4.7 | Summary | 77 |

| | | |
|----------|---|------------|
| 5 | Results 2: Identification, composition and provenance | 78 |
| 5.1 | Identification of materials and bulk compositional analysis | 78 |
| 5.2 | 2nd millennium BC glass | 80 |
| 5.3 | Later glass | 86 |
| 5.4 | Glazed ceramics | 89 |
| 5.5 | Faience and related materials | 93 |
| 5.6 | Other materials | 97 |
| 5.7 | Trace elemental compositional analysis | 98 |
| 5.8 | Summary | 99 |
| | | |
| 6 | Results 3: Preservation and weathering | 100 |
| 6.1 | 2nd millennium BC glass | 100 |
| 6.2 | Variation in alteration | 122 |
| 6.3 | Glazed ceramics | 124 |
| 6.4 | Late period glass | 127 |
| 6.5 | Other vitreous materials | 128 |
| 6.6 | Summary | 129 |
| | | |
| 7 | Results 4: Experiments (replication and dissolution) | 129 |
| 7.1 | Glass dissolution and alteration experiments | 129 |
| 7.2 | Replication of glasses | 134 |
| 7.3 | Summary | 139 |
| | | |
| 8 | Discussion | 140 |
| 8.1 | Archaeological results | 140 |
| 8.2 | Bulk compositions | 145 |
| 8.3 | Alteration of glasses | 149 |
| 8.4 | Experimental results | 160 |
| 8.5 | Summary | 164 |

| | | |
|-----------|------------------------------------|------------|
| 9 | Conclusions and Future work | 165 |
| 9.1 | Conclusions | 165 |
| 9.2 | Future work | 170 |
| 10 | References | 171 |

List of Tables

| | | |
|----|--|-----|
| 1 | Stratigraphic groupings at the site of Yorgan Tepe, including the city of Nuzi | 26 |
| 2 | List of 'ideal' samples prepared prior to museum visit | 37 |
| 3 | Samples taken from the Semitic Museum at Harvard University for analysis | 39 |
| 4 | Replica glass 1: LBA composition glasses used for dissolution experiments | 52 |
| 5 | ICP-AES results of mudbrick analyses (major elements and copper) and analysis of clay used | 53 |
| 6 | Dissolution experiments: starting weight and surface areas of glass monoliths | 54 |
| 7 | Replica glass 2: translucent LBA glass recipe | 55 |
| 8 | Replica glass 3: antimony-opacified replica glasses | 55 |
| 9 | Survey of vitreous materials in museum assemblage | 56 |
| 10 | Survey of finds notebooks, summary table | 67 |
| 11 | Bulk compositions 2nd millennium BC glasses | 79 |
| 12 | 2nd millennium BC glass by colour | 81 |
| 13 | Late period glass bulk compositions | 87 |
| 14 | Glazed ceramics composition | 90 |
| 15 | Faience and other materials composition | 94 |
| 16 | Trace elemental analysis, results | 98 |
| 17 | Objects sampled by object type and presence of glass | 100 |
| 18 | Visual survey of preservation - subgroups | 101 |
| 19 | Altered glasses subgroups (after SEM imaging) | 102 |
| 20 | Details of alteration: samples with glass present | 106 |
| 21 | Details of alteration: devitrified glasses | 107 |

| | | |
|----|--|-----|
| 22 | Altered glasses, bulk composition | 120 |
| 23 | Table showing phases identified by XRD | 121 |
| 24 | Alteration groups and details: glazed ceramics | 125 |
| 25 | Powder vs monolith: initial experiment | 129 |
| 26 | Dissolution experiment results | 131 |
| 27 | Experimental samples, clay solution and 100% RH | 132 |
| 28 | Replica antimonate glasses | 134 |
| 29 | Bulk compositional analysis experimental antimonate glasses | 137 |
| 30 | Recipes compared to analyses replica antimonate glasses | 137 |
| 31 | XRD results of experimental and archaeological antimonate glasses | 139 |
| 32 | Normalised elemental mass loss and dissolution rates of replica glasses | 161 |
| 33 | Comparison of normalised mass loss into solution from archaeological and replica glasses | 162 |

List of Figures

| | | |
|---|--|----|
| 1 | Site of Yorgan Tepe, location of the city of Nuzi, in Iraq (Starr, 1937: Plan 1) | 23 |
| 2 | Map of extent of excavations of the city of Nuzi (Starr, 1937: Plan 16) | 25 |
| 3 | Map of Stratum II city with areas marked (after Starr 1937: Plan 13) | 29 |
| 4 | Plan of the suburban houses of Zigi and Shilwi-Teshub (Starr, 1937: Plan 36) | 30 |
| 5 | Rainfall map, northern Iraq (Buringh, 1960:42) | 31 |
| 6 | a. sample with complete cross section (1930.62.82c); b. unstable sample (1930.82.73c) | 39 |
| 7 | Types of bead: top row left to right, spherical bead 1930.63.5; large inlaid cylindrical bead 1930.62.90, spacer bead 1930.61.8; middle row: yellow disc bead 1930.63.59, blue hubbed bead 1930.62.72, ribbed bead 1930.67.74, red granulated bead 1930.67.33, square inlaid bead 1930.62.82, rhomboidal bead 1930.62.84; bottom row: eye beads 1930.63.29, broken inlaid barrel bead 1930.62.78; grapes bead 1930.60.99. (not to scale) | 59 |
| 8 | Beads of various colours, all heavily weathered | 60 |
| 9 | a. polychrome glass vessel with inlaid decoration; b. fluted vessel; c. vessel fragment with fine decoration, unknown original colour | 61 |

| | | |
|----|---|----|
| 10 | a: decorated sun disk pendant (Starr 1937: Plate 120); b: amber-coloured pendant fragment, 1930.82.62e | 61 |
| 11 | a: blue glass mace head with yellow decoration; b: fragment of glass figurine (with restoration) | 62 |
| 12 | a: marbled faience vessel; b: fragment N25 | 63 |
| 13 | Egyptian blue vessel fragment 1930.47.14 | 64 |
| 14 | Egyptian blue pigment, raw lump and close up of interior | 64 |
| 15 | Cylinder seals: a. vitreous material (1930.80.29); b. stone (1930.82.30); c. terracotta (1930.80.34) | 65 |
| 16 | Drawings of typical Late glass forms (Starr 1939: Plate 140) | 65 |
| 17 | Glazed ceramics: wall nail and lion figurines | 66 |
| 18 | Page from finds notebook, with later correction | 67 |
| 19 | Extract from notebook showing 28-12-306 as a ceramic vessel rather than the Late glass vessel 1930.62.6 | 70 |
| 20 | Page of finds notebooks showing change of room number | 71 |
| 21 | Distribution map of vitreous materials in Stratum II, based on Starr, 1937: Plan 13. Key: the pink diamonds are the beads (with the number of beads at each location within this symbol); the blue triangles are glass vessels, the blue circles the glass pendants and figurines and the blue squares the raw glass; the green triangles are the glazed ceramic vessels; the green circles the glazed wall nails and the green stars the glazed ceramic figurines. | 73 |
| 22 | Examples of translucent blue, opaque blue, white and yellow glass | 82 |
| 23 | a: Calcium antimonate in opaque turquoise glass 1930.68.27c; b: Lead antimonate in yellow inlay 1930.82.15b | 83 |
| 24 | 1930.: SEM image altered ?black glass, CuS inclusions visible as bright white specks | 84 |
| 25 | Compositional difference between translucent and opaque glasses Nuzi | 85 |
| 26 | Colorant-free glass bead with tin-rich inclusions in inlay (1930.62.52) | 86 |
| 27 | Glaze sample 1930.52.1f showing alteration layers and a clear interaction layer | 91 |
| 28 | Altered white glaze, 1930.14.6b | 91 |
| 29 | 'yellow' striped glazed vessel and 'yellow' bead | 92 |
| 30 | Red lion 1930.5B.1, SEM image of paint layer | 92 |

| | | |
|----|--|-----|
| 31 | Marbleised faience sample 1930.82.1; glassy area in sample N25 | 93 |
| 32 | Faience vessel fragment; SEM image showing quartz body and heavily weathered glaze layer | 95 |
| 33 | Egyptian blue vessel fragment SEM image and compositional spectrum | 96 |
| 34 | Cylinder seal fragment, SEM image - possible glaze fragment bottom right | 97 |
| 35 | Bone bead 1930.68.26: SEM image and compositional spectrum | 97 |
| 36 | Scatterplot showing trace element groups for Egyptian and Near Eastern glass (from Shortland et al 2007) with additional data from the current project | 99 |
| 37 | 1930.82.55, well preserved translucent blue glass; 1930.69.39e, devitrified glass bead. . . . | 101 |
| 38 | a. 1930.63.40d, opaque turquoise glass with white weathering crust; b. 1930.63.37, colorant-free eye bead with beige weathering crust; c. 1930.66.90c, translucent blue glass with iridescent weathering crust. | 101 |
| 39 | Examples of the preservation groups 1 to 7 | 104 |
| 40 | Morphology of alteration layers: a. 1930.82.4; b. 1930.63.37 | 105 |
| 41 | Variation in greyscale in BSE image of secondary alteration layers, 1930.68.27c | 105 |
| 42 | Lamellar features 1: a. 1930.60.42 fine lamellar features; b. 1930.62.84c larger lamellar features; c. 1930.63.40a changes in scale; d. changes in direction of reaction front; e. 1930.69.39b smooth well-organised lamellae; f. 1930.62.84e disorganised lamellae. | 108 |
| 43 | Features of secondary layers: 1930.82.66 with compressed layers; 1930.68.27b showing significant fractures and 'fault line' behaviour of lamellae around cracks; 1930.82.15b with the alteration process moving along cracks in otherwise pristine glass. | 109 |
| 44 | Line analysis of 1930.69.39f: silicon, sodium and magnesium maps | 110 |
| 45 | Line analysis 1930.82.14, screenshot | 110 |
| 46 | Line analysis 1930.69.39b, variation in silicon counts | 111 |
| 47 | Montage of area of 1930.82.4 with 'smeared' areas in the secondary phases, BSE image . | 112 |
| 48 | 1930.82.50, opaque white glass, compositional maps | 112 |
| 49 | 1930.82.4 compositional maps | 113 |
| 50 | False coloured image of 1930.66.90g Si = green, Mg = red | 114 |
| 51 | 1930.60.140a, yellow glass bead, compositional maps showing inhomogeneity of composition in unaltered glass | 114 |

| | | |
|----|--|-----|
| 52 | 1930.82.14, manganese and iron-rich area; 1930.68.9, calcium-rich substance infiltrating along cracks; 1930.60.140b, clustering of lead colorant. | 115 |
| 53 | Various inclusions found in the glasses: a. diopsides (1930.82.70a); b. albite inclusion (1930.61.129a); calcium-phosphorus-rich (1930.66.90b); d. possible chromspinel, within diopside (1930.82.66); e. iron-rich inclusion (1930.61.91a); f. bone fragment (1930.66.89) | 116 |
| 54 | 1930.82.4 points analysis and BSE image | 118 |
| 55 | 1930.82.70a, quantified points and BSE image | 119 |
| 56 | Diffraction pattern for 1930.82.70 (2 Theta on x axis) | 121 |
| 57 | Diffraction pattern for 1930.60.140 (2 Theta on x axis) | 122 |
| 58 | Translucent vs opaque glass secondary alteration layers; a. 1930.66.90a (translucent blue); b. 1930.82.59 (opaque white) | 123 |
| 59 | 1930.60.140d with copper-rich alteration layers; point 5: 25.6%, point 6: 7.5%, point 7 13.2% and point 9 on 14.2% CuO on analysis with SEM-WDS, compared to 2.0% in the unaltered glass. | 123 |
| 60 | Glazed ceramics: a.1930.52.1g Late glaze with tin-rich inclusion (white) and wollastonite inclusions (grey); b.1930.16.3 well preserved LBA glaze; c. 1930.52.1h fine 'soft' lamellar features; d. 1930.52.1f fine lamellar features, diopside inclusions; e. 1930.52.1f interaction layer with diopside inclusions radiating from interaction layer; 1930.52.1h interaction layer between glaze and ceramic body. | 126 |
| 61 | Late glasses: a. 1930.82.21 natron glass with minimal weathering at edge; b. 1930.82.37 glass with significant secondary layers; c. 1930.82.6a 'wavy' interaction layer between glass and secondary phases; d. 1930.82.6a are of slower weathering; e. 1930.82.34 change of scale/organisation in lamellar features; f. 1930.82.34 large lamellae showing difference in structures. | 128 |
| 62 | 1930.61.91: Egyptian blue bead with devitrified glassy areas with distinct lamellar features in places. | 128 |
| 63 | Scatterplot showing loss of silicon into solution versus surface area, dissolution experiments | 130 |
| 64 | a: congruent dissolution attacking along cracks; b and d: typical appearance of experimental glasses after 28 and 56 days in solution at 60 degrees Celsius; c, e and f possible secondary phases (c - 60-28 e/f RT-56); | 132 |
| 65 | Secondary alteration phases on 84 day sample 100% RH experiments | 133 |

| | | |
|----|--|-----|
| 66 | Early alteration stages: a. archaeological glass 1930.82.21; b. experimental glass RT 56 | 133 |
| 67 | a. 60 84, congruent dissolution; b. RT 84, early stages | 134 |
| 68 | 'Frothy' replica antimonate glass (1050°C) | 135 |
| 69 | Experimental replica glasses B2-B4 and C2 (from left to right top); close-up of B4 (left) and C2 (right) | 135 |
| 70 | Experimental antimonate glasses: a. and b. glass B2, 3% Sb ₂ O ₃ ; c. and d. glass B3 (3% Sb ₂ O ₃ + 3% CaO); e. and f. glass C2 (cullet + 3% Sb ₂ O ₃) | 136 |
| 71 | Nuzi antimonate glass 1930.62.103 | 136 |
| 72 | Diffraction patterns for experimental antimonate glasses: glass B2 top and B3 bottom | 138 |
| 73 | Extract from notebook showing decorated glass fragment recorded as 'painted fragment' | 142 |
| 74 | Possible altered red glass bead 1930.61.91a | 146 |
| 75 | Scatterplot of Late period glasses compared to LBA glasses: Sassanian glasses from Brill 1999b (152-156) and Egyptian data from Shortland and Eremin 2006 | 148 |
| 76 | Early stages of alteration, 1930.82.55 | 151 |
| 77 | a. 1930.82.21, Late period vessel fragment; b. Experimental replica alteration experiment RT 28 | 151 |
| 78 | Altered glass 1930.52.1e inlay and body glass | 155 |
| 79 | Bead 1930.66.90g, significantly more altered on one side than the other | 156 |
| 80 | Excavation photograph, showing beads very close together | 156 |
| 81 | a. lead antimonate in alteration layers (1930.62.81); b. calcium antimonate in alteration layers (1930.66.90b) | 157 |

1 Introduction

1.1 Background

The scientific study of ancient glass objects has expanded considerably over the last 40 years and has moved from simple categorisation based on major element composition to highly complex studies looking at the place of manufacture, in some cases looking at the movement of individual glass batches. Projects have been concerned with the composition, technology and provenance of ancient glasses. Others have concentrated on the preservation and weathering of such artefacts both from buried and architectural contexts, such as stained glass windows. The long-term behaviour of glass in a burial environment has been studied extensively over the last 50 or 60 years, both from the perspective of preserving ancient objects and the durability of nuclear waste glasses.

A large number of glass and vitreous objects, alongside many other classes of material, from the 2nd millennium BC city of Nuzi are held at the Semitic Museum at Harvard University. The glass assemblage from the city of Nuzi, in modern Iraq, is amongst the earliest known from the Near Eastern Bronze Age (around 3500 years old). The assemblage is also one of the largest known from this early period in the history of glass. Many thousands of objects made from glass, faience and frit are present within it; all coming from a single site with the majority from a single context; the destruction layer of the LBA city. The site itself is relatively small, around 200m across and it was not significantly reoccupied after the destruction of the city until around 1000 years later. This should mean that the objects in the LBA layer were found in approximately the positions they were in at the point when the city was destroyed. Several previous studies have looked at small numbers of objects from this collection but there has not been a study looking at the collection as a whole (Vandiver 1983; Barag 1970; Thornton and Ehlers 2003).

A major international project, involving a number of researchers from institutions in several countries, has initiated a holistic study of the entire material assemblage from the site of Yorgan Tepe, which contains the city of Nuzi. The aim of this project has been to assess and then characterise in detail all categories of material, including copper alloy metal objects, ceramics, organic materials such as bone and shell, and the glass and vitreous materials from the site using multiple scientific techniques. This is in order to answer a number of questions about the technology, trade and exchange of materials and objects within this region during the Late Bronze Age (LBA). The project is also interested in the everyday use of objects and life of the people who lived at this site. Another major strand of this research is the identification of intrusive material in the LBA assemblage from later period occupation on the site. In addition to this the project is also concerned with assessing the preservation of the inorganic materials, particularly the metals and vitreous materials. Thus far the glass and vitreous materials have received the most attention with extensive studies into their technology and provenance (Shortland and Eremin 2006; Shortland et al 2007; Degryse

et al 2009). However, the metal assemblage is in the process of being characterised with an extensive non-destructive survey, as well as limited destructive analyses and a pilot study into the composition and provenance of the LBA ceramics was carried out during 2008 (Shortland et al 2008; Erb-Satullo et al in preparation).

The durability of glasses has been studied extensively for the past 60 or so years for a number of reasons. The conservation of ancient artefacts, particularly architectural elements such as stained glass windows has been a major concern for many projects. However, the preservation and alteration of glass from the Late Bronze Age period in the Near East has not been studied in any detail before the current project. A single example from Nuzi was analysed in Vandiver (1992) but a complete assessment of the assemblage as a whole has not been carried out. Devitrified glasses, of which there are a number of examples from Nuzi, have also not been studied extensively. The Nuzi vitreous assemblage, due to its size and the varied nature of the objects and materials within it allows a wide-ranging analysis of both the technology of the vitreous materials and their preservation and alteration.

1.2 Project Aims and objectives

The aims and objectives of the current project can be divided into three main areas. To reassess and evaluate the extensive collection of vitreous materials held at the Semitic Museum at Harvard University; to examine the composition and technology of the glasses and other vitreous materials within that collection; to characterise the preservation and alteration of the glasses and vitreous materials in the Nuzi collection.

1.2.1 Survey of the Late Bronze Age vitreous from Nuzi

The first major aim of the current project is to reassess the vitreous material assemblage from the site. This will include a survey of the assemblage in terms of the number and types of objects present. Where possible the original find location of the objects will also be determined and any later period or intrusive materials identified. The site archive held within the museum, including the finds notebooks, will also be studied to find out as much as possible about the original excavation of the materials, including their find locations and condition. The distribution of these materials across the site and their possible significance will also be studied as part of this project. The entire vitreous materials assemblage was examined (with the exception of some of the objects on display) as the initial stage of this project, alongside the excavation archive. An extensive set of samples (252) from the assemblage has been collected from the Semitic Museum at Harvard University where the objects and excavation archive are now stored.

1.2.2 Identification, composition and technology

The second broad aim of the current project is to examine the composition of the glasses and other vitreous materials. This will include the identification of the materials used in manufacture of the objects; this can be unclear due to post-depositional changes, especially in the smaller objects such as the beads. Major and trace element composition of the glasses will also be established, this has already been done for a number of the glass objects but the current project intends to extend the range of glass colours and other vitreous materials for these analyses. The composition of the glasses and other materials can provide significant information about their manufacture, technology and provenance. This fits well with the overall aims of the major research project noted above.

1.2.3 Alteration: characterisation and experimental work

The final strand of the project is to assess and characterise in detail the preservation and alteration of the glasses and other vitreous materials. The excavation report and other studies have indicated that the majority have suffered significant post-depositional alteration. This project intends to characterise in detail the alteration that these glasses have undergone while buried, using a number of analytical techniques including SEM-WDS, SEM-EDS, LA-ICP-MS and XRD. The nature of the post-depositional processes will also be examined and experimental work to replicate these processes will be carried out. The project will also consider the range of alteration phenomena within this assemblage. The majority of the assemblage is from a single context (the final occupation and destruction layer of the Bronze Age city) within the site, which is itself relatively small. Some examples from the assemblage are almost perfectly preserved whilst others are extremely altered, to the point that no original glass remains and the structure is extremely fragile. As the original burial locations of many of the objects are known variation in the preservation of the vitreous materials can be studied at an intra-site level. Possible factors that could have affected the alteration seen in these glasses, such as composition of the glass and burial environmental conditions, will be examined. Another aspect that will be studied within this project is the extent to which experimental alteration can replicate that found in the archaeological examples.

1.3 Why study the alteration of the glasses from Nuzi?

The assemblage of glass from Nuzi allows many questions to be asked regarding the behaviour of glasses in a long-term burial environment. These are amongst the earliest known man-made glasses so provide an opportunity to look at the alteration of buried glasses over a very long time period. This has implications for looking at the preservation and conservation of archaeological glasses as well as predicting the alteration of modern glasses in buried contexts. There is also the potential for data from these glasses to be used in

the study of the durability of nuclear waste glasses; archaeological glasses are often used as analogues for the durability of nuclear waste glasses, however, most studies published so far have looked at much younger glasses (less than 2000 years old). As already noted the degree of variation observed in the alteration of glasses from this site allows different stages of alteration processes to be studied at an intra-site level. The glass from Nuzi provides an opportunity to examine the preservation, technology and distribution of this unique assemblage from an early period in the history of glass.

2 Literature survey

2.1 Introduction

This project covers a wide range of subjects from the molecular structure of glass and the details of glass/water interactions to the archaeological and historical background of the city of Nuzi and Late Bronze Age glass. This chapter outlines the main sources of information on these topics within the context of the project aims.

2.2 Glass

2.2.1 What is glass?

A material is generally described as a glass when it has solidified from the liquid state without crystallization, an amorphous solid (Paul 1990:1,9). And more specifically as a supercooled liquid that has “frozen-in” (Scholze 1991:19) i.e. a material that has retained the structure of a liquid in its solid state (Scholze 1991:92). The most important ideas about the structure of glasses were first discussed by Zachariasen (1932) who found that the energy differences between glass and crystalline materials of the same composition were extremely small, therefore the same states of bonding had to occur in the glassy and crystalline state, but that glass had a random rather than ordered network. Therefore glass can be defined as a material that lacks long range periodic atomic structure and also exhibits glass transformation behaviour (Shelby 2005:3). Glass transformation behaviour is the temperature range within which a melt can be cooled without crystallising (Shelby 2005:4). Based on this definition any material which exhibits this behaviour can be defined as a glass (Shelby 2005:3), for example, clear boiled sweets are a glassy form of sugar.

A number of oxides can form a glass, network building polyhedrons such as SiO_2 , B_2O_3 and P_2O_5 , which are known as network formers (Zachariasen 1932). However, as ancient glasses are the subject of this project only the silicate glasses will be discussed. Silicate glasses are based upon the SiO_4 tetrahedron

(Doremus 1994:25) which retains this short-range order even within the random network of a glass (Greaves et al 1991). However, pure quartz requires a temperature of 1720°C to vitrify therefore usually a flux (an alkali such as sodium or potassium) is added to lower the melting point making the formation of a glass easier. The addition of the alkali results in the breaking of connections between the silicon-oxygen bonds in the glass network (Doremus 1994:33). The shared oxygens between silicon tetrahedra are known as bridging oxygens, unshared as non bridging oxygens (NBOs) (Rao 2002:25). Each Na⁺ ion produces an NBO thus reducing the connectivity of the glass and consequently its melting point (Le Bourhis 2007:57). As a result of this the alkali component of glasses are known as network modifiers (Zachariassen, 1932). Alkaline earths, such as calcium and magnesium, although classed as network modifiers are generally added to glasses because these oxides have a stabilising effect on the network and improve the glass's durability. The alkaline earths are less mobile than the alkali ions and are more strongly bonded to the network, thereby increasing the stability and durability of a glass by restricting the diffusion of alkali ions (Shelby 2005:90). There are also intermediate oxides, such as Al₂O₃, which may behave either as network formers or network modifiers, these are oxides which cannot easily form a glass on their own but can substitute for silicon tetrahedra in the glass network (Shelby 2005:90).

2.3 Alteration processes of buried glasses

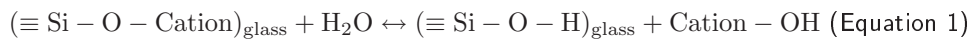
2.3.1 Terminology

The term alteration has been selected to cover all of the processes which affect glasses in contact with water. A variety of terms are used to describe the various aspects of glass/water interactions with the terms alteration, weathering, corrosion, hydration, durability, stability, deterioration, decay and dissolution all being used within the literature. Some of these terms appear to have loaded connotations such as weathering which is often applied to atmospheric effects rather than buried glasses, particularly in studies of stained glass windows (for example, Newton 1975). Lombardo et al (2005) suggest that the term corrosion should only be used to describe the network breakdown aspect of glass alteration, whereas it is used to describe all aspects in other studies (for example, Janssens et al 1996). The durability of glass is often discussed in relationship to nuclear waste disposal (for example, Wicks 1992) and hydration is more usually applied to natural glasses (for example, White 1984). However, all of these terms are used to describe the same processes or aspects of the same processes, therefore, in this project the term alteration has been selected as an overall term covering glass/water interactions.

2.3.2 Processes

The alteration of glasses is caused by the interaction of the glass surface with an aqueous solution, usually water. This interaction causes the selective leaching of alkalis from the glass, the hydration of the glass network, the breakdown of the glass network and the formation of secondary mineral phases.

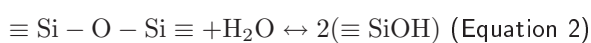
The selective leaching of alkalis from a glass surface is thought to occur through ion exchange between H^+ protons and alkali cations within the glass (Bunker 1994). The modified random network theory of Greaves et al (1991) suggests that percolation channels exist within the random network of glass structure and it is these that allow that transport of cations in diffusion processes such as ion exchange. There has been considerable debate about how exactly water diffuses into a glass (Ojovan et al 2005) but the reaction can be shown simply as:



The amount of alkali cations present in solution and the pH in a solution will affect the rate of ion exchange, for example, a larger number of alkali ions within a solution is expected to inhibit ion exchange. Ion exchange is also affected by the equilibrium constant which measures how effectively protons and alkali cations compete to occupy an anionic site (Bunker 1994). The ion exchange equilibrium constant is governed by the charge distribution of sites within the glass (Bunker 1994).

Although it often implied that an H^+ exchanges with alkali cations in glass Ernsberger (1980) has argued that a bare proton cannot exist within these conditions. A proton has no electron cloud and would embed itself in the electron cloud of the first anion it encountered. Therefore another mechanism for proton exchange in glass is required. It is suggested that H^+ is being transported into the glass alongside water molecules, possibly as hydronium ions (H_3O^+) (Ernsberger 1980), or simply as molecular water (Equation 1). About three hydrogen atoms enter the glass for each alkali ion released into solution (Grambow 2006) leading to an alkali-depleted and hydrated surface layer.

Hydrolysis and dissolution of the glass network occurs simultaneously with ion exchange but at a much slower rate than the initial hydration and ion exchange rates (Grambow 2006). Network dissolution occurs where hydroxyl groups (usually OH^-); formed by hydrolysis reactions, attack tetrahedral SiO_4 sites forming a reactive five-co-ordinated intermediate group which can decompose rupturing the Si-O-Si bonds within the glass network (Bunker 1994). Equation 2 shows the initial hydrolysis reaction, which is theoretically reversible.



In glasses with high silica content or in pure silica this reaction is suppressed by the high degree of connectivity within the glass network, which makes it difficult for SiO_4 tetrahedra to rearrange into the five co-ordinated intermediate group (Bunker 1994). Conversely when a glass contains significant NBOs,

caused by the addition of fluxes such as soda, the hydrolysis reaction occurs more easily as there are unconnected areas within the network i.e. the greater the number of NBOs the more rapid the hydrolysis reaction (Bunker 1994). The opening up of reactive sites within the network can also be created by external stresses to the glass which can deform local Si-O bonds and thus allowing rapid hydrolysis (Bunker 1994). Hydrolysis of the glass network leads to the precipitation of silica on the glass surface forming a gel layer, this is a completely separate phase rather than part of the glass itself; and may also contain an assemblage of crystalline phases (Grambow 2006) resulting from the repolymerisation of silica and other oxides from the glass network (Bunker 1994). The gel layer is highly porous and allows transport of water further into the glass network (Bunker 1994). Network dissolution may also result in the complete 'congruent' dissolution of the surface where the glass surface composition is identical to the bulk composition (Hench and Clark 1980).

The creation of secondary phases during glass alteration has been discussed in many articles, and it is generally accepted that the formation of these layers arises from recondensation of the glass network after hydrolysis and dissolution (Jégou et al 2000). The layers are created by reprecipitation of silica (and other elements) at the glass surface into a new material, which may be amorphous or poorly crystalline (Grambow 2006). However, more recently the role of both the precipitation of secondary phases in the rate of glass dissolution and the effects of the type of phase precipitated have been examined in more detail, with the type of secondary phases formed being thought to affect the overall durability of the glass (Cailleteau et al 2008; Jantzen et al 2008). The porosity of the secondary phases created appears to affect whether or not the rate of alteration will slow to a final residual rate or if dissolution will continue over the long-term (Cailleteau et al 2008).

2.3.3 Factors affecting glass/water interactions

Composition of the glass: One of the most significant factors affecting the reaction of a glass with an aqueous solution is the composition of the glass itself. Within this the level of silica within the glass is the most significant. The resistance of glass to alteration drops sharply at silica levels below 66.67 mol% which corresponds to the point where each silicon atom within the glass is associated with an alkali ion as a second neighbour (El-Shamy 1973). Therefore in glasses that contain less than 67 mol% silica an interconnected path of non-bridging oxygen sites allows the exchange of species between the solution and the glass conversely above 67 mol% silica these oxygen sites are isolated from one another by the silica network (Jantzen 1992a).

However, experiments using an 80% SiO₂ 20% Na₂O glass have shown that despite the high silica levels this glass very rapidly began to dissolve in water indicating the requirement for a network stabiliser such as lime (Hench and Clark, 1980). The effect of the addition of lime is explained as resulting from the

divalent Ca^{2+} ions, which are less mobile, reducing alkali ion diffusion through the glass network (Shelby 2005:168). The presence of lime also leads to the formation of a calcia-silicate film at the glass surface which can retard ion diffusion (Hench and Clark 1980), presumably by reducing the porosity of the gel layer. The presence of aluminium oxide, even in small quantities, within a glass can increase its stability significantly. This is because aluminium oxide is contained within glass in a formation that fixes an alkali ion for charge balance (Shelby 2005:90); it can also be favour the creation of more stable protective gel layer which retards diffusion processes (Scholze 1991:345) such as ion exchange and hydration. Although lime is the most common stabiliser experimental work has indicated that there is little difference between the divalent alkaline earths calcium and magnesium (El-Shamy 1973).

Solution pH: The pH of the attacking solution is also significant in the interaction of glass with an aqueous solution. Experimental work on soda-lime-silicate glasses has indicated that silica release (from the dissolution of the silica network) is minimal at a pH below 9 and increases at a pH above 9, the reverse being found for alkali extraction (El-Shamy et al, 1972). Therefore ion exchange is the dominant reaction in acidic to neutral conditions and network dissolution (thus releasing silica into solution) dominating in alkali conditions. In near neutral conditions ion exchange and hydration are the initial processes of alteration with hydrolysis subsequently controlling the later stages. Ion exchange reactions lead to a decrease in cation content in the surface layers of the glass, as a result of this ion exchange rates decline over time; hydrolysis reactions, however, remain constant over time and will eventually dominate the alteration of glass (Ojovan et al 2005). It has also been noted that a higher pH increases the overall dissolution rate as a result of hydrolysis and network breakdown being the primary mechanism of alteration (Pierce et al 2008).

Surface characteristics: The surface area to volume ratio (SA/V) of a glass surface within an aqueous solution has been shown to significantly affect the alteration produced. At high SA/V network dissolution predominates with selective leaching being the dominant process at lower SA/V ratios (Buckwalter et al 1982). It has also been noted that surface roughness increased alteration to a greater extent than the increase in SA/V caused by an uneven surface alone (Buckwalter et al 1982). Alteration processes have also been noted to conform to irregularities and bubbles at the glass surface (McLoughlin 2003:214).

Time and temperature: At high temperatures the switch in the dominant alteration process from ion exchange controlled to hydrolysis controlled alteration can take only a few days, rather than many years at low temperatures (Ojovan et al 2005, 2006). Experimental work has indicated that the temperature dependence of alteration reactions follows Arrhenius kinetics for most cations, because hydrolysis reactions have a higher activation energy (Ojovan et al, 2006).

Other factors: Many other factors can also affect the alteration of glasses; however, many are not relevant to buried glasses, such as sunlight and atmospheric pollution (Newton and Davidson 1996:35). However, the action of bacteria can also affect the alteration of glass; fungi, algae and bacteria have all been shown to have an effect on the alteration of archaeological glasses from medieval windows to buried environments (Krumbein et al 1991; Brehm et al 2005).

2.3.4 Modelling glass/water reactions

Numerous models have been created to predict the alteration of different types of glasses within different environments. These can be broadly divided into models based on the chemical affinity of the reactions taking place between the glass and an aqueous solution; and models based on the thermodynamics, primarily the free energy of hydration, of the glass surface/aqueous solution reactions. These models have been derived in order to predict the behaviour of glasses of different compositions within certain environmental conditions.

Thermodynamic models: Within this model the thermodynamic stability of a glass is considered to be the stability of its component oxides which is a function of the chemical potential of each oxide within a glass (Jantzen and Plodinec 1984). Within this model glass/water reactions are explained by the summation of the free energies of hydration of each component oxide species within a glass (Jantzen and Plodinec 1984) given by:

$$\Delta G_{hyd} = \sum x_i(\Delta G_{hyd})_i \text{ Equation 3: (Jantzen and Plodinec 1984)}$$

where $(\Delta G_{hyd})_i$ is the free energy change of the most stable reaction of component i at mole fraction x_i (McLoughlin 2003:50). However, it should be noted that the 'geochemical' models also use the free energy of hydration within their calculations (Aagaard and Helgeson 1982; Grambow 2006).

In thermodynamic models the glass is assumed to be a homogeneous mixture of structural units such as SiO_2 and Na_2SiO_3 , the reaction of all of these units with water is the thermodynamic stability and the hydration free energy of the glass is assumed to be the sum of the hydration stabilities for each component (ΔG°), weighted by its mole fraction (Jantzen and Plodinec 1984), the more positive the free energy the more durable the species within a glass. For example, SiO_2 has a free energy of hydration of $+5.59 \Delta G^\circ$ kcal/mol and Na_2SiO_3 $-28.815 \Delta G^\circ$ kcal/mol (Jantzen and Plodinec 1984). This assumes that hydration reactions dominate glass dissolution processes with; for example, silicate groups hydrating to silicic acids, therefore free energy of hydration values may not be applicable at extremes of temperature or pH where other reactions may take place (Jantzen and Plodinec 1984). A wide variety of glass compositions including nuclear waste glasses, natural glasses and archaeological glasses were leached in the laboratory to test the theory and the levels of structural silica released were plotted against the free energy of hydration of

each glass composition and the number of non-bridging oxygens (NBO) within that composition (Jantzen and Plodinec 1984). A linear relationship between the ΔG° and number of NBOs was found which indicated that natural glasses were the most durable and certain medieval window glasses the least durable (Jantzen and Plodinec 1984). It is argued that a thermodynamic approach using the composition of a glass can predict its durability (Jantzen and Plodinec 1984). Thermodynamics offers a “quantitative frame of reference for the relationship of any solid species with an aqueous environment on geological timescales” (Jantzen and Plodinec 1984:208).

The thermodynamic model was later expanded using Pourbaix diagrams (equilibrium pH-electrochemical potential diagrams) generated to describe the effects of environment on the corrosion of metals. Linking the thermodynamic models with these allowed the dissolution of glass to be modelled both as a function of the hydration free energy, (ΔG_{hyd}), and environmental conditions (Jantzen 1992a) and can quantitatively describe the dissolution behaviour of all glasses as a function of its environment (Jantzen 1992b). Thermodynamic modelling is currently used in predicting the alteration of nuclear waste glasses. Recent work by Jantzen et al (2008) suggests that models based on the thermodynamic approach have successfully predicted the behaviour of a nuclear waste glass buried for 24 years. This study also used the concept of mineral clusters within a glass to predict the type of secondary minerals that would form as alteration layers and their effects on the overall durability of a glass (Jantzen et al 2008).

However, it has been argued that thermodynamic approaches have certain limitations. Helebrant et al (2004) have suggested that thermodynamic models do not explain the selective leaching of alkalis from glasses. In addition Perret et al (2003) indicates that thermodynamic models do not account for secondary crust formation at the glass surface as they are not taken into account when calculating the overall free energy of hydration of a particular glass.

Kinetic models: The basis for most of the geochemical affinity based models is the extremely detailed 1982 model of Aagaard and Helgeson which looked at predicting the dissolution rates of silicate minerals and was then applied to feldspars. Aagaard and Helgeson’s model (1982) attempts to quantitatively predict the rates at which minerals react with aqueous solutions and how these might change with pressure, temperature and solution composition within a single general rate equation. The model uses Transition state theory and thermodynamics to identify the rate-limiting step(s)/reaction(s) within mineral hydrolysis, which are the decomposition of an activated complex on the glass surface driven by the chemical affinity of the overall reaction (Icenhower et al 2008). Transition state theory states that in a given set of kinetic reactions there is a single reaction that is the rate-limiting step (Eyring 1935, cited in Icenhower et al 2008). The activated complex that is the rate-limiting step may change during the hydrolysis process (Aagaard and Helgeson 1982). This model was then applied to the hydrolysis of potassium-containing feldspars (Aagaard and Helgeson 1982). Grambow (1992) then applied this model to nuclear waste glasses and argues that

silica network dissolution is the long-term rate-limiting step of glass hydrolysis once initial hydration and ion exchange by diffusion has reached a steady state. He also notes that the linear relationship between the Gibbs free energy of hydration of a glass and its corrosion rate is most probably based upon the concentration of activated surface complexes; which are rate limiting, a negative hydration free energy favours the formation of hydrolysed bonds at the glass surface resulting in a higher concentration of activated surface complexes (Grambow 1992).

A more recent model, which also uses transition state theory to predict the dissolution rates of multioxide silicate minerals, is Oelkers (2001). Within this model dissolution is seen as the progressive breaking of metal-oxygen bonds in their order of reactivity, as single hydroxides, with each bond type reaching equilibrium before the significant breakage of the next type; the last metal-oxygen bond type to break is considered to be rate-controlling (Oelkers 2001). The partial freeing of the rate-controlling component from the mineral or glass structure is considered to form a rate-controlling precursor complex which is used within the context of transition state theory to derive predictive equations (Oelkers 2001). These equations are claimed to allow description of the dissolution rate of glasses and minerals as a function of solution composition at both far-from and near equilibrium conditions – including taking into account the presence or absence of leached layers (Oelkers 2001).

Grambow and Muller (2001) have extended previous models to include ion exchange and hydration of the glass; within this model the penetration of water into the glass is presumed to be required for both diffusion processes and parallel network hydrolysis reactions using an advection/dispersion/reaction equation, based on equations originally used for modelling the transport of contaminants in a porous media. This model was then applied to experimental nuclear waste glass data finding that the rate-controlling steps are different between closed and open systems (Grambow and Muller 2001). In closed systems the rate of secondary mineral formation ultimately becomes rate-controlling and in open systems glass hydration and ion exchange become equal to the rate of network dissolution; with extremely slow dissolution rates expected in the long-term (Grambow and Muller 2001). These data also showed that silica saturation alone does not account for the significant decrease in corrosion rates observed in this and other studies but that the formation of a hydrated layer forming a barrier to diffusion is also required (Grambow and Muller 2001).

Two recent reviews of kinetic models based on chemical affinity and transition state theory have highlighted the difficulties of applying these models, particularly in complex multi-element glasses and the need for the precipitation of secondary phases to be taken in to account in any future models (Gin et al 2008; Frugier et al 2008). Frugier et al (2008) have produced a new model the GRAAL model (glass reactivity with allowance for the alteration layer). This model adds the kinetics which form the secondary phases to those of the dissolution of the silicon-oxygen network; a single phase of secondary layers is considered to have a linear relationship with the concentration of silicon in solution at the glass surface (Frugier et al 2008).

This model claims that the effect of these layers, whether in passivating or facilitating further silicon release (Frugier et al 2008).

Most of these models have their basis in the dissolution of silicate minerals – while these are generally very similar to man-made glasses there could be differences, such as the structure of the mineral. Within the literature studied it appears to be assumed that the models are applicable to natural, archaeological and nuclear waste glasses without significant changes. However, it should be noted that differences are acknowledged in the behaviour of natural and man-made glasses for example hydration can take place without any ion exchange in obsidians (Grambow 2006). Therefore there is a possibility that models derived specifically to look at silicate minerals might not be directly applicable to glasses. It should also be noted that studies of silicate mineral weathering cover a wider range of scales than studies of glasses moving from atomic and microscopic structures to regional and global weathering patterns, which are in turn linked to climate history (White and Brantley 1995). Nuclear waste glasses also have the potential effects of radionuclides to contend with. These appear to have a mixture of effects of glass alteration rates. Peugeot et al (2007) suggest that α radiation has no effect, whereas Jantzen et al (2008) suggest that γ radiation increases the thickness of alteration layers; and Van Iseghem et al (2001) note that γ radiation actually decreased the alteration rate in their experiments.

In a review paper from 2004 Helebrant et al argues that there is no generally accepted mathematical model for glass alteration processes as yet and that neither kinetic nor thermodynamic models fully describe the observed alteration processes and that a way forward is to combine these approaches. However, a more recent review paper by Grambow (2006) suggests that the real gap within the modelling of alteration processes is a need to couple the modelling of the glass itself and its interaction in detail with the near-field burial environment and this is echoed in the review papers of Gin et al (2008) and Frugier et al (2008). While solution pH is generally part of the rate equations the effects of other oxides within the near field appears a lesser consideration within most models so far. There also does not seem to be any straightforward way of looking at compositional variation within the attacking solution, which may have significant effects on buried glasses. However, work has begun to address this with several studies looking specifically at the relationship between the near field burial environment and glasses (Van Iseghem et al 2001; Grambow and Giffaut 2006; Bildstein et al 2007).

2.3.5 Archaeological glasses

The implications of glass alteration for archaeological glasses are largely concerned with the preservation and conservation of glass artefacts. For example, the exact nature of corrosion crusts on archaeological glasses is of great importance to conservators when selecting cleaning and stabilisation techniques for an artefact (Domenich-Carbo et al 2006). The importance of assessing the level of stability within objects

in museum collections to further inform their storage and conservation has also been highlighted (Fearn 2004, 2006; Robinet et al 2004, 2006). However, most studies on archaeological glasses are concerned with museum quality objects and medieval stained glass (for example, Carmona et al 2006; Vilarigues and da Silva 2006). Where alteration studies have been carried out there is considerable literature on the alteration of glass in marine environments (for example, Silvestri et al 2005; Dal Bianco et al 2004, 2005; Verney-Carron et al 2008) but far fewer projects looking at glasses buried in a land environment (for example, Salviulo et al 2004). There is also only a single current burial experiment project in the literature at the present time, the Ballidon project, (McLoughlin et al 2006) however, there are limitations in the usefulness of the data from this project as it is in extreme soil conditions (adjacent to a limestone quarry) and thus has a high soil pH. There has also been very little work on the earliest man-made glasses, particularly those from the Near East. A single bead from Nuzi is briefly mentioned by Vandiver (1992), noting the complexity of its alteration, and an Egyptian vase is mentioned in Vandiver (1993). This is surprising as a relative large corpus of material from this period in the Near East exists and is generally in a poorer state of preservation than contemporary Egyptian glasses.

2.3.6 Nuclear waste glasses

Borosilicate glasses have been used to immobilise nuclear waste for many years and in many countries, and it is argued that over 40 years of studies into this subject has validated this method as a means of long-term storage of nuclear waste (Grambow 2006). There is a very extensive set of literature concerned with the storage of nuclear waste in glass repositories, much of it concerned with modelling the stability of glass over long periods and experimental work using waste glass compositions to further assess durability (Wicks 1992). For example, Ferrand et al's (2006) study examining water diffusion coefficients within glass to model long-term durability in different environments. There have also been long-term experimental studies performed over many years such as Ojovan et al (2005) and comparative studies of different compositions of waste glasses (for example, Curti et al 2006).

2.3.7 Archaeological glasses as analogues for nuclear waste disposal

It is suggested that the use of archaeological glasses as analogues is valid as they often have a known environmental history (Macquet and Thomassin 1992) and although compositionally different to nuclear waste glasses the mechanisms for their alteration remains the same (Römich 2003). Archaeological glasses also provide an opportunity to look at alteration processes over a much wider timescale than laboratory or burial experiments and it well known that laboratory results can differ from those observed in the field (Grambow 2006; White and Brantley 2003). Archaeological glasses have been used extensively as analogues for modelling the durability of nuclear waste glasses (for example, Macquet and Thomassin 1992; Römich

2003; Sterpenich and Libourel 2006). Very recent work (Verney-Carron et al 2008) has highlighted that despite the compositional and burial environment differences between archaeological and nuclear waste glasses they can still be useful indicators of the long-term behaviour of glass.

2.3.8 Dating

The alteration of glasses has also been used a method of dating, primarily natural, glasses such as obsidian (Friedman et al 1997). The rate at which water enters volcanic glasses, such as obsidians, has been used as a method of dating the object. However, there are concerns that this may not be as accurate as originally thought due to the complexity of the processes involved (Morgenstein et al 1999). A recent study has used the diffusion coefficient of the hydration of high calcium glasses to date archaeological strata (Stevenson et al 2007). This technique may have potential but was carried out using a very specific glass composition and in an area where the environmental conditions within the burial environment had been closely monitored for several years. It is difficult to see how this technique could be more generally applied to other glass compositions and archaeological contexts.

2.4 Nuzi

2.4.1 The site and excavations

The mound of Yorgan Tepe, which contains the mid-2nd millennium BC Hurrian city of Nuzi, is situated 13km southwest of the town of Kirkuk in modern Iraq. It lies on a flat plain between the Kurdish mountains in the northeast and 130 km from the Tigris River to the southwest (Figure 1). It is a flat-topped mound around 200m across and rises on average five metres above the surrounding plain. The mound has been extensively eroded on its southeastern side, as this the direction of the prevailing winds, there are also several erosion channels on its surface. (Starr 1939:xxx) The name Nuzi is derived from the term "Nuzu" found on many of the 5000+ inscribed clay tablets found in the upper levels at the site and is considered to have been the name of city; Nuzi is the genitive case, the possessive form, of the name and this is the name that is generally used (Starr 1939:xxxv; Bernhardsson 2005:137). Inscribed tablets also gave the name of the previous city on the same site which was "Ga.Sur" (Pfeiffer 1931). Yorgan Tepe or Yorgan Tepe is the modern name for the mound itself.

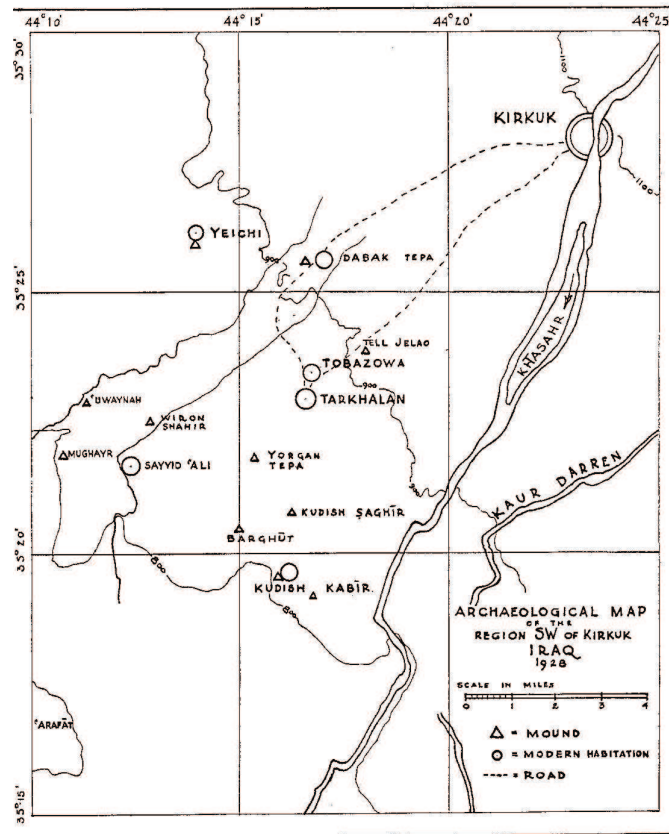


Figure 1: Site of Yorgan Tepe, location of the city of Nuzi, in Iraq (Starr, 1937: Plan 1)

2.4.2 Historical context

During the mid-second millennium BC Nuzi was a regional centre in the Hurrian kingdom of Arrapha, which was part of the Mitanni Empire, a significant power in the Near East at that time (Kuhrt 1995). The formation of the Mitanni Empire is believed to have taken place around the early to mid 16th century after destabilization of Mesopotamia and Syria by Hittite invasions and the unification of Hurrian speaking peoples in this region (Bryce 2003:35). The Mitanni are mentioned as an enemy of Egypt during the reigns of Ahmose (1550-1525 BC) and Amenhotep I (1525-1504 BC) (Redford 2003:107) and appear to have wielded significant political power in northern Mesopotamia and parts of Syria at this time, including establishing treaties with Egypt (Akkermans and Schwartz 2003:329). During the second half of the 14th century BC increasing political destabilisation in the region culminated in the overthrow and murder of the Mitanni king Tušratta (Stein 1989), which may have coincided with the destruction of Stratum II at Nuzi (Stein 1989). The Mitanni Empire largely collapsed after this and was finally annexed by the Assyrians in the 13th century BC (Akkermans and Schwartz 2003:329).

2.4.3 Excavations

The story of the excavations at Nuzi begins with the decision by Gertrude Bell, the then Director of Antiquities in Iraq, to begin looking at the history of the people or culture that had produced the inscribed clay cuneiform tablets which had occasionally been found in Kirkuk (Starr 1939: xxix). The search for the Hurrians and their civilisation was the focus of much of the archaeology carried out in northern Iraq in the late 1920s and early 1930s (Bernhardsson 2005:136). To this end Dr Edward Chiera, the Annual Professor of ASOR at that time, was commissioned to carry out a limited excavation within Kirkuk itself during 1925 and 1926. However, he decided that the city had been too densely settled to undertake excavations within it and began looking for a suitable site which did not have any modern habitation nearby (Starr 1939: xxix). Local legend had it that many tablets had been found on a small mound close to the city, which was identified as being the mound close to the larger mound of Yorgan Tepe (Starr 1939:xxix). Excavations began in 1925 finding two private houses and many inscribed tablets (Chiera and Speiser 1924-5). These excavations were the first official Iraqi excavation, although the only Iraqis who took part were labourers, as it was originally sponsored by the Iraq Museum in partnership with the American school of archaeology in Baghdad (Bernhardsson 2005:137). The 1925 campaign had a one-month permit and it had been decided between the partners that any finds would be divided between the Museum and the school, with the American school retaining the publication rights for the inscribed tablets. Dr Chiera and Gertrude Bell had also decided that the American school counted as an Iraqi institution and was therefore not subject to certain export laws (Bernhardsson 2005:137). The excavations were continued in four campaigns sponsored by several institutions including: the Fogg Art Museum and the Semitic Museum at Harvard, and the American School of Oriental Research (Bernhardsson 2005:137). During the season of 1927-28 Chiera returned as the director of the excavations during which the two houses were completely cleared and excavations on the neighbouring small mound began, revealing two more private houses (Starr 1931). Excavations on the large mound also began in this season discovering the majority of the palace complex at the centre of the city (Starr 1931). In the next season, 1928-1929, the director was Dr Robert H Pfeiffer of Harvard University, Annual Professor of ASOR for that year, during this season the rest of the palace and the residential areas to the northeast and southwest were uncovered. In addition a pit in L4 (within the palace complex) was sunk down to natural in order to look at all levels of occupation within the mound (Starr 1939:xxxiv). During the next season, 1929-1930, Richard Starr became the director of the excavations – he had been a general assistant in the years before (Starr 1939:xxxiv). The excavations from this season concentrated on the northwestern ridge, finding the temple complex and further residential areas (Starr 1931). In the final season, 1930-1931, further excavations were made in the northwestern area and also part of the city wall in the southeast region of the site was uncovered. In addition the earlier temple complexes were uncovered and the shaft in L4 was enlarged (Starr 1931; Starr 1939:xxxv), Figure

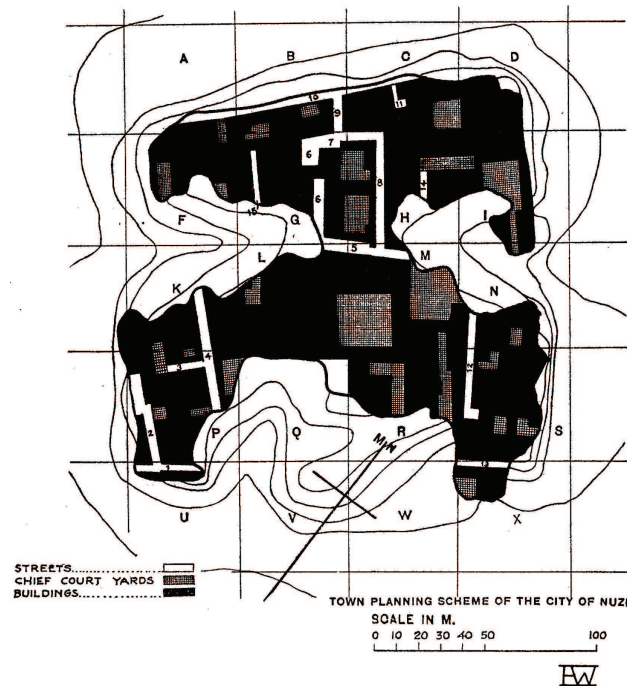


Figure 2: Map of extent of excavations of the city of Nuzi (Starr, 1937: Plan 16)

2 shows the extent of the excavations. The nearby prehistoric mound of Kudish Saghīr was also excavated during this final season (Starr 1939:xxxv).

The legislation in place governing archaeology in Iraq during this period meant that all of the objects found were to be divided between the Iraq Museum and the sponsoring institutions. The division of finds was carried out by the director of the Antiquities service, generally in the presence of the excavation director (Bernhardsson 2005:142-3). This system meant that: “The archaeologist in Iraq, therefore was caught between the desires of his sponsoring institution, his own feeling of proprietorship, and the Iraqi law, which required that a portion of the finds remain there.” (Bernhardsson 2005:141-2). The first director of Antiquities in Iraq was Gertrude Bell but after her suicide in 1926 the job was taken over by Sidney Smith (Bernhardsson 2005:145-6). Bell had been somewhat sympathetic towards the archaeologists but after her death her successors, alongside a growing awareness of the importance of archaeological and heritage matters within the Iraqi government, led to pressure to keep more finds in the country (Bernhardsson 2005:145-147); and it was in this period that the majority of the Nuzi excavations took place.

2.4.4 Stratigraphy

The stratigraphy of the site can be divided into four major periods of occupation: Prehistoric, Ga.Sur, Nuzi and Late Period. The Prehistoric period is the least well defined but would appear to be related to

| Yorgan Tepe | City of Nuzi | City wall area | Pit in L4 | Temple complex |
|------------------------|--------------|----------------|-----------|----------------|
| Late | | | | |
| Nuzi post destruction | S1 | | | |
| Nuzi destruction layer | SII | | PvI | Temple A/B |
| Nuzi | SIII | | PvIIA | Temple C |
| Nuzi | SIV | SIII | | Temple D/E |
| Ga.Sur/Nuzi transition | | SIV | PvIIB | Temple F |
| | | SV | | |
| | | SVI | | |
| | | SVII | | |
| Ga.Sur | | SVIII | PvIII-X | Temple G |
| Prehistoric | | | PvX-XII | |

Table 1: Stratigraphic groupings at the site of Yorgan Tepe, including the city of Nuzi

the lack of tablets in these early layers; Ga.Sur was considered to be the pre-Mitanni occupation of the city, with a gradual transition noted (Starr 1939:18). The Nuzi period covers the Mitanni occupation of the city when it was a small regional centre of the Mitanni empire, ending in Stratum I, not long after the destruction of Stratum II. The Late period describes all of the later occupation periods on the site, which span several hundred years (Starr 1939: xxxviii). However, periods earlier than the Nuzi levels were only excavated in limited areas of the site, with pits through to natural being excavated in the courtyard of G50, Temple complex and rooms N120 and L4 in the palace complex; only pit L4 is discussed in detail in the excavation report (Starr 1939:11). There were also limited excavations into earlier layers carried out at the main gate of the city wall (Starr 1939: 324). This is because the excavations were most concerned with the Hurrian, Mitanni, levels of the city, little was known about the Hurrian peoples at the time and so this period was considered to be the most important at this site (Starr 1939:xxix).

The stratigraphy for the site at Yorgan Tepe is highly complex and is complicated by stratigraphic layers in different parts of the site being given different names Table 1 summarises the stratigraphic sequence, extrapolated from the excavation report. In some areas the layers are termed strata which appears to have referred to a single occupation sequence across an area of the site, whereas the term pavement appears to have been used to denote individual floor levels in a limited area. The city wall area contains Stratum VIII (earliest) to Stratum III (later) with the Nuzi levels on the rest of the site being numbered from Stratum IV to Stratum I (the latest); Stratum III of the city wall area was considered to be contemporary with Stratum IV of the rest of the city (Starr 1939: 342).

The temple complex contains seven successive temples from Temple G (the earliest) to Temple A (the latest); Temple G belongs to the Ga.Sur period and F to the Ga.Sur/Nuzi transition with temples A-E belonging to the Nuzi levels; Temple A being contemporary with the destruction of Stratum II (Starr 1939:41). Within the shaft in L4 15 pavements were found, the latest being contemporary with Stratum II, numbered from XII to I (subdivisions within these making 15). Pavements XII to X (four pavements) contained objects consistent with prehistoric material from other sites in the area, including an early example

of an infant burial – common in the upper layers of the site (Starr 1939:14). Pavements IX to pavement IIB cover the Ga.Sur period of the site (seven pavements) with pavements IIB to IIA covering the transition from Ga.Sur to Nuzi, reflected in the nature of the objects found (Starr 1939:18, 29). Pavements II and I belong to the Nuzi levels with Pavement I being contemporary with Stratum II (Starr 1939:30). A number of graves were also found within the pit in L4, representing the only adult burials found in the city or surrounding area, which predate the Late cemetery.

In the city walls area the small surviving area of the wall and main gate were excavated, and were considered to be somewhat earlier than the Nuzi levels (Starr 1939:324). The successive phases of building in this area are numbered from Stratum VIII, which is considered to be when the wall and gate were originally built, and was thought to be late Ga.Sur in date, possibly contemporary with Temple G (Starr 1939:324-5). Finds from rooms nearby from Strata VII to V suggested that they were from the Ga.Sur/Nuzi transition period with Stratum IV and III being linked to the Nuzi levels in the northeastern area (Starr 1939:324).

Both the suburban residences and the nearby prehistoric mound of Kudish Saghir showed little or no evidence of material from other periods of the site, with no objects from the Late period recorded from above the suburban dwellings in the excavation report (Starr 1939:337-347). However, a number of soundings were carried out on the mounds surrounding the main tell with a number of Late period dwellings and objects being found (Ehrich 1939)

2.4.5 Chronology

The excavations showed that the site of Yorgan Tepe had been occupied, intermittently, from around 5000 BC to about 400 AD divided into four major periods of occupation, as outlined above, with an apparent hiatus in occupation between just after the destruction of the Mitanni city in the late 2nd millennium BC and reoccupation during the Parthian period in the latter part of the 1st millennium BC. The destruction of Stratum II of Nuzi was originally dated to c1500 BC by a letter bearing the seal of Saušatar within the Nuzi archives of clay tablets (Speiser 1929). However, the chronology of Stratum II, and other sites in the Near East for this period (16th to 14th century BC), has been extensively debated since the original publication of the excavation report (for example, Stein 1989; Gates 1981; Bergoffen 2005). There are very few radiocarbon dates available for Near Eastern archaeological sites from the Late Bronze Age and no dates have been run on the Nuzi material. Therefore the chronology of sites in this area is based upon textual analysis, synchronisms with other sites and archaeological evidence such as pottery.

Stein (1989) has postulated a date for the span of Stratum II, based on a reassessment of the Saušatar letter, other inscriptions, and archaeological evidence of 1450 to 1350 BC; while noting that there is a possibility that this could be raised to 1430-1330 BC. Stein (1989) concluded that the letter had been sent by a successor of this king, the use of a 'dynastic seal'. The dates are based upon correlations

between the Nuzi and Alalakh (a contemporary site in Syria) archives, synchronisms between Egyptian pharaohs and kings of the Mitanni, the scribal generations within the Nuzi archive, and other historical and archaeological evidence. Although Stein (1989) gives Stratum II a duration of 100 years it has been suggested that the scribal generations may have overlapped slightly, indicating a duration for SII of around 85 years (Friedmann 1987). The date of the destruction of Stratum II is thought to have been linked to the death of the last independent Mitanni king, Tušratta (Stein 1989). de Martino (2005) notes that Stratum II is synchronised with the Egyptian chronology by inter-dynastic marriages between various pharaohs and Near Eastern princesses including Amenophis III and IV (Akhenaten) whose reigns covered 1391 to 1334 BC. He also notes that the death of Tušratta may be indirectly mentioned in Amarna letter 43 from Suppiliuma I of Hatti to Akhenaten (de Martino 2005). This suggests that the latter part of Stratum II of Nuzi is contemporary with the Amarna period of Egypt. Although a direct relationship between the death of Tušratta and the destruction of Nuzi cannot be verified it would make historical sense that a provincial city was attacked and destroyed during the period of turmoil that the death of a king would cause. Based on the current evidence it would appear that the destruction of Stratum II of Nuzi is dated to between 1350 BC and 1330 BC.

2.4.6 Architecture

The primary building material at Nuzi was sun dried mud brick (libin) used for all walls and buildings which were laid with a mixture of clay and chopped straw for mortar (Starr 1939:42-3). Baked bricks were also used but were less common and usually used for specific areas or surfaces such as drains, pavements hearths etc (Starr 1939:43). Bitumen was used to seal brick pavements in areas where water would be a problem (Starr 1939:44). The buildings are considered to have been almost universally on a single storey with only a very few examples of a superstructure (Starr 1939:48). They are also thought to have had flat roofs made from wooden poles over which a layer of brush or reeds covered with a mixture of mud and chopped straw was placed (Starr 1939:48).

2.4.7 The Hurrian city

The greater proportion of the Stratum II city was excavated and consisted of the temple and palace complexes, three residential areas, the city wall (Figure 3) and the suburban dwellings outwith the city boundary. The final phase of the temple complex, Temple A, consists of two ranges of buildings, the northwestern temple, which is relatively well preserved and was abandoned after it was looted and destroyed at the end of Stratum II (Starr 1939:87), probably by the Assyrians (Starr 1930); and the southeastern temple which has been badly damaged by erosion (Starr 1939:87). On the basis of the fragments excavated of the cult statue and other objects found in the temple it is believed that the northwestern temple was



Figure 3: Map of Stratum II city with areas marked (after Starr 1937: Plan 13)

dedicated to Ishtar (Starr 1930). The southeastern temple, however, is believed to have been dedicated to a different god as the types of objects and ritual equipment suggest that different rites were performed here (Starr 1939:113). Starr has suggested that this temple was dedicated to Teshub, as the name is frequently found in the Nuzi tablets and Teshub was considered to be a companion to Ishtar (Starr 1939:113).

The palace of Nuzi consists of a large complex of buildings in the centre of the city area. It is considerably larger than any other group of rooms within the city (Starr 1939:123). This area had been badly affected by erosion, especially in the southeastern quarter and there were erosion channels at the northern and western corners of the complex (Starr 1939:123). It is considered to have been of great importance to the city and is thought to have been the 'Palace of the City of Nuzi' referred to in the inscribed tablets (Starr 1939:123). In addition to being much larger than other buildings in the city the palace also has larger and thicker walls, a greater use of baked brick paving and more extensive drainage, it is thought that the palace was the residence of the city governor (Starr 1939:125).

The northwestern residential area is on the rise between the palace and the northwestern edge of the mound which includes the temple and it is believed to have been a wealthier area than the other residential districts

(Starr 1939:180). The buildings of Stratum II are concentrated at either end of the ridge, the intervening buildings having been lost (Starr 1939:207). The southwestern residential area is slightly smaller than the northwestern ridge and is next to the southwestern palace wall stretching to the erosion channels at the northwest wall and the south edge of the mound (Starr 1939:267). This is interpreted as a residential area with few notable objects being found within it (Starr 1939:288). The third major residential area within the city flanks the northeastern wall of the palace (Starr 1939:296). The southeastern end has been heavily eroded (Starr 1939:296). Some of the buildings in this area appear to have had a possible administrative purpose (Starr 1939:302-3). It is also suggested that this section may have been less desirable than the other residential areas as the buildings lack the careful planning of the other sections and whilst they are larger the quality of the construction is often inferior (Starr 1939:304).

Four large houses were found on small rises to the north of the main mound (Starr 1939:333). They are known as the House of Tehip-Tilla, the House of Shirka-Tilla, the House of Shilwi-Teshub the “son of the King” (Starr 1939:337) which was second only to the palace in size (Starr 1939:337) and the House of Zigi, Figure 4 shows the plans of these two houses. The owners’ names were extrapolated from the inscribed tablets found within the houses and they were all considered to be contemporary with Stratum II and showed similar signs of burning and destruction as the city proper (Starr 1939:347).

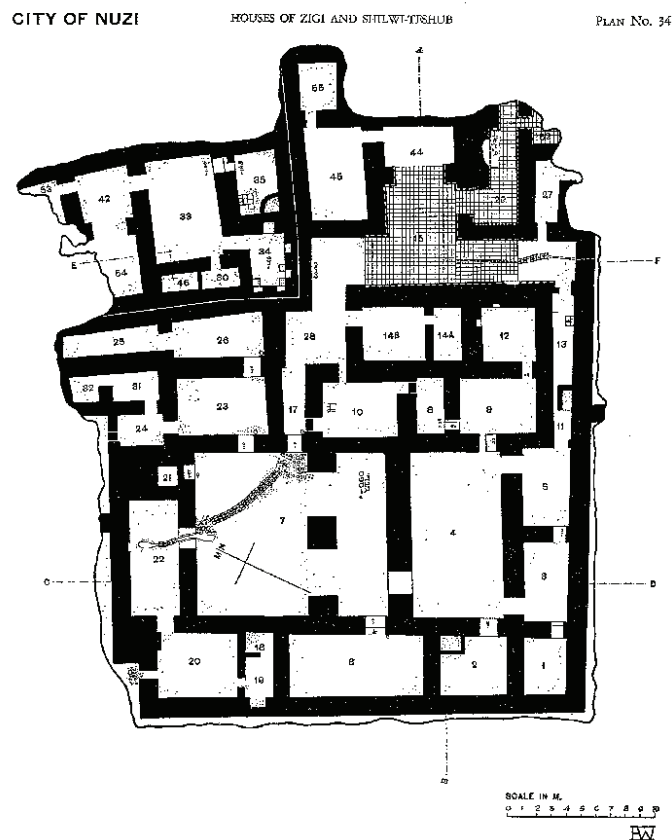


Figure 4: Plan of the suburban houses of Zigi and Shilwi-Teshub (Starr, 1937: Plan 36)

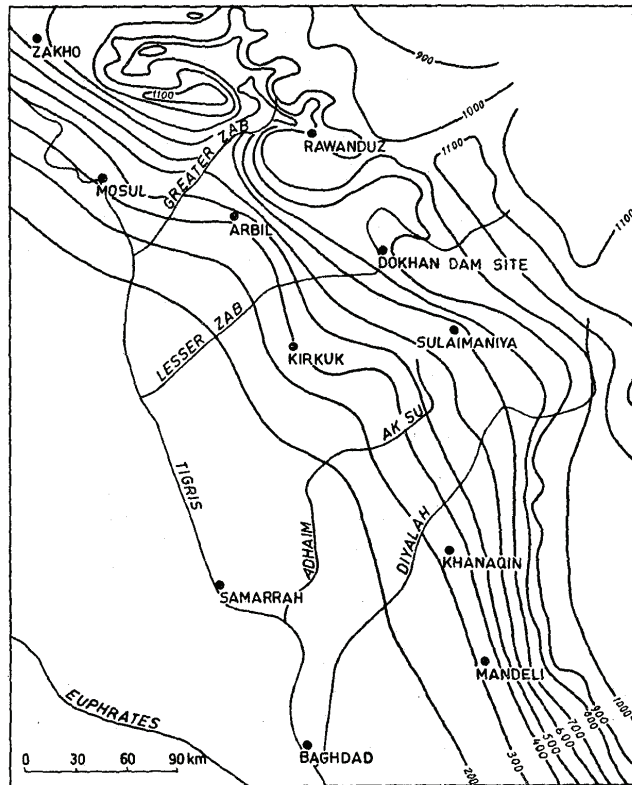


Figure 5: Rainfall map, northern Iraq (Buringh, 1960:42)

2.4.8 Environment

Nuzi sits at the 400mm isohyet of rainfall in northern Iraq, well within the boundary for non-irrigated farming, Figure 5 (Buringh 1960:42). Winters are generally wet and summers warm and dry and the prevailing rain-bearing winds are generally from the south and southwest (Buringh 1960:42,47). The climate is not thought to have changed significantly over the last 6000 years (Buringh 1960:47). The soil type in this region is a 'deep Brown Soil' from fluvial and aeolian material over limestone geology (Buringh 1960: 218; 302). However, because Nuzi is a tell site the soils are most likely to be anthropogenic and consist primarily of decomposed mud brick, organic matter and broken pottery (Buringh 1960:208). Starr notes that in many areas the fill of the rooms consists predominantly of deteriorated mud bricks fallen from the walls, in some cases so decomposed that following the lines of the walls was extremely difficult (Starr 1935)

2.4.9 Material assemblage

A very large number of objects in a variety of materials were found at the site including: ceramics, plain, painted and glazed; copper alloy metal objects; glass and other vitreous materials; and numerous other object types such as stone, bone, shell and pigments. In addition to the current project, which

has concentrated on the vitreous materials, there are also extensive studies of the metal and ceramic assemblages underway at the moment (Shortland et al 2008; Erb-satullo et al in preparation) and the organic materials and infant remains have been catalogued and initial studies carried out (Cochrane et al in preparation).

2.4.10 Vitreous materials in the excavation report

The excavation report details many of the vitreous materials found on the site. The earliest glass from the site comes from a burial (Grave 5A) found in the shaft dug down to natural in Room L4. A spherical blue glass bead, attached to a copper pin, was found as part of the grave goods within this burial which also included two small gold beads, a gold earring a marble cylinder seal and two ceramic vessels; these suggest that the individual buried there was a “personage of importance” (Starr 1939:32). On the basis of a cylinder seal found in the grave it is believed to date to the second half of the 3rd millennium BC (Moorey 1994:190). The physical depth of the burial, around 4 metres below Stratum II, (Starr 1937: Plan 5B) indicates that it is likely to date from considerably before the Nuzi levels. Glass beads were also found in Room 2 of Pavement IIA (SIV), also in the pit in L4; the purpose of this room is debateable but may have been connected to metalworking or other craft activities (Starr 1939:29). The majority of the vitreous materials from Nuzi, however, come from Stratum II with some later glass objects and glazed ceramics from the Parthian and Sassanian levels of the site.

2.4.11 Previous work on the Nuzi vitreous assemblage

Several previous studies have examined the vitreous assemblage from Nuzi. Contemporary with the excavations, analysis of the glazed objects was carried out by Gettens in 1931. This involved the microscopic analysis of thin sections and several wet chemistry methods; the study concluded that that the glazes were of a “soda and lime silicate glass which derives its colour from copper” (Gettens 1939:524), a conclusion that has been borne out by more recent studies (Paynter 2009). Barag (1970:135-141) carried out a survey of Mesopotamian glass of the Late Bronze Age, including the Nuzi material, publishing 15 vessels in detail alongside the moulded pendants, figurines and ingot fragments. This survey also covered glass vessels and other objects from Late Bronze Age contexts from several Near Eastern sites (Barag 1970). In the early 1980s a study was carried out on the beads and other glass objects by Pamela Vandiver (1983) and a small number of samples were taken for analysis by electron microprobe. This study concentrated on the manufacturing technology of the beads and other small objects alongside the analysis of several glass samples and a single glaze sample. This study concluded that the diversity, complexity, technical excellence and range of manufacturing techniques and colours seen in the glass assemblage indicated that glassmaking

and working technology were well established in this region at the time of the destruction of Stratum II (Vandiver 1983).

Several further analyses were done by Robert Brill, published in 1999, where 22 samples of vitreous material from Nuzi were analysed by electron microprobe; of these six are of the marbled faience material, one of limestone and there are two colourless fragments which may not be 2nd millennium BC in date (Brill 1999b:41-2). The Nuzi material was discussed in some detail in the reports section in the same publication (Brill 1999a:279-283). A small number of glaze samples from the glazed ceramics were analysed by Sarah Paynter and their relationship to the glasses discussed (Paynter and Tite 2001; Paynter 2009). More recently a number of the glass objects have been analysed using SEM-WDS, LA-ICPMS and isotopic analysis to look at the Nuzi glasses compared to contemporary glasses from Egypt, other areas of the Near East and the Aegean (Shortland and Eremin 2006; Shortland et al 2007; Walton et al 2009; Degryse et al 2009).

2.5 Late Bronze Age vitreous materials

2.5.1 Glass

The very first glass objects known come from the Near East and are almost universally beads or other small objects, the first examples date from the 3rd millennium BC (Peltenberg 1987; Moorey 1994:190-2; Lilyquist and Brill 1993:23-5). Glass objects increased in number, the range of colours present, and the types of object through the first half of the 2nd millennium BC with regular production of glass apparently in place by the mid 15th century BC (Moorey 1994:193-8). New colours of glass appear, including white and yellow, alongside new forms including moulded objects such as complex beads and figurines (Moorey 1994:193); polychrome beads and moulded figurines are noted from Level VII at Alalakh (Woolley 1955:269;302) and then slightly later core-formed vessels appear. The earliest known core-formed vessel fragments come from Level VI at Alalakh in Syria which may date from the early 16th century BC, however, the dating of this site has been hotly debated (Gates 1981; Stein 1989; Lilyquist 1993; Bergoffen 2005) and the glass was originally thought to have been considerably older with level VI originally dated to 1750 to 1595 BC (Woolley 1955:399). Other early vessel fragments have also been noted from Tell Brak; a single fragment embedded in a wall from Level VI may date to the mid 16th century (Oates et al 1997:81;84). Glass vessels appear to have been relatively unusual and have only been found on a limited number of sites the main ones being Alalakh (Woolley 1955:300-2), Tell Brak (Oates et al 1997:81-5), Nuzi (Starr 1939:457-9) and Tell al Rimah (Oates 1966; 1967, 1968 and 1970). Barag (1970:143-5; 147; 153) also notes glass vessels from Assur, Ur and Megiddo (in the Levant) and moulded glass axe heads are documented from Nippur (Barag 1970:148).

Glass in Egypt appears at around the same time in the Near East with some small objects, predominantly beads, dating from the late 16th century onwards (Lilyquist and Brill 1993:5; Bimson and Freestone 1998). Core-formed vessels, however, do not appear until the reign of Tuthmosis III (1479-1425 BC) and are thought to be a mixture of imported and locally produced objects (Lilyquist and Brill 1993:25-6). By the beginning of the 15th century BC significant glassmaking is occurring in Egypt based on archaeological evidence from Malkata and Amarna (Jackson et al 1998; Jackson 2005, Shortland and Eremin 2006). Glassmaking as part of an industrial complex is documented in Egypt at a slightly later date from the Ramesside factories at Qantir (Rehren and Pusch 1997; Rehren and Pusch 2005).

No archaeological evidence exists for the furnaces used to make glass in the Near East dating to the Late Bronze Age, however, some information about the possible processes and recipes used has been gained from cuneiform texts dealing with glassmaking. These texts are part of a larger collection dealing with range of subjects such as medicine and ritual practices. (Robson 2001). There are 12 tablets which appear to relate to glassmaking (Robson 2001), and which take the form of 'procedural instructions' both in terms of raw materials and the rituals needed to successfully set up a furnace (Oppenheim 1970:4-5). The texts mention reasonable raw materials and methods known in glassmaking such as fritting and melting (Shortland 2007). However, it is thought that glassmaking in this period may have been an "alchemical process", bounded by ritual and magic and controlled by the elite (Shortland 2007:272).

Various methods of forming glass objects are known from this period including the moulding, of beads, pendants and figurines, and core-forming of vessels and rod-forming of beads. Core-forming uses a pre-formed core, usually of clay and animal dung which then has molten glass wound around it to form the body; decoration in other colours of glass can then be added by the same method (Goldstein 1979:27-9). Another possible technique was to roll a preheated core in glass chips or powder and then heat so that it would fuse into the body (Stern and Schlick-Nolte 1994:31, cited in Nicholson and Henderson 2000). Moulding of small objects could be done using open moulds, the objects being ground and polished afterwards (Moorey 1994:204). Cold-working techniques related to stoneworking could be used to shape solid glass objects (Moorey 1994:5).

Glass in the Bronze Age of the Near East and Egypt, appears to have been closely associated with the elite with both vessels and raw glass being used in gift exchanges between rulers (Feldman, 2006:117; Nicholson et al 1997; Shortland et al 2001). Evidence of this trade is gained from the presence of glass ingots and ingot fragments at several sites across the Near East for example at Tell Brak and Nuzi (Oates et al 1997:85-6; Barag 1970:140-1) including an of ingots, which have similarities to crucibles found at Amarna in the Ulu Burun shipwreck (Nicholson et al 1997). This is dated to 1316 BC by dendrochronology on timber from the ship and by the presence of a bead bearing the head of Nefertiti (Nicholson et al 1997), suggesting that it is contemporary with the Amarna period in Egypt which is also contemporary with the

later part of Stratum II at Nuzi.

2.5.2 Faience and frit

Faience consists of a quartz core with an alkali glaze, often containing metal colorants (Moorey 1994: 167). In contrast to glass faience objects were first noted from Egypt and the Near East from the 5th millennium BC onwards (Moorey 1994:17). Frits are related to both faience and glass being deliberately sintered materials made from similar raw materials to faience, but lacking a separate glaze layer (Moorey 1994:167). The best known of these is Egyptian blue which was used both to make objects, such as beads and vessels and as a pigment (Hatton et al 2008).

2.5.3 Glazed ceramics

Glazed ceramics appear in the archaeological record at the same time as glass vessels. The first recorded examples are from Alalakh Level VI (Woolley 1955:299). Paynter (2009) has suggested that the glaze used on the Nuzi glazed ceramics may have been powdered glass as it is compositionally similar to the blue glasses from Nuzi. It is thought that glazed ceramics and glass production arose at around the same time due to the difficulties of working with glazed ceramics - the glaze and ceramic bodies having different thermal expansion coefficients and a knowledge of glass behaviour and properties would be required to successfully create these objects (Moorey 1994:195).

2.6 Summary

The alteration of glasses has been studied in detail for a number of decades, particularly with reference to the preservation and conservation of archaeological materials and in terms of the use of glass to vitrify nuclear waste for long-term disposal. Despite this, however, questions remain about the mechanisms which cause glass alteration and relatively little work has been done on the earliest man-made glasses, which have been in their burial environment for over 3000 years.

The vitreous assemblage from Nuzi is one of the largest and most important from this period in the Near East. It dates from an early period of glass vessel manufacture and consists of an unusually large numbers of objects, particularly beads. As Nuzi was not extensively reoccupied after the destruction of Stratum II, a much clearer picture of the quantity and distribution of objects across the site emerges. In contrast to sites with continuous occupation where older material could be removed and discarded - making it more difficult to assess the quantity and distribution of any class of objects during a particular period of occupation. The glass assemblage from Nuzi provides a unique opportunity to examine the deterioration, technology and context of glass vessels, beads and other objects at an early point in the history of glass.

3 Methodology

3.1 Introduction

A number of analytical techniques and experimental methods have been used to analyse the glass and vitreous material samples from Nuzi. The sampling methodology, analytical techniques used, sample preparation for analysis, and methods for the different experiments, from replicating antimony-opacified LBA glasses to the dissolution of replica and archaeological glasses, are detailed within this chapter. The specifications and set-up of the equipment used for the analyses is also contained within this chapter.

3.2 Sampling

The glass and other vitreous materials excavated from the site of Nuzi consist of a considerable number (many thousands) of beads, numerous vessel fragments and hundreds of other objects. Therefore a means of selecting which samples would be the most appropriate for the research questions of the current project was required. The variables that could have affected the alteration of the glass were considered, such as: location on the site, composition, the form of the object, age, local conditions, depth of burial, and their treatment prior to burial. A list of 'ideal' samples, based on these factors, was drawn up, using information from the excavation report and this formed the basis of the sampling strategy prior to examining the collection held at the Semitic Museum at Harvard University; Table 2 shows this in detail. The entire vitreous material assemblage held at the Semitic Museum was examined and recorded to assess where samples could be taken, Table a in Appendix 1 details this survey.

| Sample | Location | Factor | Factor |
|-------------------------------|--|--|-------------------------------|
| Beads (blue) | Temple A (G51, G29, G56, H20), temple courtyard (G50, H14), NE residential area (S110, S111), NW residential area (F2, F25, F37), suburban area (House of Shilwi Teshub) | Intrasite variability of preservation | Differences in form/technique |
| Glass vessel fragments | Temple A (H5, H10), NW residential area (A4, A5, F27, F29, F35), Palace (L8, M79, M100), NE residential area (S157), suburban area (House of Shilwi Teshub) | Intrasite variability of preservation | |
| Moulded objects | Temple A, NE residential area | Intrasite variability of preservation | |
| Beads (other colours) | Temple A | Differences in preservation between colours of glass | Differences in composition |
| SIII beads | Temple B/C (G50) | Chronological differences | |
| Beads not identified as glass | NW residential area (F2, F14, F19, H13), SW residential area (N383, P467, P340, P348) | Identification of material | |
| Glazed ceramics | Temple A (G29, G50) | Relationship to the glass | Comparison of alteration |

Table 2: List of 'ideal' samples prepared prior to museum visit

3.2.1 Glass

The ideal list of samples created prior to visiting the museum had indicated that in order to look at variation in the preservation of 2nd millennium BC glasses from different locations on the site and of different object types it would be necessary to concentrate on one colour of glass. It was decided to sample translucent blue glasses as widely as possible as these were reported to be the most abundant in the assemblage (Starr 1939: 446). Within these samples a range of object types was sought including beads, vessels and pendants to look at variation in preservation between object types. In addition examples of all of the colours of glass found were taken for comparison to see if there was any variation between them. As variation between locations on the site had been highlighted as an important aspect of this project it was attempted to sample from as many locations as possible. However, many objects in the assemblage had lost their field numbers or did not have a room number on their label; therefore, they could not be assigned to a particular location in Stratum II. Thus the sampling strategy concentrated, as far as possible, on examples where the original location of the find was known. Limitations were present in that many of the glass objects have completely devitrified and so their original colour could not be determined, indeed it was not always possible to determine the material used to manufacture an object. Where the original colour of an object could not be determined due to complete devitrification the objects were sampled on the basis of their location and their the degree of preservation to get as much of the range as possible.

In several cases it was not possible to take samples from some objects as it would have been detrimental to their appearance; for example, a pale blue glass mace head and a decorated polychrome mace head, both of which are display quality; the pale blue one is currently on display. However, due to the large number of beads and the fragmentary nature of the decorated vessels it was possible to take an extensive set of samples of almost all of the vessels and every style/colour of bead and pendant, although the only decorated complete pendant could not be sampled. The figurines could also not be sampled as they have completely devitrified and are extremely fragile. A number of samples were also taken from glasses that were considered to be from the late period of the site; these were identified by usually being of colourless glass with forms and decorative techniques, such as faceted decoration, not seen in the earlier glasses. The majority of these are in a much better state of preservation than the 2nd millennium BC glasses. A few strongly coloured beads which were of uncertain date were also sampled including yellow, red and green.

3.2.2 Frit and faience

A number of samples from objects which did not appear to be made of glass were taken, both to identify the material where this was not clear and to look at their composition and technology. Several samples of marbled faience were taken. It was not possible to sample the blue glassy areas on the largest fragment as it is currently on display. However, a new fragment with glassy areas was found during the sampling process (sample N25). A number of samples were taken from other objects believed to be manufactured from frit and faience, including several beads and vessel fragments.

3.2.3 Glazed ceramics

In order to compare the glaze component of the glazed ceramics to the glasses a number of samples were taken. The samples from the glazed ceramics in the assemblage from Nuzi were grouped into wall nails, figurines and other objects, and glazed ceramic vessels. There are considerable numbers of these glazed ceramics within the assemblage and it was attempted to get a representative sample across all classes of objects, although samples of unaltered glaze were very difficult to find.

3.2.4 Cylinder seals

Many cylinder seals, usually intricately inscribed, were found at Nuzi; 36 were noted in the current assemblage. Most of these are intact and due to their importance it was not possible to take samples for destructive testing. However, a single seal had been broken in the past, 1930.80.13, and we were allowed to take a small sample from the broken edge. The material used to make many of the cylinder seals was unclear and it was thought that it could be faience or a related material.

| Sample type | Number | Location known | No. of locations |
|--------------|--------|----------------|------------------|
| Beads | 127 | 79% | 21 |
| Vessels | 34 | 85% | 10 |
| Pendants | 4 | 100% | 3 |
| Other | 9 | 78% | 4 |
| Late glasses | 27 | 4% | 1 |
| Frit/faience | 8 | 50% | 3 |
| Ceramic | 43 | 47% | 6 |
| Total | 252 | 65% | 48 |

Table 3: Samples taken from the Semitic Museum at Harvard University for analysis

3.2.5 Sampling method

A small sample was removed from each object selected. This was done by taking a small fragment, usually from the edge, using box-ended snips. In most cases it was attempted to remove a complete or partial cross-section so that the preservation of an object could be studied in detail such as in 1930.62.82c. This was extremely challenging with some samples, particularly where both glass and weathering layers were present. The weathering layers being much softer and more fragile than the glass, in some cases these flaked off and were lost during the sampling process, as can be seen in sample 1930.82.73c, Figure 6.

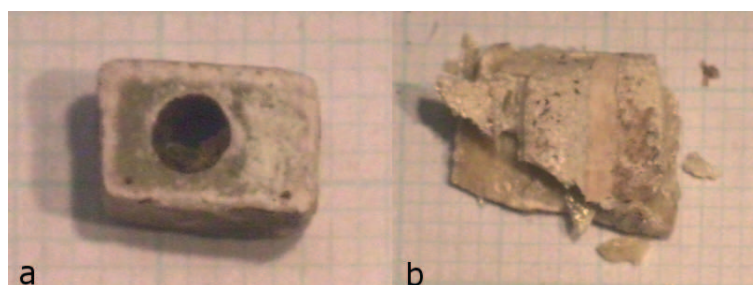


Figure 6: a. sample with complete cross section (1930.62.82c); b. unstable sample (1930.82.73c)

3.2.6 Samples

Table 3 lists a summary of the samples taken from the Semitic Museum, broken down into beads, vessel fragments (2nd millennium BC and Late period), other glass objects, glazed ceramics, faience, and other vitreous materials; the detailed table with a description of each sample is in Table b in Appendix 1. The samples were selected and removed during two visits to the Semitic Museum in 2007 and 2008. With the exception of the Late period glasses finds locations are known for most of the objects sampled. For some classes of object this information was harder to find, such as the glazed ceramics; samples were taken despite this where the objects could still provide useful information, were rarer, or were highly representative of their type, colour or state of preservation.

3.3 Analytical techniques

3.3.1 Scanning electron microscopy (SEM)

Scanning electron microscopy is the creation of an image by directing a beam of electrons at a specimen, rather than light as in optical microscopy. These electrons interact with the specimen in various ways, creating the image. The main differences between the creation of an image by light and by electrons is that electrons have much smaller wavelengths than light and are more easily scattered by gases, resulting in the requirement of a vacuum (Goodhew et al 2001:17). The possible spatial resolution is also much higher than with light microscopy with 10nm being possible in secondary electron mode and 100nm in backscattered electron mode (Reed 2005:2). Another important difference is that the interaction of the electron beam with the specimen in an electron microscope can also give compositional information about the specimen in addition to an image (Egerton 2005:137).

SEM generally uses a thermionic emission gun to create an electron beam by heating a filament, usually tungsten, which then emits light and electrons. An electron beam is created by accelerating these electrons across an electrical potential difference of tens or hundreds of kilovolts (Goodhew 2001:24). The brightness of the beam is constrained by the material used as the filament and can be increased by using a lanthanum/boron filament (Goodhew et al 2001:26). An alternative method of creating the electron beam, which creates an even brighter beam, is by using a field emission gun (Goodhew et al 2001:27). A field emission gun consists of an emitter, usually tungsten, which has a very sharp point, a strong electric current is then applied to the tip of the emitter by an anode, the electrons are then accelerated down the column by a second anode which is at a much higher potential (Goodhew et al 2001:26-7).

Once the electron beam has been generated it has to be focused. In SEM this is done by a series of electromagnetic lenses which consist of an axial magnetic field that has rotational symmetry (Reimer 1998:20). This makes the electrons move in a helical pattern down the column which, with an ever-decreasing radius of the spiral, forces the beam into a point, just as a lens focuses light in an optical microscope (Goodhew et al 2001:28). There are usually several lenses with the final beam forming lens usually being small and asymmetric to reduce the magnetic field on the specimen surface (Reimer 1998:22). There are several possible lens aberrations that can affect the electron beam, and thus the functioning of the SEM. The most important of these are spherical aberration where an enlargement of the beam diameter at the focal point is caused by the lens focusing the outer part of the beam more strongly than the inner (Reed 2005:26) and astigmatism which is caused by magnetic inhomogeneities in any part of the lens creating asymmetry in the focused beam (Reimer 1998:25).

The incident beam then interacts with the specimen in several ways – the primary electrons enter the specimen and it is the scattering of these, or different, electrons leaving the specimen that create the

image. The scattering of electrons can either be elastic, where the electron changes direction but does not lose significant energy and inelastic where the electron loses significant energy (Goodhew et al 2001:30-1). Elastic scattering is an important mechanism for the deflection of electrons and can also be used to get diffraction information from the specimen (Goodhew et al 2001:30). The energy loss caused by inelastic scattering can be caused by several types of interaction between electrons and the specimen which can result in the generation of heat within the specimen or the production of light, X-rays and secondary electrons (Reed 2005:19).

Secondary electrons (SE) escape from the near-surface of the specimen and have low energies, they are most likely to be electrons that have had energy transferred to them by the primary electron beam, the yield compared to this beam is around 1 so they are very abundant (Goodhew et al 2001:34; Reimer 1998:6). They may also be generated by the escape of back-scattered electrons from deeper within the specimen (Reimer 1998:6). Secondary electrons are detected by an Everhart-Thornley detector which is a scintillator/photomultiplier system. The secondary electrons, which have been accelerated by a bias voltage, hit the scintillator which emits light; the light is transmitted to the photomultiplier which converts the photons into pulses of electrons. These pulses modulate the intensity of the CRT creating the image (Goodhew et al 2001:122). The yield of secondary electrons is dependent on the angle of the specimen surface; edges have increased collection with contrast from incomplete collection areas on the surface, thus creating an image of the surface topography (Reimer 1998:7). SE output is dependant on variations in the electrostatic field on the specimen surface and this creates a voltage contrast with negatively biased areas appearing bright and positively biased areas dark (Reimer 1998:7).

Backscattered electrons (BSE) are electrons from the primary beam which are ejected from the specimen surface before losing all of their energy, BSE are less numerous than secondary electrons but carry higher energies (Goodhew et al 2001:34-5). Detection of BSE is either by a scintillator type detector measuring light intensity (Reimer 1998:180) or by a solid-state detector based on the creation of electron hole pairs by the impact of high energy electrons onto a semiconductor (Goodhew et al 2001:130). The means of contrast in BSE imaging is the dependence on atomic number (Z) of the BSE coefficient (Reed 2005:9) which varies according to the composition of the specimen (Egerton 2005:137).

Other forms of interaction include cathodoluminescence, Auger electrons and the production of X-rays, which are all caused by an electron being knocked out of an atom by the incident beam, the empty electron is then filled causing the atom to relax and emit any excess energy as photons (cathodoluminescence), Auger electrons and X-rays (Goodhew et al 2001:35). Cathodoluminescence and Auger electrons are not being used within the current project so will not be dealt with further. The emission of X-rays will be discussed in more detail in the compositional analysis sections of this chapter.

An SEM image, either of secondary or backscattered electrons, is produced by magnetic fields scanning the

electron beam across the specimen (Goodhew et al 2001:29) in a raster while simultaneously displaying the output from the electron detector on a synchronously scanned VDU (Reed 2005: 29). In a digital system the computer-controlled primary beam dwells on each point on the specimen (pixel) for a set time and the image is created by recording the intensity of that pixel, as a number, into a framestore which is then displayed on-screen (Goodhew et al 2001: 162; Reed 2005: 29-30). This has some advantages over analogue systems as the digital image, consisting of the 'address' of each pixel and its intensity, can be stored (Egerton 2005:128).

This technique was selected as it is capable of producing high resolution images which could be used to characterise the altered glasses being studied. It also allows areas of particular interest to be selected for further analysis. In BSE mode it allows the homogeneity of the glass to be checked, which could cause problems with bulk analyses. In SE mode the topography of the samples, particularly the altered glasses could be assessed to make sure that they were relatively smooth; uneven surfaces can cause problems for quantitative analysis by SEM-WDS due to the exact geometry required between the specimen and detection system.

While some compositional information about a specimen can be gained from the BSE image it is the ability of the electron beam to excite X-ray emission from the specimen that allows detailed qualitative and quantitative compositional information to be sought. Interaction between the primary incident beam and the specimen may cause electrons to be knocked out of atoms within the specimen if a single electron then moves into the inner shell vacancy created an X-ray is emitted (Goodhew et al 2001:35). The energy of the X-ray is dependent on the energy difference between the two excited states and is characteristic of the element present (Goodhew et al 2001:35). X-rays that are not characteristic of an element may also be emitted where the primary electron excites an X-ray but does not knock out an inner shell electron; this gives a background of X-rays in any electron-generated analysis, it is also known as the Bremsstrahlung (Goldstein et al 2003:271). In order to carry out compositional analysis it is important to understand which of the characteristic X-ray lines of an element is the strongest, and therefore the one that will be used for analysis (Goodhew et al 2001:170). The $K\alpha$ line doublet ($K\alpha_1$ $K\alpha_2$) is the most intense, around 7-8 times the next line doublet $K\beta_1$ $K\beta_2$, and is the most commonly used for compositional analysis (Goodhew et al 2001:170). However, the energy required to knock out a K-shell electron increases with atomic number and it is not always possible to excite a K-line, for example elements above $Z=50$ require energy above 25keV to knock out K-shell electrons and are inefficient until around 75 keV (Goodhew et al 2001:171). Therefore L lines, and in some cases M lines, which require less energy to excite X-rays are used for heavier elements, again there are more intense lines within these that can be selected for analysis (Goodhew et al 2001:171). All elements have at least one characteristic X-ray line which can be excited at energies below 10keV meaning that they can all be analysed within an SEM (Goodhew et al 2001:171). There are two

main types of technique used in counting the X-rays emitted by the interaction of the electron beam with a specimen, energy dispersive spectrometry (EDS) and wavelength dispersive spectrometry (WDS) each has their own advantages and disadvantages and are discussed in more detail below.

3.3.2 Scanning electron microscopy-Energy Dispersive Spectrometry (SEM-EDS)

An EDS detector typically consists of a silicon or germanium semiconductor which is positioned within the SEM so that the largest fraction of the X-rays emitted can fall onto it (Goodhew et al 2001:175). The emitted X-rays excite a number of electrons into the conduction band of the semiconductor resulting in an identical quantity of positively charged holes in the electrons' outer shells. The number of hole pairs produced is relative to the energy of the X-ray being detected, for example, $AlK\alpha$ produces 391 hole pairs (Reed 2005:79). However, the resistivity of pure silicon is too low i.e. the current generated is too small to be detected compared to the normal current flow when voltage is applied so its resistivity is increased by doping the silicon with lithium or by cooling the detector with liquid nitrogen to 77K (Goodhew et al 2001:176; Reed 2005:79). This reduces the normal current allowing the current generated by an X-ray entering the detector to be easily detected (Reed 2005:79). The detector is protected by a thin window, typically of beryllium, which absorbs a proportion of low-energy X-rays (generally those less than 1KeV); this makes detection of light elements more difficult and it is impossible to detect elements lighter than sodium unless a specialist ultra-thin polymer or windowless detector is used (Reed 2005:79). The current created by an X-ray hitting the detector is usually described as a pulse; these pulses are collected into a histogram of all the X-rays entering the detector by a multi-channel analyser (MCA) on a computer, the MCA selects which channel a pulse will be stored into, and is displayed on screen with the relative counts of each X-ray energy in each channel (Goodhew et al 2001:177-8). An important aspect of this type of analysis is the pulse processing speed, as the X-ray count rate increases the number of counts that are rejected by the MCA also increases, therefore the count rate from a specimen includes both the live time, when the detector was counting and dead time when the pulses were ignored (Goodhew et al 2001:178). The data are then shown as a histogram based on intensity by voltage, these then pass to a computer for processing into peak identification or quantification (Goldstein et al 2003:299)

EDS detectors are very efficient and allow quick analysis of all the elements present within a specimen (with the exception of the light elements mentioned above). However, as the X-rays lines are detected as peaks rather than sharp lines the resolution of the detector is relatively poor and it can be difficult to separate closely spaced lines (Goodhew et al 2001:180) such as lead and molybdenum. The system also produces a fairly high level of background electronic noise which reduces the peak to background ratio, this can be significant in quantifying the analysis and can decrease possible detection limits as a peak can only be detected if it is possible to distinguish it from the background (Goodhew et al 2001:180, 200). Two

further problems with EDS analysis are the potential presence of false peaks, the most important of which are the sum peak and silicon escape peak. Sum peaks are produced when identical photons impact the detector simultaneously causing twice as many hole pairs to be produced, the detector interprets this as being caused by a single high energy photon and produces a sum peak with twice the energy (Goodhew et al 2001: 180). Silicon escape peaks result from the ionisation of a silicon atom within the detector crystal the initial photon loses the equivalent energy of the SiK α line and a peak at this energy below the main peak is produced (Goldstein et al 2003:318).

X-ray microanalysis using an energy dispersive spectrometer allows the elements present within a sample to be assessed relatively quickly, both in the bulk glass and in any alteration layers. This provides information about which elements are present for further analyses and also allowed any areas of interest such as mineral phases and opacifying crystals within the glass to be quickly characterised. SEM-EDS was also selected as in the piece of equipment used, a JEOL 5900 LV with an Oxford Inca EDS X-ray analysis system, can produce both line analyses, where the composition across a predetermined line is analysed, and digital maps of the composition of the sample. It is also possible to produce montages of larger areas of samples both as images and digital maps. This was felt to be extremely useful in looking at possible contrasts in composition between the glass and alteration layers.

In the SEM-EDS system used in this project quantification is carried out by initially subtracting the background below the peaks using a channel-by-channel top-hat digital filter. The measured area of each peak reflects the concentration of each element which is then compared to the concentrations in known standards. The standards are acquired prior to analysis and are stored within the software. Regular calibrations analysing the known standards have to be carried out. Detection limits for EDS are typically 0.1% for most elements (Kuisma-Kursala 2000). Although quantification is possible using this system it was decided to use a different technique for quantitative analysis of the glasses.

Analytical parameters: For both the SEM imaging and SEM-EDS analysis a JEOL 5900 LV with Oxford Inca EDS X-ray analysis and a solid-state backscattered electron detector was used. An accelerating voltage of 20 KeV was used as this would excite enough X-rays for analysis, with a spot size of 20 μ m for the analytical spectra.

3.3.3 Scanning electron microscopy-Wavelength Dispersive Spectrometry (SEM-WDS)

In contrast to EDS detectors which detect all of the elements present within a specimen simultaneously WDS detectors analyse a single element at a time. The X-rays being emitted by the specimen are filtered so that only a chosen wavelength falls onto the detector. A crystal spectrometer which separates the wavelengths of the emitted X-rays by diffraction is used as the filter. This works by the X-rays being

emitted from the specimen at a specific angle (φ), falling onto a crystal of known lattice spacing (d) assuming that the angle between the X-rays and the crystal lattice planes is theta (θ), then the only X-rays that will be diffracted from the crystal and thus reach the detector will be those obeying Bragg's Law. The wavelength of the transmitted X-rays is therefore given by:

$$\lambda = \frac{2d \sin \theta}{n} \text{ (Equation 4)}$$

The X-ray wavelength (λ) of the desired element is substituted into this equation and the value of θ can be calculated for that crystal (Goodhew et al 2001:181). Therefore with the spectrometer at the required angle only a single wavelength of X-rays will reach and be counted by the detector. The X-rays must be collimated by the means of slits prior to reaching the spectrometer and need to be focused so that all of the X-rays reach the detector (Goodhew et al 2001:181). The X-rays are focused by the specimen, spectrometer and detector all lying on a circle of known radius (Rowland circle), the spectrometer crystal also has to be curved (Goodhew et al 2001:181). This means that θ can only be altered for a small range of angles thus several crystals with different lattice spacings are required to cover all the elements (Goodhew et al 2001:182). The need for precise geometry and accuracy of movement of the components means that WDS systems are expensive to manufacture (Goodhew et al 2001:181-2). Multi-element analysis can also be time-consuming as each element is analysed separately (Goodhew et al 2001:183). In addition, due to the rotational geometry required for quantitative analysis in the SEM-WDS the sample must be completely flat if the sample is even slightly off the Rowland circle the number of X-rays reaching the spectrometer and detector is severely reduced (Reed 2005:31). However, the WDS system has several advantages over the faster and cheaper EDS systems for microanalysis. It has greater resolution between closely spaced lines, overlapping lines are rare; it can detect lighter elements more easily, with appropriate crystals; the peak to background ratio is considerably higher, thus improving detection limits and precision compared to EDS, particularly in quantitative analysis (Kuisma-Kursala 2000).

Quantification of the SEM-WDS involves a number of stages; well characterised standards of known composition are run to calibrate the instrument before each analysis session. These standards need to be not only compositionally similar to the elements sought in the sample material but also of a similar nature, particularly in terms of density and mean atomic weight (Goldstein et al 2003:394). The crystal and detector are rotated on the Rowland circle to the peak position of a selected emission line; this is precisely determined by the calibration run on the standards. The number of counts detected on that peak is recorded for a fixed time interval with background measurements being taken close to the peak, the background is then subtracted from the centroid of the peak (Goldstein et al 2003:400). The detection limits for this technique are quoted in the literature as being as good as 0.01% (Kuisma-Kursala 2000). However, with the instrument used in this project the detection limits are calculated for each element sought during every point analysed. Using this instrument under the analytical parameters set for these

analyses detection limits are typically between 70 and 1000ppm (elemental concentration); 0.01 to 0.12 oxide weight percentage. Table a in Appendix 1 shows a typical set of detection limit data for a run of over 100 analytical points. Elements such as sodium and chromium have very low detection limits, usually around 100ppm whereas heavier elements such as zinc and lead have much higher detection limits, in the case of zinc this is usually above 1000ppm.

This technique was selected to carry out bulk compositional analysis of the glass and to analyse specific points within the alteration layers. This technique has been extensively used to characterise the composition of many types of ancient glass (for example, Janssens et al, 1996; Silvestri et al, 2005; Shortland and Eremin, 2006). Therefore direct comparisons with previous analyses of similar glasses and different types of ancient glasses are possible. SEM-WDS was selected for quantitative analysis over SEM-EDS due to the better detection limits for many elements, and more accurate quantification. The time-consuming nature of the analyses was outweighed by the potential quality of compositional information that could be gained.

Analytical parameters: The machine used for SEM-WDS analysis was a Cameca SX100 based at the Natural History Museum in London. The elements selected for analysis by SEM-WDS in these glasses, vitreous materials and weathering crusts are: list Si, Al, Ca, Mg, Na, K, Fe, Ti, Co, Cu, Mn, Ni, Zn, Sn, Sb, Ba, Pb, Cr, P, S, Cl, Sr. The elements were selected to cover all of the major and minor oxides expected in a glass from this period and also to allow the results to be directly compared with previous work on the site (Shortland and Eremin 2006). These elements are assigned to the five spectrometers in order to cover all of the elements sought, as each crystal can only cover a limited range of X-ray wavelengths (Goldstein et al 2003:328). The machine was run with an accelerating voltage of 20keV in order to cover all of the elements sought and a spot size of 20µm was used. The smallest possible spot size was required in order to look at small features and changes in composition across the samples and it was found that this spot did not result in volatilization of the lighter elements such as sodium. The lighter elements were analysed first and for shorter counting times to also reduce the possibility of volatilisation. For bulk analysis, three points were taken for each sample and then averaged to give the result. The standards used and their compositions are contained in Appendix 1.

3.3.4 Problems with Quantitative analysis

Quantitative analysis is however, highly complex and can be affected by numerous factors. The volume of X-rays being analysed depends on where in the sample they were generated, how much has been absorbed by the specimen on exit, the energy of the electron beam, the mean atomic weight of the sample, the wavelengths of the X-rays and their incident angle at the surface (Goodhew et al 2001:199). All of these factors can affect the compositional analysis from a specimen and it may be necessary to apply

correction factors these are usually performed by a computer using iterative calculations to correct for atomic number (Z), absorption (A) and fluorescence (F), often known as ZAF corrections (Goodhew et al 2001:201) or matrix corrections (Goldstein et al 2003:402). Atomic number corrections are concerned with the productivity of X-ray generation within an element, which varies between elements (Goldstein et al 2003:406); if the standard differs significantly in mean atomic number from the specimen then the count rates for each element may be different (Goodhew et al 2001:202). The absorption of electrons without any X-rays being generated depends primarily on the mass absorption coefficient of the elements present within a specimen and this is unlikely to be replicated within the standard so again differences may arise (Goodhew et al 2001:202). Fluorescence is caused when X-rays produced by the incident beam travelling through a specimen excite atoms which then produce further characteristic X-rays, although of somewhat lower energy (Goodhew et al 2001:171). However, although this is an inefficient process as only a few of the higher energy X-rays will excite the lower energy lines, it can affect the relative quantities of compositional X-ray lines emitted from some materials (Goodhew et al 2001:171).

3.3.5 ICPS

Inductively Coupled Plasma Spectroscopy (ICPS) Plasma Spectroscopy covers a range of techniques generally used for the analysis of trace elements. All of the techniques initially require the creation of the sample into a plasma. Dean (2005:55) defines a plasma as “the coexistence, in a confined space, of the positive ions, electrons and neutral species of an inert gas”. Inductively coupled plasma is produced by a plasma torch consisting of three concentric glass tubes (Dean 2005:58). The plasma is created by inducing an oscillating magnetic field between the inside, containing the carrier gas, and outside of the torch, where there is a copper induction coil (Dean 2005:58). A spark is added, while the carrier gas flow is briefly switched off, this spark causes the carrier gas to ionise creating the plasma (Dean 2005:58). The sample is introduced through the innermost tube usually via a nebuliser and then a spray chamber, as an aerosol consisting of sample solution and carrier gas (Dean, 2005:40). The emission from the plasma can then be measured by several methods.

Inductively Coupled Plasma-Atomic Emission Spectroscopy (ICP-AES): Atomic emission spectroscopy uses the emission generated by energy changes within an atom to find out what elements are present, and in what concentration, within the sample (Dean 2005:66). Emission is defined as the return of an atom from a high-energy (excited) to a lower-energy state (ground state) (Dean 2005:67). If thermal energy is applied to an atom it absorbs radiation and electronic transitions from lower to higher states can occur within the electron orbital shells (Dean 2005:67). Both absorption and emission occur at specific wavelengths or frequencies of electromagnetic radiation creating emission lines that are characteristic both of the element and the transition (Dean 2005:67-9). The intensity of these spectral lines is dependent

on the relative amounts of atoms in the ground and excited state within the sample (Dean 2005:69-70). The spectral lines emitted are then separated by the spectrometer into their component wavelengths via a diffraction grating, which consists of a mirror with a series of grooves etched into it, the light hitting the grating is diffracted depending on the distance between grating lines and the groove angle, from this it is possible to work out the wavelength (Dean 2005:76). However, more commonly a blazed diffraction grating is used i.e. one where the grooves are ruled at a specific angle – this reduces interference images from overlapping wavelengths (Dean 2005:76). Some spectrometers only detect a single wavelength at a time but the majority can undertake simultaneous multi-element analysis. Either a polychromator, such as the Paschen-Runge mounting, where the diffraction grating, multiple exit slits and source entrance are mounted around a Rowland circle; and the Echelle spectrometer which uses a grating with a smaller number of lines and spectral order to separate the wavelengths, may be used (Dean 2005:78). The wavelengths are then detected either by a photomultiplier tube or more commonly using a multi channel detector based on charge transfer technology (Dean 2005:82). Charge transfer devices consist of a series of diodes on semiconductor wafers that store charge when exposed to light; the amount of charge accumulated is proportional to the light detected, this can then be read (Dean 2005:84) and allows the elements present and their concentration to be ascertained, quantitative analysis is achieved by comparison of the analysis with calibration solutions made from high purity reagents (Dean 2005:8-9). Potential problems with this technique come from interferences between emission lines. These may be caused by fully, or partially overlapping, lines or by an elevated background; increasing the resolution of the spectrometer or choosing an alternative characteristic line are possible solutions (Dean 2005:85). Interference may also be caused by the inclusion of ionisable elements in the plasma source or by problems in the nebulisation of the sample (Dean 2005:85).

Within the current project a technique that could determine the levels of small quantities of elements, such as silica, within the solutions from experimental weathering dissolution experiments was required. This technique was also selected as being able to analyse samples quickly and with no further sample preparation, unless further dilution was required. ICP-AES has been previously used in determining elemental release in glass dissolution experiments (Chave et al 2007).

Analytical parameters: The equipment used for the analysis of the solutions was an axially-viewed Varian-Vista-Pro ICP-AES with a charge-coupled device (CCD) detector and an SP5-S autoloader based at the Natural History Museum, London. The software used was ICP Expert 4.1.0 and the calibration solutions described in section 3.4.3 were used to calculate the detection limits which ranged from 0.001 ppm for magnesium to 0.15 ppm for potassium (Table 26, Section 7.1).

Laser Ablation-Inductively Coupled Plasma Mass Spectroscopy (LA-ICPMS): Laser ablation permits the analysis of solid samples with minimal destruction. A small area of the sample is ablated using a laser, most commonly Nd:YAG, which may be operated at several wavelengths depending on the gas being used (Dean 2005:49). The laser is focused onto the sample within the ablating chamber through a fused silica window, typically a crater of between 10 and 100 μm is created and the vaporised sample is carried from the chamber to the plasma torch via the carrier gas (Dean 2005:49-50). The inductively-coupled created plasma is then analysed via a mass-spectrometer. The mass spectrometer separates the ions within the sample based on their mass/charge ratio; transmitting ions with a pre-selected mass/charge ratio to be detected and displayed (Dean 2005:96). There are several types of mass spectrometer including quadrupole, ion trap and time-of-flight (Dean 2005:96). Detection is usually by continuous dynode electron multiplier, within which positive ions are attracted to negative potential of a lead oxide covered cone on impact secondary electrons are ejected which are then attracted to the collector further down the cone and recorded as ion counts per second (Dean 2005:104). Interferences are less problematic than for ICP-AES but can still occur, including spectral interferences from overlapping atomic masses of different elements and non-spectral causing signal enhancement or depression (Dean 2005:104).

This technique was selected as being able to analyse the trace element composition of the glass samples with minimal further sample preparation or destruction of the samples. SEM-WDS can only detect most elements above several hundred ppm. The trace element composition of glass can be used to gain information about its original place of manufacture and is now becoming a standard technique in analysing ancient glasses (Shortland et al 2007; Walton et al 2009). Laser ablation destroys only a miniscule part of a solid sample and gives results for trace elements down to ppb levels in some cases. It was therefore considered to be a useful technique in the characterisation of the glasses studied within this project.

Analytical parameters: The equipment used for this analysis was a GBC Optimass G500 Inductively coupled plasma, time-of-flight, Mass spectrometer, linked to a New Wave Laser UP213 ablation system, operated at 40J/cm² in a helium sweep gas, based at the Getty Conservation Institute, Los Angeles, USA. Each spot was collected for 25 seconds with a spot size of 60 μm and calcium, based on the SEM-WDS results, was used as an internal standard.

3.3.6 X-ray diffraction (XRD)

X-ray diffraction (XRD) uses the Bragg equation used in SEM-WDS to look at the lattice spacings of materials. X-ray diffraction uses X-rays of a known wavelength (λ) and measuring theta (θ) to determine the d-spacings of different materials which can then identify unknown materials (Cullity 1978:88). In X-ray powder diffraction a fine powder is placed into an X-ray beam, the powder contains crystals orientated at

random so some will be correctly orientated so that their planes are at the correct angle to fulfil the Bragg law and are capable of reflection (Cullity 1978:96-7). The resulting diffraction lines are made up of many tiny spots, each caused by reflection from a single crystal particle, so close together that they appear as a continuous line, which usually appears curved (Cullity 1978:97). The position of these lines allows the identification of unknown materials (Cullity 1978:97). The size of the particles can affect the diffraction patterns produced and the presence of amorphous materials produced broad peaks rather than sharp lines, making interpretation more difficult (Cullity 1978:105).

This technique was selected as it could give information about the degree of re-crystallisation within the secondary alteration layers as well as the mineral phases present. This technique has been used to successfully characterise the secondary alteration layers of glasses from a number of periods and settings, for example Cox and Ford (1989) for glasses buried on the sea bed and Curti et al (2006) for nuclear waste glasses. XRD also makes it possible to look at any additional mineral phases, such as opacifying crystals, present within the glass. For example, calcium antimonate, used to opacify glasses, has more than one phase the formation of which can be related to the temperature and composition of the melt from which it was formed (Butler et al 1950).

Analytical parameters: *Powder diffraction*

X-ray powder diffraction analysis was carried out using a PANalytical X'Pert PRO Multi-Purpose Diffractometer with Cu K α radiation at 40kV. A PIXcel detector was used to collect data over an angular range of 10 - 80 $^{\circ}/2\theta$ with a step size of 0.01 $^{\circ}/2\theta$ and a count time of 300 seconds at each step. SearchMatch software was used to identify the diffraction patterns produced.

Point XRD analysis

The point X-ray diffraction analyses were carried out using a Bruker D8 X-ray diffractometer with Cu K α radiation at 40kV. A General Area Detector Diffraction System (GADDS) and a 500 μm collimator were used to collect data over an angular range of 21 - 55 $^{\circ}/2\theta$ with a count time per frame of 180 seconds. The detector was centred at 38 $^{\circ}/2\theta$ and rotated through 360 $^{\circ}$ over the count time. SearchMatch software was used to identify the diffraction patterns produced.

3.4 Sample preparation

3.4.1 SEM-EDS, SEM-WDS, LA-ICPMS, point XRD

For the first batch of analyses 98 samples were selected from those taken at the museum in 2007; this was based upon the original sampling strategy and on which would give the most information (i.e. had an appropriate cross-section). They were sorted into categories of preservation state because the more

poorly preserved samples were softer and would require more careful sample preparation than the better preserved samples. A further 154 samples were selected and prepared after my second visit to the Semitic Museum in 2008. A number of samples were not prepared due to time constraints and their similarity to other examples.

For SEM-WDS the samples have to be mounted in resin and then ground and polished so that the surface is completely smooth due to the geometry required. The first 98 samples were set (usually 3-8 per mount depending on size and condition) into 25mm mounts using MetPrep KleeSet acrylic resin; ground using graded silicon carbide papers and then polished with 3 μm and 1 μm diamond pastes. Several had to be reimpregnated using a different grade of resin (Struers Specifix 20) and repolished later on as problems getting a sufficiently smooth surface for analysis were encountered due to the original resin setting too quickly and some of the alteration layers 'plucking out' while grinding. Due to the problems noted above, all subsequent samples were mounted using this epoxy resin (Struers Specifix 20). The mounted samples were coated with a very thin layer of carbon for both SEM-EDS and SEM-WDS to prevent charging. The surface of a sample under an electron beam has to be conductive as surplus electrons from the incident beam build up on the surface and if they are not conducted away and earthed they can repel an incoming beam, thereby distorting the image; this is known as charging (Goodhew et al 2001:164). The mounted samples were used for both SEM-EDS and SEM-WDS analysis; with their coating removed it was also possible to carry out LA-ICPMS and point XRD on these samples.

3.4.2 Powder XRD

Five samples of the weathering layers from the Late Bronze Age glasses were examined by powder XRD. This material was from examples where the weathering layer had disintegrated either on sampling, or during transit of the samples from the USA to the UK. The material was ground in an agate mortar and pestle until the resulting powder would pass through a fine-meshed sieve. Around 1g of the resulting powder was then pressed into stainless steel sample holders for analysis.

3.4.3 ICP-AES

The solutions from the dissolution experiments were analysed using ICP-AES. In order to prepare the samples for analysis the solutions were acidified at the end of each experimental period to stop any further reactions. 9.8ml of each solution was combined with 0.2ml of 1M nitric acid within LDPE containers which were then sealed. A range of calibration solutions were prepared prior to analysis, based on the mass loss of the major elements during the experiments. Solutions were prepared with 0.1ppm, 0.5ppm, 1ppm, 5ppm, 10ppm and 20ppm of silicon, calcium, potassium, sodium, and copper, the major elements within the replica glasses, alongside a blank. The solutions were prepared using 1% nitric acid in deionised water

| Oxide % | Recipe | Batch 1 | Egyptian batch |
|--------------------------------|--------|---------|----------------|
| SiO ₂ | 67.2 | 67.1 | 62.8 |
| Al ₂ O ₃ | 0.6 | 0.8 | 1.1 |
| CaO | 6.0 | 6.5 | 8.7 |
| MgO | 4.5 | 5.4 | 8.0 |
| Na ₂ O | 16.8 | 15.3 | 17.1 |
| K ₂ O | 3.0 | 2.9 | 2.4 |
| FeO | 0.3 | 0.4 | 0.4 |
| CuO | 1.6 | 1.6 | 0.0 |
| | 100.0 | 100.0 | 100.5 |

Table 4: Replica glass 1: LBA composition glasses used for dissolution experiments

with varying quantities of standard solutions for each element; the solutions used were Spectrosol standard solutions with 1000ppm of the element required, except silicon which was a BDH standard solution with 1ml = 1.00mg Si and magnesium which was Spectrosol magnesium nitrate 1ml = 1.00mg Mg.

3.5 Dissolution experiments

3.5.1 LBA replicate glass

The glass used in the dissolution experiments was produced by the Roman Glassmakers, Andover, to a simplified LBA translucent blue glass recipe. Translucent blue is the most common colour of glass found at Nuzi and colourless glasses are extremely rare in the Near East at this time. Therefore it was decided to base the glass recipe on the bulk compositions of the translucent blue glasses from Nuzi. Table 4 shows the recipe used and the composition of the finished glass, verified by SEM-WDS analysis. The glass produced was provided as rods of around 5mm diameter which were then cut into small cylinders 2-3mm high. This shape was chosen as it is simple to calculate the surface area of a cylinder, surface area being an possible factor in glass/water reactions. The resulting monoliths had their original fire-polished surface on their circumference with a finely ground surface on their flat surfaces from being cut to size.

3.5.2 Experiments

Powdered glass vs monolith: An initial experiment was carried out to look at whether monoliths of glass would be reactive enough over short term experiments using powdered glass, <250µm, versus a small monolith (1g). For this experiment some existing glass made by the Roman glassmakers to a Late Bronze Age Egyptian glass recipe, was used as it was of known composition and at this stage the LBA composition blue glass was not yet ready, the composition of this glass is also shown in Table 4.

Precipitation of secondary layers: Almost all of the glass objects from Nuzi had some kind of weathering apparent at their surface ranging from a negligible surface change to complete devitrification, which retained

| Sample | Al ₂ O ₃ | Fe ₂ O ₃ | MgO | CaO | Na ₂ O | K ₂ O | TiO ₂ | P ₂ O ₅ | Cu (ppm) |
|------------------|--------------------------------|--------------------------------|------|-------|-------------------|------------------|------------------|-------------------------------|----------|
| 1930.13B.2 | 8.57 | 4.34 | 3.37 | 19.14 | 0.72 | 1.77 | 0.47 | 0.11 | 29 |
| 1930.41.112 | 8.70 | 4.56 | 3.77 | 17.69 | 0.59 | 1.83 | 0.48 | 0.21 | 36 |
| 1930.40F.2 | 8.99 | 4.58 | 3.85 | 17.80 | 0.71 | 1.89 | 0.48 | 0.22 | 33 |
| Average | 8.75 | 4.49 | 3.66 | 18.21 | 0.67 | 1.83 | 0.48 | 0.18 | 33 |
| | | | | | | | | | |
| BPS AT ball clay | 29.0 | 2.4 | 0.4 | 0.3 | 0.50 | 3.00 | 1.10 | - | - |

Table 5: ICP-AES results of mudbrick analyses (major elements and copper) and analysis of clay used

the original form of the object rather than the glasses dissolving completely into the soil. Therefore it was decided to carry out some experiments to examine the creation of these layers. In the first of these a replica soil environment was created using powdered clay and artificial hard water (EPA 2002:33). The composition of clays from Nuzi had been studied within another project (Erb-Satullo et al in preparation) by solution ICP-AES and these data were used to select the clays used in the experiments (Table 5). The clay selected, Bath Potters' Supplies AT ball clay, is not a perfect match to the Nuzi mudbricks; but clay even close to the mudbricks in composition could not be found due to the very high lime and low aluminium oxide content, which could be a result of the very large organic fraction within these objects. However, the chosen clay was the closest that could be found to other components such as potash, titanium and iron oxide; it was also available in a fine powdered form, free of inclusions, which was suitable for the experiments.

For this experiment eight monoliths were placed into two PTFE beakers (four in each) alongside 10g of clay and 100ml of artificial hard water in each beaker, as described above. These beakers were sealed and then one was placed into an oven at 60 °C with a monolith removed at 14, 28, 56 and 84 days, with the other kept at room temperature as a control. A temperature of 60 °C was chosen as it was hoped that reaction rates at the glass/environment interface would increase without the temperature speeding up the reactions to the point where the glass dissolved congruently. Another set of experiments were carried out at the same temperature with four monoliths held for 14, 28, 56 and 84 days in 100% RH (or as close as possible) at 60 °C within a sealed PTFE beaker. RH was measured by a hygrometer at regular intervals. This was to compare the effects of clay compared to just water on the precipitation of secondary layers at the glass surface. The phase vapour test, 100% RH in steam, was chosen as it is a well established test for looking at the precipitation of secondary phases at the surface of glasses in nuclear waste glass testing (Strachan 2001).

Dissolution experiments A further set of dissolution experiments were carried out to try and establish a baseline dissolution rate for the LBA replica glasses, and some actual archaeological, glasses. Six replica monoliths were held in 100ml of the artificial hard water, described above, in PTFE beakers for seven days alongside three archaeological examples which had had any weathering layers removed; these were not

| Sample | Colour | Start weight (g) | Diameter (mm) | Height (mm) | Surface area (mm ³) |
|-------------|------------------|------------------|---------------|-------------|---------------------------------|
| 7-90-1 | translucent blue | 0.127 | 4.71 | 2.81 | 76.7 |
| 7-90-2 | translucent blue | 0.141 | 4.77 | 2.97 | 80.5 |
| 7-90-3 | translucent blue | 0.162 | 5.30 | 2.95 | 93.6 |
| 7-90-4 | translucent blue | 0.142 | 4.91 | 2.96 | 83.3 |
| 7-90-5 | translucent blue | 0.132 | 4.76 | 2.94 | 79.6 |
| 7-90-6 | translucent blue | 0.157 | 5.30 | 2.88 | 92.0 |
| 1930.82.55 | translucent blue | 0.185 | | | 133.7 |
| 1930.66.90b | opaque turquoise | 0.239 | | | 149.7 |
| 1930.82.15a | translucent blue | 0.210 | | | 129.9 |
| 28-90-1 | | 0.159 | 5.14 | 2.98 | 89.6 |
| 28-90-2 | | 0.156 | 5.25 | 3.01 | 92.9 |
| 28-90-3 | | 0.178 | 5.65 | 3.03 | 103.4 |
| 1930.82.55 | | 0.190 | | | 133.7 |
| 1930.66.90b | | 0.269 | | | 149.7 |
| 1930.82.15a | | 0.217 | | | 129.9 |

Table 6: Dissolution experiments: starting weight and surface areas of glass monoliths

cylinders but more irregular fragments. The surface area measurements for these samples were calculated from their entire surface; each flat area, rectangle, triangle or polygon was measured and the various sections added together. A further three monoliths and three archaeological examples were dissolved for 28 days in a solution of the same composition, as described above; a blank solution which did not contain a glass monolith was used in each run to check for any changes caused by the beakers used. Table 6 lists all of the details and measurements of each sample prior to the experiments. The pH of the solution was monitored regularly during the experiment to make sure it did not reach above 9 using a Hanna pH checker calibrated using buffer solutions of pH 4, 7.01 and 11.

3.6 Experimental replication of antimonate glasses

The bulk compositional analysis of the glasses indicated that there were compositional differences between the translucent and antimony-opacified blue glasses from Nuzi. In order to examine this further a number of antimony-opacified glasses were recreated in a range of compositions and at a range of melting temperatures. The purpose of these experiments was to examine the phases of calcium antimonate produced with different compositions and melting temperatures of the glass; the effects of additional lime on the phases produced; the effects of pre-roasting calcium and antimony on the composition of the final glass, and the phase(s) of calcium antimonate produced.

Tables 7 and 8 detail the glass recipes and the melting temperatures used in these experiments. The glass recipe is based on the composition of the translucent blue glasses from Nuzi. The glass batches were prepared by weighing and then mixing the reagents together in a sealed plastic bag to ensure that they were evenly distributed. To this original batch mixture various quantities of antimony oxide and lime; and in one case a pre-roasted mixture of calcium antimonate. The pre-roasted mixture was prepared by heating

calcium carbonate and antimony trioxide in stoichiometric proportions (for $\text{Ca}_2\text{Sb}_2\text{O}_7$); 120g of calcium carbonate with 33g of antimony trioxide then roasting this mixture in a mullite tray at 850 °C which was held for two hours at this temperature. This was based on the methodology in US patent no. 2329161 (Harbert and Bateman 1943) on the manufacture of calcium antimonate.

| Oxide % | Glass batch | Reagent | Weight (g) |
|-------------------------|-------------|--------------------------|------------|
| SiO_2 | 68 | SiO_2 | 68 |
| Al_2O_3 | 0.5 | Al_2O_3 | 0.5 |
| CaO | 6 | CaCO_3 | 10.7 |
| MgO | 5 | MgO | 5 |
| Na_2O | 17 | Na_2CO_3 | 29.1 |
| K_2O | 3 | K_2CO_3 | 4.4 |
| FeO | 0.5 | FeO | 0.5 |
| Totals | 100 | | 118.2 |

Table 7: Replica glass 2: translucent LBA glass recipe

| Glass | 1050°C | Glass | 1150°C |
|-------|---|-------|---|
| A1 | colourless glass | B1 | colourless glass |
| A2 | colourless glass + 3% Sb_2O_3 | B2 | colourless glass + 3% Sb_2O_3 |
| A3 | colourless glass + 3% Sb_2O_3 +3% CaO | B3 | colourless glass + 3% Sb_2O_3 +3% CaO |
| A4 | colourless glass + pre-roasted Sb_2O_3 + CaO | B4 | colourless glass + pre-roasted Sb_2O_3 + CaO |
| C1 | cullet | | |
| C2 | cullet + 3% Sb_2O_3 | | |

Table 8: Replica glass 3: antimony-opacified replica glasses

In addition a glass made from cullet with added antimony oxide, as opposed to the other replica glasses made by fusing raw glass batch materials, was made in order to compare opacified glasses made by these different methods. Each of the glass recipes/batches were fired in a mullite crucible within an electric furnace for and held at the selected temperature for 12 hours. The glasses were then cooled to below 800 °C and then quenched in water; this was done for reasons of time, as it was generally not possible to allow the glasses to cool down in the furnaces as they were needed for other applications, as well as standardising the cooling regime of the glasses. Calcium antimonate precipitates from the melt on cooling so variations in the cooling regime of the experimental glasses could affect the crystallisation of these phases and thus the results. The standard form mullite crucibles and trays were manufactured by the Materials Advice and Research Centre, Department of Engineering, University of Sheffield.

4 Results 1: Typology and distribution

4.1 Introduction

One of the major aims of the current project was an examination of the effects of differential burial conditions on the preservation of vitreous materials from a single assemblage and time period. In order to be able to look at this in detail it was necessary to survey the vitreous assemblage, from the 2nd millennium BC site of Nuzi, stored at the Semitic Museum Harvard University, to assess the nature and state of preservation of the material held there. In addition, the treatment and storage of the materials since their excavation was assessed where possible. It was also necessary to evaluate the accuracy of find locations recorded for these artefacts which involved reviewing the original excavation finds notebooks and the excavation report alongside the material held within the museum. The extent of possible intrusion into Bronze Age contexts from later occupation on the site has also been evaluated.

4.2 Survey of the vitreous assemblage

As part of this project the entire vitreous assemblage from Nuzi stored at the Semitic Museum at Harvard University was re-examined prior to samples being taken for analysis. Several classes of objects were noted including: beads, in a variety of materials; monochrome and decorated polychrome glass vessels; glazed ceramic vessels, figurines and wall nails; glass pendants, mace heads, figurines and inlays; and other miscellaneous objects. The full survey is presented in Appendix 1, Table b with a summary in Table 9.

| Object type | Number | Location known | Percentage |
|----------------------------------|--------|----------------|------------|
| Beads | 4677 | 3209 | 69% |
| Glass vessel fragments | 159 | 112 | 70% |
| <i>2nd millennium BC</i> | 133 | 106 | 80% |
| <i>Late</i> | 26 | 6 | 23% |
| Glass pendants/fragments | 17 | 10 | 59% |
| Other glass objects | 16 | 7 | 44% |
| Glazed ceramic vessels/fragments | 197 | 80 | 41% |
| Glazed ceramic wall nails | 26 | 23 | 88% |
| Other glazed ceramic objects | 11 | 6 | 55% |
| Faience/frit objects | 7 | 5 | 71% |
| Cylinder seals (vitreous) | 20 | 0 | 0% |
| Cylinder seals (non-vitreous) | 16 | 0 | 0% |
| Total | 5305 | 3564 | 67% |

Table 9: Survey of vitreous materials in museum assemblage

4.2.1 Numbering system

The numbering system of the Nuzi assemblage within the Semitic Museum is somewhat complex and a brief outline is given here as an attempt to clarify this. Each object, or small group of objects in some

cases, was given a museum number on its accession into the museum collection. This number is prefixed by 1930, the year the majority of the finds were imported, then two further two digit numbers which were assigned sequentially, therefore a typical accession number for an item from the Nuzi collection would be 1930.82.15, which relates to a group of glass vessel fragments. In addition to this number many of the objects also have field numbers either recorded on the object itself or on its accompanying label. These field numbers relate to the year and month that the object was found and recorded at the site then a further find number, for example, 30-2-71, relates to glass pendant fragments excavated during February of 1930 these being the 71st object recorded that month; the field number is also linked to the original find location of the object. Some objects also have a room number recorded either on the object or on its label. This is discussed further in section 4.4.

4.2.2 Beads

Beads are the most numerous object type noted from Nuzi. Starr estimated that 16,000 beads were present in the temple complex alone (1939:94). A review of the assemblage currently held at the Semitic Museum estimates that there are between four and five thousand beads currently in the museum assemblage, excluding the large number of beads on display. Only where a total number of beads was noted within the labelling was the number of beads within an accession group recorded, or where the number could be quickly counted – otherwise beads were noted as being ‘numerous’ i.e. there were too many to count quickly, or ‘various’ which means that the beads were fragmentary so the original number could not easily be assessed. Three thousand, three hundred and thirteen beads were counted individually and if an average of 50 is used where ‘numerous’ has been noted and an average of 10 for ‘various’ the total is 4603, which may well be an underestimate; the exact number is difficult to assess precisely as many are broken and fragmentary. There are also hundreds of beads currently on display so the actual total is likely to be much higher.

The beads consist of a very wide of range of designs, colours, sizes and materials. The vast majority appear to be made from vitreous material, but post-depositional processes can make it difficult to assess the exact material used: glass, faience or frit. Glass, faience and frit are related vitreous materials. The definitions of these materials has varied considerably, however, for the purposes of this project glass is defined as material that is completely vitreous i.e. has no crystalline structure; faience is defined as a vitreous material consisting of a quartz core with a deliberately produced glaze layer and frit, rather than its alternative meaning of an intermediate stage between raw materials and glass, is defined here as being a deliberately-heated material containing silica, alkali and colorant which has then been shaped into its final form. In many cases it was not possible to definitively identify the material used without further analysis of the object.

Typology: The beads contained within the museum assemblage consist of a very wide range of types and sizes. Examples of almost all of the types of beads reported in the original excavation report were found. These included: spherical beads, cylindrical beads, eye beads, hubbed beads, ribbed/fluted beads, barrel beads, disc beads, square/rectangular beads, moulded spacer beads, zoomorphic beads, and granulated beads.

- Spherical beads: these beads were found in a range of sizes ranging from a few millimetres across to several centimetres. There were also various colours observed; however, assessing the exact proportions of different colours present was not possible due to post-depositional alteration. Some spherical beads were also inlaid with glass of a contrasting colour.
- Cylindrical beads: again these beads were found in a range of sizes from tiny ones, a few millimetres long, in what appeared to be blue, red and white frit, to some very large glass examples, including bead 1930.62.90, which is around $4\frac{1}{2}$ centimetres long and had inlay of a contrasting colour at each end.
- Eye beads: these beads consist of several layers of glass, usually of different colours built up to resemble an eye. Again they are present in a range of sizes from 1-2cm in diameter up to 6-7cm in a few cases.
- Hubbed beads: these are present in glass and other materials, consisting of a round central bead with a 'hub' or disc shape at either end. They can either be made in one piece or have hubs of a contrasting colour; Starr notes that many of the glass examples appeared to have been of blue glass with yellow hubs (Starr 1939:449).
- Ribbed/fluted beads: a number of spherical beads with distinct ribbing or fluting were also noted in the assemblage. The exact nature of the materials used to make, and the original colours of, these beads was difficult to assess. 1930.67.74, pictured, is a typical example in what appears to be either an altered glass or frit.
- Barrel beads: a variant on the cylindrical beads was the barrel beads which taper at each end. A number of sizes and colours were noted with some inlaid examples also being present.
- Disc beads: a number of simple disc beads were also observed within the assemblage. Again several colours are present, including some yellow beads such as 1930.63.59 pictured in Figure 7.
- Square/rectangular beads: the assemblage also contains a number of beads with a square or rectangular cross section. These appear to be predominantly of glass; however, it is difficult to be certain in many cases.

- Spacer beads: the ribbed rectangular spacer beads are fairly common in the assemblage and are present in different types of materials and several colours, as far as can be observed. Again a range of sizes are present from smaller examples around 1cm across to larger ones several centimetres across; 1930.61.8, is a medium sized example in what appears to be dark blue frit.
- Zoomorphic beads: a small number of beads in the shape of various animals were noted in the assemblage, the commonest being frogs and flies. These appear to be made from blue or white frit.
- Granulated beads: a small number of granulated beads were observed in the assemblage, consisting only of red or white frit, most of these are on display but 1930.67.33 (pictured) clearly shows the 'granules' placed onto a small spherical bead.

The spherical, cylindrical, barrel and disc beads were the most common type, with eye beads also being relatively common; many other types were much rarer such as the granulated beads, of which only eight were found, and there were also a number of unique types such as the blue frit or faience bead, 1930.60.99, which is in the shape of a bunch of grapes, Figure 7 illustrates most of the types mentioned.



Figure 7: Types of bead: top row left to right, spherical bead 1930.63.5; large inlaid cylindrical bead 1930.62.90, spacer bead 1930.61.8; middle row: yellow disc bead 1930.63.59, blue hubbed bead 1930.62.72, ribbed bead 1930.67.74, red granulated bead 1930.67.33, square inlaid bead 1930.62.82, rhomboidal bead 1930.62.84; bottom row: eye beads 1930.63.29, broken inlaid barrel bead 1930.62.78; grapes bead 1930.60.99. (not to scale)

Colour: The majority of the beads examined are blue, in one shade or another, with smaller numbers of red, white, yellow, amber/brown and black beads, however later analysis indicated that the colour seen did not always represent the original colour due to post-depositional alteration. There were also very many beads of indeterminate colour, such as those illustrated in Figure 8. Many of the glass beads found were decorated with inlays of different colours as can be seen in Figure 7.



Figure 8: Beads of various colours, all heavily weathered

4.2.3 Glass vessels

The 2nd millennium BC glass vessels within the museum assemblage consist of over 120 fragments from an unknown number of core-formed glass vessels; again this does not include objects on display. Starr reports that no intact vessels were found and that it was possible that the vessels had been deliberately smashed during the looting and destruction of Stratum II (1939:457). If a single accession group is taken as representing a single vessel then 27 vessels are represented within the museum assemblage. However, there are accession groups which appear to share a single vessel and others which contain more than one vessel based on the form and decoration of the fragments. The fragments in 1930.82.10 and 1930.82.17 appear to all come from the same vessel based on their thickness and the black staining seen on many of the shards. 1930.82.15 contains fragments from at least two vessels, possibly more and 1930.82.73 also contains at least two vessels and there may well be other groups with multiple vessels. Therefore the exact number of vessels within the assemblage is most likely to be higher than 27, but this cannot be verified due to the fragmentary nature of the objects.

The majority of the vessel fragments are decorated either by inlays of coloured glass or in several cases by additional fluted decorations. Where the original colour of the glass could be assessed all of the vessels appeared to be translucent blue with yellow and white decoration. However, many were very heavily altered and the original colours of the both the vessel and its decoration could not be ascertained from their appearance (Figure 9). A single small fragment of a translucent amber-coloured glass vessel was also found, 1930.82.13, this had appeared similar to other heavily altered fragments but on sampling the original colour was revealed.

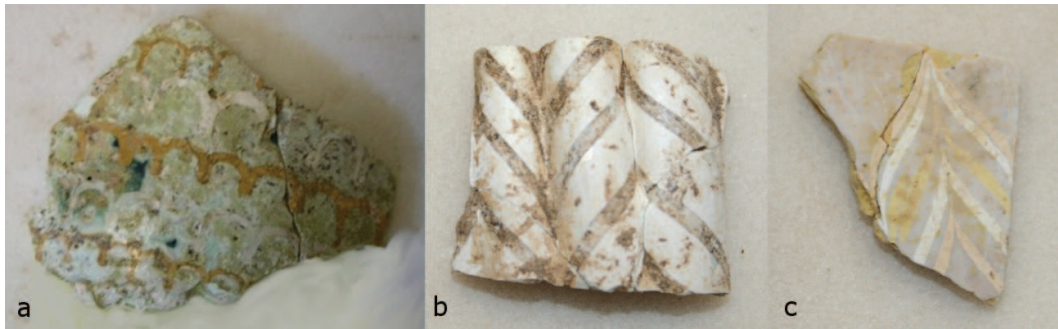


Figure 9: a. polychrome glass vessel with inlaid decoration; b. fluted vessel; c. vessel fragment with fine decoration, unknown original colour

4.2.4 Glass pendants

Several examples of glass sun disk pendants were found within the assemblage, the fragments suggesting six or seven pendants. The excavation report suggests that these could be both decorated (Figure 10a) and plain, however, only a single decorated fragment was noted (1930.69.30). All of the fragments are heavily altered but the original colour could be seen on the broken edges. The pendants are a mixture of translucent blue and opaque turquoise glasses, as far as could be observed. In addition to these a further small decorated fragment was found, 1930.82.62e. This fragment was very heavily altered with only a thin core of glass remaining, on sampling this was shown to be amber-coloured with a possible remnant of moulding visible within the external alteration layers (Figure 10b). This would appear to be a unique object, there was no mention of pendants in this colour of glass within the excavation report or finds notebooks and thus far no parallels from contemporary Near Eastern sites have been found.

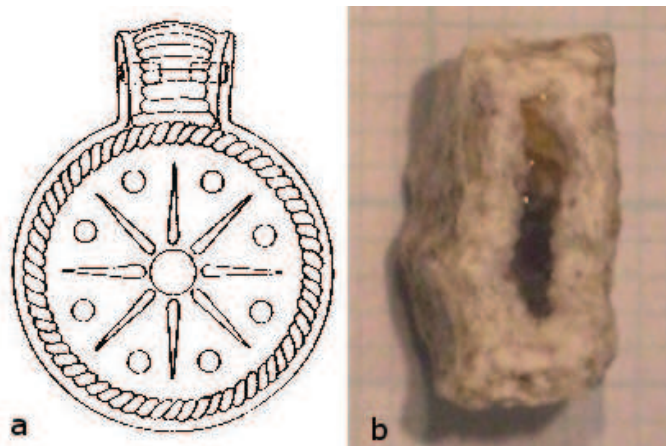


Figure 10: a: decorated sun disk pendant (Starr 1937: Plate 120); b: amber-coloured pendant fragment, 1930.82.62e

4.2.5 Raw glass

Three lumps of raw glass, two dark blue and one green, were found within the assemblage alongside an unknown object of white glass which could potentially be an ingot. 1930.82.48 and 1930.82.50 consist of several fragments of translucent dark blue glass in a very good state of preservation. 1930.82.47 is a large lump of translucent pale green glass containing multiple air bubbles. 1930.82.59 is a curved bar of opaque white glass covered by a thick beige alteration layer, the exact form of the object is unclear but it could be a fragment from a much larger object or an ingot of raw glass.

4.2.6 Other glass objects

Several other types of glass objects were noted within the museum assemblage including a mace head, figurines and a stone plaque with coloured glass inlay. Several mace heads are described within the excavation report (Starr 1939:96) but only two examples were found within the museum assemblage, 1930.82.26, consisting of blue glass with yellow glass globules added as decoration (Figure 11a) and a plain pale blue mace head, currently on display. Three figurines are noted within the assemblage, although only two are mentioned in the excavation report, an animal figurine from the palace; and an Ishtar figurine from the northeastern residential area (Starr 1939: 143;307). All of the figurines are extremely altered and in a very fragile state making it difficult to see what their original form and colour might have been; the illustrated example, Figure 11b, has also been extensively restored masking many details. One of the two glass inlaid plaques mentioned within the excavation report was found in the museum assemblage consisting of white limestone overlain by a thin layer of yellow glass in poor condition, 1930.82.20. Eight other small objects including several amulets were also noted in the assemblage.

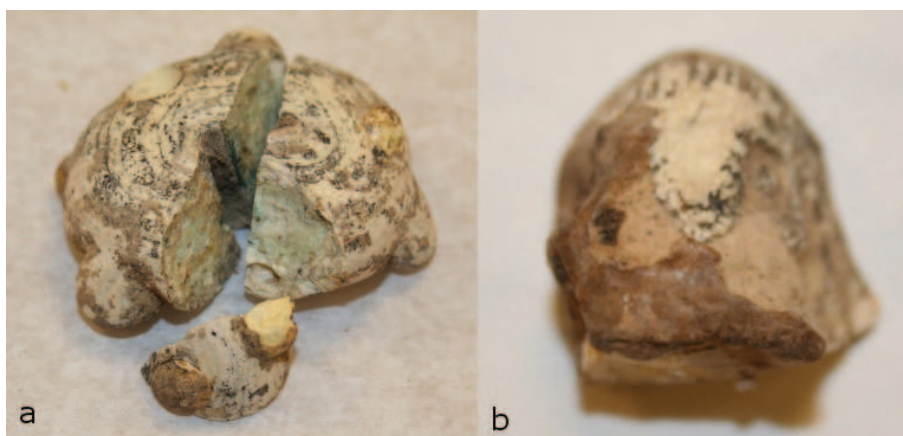


Figure 11: a: blue glass mace head with yellow decoration; b: fragment of glass figurine (with restoration)



Figure 12: a: marbled faience vessel; b: fragment N25

4.2.7 Faience

The marbled faience vessel fragments are amongst the best known objects found at Nuzi. They consist of layers of different coloured material in red, white, yellow and brown with blue glass areas reported in one sample (Figure 12a). These objects have been studied in some detail and there has been considerable debate as to what material they are made of with it being described as mosaic glass (Barag 1970:139), faience and glassy faience at different stages (Lilyquist and Brill 1993:10). Previous work has suggested that these objects are not traditional faience, lacking a separate glaze layer, but they do not appear to be glasses either (Lilyquist and Brill 1993:10). Three fragments were found in the museum assemblage and there is a very large fragment on display. No blue glassy areas were found in any of the fragments examined in this study and one sample (1930.82.2) had an extremely thick base and showed signs of significant consolidation and conservation. A new sample of this material, shown in Figure 12b, was found during a survey of some unaccessioned artefacts in the summer of 2008 (sample N25) it had been misidentified and placed amongst a collection of organic materials. This sample was interesting as it contained apparently glassy areas of a creamy colour amongst the red, white and yellow areas. A single example of a glazed faience vessel fragment was found in the assemblage (1930.57.4) the glaze layer appeared to be a creamy yellow colour but it was unclear whether this was its original colour or not. Several beads thought to be of faience were found as well, however, it is often difficult to distinguish between faience where the glaze has disappeared through alteration processes, and other materials such as frit.

4.2.8 Egyptian Blue

An unexpected find was a vessel fragment which was appeared to be made of blue frit. This had been thought to be a glazed or painted vessel but on sampling the blue colour was found to extend right through the fragment (Figure 13). The vessel fragment appears to be from a large shallow dish which, based on the curve of the rim, must have been of some considerable diameter; it would appear to have been made by moulding as some of the original moulded decoration remains (Figure 13). The vessel fragment is possibly the frit cup fragment mentioned in the excavation report (Starr 1939:91), although it lacks the pierced rim mentioned in the report. Another unusual find was a raw lump of blue pigment, this object had appeared to be a stone with some green coloration attached to it, however, on sampling the blue pigment underneath was revealed (Figure 14). The lump was loose and crumbly rather than solid, like the vessel fragment, perhaps suggesting that this was intended for wall painting or other decoration.



Figure 13: Egyptian blue vessel fragment 1930.47.14



Figure 14: Egyptian blue pigment, raw lump and close up of interior

4.2.9 Cylinder seals

A survey was also made of the cylinder seals as several of them appeared to be made from vitreous materials. Thirty-six cylinder seals are held within the museum assemblage, including the ones currently on display. Of these 20 appeared to be potentially made from vitreous material, Figure 15a, although whether this was frit or faience was unclear. The rest appear to be stone or terracotta, Figure 15b and 15c.

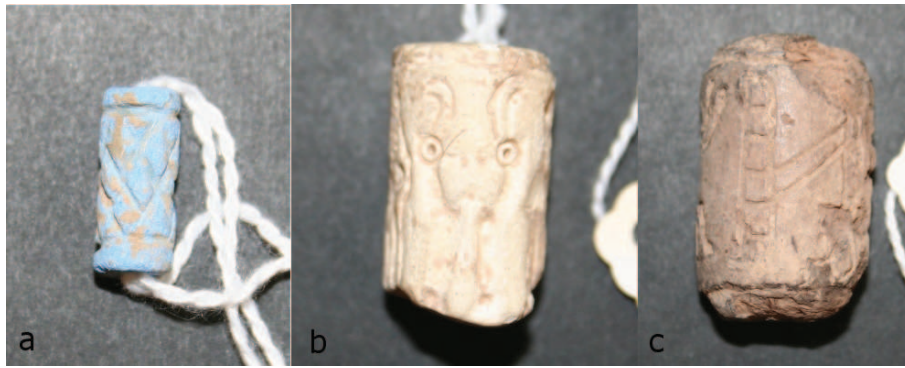


Figure 15: Cylinder seals: a. vitreous material (1930.80.29); b. stone (1930.82.30); c. terracotta (1930.80.34)

4.2.10 Late glasses

Twenty-six fragments from 14 vessels, a single bead and a bracelet fragment considered to be from later contexts were found within the museum assemblage. The vessels differ from the Bronze Age glasses in that they are usually colourless and translucent and have much thinner walls due to having been blown rather than core-formed; some examples also have mould blown, faceted or inscribed decoration, as can be seen in the drawings of these glasses from the excavation report, Figure 16. These glasses display a range of tints from being completely colourless to a pale blue-green or green tint; however, 1930.82.38 is translucent blue and the bracelet fragment (N124) is black glass.

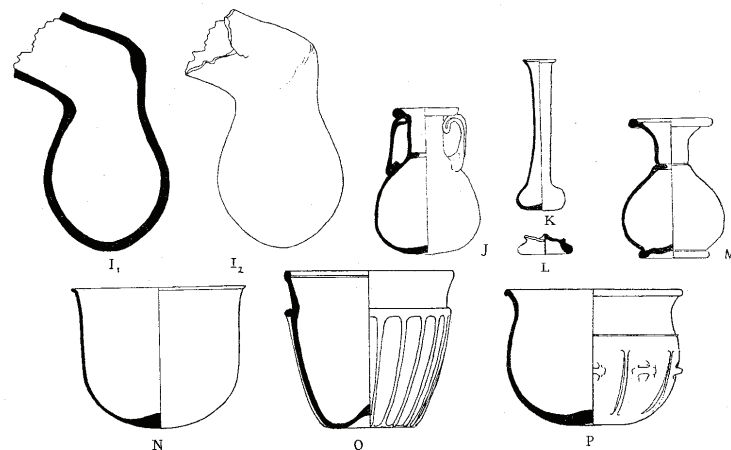


Figure 16: Drawings of typical Late glass forms (Starr 1939: Plate 140)

4.2.11 Glazed ceramics

A large number of glazed ceramic objects are contained within the museum assemblage. They include glazed ceramic vessels, animal figurines, wall nails and other object types such as an offering stand and

wall decorations . Twenty seven wall nails of different sizes, shapes and states of preservation are present within the museum collection with 11 figurines (Figure 17) and other object types. Ten largely intact glazed ceramic vessels were noted alongside 187 glazed ceramic vessel fragments, many from accession groups 1930.52.1, 1930.51.2 and 1930.52.6.



Figure 17: Glazed ceramics: wall nail and lion figurines

4.2.12 Preservation of the vitreous materials

The preservation of the beads appeared to vary widely across the assemblage from solid examples which retained their original form and much of their original colour to extremely fragile and fragmentary examples. The glass vessels also showed a wide variation in their preservation again with some in a good state of preservation with significant amounts of the original glass present and others in a poor state having completely devitrified. The glass pendants generally retained some original glass, but had significant alteration layers some apparently chalky and white, other showing a greenish tinge. Without exception the figurines appeared in extremely poor condition, being light and flaky with no original glass remaining, the mace head was better preserved retaining a solid character. By contrast, the raw glass was in excellent condition with little or no alteration visible. The preservation and alteration of the glasses will be discussed in detail in chapter 6.

4.3 Survey of vitreous materials recorded in finds notebooks

In addition to surveying the vitreous material held in the museum it was also decided to review the vitreous finds recorded in the finds notebooks. These notebooks give the field numbers for each object or group of objects alongside a brief description of the item and the location in which it was found (Figure 18). The majority of these records were kept by the wife of the excavation architect, Emanuel Wilensky, (Starr 1931) each season from November 1928 and March 1931. The 1927-28 notebooks are much less detailed and are in a different hand; unfortunately it was not possible to ascertain who wrote these. Table c in Appendix

1 details the vitreous materials noted within these texts with a summary table below (Table 10). A part of this process involved creating a digital record of the finds notebooks by photographing each page; this was done because the notebooks are rapidly deteriorating due to age and handling.

February 1930

№ 349 *

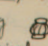
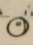
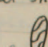
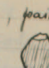
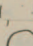
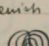

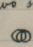
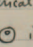
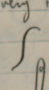

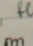
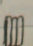
| No. | Material | Site | Description | Loca- tion | Date | | Remarks |
|-----|----------|--------|---|---------------|--------|---|---------------------|
| | | | | | D M | Y | |
| 281 | Compos | D10-D4 | 4 beads, ribbed, terminal bending  | H10 | | 4 | D:02 |
| 282 | " | D11-D3 | 5 spherical beads, in yellow & white  | " | " | " | C:1 |
| 283 | " | L20-L4 | 4 barrel shaped beads, painted  | " | " | " | D:02 |
| 284 | " | L 25 | Bead, lozenge, painted in yellow & grey  | " | " | " | D:05 |
| 285 | " | D 14 | Bead, disc shaped, blue  | " | " | " | D:06 |
| 286 | " | D 18 | Bead, ribbed, greenish blue  | H16 | " | " | C:9 |
| 287 | " | | Painted fragment  | " | " | " | for decorated glass |
| 288 | " | D8-D5 | 4 beads, two spherical, and two ribbed   in yellow & blue | C39 | " | " | D:0 |
| 289 | Brone | | Wire fragment, very thin | H32 | " | " | C:7 |
| 290 | Bone | L95 | Needle, complete  | C31 | " | " | D:1 |
| 291 | Compos | L 24 | Cylinder seal  yellow | C43 | | 2 | D:2 |
| 292 | " | D11 | Two ribbed beads, blue, spherical  | " | " | " | " |
| | " | D3 | & rectangular  | " | " | " | " |

Figure 18: Page from finds notebook, with later correction

| Object type | Number |
|----------------------------------|--------|
| Beads | 9434 |
| Glass vessel fragments | 27 |
| 2nd millennium BC | 20 |
| Late | 7 |
| Glass pendants/fragments | 9 |
| Other glass objects | 26 |
| Glazed ceramic vessels/fragments | 26 |
| Glazed ceramic wall nails | 65 |
| Other glazed ceramic objects | 15 |
| Faience/frit objects | 5 |
| Cylinder seals (vitreous) | 25 |
| Cylinder seals (non-vitreous) | 30 |
| Total | 9689 |

Table 10: Survey of finds notebooks, summary table

4.3.1 Beads

9434 beads, listed as being of glass, frit, faience, paste and composition, are recorded in the finds notebooks. Where a number was not present i.e. where an entry stated 'various' beads or 'group' of beads 13 was used, being the average of all of the groups noted in the finds record. Composition and paste appear to have been general terms used where the exact material was not clear and it is probable that most of the beads listed as such are of vitreous material. Given Starr's estimate that 16,000 beads were recovered from Temple A alone (1939:94), it would appear that many were either not recorded at the time or did not make it into the museum collection. In the 1927-28 season notebooks beads were only recorded by numbers, however, in the later notebooks each bead was recorded individually with a description, measurements, and often a small drawing. This level of detail persisted until the very large groups of beads began appearing once the excavation of Temple A was underway when the beads are again only recorded as numbers with a general description of the group.

4.3.2 Glass vessels

Twenty seven instances of glass vessels, vessel fragments or group of fragments are recorded in the finds notebooks; unfortunately the number of fragments within a group was not usually recorded. Of these, seven are recorded as coming from graves in the later cemetery, leaving 20 instances as being from Bronze Age contexts. This is fewer than suggested by the accessioned groups present in the museum. It is possible that some of the glass was not recorded in the finds notebooks either because there was not time to record them or that glass vessel fragments were misidentified and recorded as another material. It is clear from the finds notebooks that the decorated glass was often recorded as painted pottery, or another material such as composition, and many entries have a correction added at a later date, possibly by Richard Starr (Figure 18). There is also a lack of correlation between the find locations recorded in the notebooks and the locations recorded in the museum assemblage suggesting that many of the glass objects recovered were either not accessioned into the museum collection or their field numbers/locations were not recorded on accession.

4.3.3 Glass 'sun disk' pendants and other objects

There are nine instances of glass pendants or pendant fragments recorded in the finds notebooks including one group of three pendants. This compares to eight pendants or group of pendant fragments found in the museum assemblage, including a small amber-coloured fragment with moulded decoration. However, all but two of the pendants in the museum assemblage are undecorated. Two decorated pendants are mentioned in the finds notebooks, 30-2-172 and 30-2-426, both of which are recorded as intact. Either of

these could be 1930.69.30 but the amber-coloured fragment does not appear to be mentioned in the finds notebooks. Additionally the excavation report indicates that there were three distinct types of decorated pendants, implying that there were multiple examples of each type (Starr 1939:451). Three glass mace or staff heads are reported from the finds notebooks alongside five probable glass plaques, two glass figurines and 14 small objects described as amulets or pendants. There is also a glass eye from a statue and a unknown object of plain white glass.

4.3.4 Faience and frit

Only five objects, excluding beads and cylinder seals are listed as being manufactured from faience or frit within the finds notebooks. This includes only one mention of the marbled faience material, although similar-looking objects were searched for under different material types within the notebooks, with four fragments or groups of fragments being present in the museum collection. Among the other objects listed in Table c (Appendix 1) the frit cup (30-1-204) appears to have been accessioned as 1930.60.73 noted as 'possible glass fragments' in the recent survey; in addition a 'composition cup fragment' (31-2-11) is the faience vessel fragment, 1930.57.4. This demonstrates the difficulty of assigning material types by visual observation alone and that different interpretations of the same object are possible.

4.3.5 Glazed ceramics

Twenty six glazed ceramic vessels are recorded in the finds notebooks, compared to 197 fragments recorded in the museum assemblage, suggesting that many of the glazed vessel fragments were not recorded – the intact vessels perhaps being considered of greater importance. Of the 26 vessels in the notebooks three are noted to be from later contexts, either based on the appearance of the object (28-10-41) or are recorded as being from a late grave (29-12-203). The finds notebooks contained 65 records relating to glazed wall nails or wall nail fragments; 26 were found in the museum assemblage so again many examples were not accessioned into the museum. Fifteen other ceramic objects were also mentioned in the notebooks, including several figurines, with 11 objects recorded in the survey of the museum assemblage. The excavation report indicates that there were several more examples of glazed figurines, including a glazed boar's head which are not present in the museum assemblage (Starr 1939:98).

4.3.6 Differences between the notebooks and current assemblage

It is clear from the above survey that many of the objects recovered from the excavation at Nuzi were not taken to the Semitic Museum at Harvard University. A few objects are in other museums in the USA, including the Sackler Museum, also at Harvard; but the rest of the finds remained in Iraq in the Baghdad

museum collection, see Section 2.4 for details. Unfortunately there are no detailed records of what went to the Baghdad museum, however, it is likely that many of the objects described in the finds notebooks and excavation report that are not present in the USA went to Baghdad. One of the few objects known to have gone to Baghdad is a glazed boar's head in addition to a bone Ishtar figurine (Starr 1931) and there must have been many others. Given recent events it is uncertain what the fate of these objects is today.

4.4 Assignment of find locations to objects

One major part of the survey of vitreous materials in the museum was to assign as many find locations as possible to the assemblage. As already noted each object, or group of objects had two possible numbers the museum accession number, and the field number which links to a location recorded in the original finds notebooks. In addition to this many objects also had a room number recorded on their labels, even if a field number was not present. For each object or group bearing an accession number the field number or room number, if present, was recorded and then the field numbers were checked against the notebooks. In most cases it was possible to assign a find location to an object.

However, there were 27 instances where the room number in the notebook could not be found, either in the excavation report or on the plans. There were also examples where the object listed in the finds book was not the object bearing the relevant field number, for example colourless Late period glass vessel fragment 1930.82.6, which has the field number 28-12-306. This field number relates to a ceramic vessel from room S189 in the notebook from that season, Figure 19.

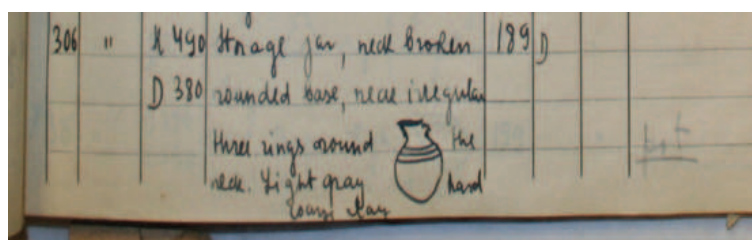


Figure 19: Extract from notebook showing 28-12-306 as a ceramic vessel rather than the Late glass vessel 1930.62.6

This process was further complicated by a change in numbering system that took place during 1929. In this year Richard Starr became the director of the excavations and instituted a new numbering system for the site. During 1929 the site, excluding the suburban area, was divided into 50m squares labelled A to X with each room number now being given its appropriate square as a prefix, for example room 110, excavated at the start of 1929, became S110. After this newly discovered rooms were numbered within their squares. Prior to this the excavated area within the city was known as 'C' and the suburban area as 'A'. As there is both a square A and square C in the later numbering system there is the possibility for confusion.

One notable example of this is the raw lump of glass 1930.82.48, which is labelled as having come from C62. Barag (1970:141) noted that there is no room C62 mentioned in either the excavation report or on any of the published plans and that it was impossible to tell where this object was originally found on the site. There was also no mention of this object in the finds notebooks and there was no field number recorded on the museum label or in the museum catalogue. However, there is one possible find location for this artefact, room K62, which is part of the palace complex and was excavated prior to November 1929. Therefore the original designation of this room would have been C62, indeed the finds notebooks from the early years of the excavations have been corrected to show the correct room numbers. Figure 20 shows the original notebook with C62 corrected to K62 by Richard Starr, although unfortunately the raw glass object itself was not recorded.

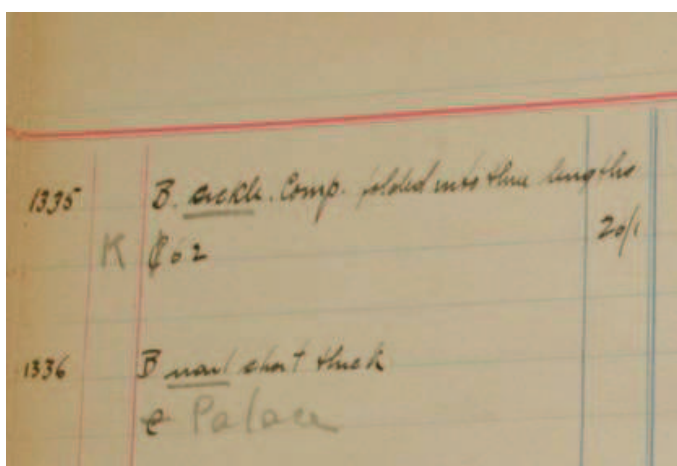


Figure 20: Page of finds notebooks showing change of room number

Despite all of this, it was possible to link 96% of the groups of vitreous objects and beads recorded in the notebooks to their original find spots. This work provided the basis of the distribution of vitreous materials results reported below; it also informed the current project's work on the variability of preservation observed within the glass and other vitreous objects.

4.5 Distribution of vitreous materials

The majority of the vitreous materials found during the excavation at Nuzi came from the northwestern temple, the 'Ishtar' temple. However, many of the glass vessels found were from locations in the palace complex and the suburban dwellings; the map of Stratum II, Figure 21, shows the distribution of glass vessels, other glass objects, glazed ceramic vessels, figurines and wall nails as well as beads, with the numbers denoting the number of beads in that location. This data has been extrapolated from both the survey of the actual material present in the museum assemblage and from the finds notebooks and excavation report. As has already been discussed, the exact nature of many of the beads is difficult to

assess, but because the vast majority of them are of vitreous material, they have been treated as a single group. It is clear from the distribution map that there are few glass and glazed ceramic objects (excluding beads) outwith the temple and palace complexes. There are also certain types of objects, such as the sun disk pendants, that are not found anywhere except within the temple complex.

4.5.1 Beads

Beads are found across all parts of the site, however, the vast majority of the beads recorded, 8203, were from the temple complex. Relatively few are from the palace, with only 222 beads being recorded as coming from the entire complex. Across the rest of the northwestern residential area, beads were found in 51 of the 177 rooms or locations, all were in groups of under 10 with 28 single beads, except a group of 12 in C19, 13 in G32, 37 in C30 and 78 in F2. In the southwestern residential area, beads were recorded in 35 of the 113 rooms and locations, all in groups of under 10 beads with 21 single beads, apart from a group of 14 in P470. The northeastern residential area contained the fewest beads with all of the groups found consisting of less than 10 beads with 13 single beads; beads were recorded from 26 of the 55 rooms in this region.

4.5.2 Glass

The majority of the Late Bronze Age glass vessel fragments were recorded as coming from the palace and temple complexes. Within the temple complex, glass vessel fragments are reported from the cella of the Ishtar temple, the courtyard outside the cella, G50, room H5 and from the street outside the temple. Starr suggests that the fragments from the courtyard and in the street were displaced during the looting and destruction of the temple, originally being part of the cella furniture (Starr 1939:90, 102-3). Fragments of glass vessels were found in seven locations within the palace complex: M100 and M94, the main courtyards; R87 the private entrance to M100 (Starr 1939:132); L22 which is thought to have been an important storage room (Starr 1939:148); M79 a high status room which may have been a bedroom (Starr 1939:134); L4, which is part of L11 the main state room of the palace (Starr 1930:138) and in room L8, which is thought to have been part of the palace's private 'chapel' (Starr 1939:156).

Only ten find locations containing glass vessel fragments were recorded outside the temple and palace complexes. The first three are several fragments of decorated glass from Rooms 7, 15 and 44 of the House of Shilwi-Teshub in the suburban area. The owner of this house is considered to be of very high status and to have had royal connections (Starr 1939:337). Several glass vessel fragments were also found in a small linked group of buildings A5/A4/F27/F29/F35 with no external or internal doors accessible only through openings high in the walls, which were interpreted as being a secure storage area, possibly linked to the temple or palace (Starr 1939:224). A single vessel fragment is reported from room C28 in

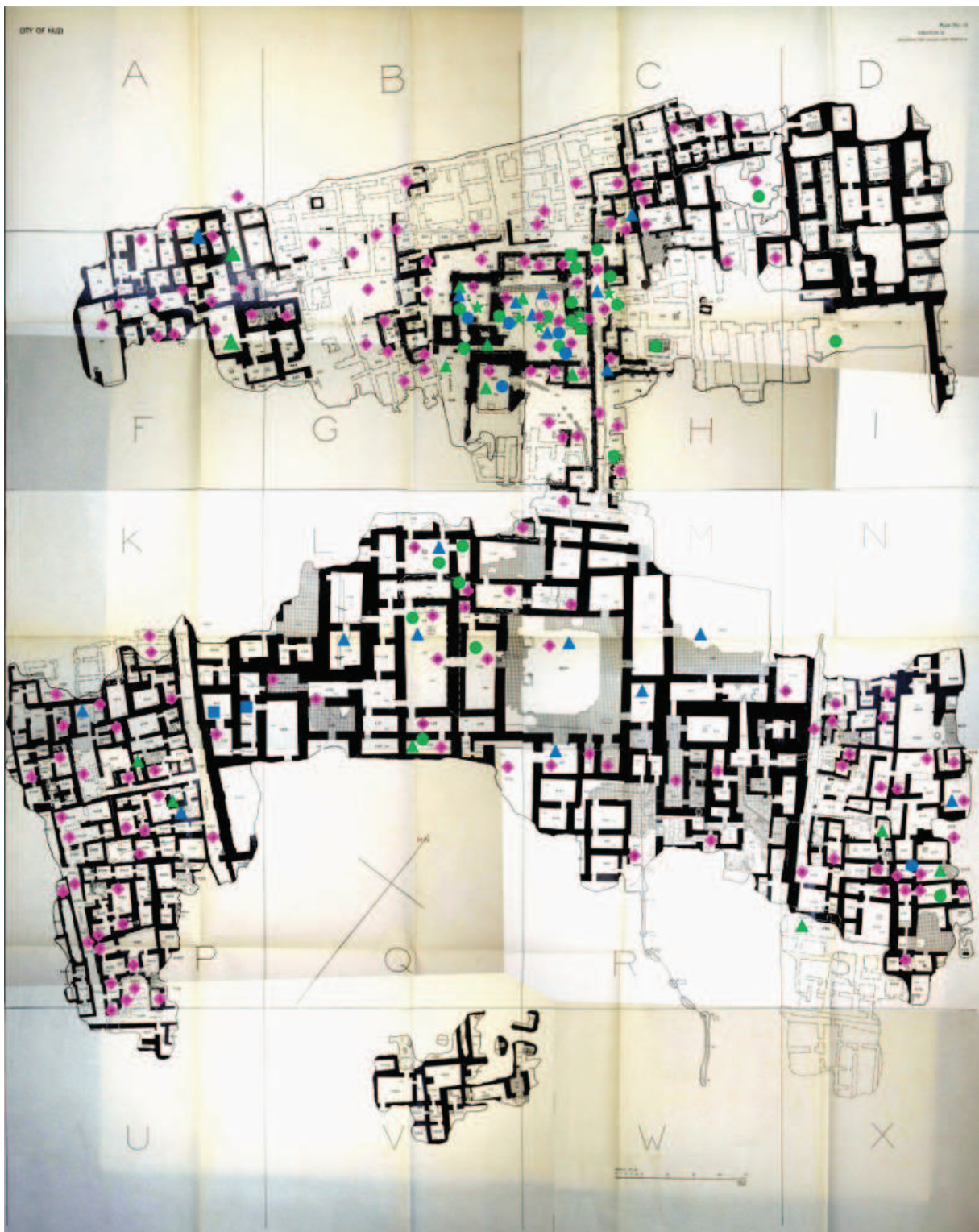


Figure 21: Distribution map of vitreous materials in Stratum II, based on Starr, 1937: Plan 13. Key: the pink diamonds are the beads (with the number of beads at each location within this symbol); the blue triangles are glass vessels, the blue circles the glass pendants and figurines and the blue squares the raw glass; the green triangles are the glazed ceramic vessels; the green circles the glazed wall nails and the green stars the glazed ceramic figurines.

the northwestern residential area, this particular room is only distinguishable from domestic areas by the presence of around 80 inscribed tablets (Starr 1939:234). Another fragment is reported from H35 which in part of a group of rooms situated opposite the temple complex Starr (1939:232) noted that this group of rooms had significantly more drains and brick pavements than would be expected in a private dwelling, suggesting that they may have been a service area for the temple staff. Several vessel fragments are noted from S104 and a single fragment from K314, both of which are thought to have been domestic dwellings (Starr 1939:312;284) indeed the house group containing K314 is described as a “humble residence” (Starr 1939:284). Vessel fragments are also noted from a room of unknown use, S157 (Starr 1939:305). The final fragment is a little more ambiguous, a black glass fragment reported from P341, which is a courtyard in a standard residential group; although a buried jar which may have votive connotations was also present in this room (Starr 1939:280). Black glass is unusual in the Bronze Age assemblage and it is unclear whether this was a vessel or another type of object; it has not been possible to locate this find in the museum assemblage so some questions as to its exact nature remain.

All nine glass pendants, pendant fragments, or groups of pendants are from the temple complex, coming from both the Ishtar temple and the southwestern temple. A glass animal figurine is reported from L11, the main state room of the palace. The glass figurines noted from the assemblage are both from the Ishtar temple. A further glass figurine is recorded from S111, in the northeastern residential area, and a possible glass plaque from room S110 in the same region; these locations are discussed in more detail below.

4.5.3 Glazed ceramics

Similarly to the glass objects the majority of the glazed ceramics were also found in the temple and palace complexes, as can be seen from the distribution map. However, there are a number of glazed ceramic objects from outwith the temple and palace complexes including vessels, figurines and wall nails. A glazed ceramic vessel was found in F10, which is linked to the set of storage rooms mentioned above, however, Starr notes that F10 contains objects consistent with it being a domestic area (Starr 1939:224). A further glazed vessel is reported from F24 which is considered to be the principal room of a large and possibly high-status residential property (Starr 1939:214;217). This room also contained a large wall painting, the best preserved of several examples at Nuzi, and many inscribed tablets – including the only copper example found at this site, indicating that this was an important room (Starr 1939:217). Another glazed vessel was found in S129 which was part of a domestic dwelling; however, the room did contain a brick hearth and several tablets (Starr 1939:314). Glazed ceramics were also found in P344 and P329, which are in the same house group as P341; P344 is described as a storage room and P329 as “living quarters” (Starr 1939:279;281). In contrast room P311 which also contained a glazed ceramic vessel may have been a private ‘chapel’ within a domestic setting (Starr 1939:285). House Group 16, within which are rooms

S144, glazed ceramic vessel, and S111 which contained a glass figurine, as well as a copper deity statue, is also thought to have been religious rather than domestic in nature (Starr 1939:306-8). Glazed ceramics were also found in room S108 and a possible glass plaque in S110, another group of rooms thought to have a religious purpose (Starr 139:309). A number of glazed vessels were found in other areas of the site where no indication of the purpose of the room was found: K421 in the southwestern region, C48, D10, H32 and H42 in the northwestern region.

Only one glazed figurine was also found in the residential areas of the city, in room D14 which is on the edge of the excavated area of the northwestern ridge, part of a group of buildings distinguished only by an elaborate drainage system (Starr 1939:243). A few glazed wall nails were also reported from locations outside the temple and palace complex: room D11 is in a Stratum III courtyard in the NW region, unusual for having the remains of a wall painting (Starr 1939:198), I21 is also in the NW region and also dates to Stratum III when it was an area devoted to metal-working (Starr 1939:205). H50 and H64 are both Stratum III rooms in the NW region and both are considered to have possibly been related to the temple (Starr 1939:195; 203). Room S105, however, is in the northeastern residential area and is a room containing a wide variety of objects including two infant burials, burnished ceramic fragments, beads and numerous copper metal objects (Starr 1939:306).

There were also several other glazed ceramic objects which, based on their recorded location, date from earlier than the destruction layer at the end of Stratum II. A glazed ceramic vessel is reported from Stratum III in S168 this would put this vessel in the mid 15th century BC and is one of the earlier glazed ceramic objects found at Nuzi. There are also several objects from room H11 in Temple B which is thought to date from the earlier part of Stratum II, most probably to the late 15th century BC. The earliest glazed ceramic object recorded is a single wall nail from H27 a room assigned to Temples D and E, which predate Stratum II, and could perhaps be dated as early as the late 16th century BC .

4.5.4 Other vitreous materials

The blue pigment was labelled as having been found in one of the suburban dwellings, the House of Shilwi-Teshub. The blue frit vessel fragment (1930.47.14) was labelled on the sherd itself as being from G29 Temple A, the cella of the Ishtar temple, and the faience vessel fragment (1930.57.4) also comes from G29. One of the marbled faience fragments (1930.82.3) is from the house of Zigi in the suburban area. The others, where the location is known, are reported as having been found in the palace complex, one in the courtyard of the palace, M100 and the other from L2A, also in the palace.

4.6 Intrusion into Stratum II

As has already been noted a number of late period glass vessels, glazed ceramic vessels, alongside other objects, were recovered from later graves dug into the city mound. A large number of graves were present across the surface of the tell, 103 in total concentrated in the northwestern region, ranging from 25cm below the surface to over 2m deep (Ehrich 1939). It was noted that these graves cut into LBA walls and rooms in some areas (Ehrich 1939). As part of this review of the museum assemblage and the original excavation report it was decided to examine the late cemetery in relation to the Bronze age layers beneath in as much detail as was possible from the data available. Despite the relationship between the later and earlier strata not being extensively discussed within the excavation report the plan for the cemetery can be used to look at where the graves overlie LBA rooms. The cemetery plan was laid over a copy of the relevant Stratum II squares and the position and depths of the graves noted. In many cases it is clear that the later graves are cutting across Stratum II walls and in some cases actually into the pavements below. This can be seen by comparing the levels taken at the heads of the graves and the levels taken within the rooms; in eight rooms the graves were above the recorded floor level and in 26 number they had cut into the floor - the full details are within Table d in Appendix 1.

Several other areas where later occupation may have intruded into the Bronze Age layers are noted in the excavation report. Within the temple complex there was evidence of two periods of habitation post-dating the destruction of Stratum II. A brick pavement was found extending over H6, H7, H9, H10 and H12 which was interpreted as being later than Stratum I (Starr 1939:116 and cross reference with stratigraphy/chronology sections of literature review). Several fragments of Nuzi lion figurines were found indicating intrusion into the Bronze Age temple; Starr (1939:116) says "... since we know that there was intrusive digging into the temple area they are probably displaced objects, the results of excavations long preceding ours". In addition to this Starr also reports several pits being dug into the temple complex and suggests that this is due to people deliberately digging in areas where they thought they would find foundation deposits of some value (Starr 1939:116). This affected the northern, eastern and western corners of G29 and the southern and eastern corners of the doorway to G53. Beads and lion jar fragments were found in the fill of the intrusive pit in G53 suggesting that they had been dumped in as backfill. All of the pits are dated to between SI and the Parthian period (Starr 1939:116). In addition, four beehive storage pits were found in G32 and one in the east corner of G50 (Starr 1937: Plan 7) these are dated by the glazed pottery found within them, these pits also cut into Stratum II layers (Starr 1939:116).

Within the palace complex there was much less evidence of intrusion into the Bronze Age layers. Some scrap brick pavement was found near R96 and R426 dated to Stratum I this was interpreted as an isolated building rather than rebuilding any of the palace structures (Starr, 1939:178). More areas of pavement were found near room K36 and near M100, the palace courtyard, with a ceramic vessel sunk into the wall

of L25; these are all thought to be from the Late period occupation of the site (Starr 1939:178-9).

Across the residential areas of the northwestern ridge, however, an “extensive habitation” (Starr 1939:263) is reported to have been present after the destruction of Stratum II (Starr 1937:Plan 29). “A small but thriving village” is described on the northwestern ridge at that time (Starr 1939:263). Walls were found in rooms F18, F19 and F28, dated to Stratum I, which were then reused in the Late period settlement (Starr 1939:261). Numerous artefacts from the late period were found in several rooms: F21 contained a bone pin, F18 glazed and plain ceramics of Parthian/Sassanian type, a long bone knitting needle and a pair of iron shears (PI 142 E) (Starr 1939:263). A late period infant burial was also found in F16 (Starr 1939:264). F8 Several Late ceramics and iron fragments were found in F8, suggesting its reuse during the Late period (Starr 1939:264). F17 and H40 also show signs of reuse (Starr 1939:265). A pit was found in room F41; a circular storage pit cutting the wall between F1 and F32; two pits in F2 and F3; brick pavement in B29, another over the walls of G2-B4, G11-12 and B7 (Refs). Rooms C15, G18, B17 and B21 in this region also have signs of later occupation (Starr 1939:265). B36 contains an oven which may be Stratum I or later, G7 contained iron rings; and G5, F10, G4, F24 and F5 all contained artefacts consistent with Late period occupation (Starr 1939:266). A silver coin of Shapur 1 (3rd century AD) was also found within a grave in this region (Starr 1939:266).

The southwestern region also has evidence of later occupation; a single Late ceramic vessel was found in P400 with glazed ceramics in rooms P482 and K421 (Starr 1939:294). Three silver Parthian coins (Vologases III) were found on the floor of P351 (Starr 1939:294). A pit had been cut through the doorway of P353 and P362 which was thought to be either Stratum I or Late period in date (Starr 1939:294). Iron fragments were found in P467 (age unknown) and potentially late glass from P356 (Starr 1939:294). Late period ceramics and fragments of pavement were also found in rooms P347, P321 and P362. Several Islamic period burials were found in this region lying over P198, P321, P360, P375, P376, P445 and between P387B and Street 1 (Starr 1939:294). The last one was a brick-built tomb cutting into the Stratum II walls and was considered to be Islamic in date due to the lack of grave goods and the position of the body (Starr 1939:294-5).

Very little evidence of later occupation is reported in the northeastern region of the site. Starr (1939:322) reports a few scraps of pavement belonging to Stratum I in S142 and N171, but there is no evidence of any Late period or Islamic occupation. However, this area was heavily eroded so it is possible that the upper layers may have been destroyed (Starr 1939:322-3).

4.7 Summary

Almost 5000 objects made from various vitreous materials are noted from the museum assemblage held at the Semitic Museum at Harvard University, this compares to around 10000 recorded in the finds notebooks.

The vast majority of the vitreous materials, both within the assemblage and in the notebooks, are beads but also include decorated glass vessels, glass pendants, amulets and figurines; frit and faience vessels and plaques; as well as glazed ceramic vessels, wall nails and figurines. The differences in numbers recorded from the assemblage and notebooks is due to several factors including the division of finds between several museums, field numbers being lost or not recorded when the collection was accessioned into the museum; there is also the possibility that some objects may have deteriorated further since excavation. In addition a number of samples have been taken for scientific analysis during the last twenty to thirty years. The preservation of vitreous objects across the museum collection is highly variable ranging from objects in an extremely good state of preservation, which are relatively rare, to those in very poor and often extremely fragile condition. The vast majority of objects within the collection, however, showed post-depositional alteration in one form or another. The surveys done on the museum assemblage and the finds notebooks have shown that of the vitreous objects held in the museum 67% can be assigned original finds locations. It is also clear, however, that some intrusion of later materials into the 2nd millennium BC layers may have taken place and this does have to be considered when looking at find locations.

The glass assemblage held at the Semitic Museum at Harvard University from the 2nd millennium BC city of Nuzi is extremely large and varied, despite the depredations of time, burial, division, transport, storage and extensive study. A remarkable number of objects have survived, including many small 'everyday' items such as the tiny blue beads found in large numbers and more common ceramics. This is particularly surprising as at the time when this site was excavated the larger and decorative objects suitable for museum display were more highly valued, with many smaller or 'less important' objects being discarded or destroyed. This factor combined with the large proportion of objects that it was possible to assign finds location to on the site has made it ideal for studying variability in the preservation of long-buried vitreous materials.

5 Results 2: Identification, composition and provenance

5.1 Identification of materials and bulk compositional analysis

SEM-EDS, analytical scanning electron microscopy, was used to characterise and identify unknown materials such as the vessel fragment 1930.47.14 and a number of beads whose nature was not clear from visual examination. Quantitative analysis of the glasses, glazed ceramics and other materials was carried out using SEM-WDS. Tables 11-15 shows the bulk compositional data (SEM-WDS) from all of the vitreous materials analysed so far. These are divided into 2nd millennium BC (Table 11) and Late period glasses (Table 13), with Table 12 being a breakdown of the 2nd millennium BC glasses by colour. Table 14 contains analyses of the glazed ceramics and Table 15 the analyses of other materials such as faience and frit. Table 16 shows the trace elemental analysis results, using LA-ICPMS, of a range of glass samples from Nuzi.

| Sample | Colour | Object type | SiO ₂ | Al ₂ O ₃ | CaO | MgO | Na ₂ O | K ₂ O | Fe ₂ O ₃ | TiO ₂ | CoO | MnO | NiO | ZnO | SnO | Sb ₂ O ₃ | BaO | PbO | Cr ₂ O ₃ | P ₂ O ₅ | SO ₂ | Cl | SiO | Total | |
|--------------|---------------|-------------|------------------|--------------------------------|------|-----|-------------------|------------------|--------------------------------|------------------|-----|-----|-----|-----|-----|--------------------------------|-----|-----|--------------------------------|-------------------------------|-----------------|-----|-----|-------|-------|
| 1930.60.140a | yellow | bead | 67.4 | 1.2 | 3.1 | 3.9 | 13.9 | 1.5 | 0.5 | 0.1 | 0.0 | 0.0 | 0.0 | 0.0 | 0.0 | 0.0 | 0.0 | 0.0 | 0.0 | 0.0 | 0.1 | 0.3 | 0.6 | 0.0 | 101.2 |
| 1930.60.140d | blue | bead | 66.2 | 0.5 | 4.2 | 3.8 | 15.9 | 3.0 | 0.3 | 0.1 | 0.0 | 2.0 | 0.1 | 0.0 | 0.0 | 0.0 | 0.0 | 0.0 | 0.0 | 0.0 | 0.2 | 0.2 | 0.2 | 0.9 | 97.2 |
| 1930.62.103 | turquoise | bead | 63.1 | 0.5 | 8.8 | 3.5 | 16.9 | 3.0 | 0.3 | 0.0 | 0.0 | 0.0 | 0.0 | 0.0 | 0.0 | 0.0 | 0.0 | 0.0 | 0.0 | 0.0 | 0.4 | 0.4 | 1.0 | 0.1 | 100.5 |
| 1930.62.31b | blue | bead | 71.7 | 0.3 | 3.5 | 3.4 | 14.2 | 2.5 | 0.2 | 0.0 | 0.0 | 2.1 | 0.0 | 0.0 | 0.0 | 0.0 | 0.0 | 0.0 | 0.0 | 0.0 | 0.2 | 0.2 | 0.7 | 0.0 | 98.3 |
| 1930.62.52 | colorant-free | bead | 63.1 | 2.0 | 5.4 | 4.8 | 17.7 | 4.1 | 0.7 | 0.1 | 0.0 | 0.0 | 0.1 | 0.0 | 0.0 | 0.0 | 0.0 | 0.0 | 0.0 | 0.0 | 0.5 | 0.4 | 0.9 | 0.0 | 99.9 |
| 1930.63.37 | colorant-free | bead | 63.6 | 0.6 | 6.1 | 4.7 | 16.1 | 2.3 | 0.3 | 0.1 | 0.0 | 0.0 | 0.0 | 0.0 | 0.0 | 0.0 | 0.1 | 0.0 | 0.0 | 0.0 | 0.2 | 0.2 | 1.1 | 0.0 | 95.4 |
| 1930.63.40d | turquoise | bead | 68.7 | 0.4 | 9.0 | 3.6 | 12.1 | 1.0 | 0.1 | 0.0 | 0.0 | 1.3 | 0.0 | 0.0 | 0.0 | 0.0 | 0.0 | 0.0 | 0.0 | 0.0 | 0.1 | 0.3 | 0.8 | 0.0 | 99.2 |
| 1930.65.90a | blue | bead | 66.0 | 0.3 | 6.9 | 4.0 | 17.6 | 3.0 | 0.2 | 0.0 | 0.0 | 0.0 | 0.0 | 0.0 | 0.0 | 0.0 | 0.0 | 0.0 | 0.0 | 0.0 | 0.2 | 0.2 | 1.0 | 0.0 | 100.6 |
| 1930.66.90b | turquoise | bead | 65.2 | 0.3 | 8.9 | 3.5 | 12.5 | 2.6 | 0.1 | 0.0 | 0.0 | 1.7 | 0.0 | 0.0 | 0.0 | 0.0 | 0.0 | 0.0 | 0.0 | 0.0 | 0.2 | 0.3 | 0.8 | 0.0 | 99.1 |
| 1930.66.90c | turquoise | bead | 64.1 | 0.9 | 10.4 | 3.4 | 14.1 | 2.5 | 0.6 | 0.1 | 0.0 | 1.1 | 0.0 | 0.0 | 0.0 | 0.0 | 0.0 | 0.0 | 0.0 | 0.0 | 0.2 | 0.3 | 1.0 | 0.1 | 100.3 |
| 1930.66.90d | turquoise | bead | 66.8 | 0.3 | 9.0 | 3.7 | 12.6 | 2.5 | 0.1 | 0.0 | 0.0 | 1.7 | 0.0 | 0.0 | 0.0 | 0.0 | 0.0 | 0.0 | 0.0 | 0.0 | 0.2 | 0.3 | 0.8 | 0.2 | 100.3 |
| 1930.66.90e | blue | bead | 66.4 | 0.3 | 6.9 | 4.3 | 17.4 | 3.0 | 0.2 | 0.0 | 0.0 | 1.0 | 0.0 | 0.0 | 0.0 | 0.0 | 0.0 | 0.0 | 0.0 | 0.0 | 0.2 | 0.3 | 1.0 | 0.0 | 101.3 |
| 1930.66.90f | turquoise | bead | 62.0 | 0.6 | 10.6 | 4.5 | 14.5 | 2.5 | 0.3 | 0.0 | 0.0 | 1.1 | 0.0 | 0.0 | 0.0 | 0.0 | 0.0 | 0.0 | 0.0 | 0.0 | 0.1 | 0.3 | 1.0 | 0.1 | 99.5 |
| 1930.66.90g | blue | bead | 65.9 | 0.3 | 5.5 | 6.8 | 15.5 | 3.8 | 0.2 | 0.0 | 0.0 | 1.2 | 0.0 | 0.0 | 0.0 | 0.0 | 0.0 | 0.0 | 0.0 | 0.0 | 0.1 | 0.2 | 0.8 | 0.0 | 100.6 |
| 1930.67.42 | green opaque | bead | 64.1 | 2.0 | 5.6 | 3.4 | 17.2 | 3.1 | 1.2 | 0.1 | 0.0 | 0.8 | 0.0 | 0.0 | 0.0 | 0.0 | 0.1 | 0.0 | 0.0 | 0.0 | 0.4 | 0.2 | 1.1 | 0.0 | 100.2 |
| 1930.67.67 | turquoise | bead | 63.9 | 0.5 | 9.9 | 3.4 | 13.5 | 2.6 | 0.3 | 0.0 | 0.0 | 1.3 | 0.0 | 0.0 | 0.0 | 0.0 | 0.0 | 0.0 | 0.0 | 0.0 | 0.2 | 0.3 | 0.8 | 0.2 | 99.0 |
| 1930.67.82 | turquoise | pendant | 66.8 | 0.5 | 8.3 | 3.0 | 13.6 | 2.7 | 0.3 | 0.0 | 0.0 | 1.5 | 0.0 | 0.0 | 0.0 | 0.0 | 0.0 | 0.0 | 0.0 | 0.0 | 0.3 | 0.2 | 1.0 | 0.1 | 100.4 |
| 1930.68.16 | green | bead | 64.1 | 0.8 | 5.6 | 3.8 | 15.3 | 2.2 | 4.7 | 0.0 | 0.0 | 2.5 | 0.1 | 0.1 | 0.0 | 0.0 | 0.0 | 0.0 | 0.0 | 0.1 | 0.2 | 0.3 | 0.9 | 0.0 | 100.6 |
| 1930.68.27c | turquoise | bead | 67.1 | 0.5 | 8.6 | 2.8 | 12.9 | 2.0 | 0.2 | 0.0 | 0.0 | 0.9 | 0.0 | 0.0 | 0.0 | 0.0 | 0.0 | 0.0 | 0.0 | 0.0 | 0.2 | 0.3 | 0.8 | 0.0 | 98.4 |
| 1930.68.27h | turquoise | bead | 65.0 | 0.4 | 8.3 | 2.6 | 15.0 | 2.7 | 0.2 | 0.0 | 0.0 | 1.2 | 0.0 | 0.0 | 0.0 | 0.0 | 0.0 | 0.0 | 0.0 | 0.0 | 0.2 | 0.3 | 0.9 | 0.1 | 98.5 |
| 1930.68.27k | blue | bead | 66.4 | 0.3 | 6.9 | 4.3 | 17.4 | 3.0 | 0.2 | 0.0 | 0.0 | 1.0 | 0.0 | 0.0 | 0.0 | 0.0 | 0.0 | 0.0 | 0.0 | 0.0 | 0.2 | 0.3 | 1.0 | 0.3 | 101.3 |
| 1930.69.39d | blue | bead | 59.6 | 0.4 | 6.4 | 4.5 | 19.5 | 2.5 | 0.2 | 0.0 | 0.0 | 1.2 | 0.0 | 0.0 | 0.0 | 0.0 | 0.0 | 0.0 | 0.0 | 0.0 | 0.2 | 0.2 | 1.2 | 0.0 | 95.9 |
| 1930.69.39f | blue | bead | 62.5 | 0.4 | 7.1 | 4.5 | 19.6 | 2.8 | 0.2 | 0.0 | 0.0 | 1.4 | 0.1 | 0.0 | 0.0 | 0.0 | 0.0 | 0.0 | 0.0 | 0.0 | 0.2 | 0.3 | 1.3 | 0.0 | 100.3 |
| 1930.82.13 | colorant-free | vessel | 66.5 | 0.7 | 6.2 | 4.4 | 17.3 | 3.0 | 0.3 | 0.1 | 0.0 | 0.0 | 0.0 | 0.0 | 0.0 | 0.0 | 0.1 | 0.0 | 0.0 | 0.0 | 0.2 | 0.3 | 1.1 | 0.0 | 100.0 |
| 1930.82.15a | blue | vessel | 66.7 | 0.4 | 4.8 | 4.8 | 15.5 | 2.7 | 0.2 | 0.0 | 0.0 | 3.0 | 0.0 | 0.0 | 0.0 | 0.0 | 0.0 | 0.0 | 0.0 | 0.0 | 0.1 | 0.2 | 1.0 | 0.0 | 99.6 |
| 1930.82.15b | blue | vessel | 66.8 | 0.5 | 4.9 | 4.9 | 15.5 | 2.8 | 0.2 | 0.0 | 0.0 | 2.9 | 0.0 | 0.0 | 0.1 | 0.0 | 0.0 | 0.0 | 0.0 | 0.0 | 0.2 | 0.2 | 1.0 | 0.0 | 99.9 |
| 1930.82.15b | yellow | inlay | 54.9 | 0.3 | 4.4 | 5.5 | 16.6 | 2.3 | 0.9 | 0.0 | 0.0 | 0.6 | 0.0 | 0.0 | 0.0 | 0.0 | 0.0 | 0.0 | 0.0 | 0.0 | 0.1 | 0.2 | 0.9 | 0.2 | 101.0 |
| 1930.82.16 | blue | vessel | 63.5 | 0.9 | 4.9 | 5.3 | 16.9 | 3.0 | 0.4 | 0.1 | 0.0 | 1.2 | 0.0 | 0.0 | 0.0 | 0.0 | 0.0 | 0.0 | 0.0 | 0.0 | 0.2 | 0.4 | 0.6 | 0.0 | 97.4 |
| 1930.82.17 | blue | vessel | 65.3 | 0.9 | 4.8 | 4.9 | 17.2 | 3.0 | 0.4 | 0.0 | 0.0 | 1.2 | 0.1 | 0.0 | 0.0 | 0.0 | 0.0 | 0.0 | 0.0 | 0.0 | 0.2 | 0.4 | 0.6 | 0.0 | 99.0 |
| 1930.82.18 | black | bead | 64.8 | 0.6 | 6.5 | 5.4 | 17.3 | 3.0 | 0.3 | 0.0 | 0.0 | 0.0 | 0.0 | 0.0 | 0.0 | 0.0 | 0.0 | 0.0 | 0.0 | 0.0 | 0.2 | 0.3 | 1.2 | 0.0 | 99.6 |
| 1930.82.4 | blue | vessel | 63.4 | 1.3 | 6.6 | 4.9 | 17.2 | 2.5 | 1.6 | 0.0 | 0.0 | 1.3 | 0.0 | 0.0 | 0.0 | 0.0 | 0.0 | 0.0 | 0.0 | 0.0 | 0.1 | 0.3 | 0.9 | 0.0 | 100.1 |
| 1930.82.48 | blue | pendant | 72.4 | 0.5 | 4.3 | 3.6 | 13.4 | 2.6 | 0.3 | 0.0 | 0.0 | 1.3 | 0.0 | 0.0 | 0.0 | 0.0 | 0.0 | 0.0 | 0.0 | 0.0 | 0.2 | 0.1 | 0.8 | 0.0 | 99.7 |
| 1930.82.50 | blue | raw glass | 65.5 | 0.4 | 8.6 | 4.0 | 14.3 | 3.1 | 0.2 | 0.0 | 0.0 | 2.1 | 0.0 | 0.0 | 0.0 | 0.0 | 0.0 | 0.0 | 0.0 | 0.0 | 0.1 | 0.2 | 1.1 | 0.0 | 99.6 |
| 1930.82.55 | blue | vessel | 60.9 | 0.7 | 6.0 | 6.2 | 16.6 | 4.7 | 0.3 | 0.0 | 0.0 | 1.1 | 0.0 | 0.0 | 0.0 | 0.0 | 0.0 | 0.0 | 0.0 | 0.0 | 0.2 | 0.4 | 0.6 | 0.0 | 97.7 |
| 1930.82.55 | white | unknown | 64.6 | 0.4 | 7.8 | 4.7 | 15.2 | 2.8 | 0.2 | 0.0 | 0.0 | 0.0 | 0.0 | 0.0 | 0.0 | 0.0 | 0.0 | 0.0 | 0.0 | 0.0 | 0.2 | 0.3 | 0.8 | 0.2 | 99.4 |
| 1930.82.62a | colorless | bead | 61.4 | 2.1 | 6.5 | 4.4 | 16.6 | 3.0 | 0.3 | 0.1 | 0.0 | 1.1 | 0.0 | 0.0 | 0.0 | 0.0 | 0.0 | 0.0 | 0.0 | 0.0 | 0.1 | 0.2 | 0.9 | 0.0 | 96.7 |
| 1930.82.62b | colorless | raw glass | 65.2 | 1.7 | 7.3 | 4.0 | 18.2 | 3.6 | 0.8 | 0.1 | 0.0 | 0.0 | 0.1 | 0.0 | 0.0 | 0.0 | 0.0 | 0.0 | 0.0 | 0.0 | 0.3 | 0.3 | 0.8 | 0.0 | 102.5 |
| 1930.82.62c | colorless | raw glass | 61.8 | 1.8 | 6.6 | 5.2 | 17.5 | 3.0 | 0.6 | 0.1 | 0.0 | 0.0 | 0.6 | 0.0 | 0.0 | 0.0 | 0.0 | 0.0 | 0.0 | 0.0 | 0.2 | 0.2 | 0.8 | 0.0 | 68.4 |
| 1930.82.62e | colorant-free | pendant | 64.4 | 0.5 | 7.1 | 4.8 | 16.8 | 2.3 | 0.2 | 0.0 | 0.0 | 0.0 | 0.0 | 0.0 | 0.0 | 0.0 | 0.0 | 0.0 | 0.0 | 0.0 | 0.3 | 0.2 | 0.9 | 0.0 | 97.6 |
| 1930.82.7 | blue | vessel | 65.0 | 0.3 | 4.6 | 4.8 | 17.0 | 4.3 | 0.2 | 0.0 | 0.0 | 1.1 | 0.0 | 0.0 | 0.0 | 0.0 | 0.0 | 0.0 | 0.0 | 0.0 | 0.2 | 0.3 | 0.9 | 0.0 | 98.7 |
| 1930.82.7 | blue | inlay | 61.7 | 0.5 | 7.6 | 4.7 | 16.1 | 4.2 | 0.3 | 0.0 | 0.0 | 0.7 | 0.0 | 0.0 | 0.0 | 0.0 | 0.0 | 0.0 | 0.0 | 0.0 | 0.2 | 0.3 | 0.9 | 0.2 | 99.1 |

Table 11: Bulk compositions 2nd millennium BC glasses

5.2 2nd millennium BC glass

The major oxides present in the 39 2nd millennium BC glasses analysed are: silica, lime, magnesia, soda and potash, defined here as elements present consistently at above 1% oxide weight, excluding deliberately added colorants. Silica is present at levels between 54.9% and 72.4%, however, only a single example is significantly below 60% (1930.82.15a a yellow glass inlay) and two above 70% (1930.62.31b and 1930.82.48, a translucent blue bead and pendant) with the average being 64.6%. Lime is present in the range 3.1% and 10.6% with an average of 6.7%; magnesia between 2.6% and 7.7%, average 4.4%; soda 12.1% to 19.6% average 15.9% and potash 1% to 4.7%, average 2.9%. The glasses also contain several minor oxides, those present at less than 1% oxide weight. Aluminium oxide is present in the range of 0.3% to 2.1%, however, only five samples contain more than 1% and the majority contain less than 0.5%. Iron oxide is also present at less than 1% apart from two examples over 1% and one sample (1930.82.16) which contains 4.7% iron oxide. Chlorine, sulphur and phosphorous are also present and there are small quantities of other elements, such as titanium dioxide, present at below 0.1% in some samples.

5.2.1 Raw materials

The compositional analysis of the glasses has indicated that they are soda lime silicates comprising of three main classes of raw materials: the network formers (silica); the network modifiers (fluxes) and colorants, usually metals. The major oxide composition of a glass can give information about the possible sources of raw materials used in its manufacture.

Silica source: The low levels of aluminium oxide, iron oxide and titanium dioxide found in the 2nd millennium BC glasses suggest that the silica source used to manufacture these glasses was relatively pure. Quartz pebbles have been suggested as the possible source of silica for glasses of this period (Turner, 1956; Shortland and Eremin 2006).

Fluxes: The level of potash and magnesia present in the 2nd millennium BC glasses indicate that these glasses were most probably manufactured using plant ashes as a flux. High levels of these oxides (usually >1.5%) are considered to indicate a plant ash alkali source as opposed to a mineral source of alkali such as natron (Brill, 1970:111). The plant ashes are thought to have come from desert or coastal plants, which contain high levels of soda, with the genera *Salicornia* and *Salsola* being suggested (Turner, 1956).

Colorants: Table 12 shows the 2nd millennium BC glasses broken down by colour. Almost all of the LBA glasses analysed are deliberately coloured using a variety of colorants and techniques; Figure 22 shows the main colours of glass.

| Sample | Colour | Object type | SiO ₂ | Al ₂ O ₃ | CaO | MgO | Na ₂ O | K ₂ O | Fe ₂ O ₃ | TiO ₂ | CoO | CuO | MnO | NiO | ZnO | SnO | Sb ₂ O ₃ | BaO | PbO | Cr ₂ O ₃ | P ₂ O ₅ | SO ₃ | Cl | SrO | Total | |
|--------------|---------------|-------------|------------------|--------------------------------|------|-----|-------------------|------------------|--------------------------------|------------------|-----|-----|-----|-----|-----|-----|--------------------------------|-----|-----|--------------------------------|-------------------------------|-----------------|-----|-----|-------|-------|
| 1930.60.140d | blue | bead | 66.2 | 0.5 | 4.2 | 3.8 | 15.9 | 3.0 | 0.3 | 0.1 | 0.0 | 0.0 | 2.0 | 0.1 | 0.0 | 0.0 | 0.0 | 0.0 | 0.0 | 0.0 | 0.0 | 0.2 | 0.2 | 0.0 | 0.0 | 97.2 |
| 1930.62.31b | blue | bead | 71.7 | 0.3 | 3.5 | 3.4 | 14.2 | 2.5 | 0.2 | 0.0 | 0.0 | 0.0 | 2.1 | 0.0 | 0.0 | 0.0 | 0.2 | 0.1 | 0.0 | 0.0 | 0.0 | 0.2 | 0.2 | 0.7 | 0.0 | 99.3 |
| 1930.66.90a | blue | bead | 66.0 | 0.3 | 6.9 | 4.0 | 17.6 | 3.0 | 0.2 | 0.0 | 0.0 | 0.0 | 1.0 | 0.0 | 0.0 | 0.0 | 0.0 | 0.0 | 0.0 | 0.0 | 0.0 | 0.2 | 1.0 | 0.0 | 100.6 | |
| 1930.66.90a | blue | bead | 66.4 | 0.3 | 6.9 | 4.3 | 17.4 | 3.0 | 0.2 | 0.0 | 0.0 | 0.0 | 1.0 | 0.0 | 0.0 | 0.0 | 0.0 | 0.0 | 0.0 | 0.0 | 0.0 | 0.2 | 0.3 | 1.0 | 0.0 | 101.3 |
| 1930.68.27k | blue | bead | 66.4 | 0.3 | 6.9 | 4.3 | 17.4 | 3.0 | 0.2 | 0.0 | 0.0 | 0.0 | 1.0 | 0.0 | 0.0 | 0.0 | 0.0 | 0.0 | 0.0 | 0.0 | 0.0 | 0.2 | 0.3 | 1.0 | 0.0 | 101.3 |
| 1930.69.35d | blue | bead | 59.6 | 0.4 | 6.4 | 4.5 | 19.5 | 2.8 | 0.2 | 0.0 | 0.0 | 0.0 | 1.2 | 0.0 | 0.0 | 0.0 | 0.0 | 0.0 | 0.0 | 0.0 | 0.0 | 0.2 | 0.2 | 1.2 | 0.0 | 95.9 |
| 1930.69.39f | blue | bead | 62.5 | 0.4 | 7.1 | 4.5 | 19.6 | 2.8 | 0.2 | 0.0 | 0.0 | 0.0 | 1.4 | 0.1 | 0.0 | 0.0 | 0.0 | 0.1 | 0.0 | 0.0 | 0.0 | 0.1 | 0.0 | 1.3 | 0.0 | 100.3 |
| 1930.82.15a | blue | vessel | 66.7 | 0.4 | 4.8 | 4.8 | 15.5 | 2.7 | 0.2 | 0.0 | 0.0 | 0.0 | 3.0 | 0.0 | 0.0 | 0.0 | 0.0 | 0.2 | 0.0 | 0.0 | 0.0 | 0.1 | 0.0 | 0.0 | 0.0 | 99.6 |
| 1930.82.15b | blue | vessel | 66.8 | 0.5 | 4.9 | 4.9 | 15.5 | 2.8 | 0.2 | 0.0 | 0.0 | 0.0 | 3.0 | 0.0 | 0.0 | 0.0 | 0.0 | 0.2 | 0.0 | 0.0 | 0.0 | 0.1 | 0.0 | 0.0 | 0.0 | 99.9 |
| 1930.82.16 | blue | vessel | 63.5 | 0.9 | 4.9 | 5.3 | 16.9 | 3.0 | 0.4 | 0.1 | 0.0 | 0.0 | 1.2 | 0.0 | 0.0 | 0.0 | 0.0 | 0.0 | 0.0 | 0.0 | 0.0 | 0.2 | 0.4 | 0.6 | 0.0 | 97.4 |
| 1930.82.17 | blue | vessel | 65.3 | 0.9 | 4.8 | 4.9 | 17.2 | 3.0 | 0.4 | 0.1 | 0.0 | 0.0 | 1.2 | 0.0 | 0.0 | 0.0 | 0.0 | 0.0 | 0.0 | 0.0 | 0.0 | 0.2 | 0.4 | 0.6 | 0.0 | 99.0 |
| 1930.82.4 | blue | vessel | 63.4 | 1.3 | 6.6 | 4.9 | 17.2 | 2.5 | 1.6 | 0.0 | 0.0 | 0.0 | 1.0 | 0.1 | 0.0 | 0.0 | 0.0 | 0.0 | 0.0 | 0.0 | 0.0 | 0.1 | 0.3 | 0.9 | 0.0 | 100.1 |
| 1930.82.48 | blue | pendant | 72.4 | 0.5 | 4.3 | 3.6 | 13.4 | 2.6 | 0.3 | 0.0 | 0.0 | 0.0 | 1.3 | 0.0 | 0.0 | 0.0 | 0.0 | 0.0 | 0.0 | 0.0 | 0.0 | 0.2 | 0.1 | 0.8 | 0.0 | 99.7 |
| 1930.82.50 | blue | raw glass | 60.9 | 0.4 | 8.6 | 4.0 | 14.3 | 3.1 | 0.2 | 0.0 | 0.0 | 0.0 | 2.1 | 0.0 | 0.0 | 0.0 | 0.0 | 0.0 | 0.0 | 0.0 | 0.0 | 0.1 | 0.2 | 1.1 | 0.0 | 99.6 |
| 1930.82.55 | blue | vessel | 65.9 | 0.7 | 6.0 | 6.2 | 16.6 | 4.7 | 0.3 | 0.0 | 0.0 | 0.0 | 1.1 | 0.0 | 0.0 | 0.0 | 0.0 | 0.2 | 0.0 | 0.0 | 0.0 | 0.1 | 0.2 | 0.6 | 0.0 | 97.7 |
| 1930.82.62a | blue | bead | 61.4 | 2.1 | 6.5 | 4.4 | 16.6 | 3.0 | 0.3 | 0.1 | 0.0 | 0.0 | 1.1 | 0.0 | 0.0 | 0.0 | 0.1 | 0.0 | 0.0 | 0.0 | 0.0 | 0.1 | 0.2 | 0.9 | 0.0 | 96.7 |
| 1930.82.7 | blue | vessel | 65.0 | 0.3 | 4.6 | 4.8 | 17.0 | 4.3 | 0.2 | 0.0 | 0.0 | 0.0 | 1.1 | 0.0 | 0.0 | 0.0 | 0.0 | 0.0 | 0.0 | 0.0 | 0.0 | 0.2 | 0.3 | 0.9 | 0.0 | 98.7 |
| 1930.82.7 | blue | inlay | 61.7 | 0.5 | 7.6 | 4.7 | 16.1 | 4.2 | 0.3 | 0.0 | 0.0 | 0.0 | 0.7 | 0.0 | 0.0 | 0.0 | 1.8 | 0.0 | 0.0 | 0.0 | 0.0 | 0.2 | 0.3 | 0.9 | 0.2 | 99.1 |
| 1930.66.90g | blue | bead | 65.9 | 0.3 | 5.5 | 6.8 | 15.5 | 3.8 | 0.2 | 0.0 | 0.0 | 0.0 | 1.2 | 0.0 | 0.0 | 0.0 | 0.0 | 0.0 | 0.0 | 0.0 | 0.0 | 0.1 | 0.2 | 0.8 | 0.0 | 100.6 |
| Average | | | 65.1 | 0.6 | 5.8 | 4.6 | 16.5 | 3.1 | 0.3 | 0.0 | 0.0 | 0.0 | 1.4 | 0.0 | 0.0 | 0.0 | 0.2 | 0.0 | 0.0 | 0.0 | 0.0 | 0.2 | 0.3 | 0.9 | 0.0 | |
| Sample | Colour | Object type | SiO ₂ | Al ₂ O ₃ | CaO | MgO | Na ₂ O | K ₂ O | Fe ₂ O ₃ | TiO ₂ | CoO | CuO | MnO | NiO | ZnO | SnO | Sb ₂ O ₃ | BaO | PbO | Cr ₂ O ₃ | P ₂ O ₅ | SO ₃ | Cl | SrO | Total | |
| 1930.62.103 | turquoise | bead | 65.1 | 0.5 | 8.8 | 3.5 | 16.9 | 3.0 | 0.3 | 0.0 | 0.0 | 0.0 | 1.0 | 0.0 | 0.0 | 0.0 | 0.0 | 1.6 | 0.0 | 0.0 | 0.0 | 0.4 | 0.4 | 1.0 | 0.1 | 100.3 |
| 1930.63.40d | turquoise | bead | 68.7 | 0.4 | 9.0 | 3.6 | 12.1 | 1.0 | 0.1 | 0.0 | 0.0 | 0.0 | 1.3 | 0.0 | 0.0 | 0.0 | 0.0 | 1.8 | 0.0 | 0.0 | 0.0 | 0.1 | 0.3 | 0.8 | 0.0 | 99.2 |
| 1930.66.90b | turquoise | bead | 65.2 | 0.3 | 8.9 | 3.5 | 12.5 | 2.6 | 0.1 | 0.0 | 0.0 | 0.0 | 1.7 | 0.0 | 0.0 | 0.0 | 0.0 | 3.1 | 0.0 | 0.0 | 0.0 | 0.2 | 0.3 | 0.8 | 0.0 | 99.1 |
| 1930.66.90c | turquoise | bead | 64.1 | 0.9 | 10.4 | 3.4 | 14.1 | 2.5 | 0.6 | 0.1 | 0.0 | 0.0 | 1.1 | 0.0 | 0.0 | 0.0 | 0.0 | 1.6 | 0.0 | 0.0 | 0.0 | 0.2 | 0.3 | 1.0 | 0.1 | 100.3 |
| 1930.66.90d | turquoise | bead | 66.8 | 0.3 | 9.0 | 3.7 | 12.6 | 2.5 | 0.1 | 0.0 | 0.0 | 0.0 | 1.7 | 0.0 | 0.0 | 0.0 | 0.0 | 2.7 | 0.0 | 0.0 | 0.0 | 0.2 | 0.3 | 0.8 | 0.2 | 100.3 |
| 1930.66.90f | turquoise | bead | 62.0 | 0.6 | 10.6 | 4.5 | 14.5 | 2.5 | 0.3 | 0.0 | 0.0 | 0.0 | 1.1 | 0.0 | 0.0 | 0.0 | 0.0 | 1.8 | 0.0 | 0.0 | 0.0 | 0.1 | 0.3 | 1.0 | 0.1 | 99.5 |
| 1930.67.67 | turquoise | bead | 63.9 | 0.5 | 9.9 | 3.4 | 13.5 | 2.6 | 0.3 | 0.0 | 0.0 | 0.0 | 1.3 | 0.0 | 0.0 | 0.0 | 0.0 | 2.0 | 0.0 | 0.0 | 0.0 | 0.2 | 0.3 | 0.8 | 0.2 | 99.0 |
| 1930.67.82 | turquoise | pendant | 66.8 | 0.5 | 8.3 | 3.0 | 13.6 | 2.7 | 0.3 | 0.0 | 0.0 | 0.0 | 1.5 | 0.0 | 0.0 | 0.0 | 0.0 | 1.9 | 0.0 | 0.0 | 0.0 | 0.2 | 0.3 | 0.8 | 0.2 | 99.0 |
| 1930.68.27c | turquoise | bead | 67.1 | 0.5 | 8.6 | 2.8 | 12.9 | 2.0 | 0.2 | 0.0 | 0.0 | 0.0 | 0.9 | 0.0 | 0.0 | 0.0 | 0.0 | 2.2 | 0.0 | 0.0 | 0.0 | 0.2 | 0.3 | 0.8 | 0.0 | 98.4 |
| 1930.68.27h | turquoise | bead | 65.0 | 0.4 | 8.3 | 2.6 | 15.0 | 2.7 | 0.2 | 0.0 | 0.0 | 0.0 | 1.2 | 0.0 | 0.0 | 0.0 | 0.0 | 1.7 | 0.0 | 0.0 | 0.0 | 0.2 | 0.3 | 0.9 | 0.1 | 98.5 |
| Average | | | 65.3 | 0.5 | 9.2 | 3.4 | 13.8 | 2.4 | 0.2 | 0.0 | 0.0 | 0.0 | 1.3 | 0.0 | 0.0 | 0.0 | 0.0 | 2.0 | 0.0 | 0.0 | 0.0 | 0.2 | 0.3 | 0.9 | 0.1 | |
| Sample | Colour | Object type | SiO ₂ | Al ₂ O ₃ | CaO | MgO | Na ₂ O | K ₂ O | Fe ₂ O ₃ | TiO ₂ | CoO | CuO | MnO | NiO | ZnO | SnO | Sb ₂ O ₃ | BaO | PbO | Cr ₂ O ₃ | P ₂ O ₅ | SO ₃ | Cl | SrO | Total | |
| 1930.62.52 | colorant-free | bead | 63.1 | 2.0 | 5.4 | 4.8 | 17.7 | 4.1 | 0.7 | 0.1 | 0.0 | 0.0 | 0.0 | 0.1 | 0.0 | 0.0 | 0.0 | 0.1 | 0.0 | 0.0 | 0.0 | 0.5 | 0.4 | 0.9 | 0.0 | 99.9 |
| 1930.63.37 | colorant-free | bead | 63.6 | 0.6 | 6.1 | 4.7 | 16.1 | 2.3 | 0.3 | 0.1 | 0.0 | 0.0 | 0.0 | 0.0 | 0.0 | 0.0 | 0.0 | 0.1 | 0.0 | 0.0 | 0.0 | 0.2 | 0.2 | 1.1 | 0.0 | 95.4 |
| 1930.82.13 | colorant-free | vessel | 66.5 | 0.7 | 6.2 | 4.4 | 17.3 | 3.0 | 0.3 | 0.1 | 0.0 | 0.0 | 0.0 | 0.0 | 0.0 | 0.0 | 0.0 | 0.1 | 0.0 | 0.0 | 0.0 | 0.2 | 0.3 | 1.1 | 0.0 | 100.0 |
| 1930.82.62a | colorant-free | pendant | 64.4 | 0.5 | 7.1 | 4.8 | 16.8 | 2.3 | 0.2 | 0.0 | 0.0 | 0.0 | 0.0 | 0.0 | 0.0 | 0.0 | 0.0 | 0.1 | 0.0 | 0.0 | 0.0 | 0.3 | 0.2 | 0.9 | 0.0 | 97.6 |
| 1930.82.18 | black | bead | 64.8 | 0.6 | 6.5 | 5.4 | 17.3 | 3.0 | 0.3 | 0.0 | 0.0 | 0.0 | 0.0 | 0.0 | 0.0 | 0.0 | 0.0 | 0.1 | 0.0 | 0.0 | 0.0 | 0.2 | 0.3 | 1.2 | 0.0 | 99.6 |
| Average | | | 64.5 | 0.9 | 6.3 | 4.8 | 17.0 | 2.9 | 0.4 | 0.1 | 0.0 | 0.0 | 0.0 | 0.0 | 0.0 | 0.0 | 0.0 | 0.1 | 0.0 | 0.0 | 0.0 | 0.2 | 0.3 | 1.0 | 0.0 | |
| Sample | Colour | Object type | SiO ₂ | Al ₂ O ₃ | CaO | MgO | Na ₂ O | K ₂ O | Fe ₂ O ₃ | TiO ₂ | CoO | CuO | MnO | NiO | ZnO | SnO | Sb ₂ O ₃ | BaO | PbO | Cr ₂ O ₃ | P ₂ O ₅ | SO ₃ | Cl | SrO | Total | |
| 1930.82.59 | white | unknown | 64.6 | 0.4 | 7.8 | 4.7 | 15.2 | 2.8 | 0.2 | 0.0 | 0.0 | 0.0 | 0.0 | 0.0 | 0.0 | 0.0 | 0.0 | 2.3 | 0.0 | 0.0 | 0.0 | 0.2 | 0.3 | 0.8 | 0.2 | 99.4 |
| 1930.60.140a | yellow | bead | 67.4 | 1.2 | 3.1 | 3.9 | 13.9 | 1.5 | 0.5 | 0.1 | 0.0 | 0.0 | 0.0 | 0.0 | 0.0 | 0.0 | 0.0 | 0.5 | 0.0 | 0.0 | 0.0 | 0.1 | 0.3 | 0.6 | 0.0 | 101.2 |
| 1930.82.15b | yellow | inlay | 54.9 | 0.3 | 4.4 | 5.5 | 16.6 | 2.3 | 0.9 | 0.0 | 0.0 | 0.0 | 0.6 | 0.0 | 0.0 | 0.0 | 0.0 | 3.2 | 0.0 | 0.0 | 0.0 | 0.1 | 0.2 | 0.9 | 0.2 | 101.0 |
| 1930.82.62b | colourless | raw glass | 65.2 | 1.7 | 7.2 | 4.0 | 18.2 | 3.6 | 0.8 | 0.1 | 0.0 | 0.0 | 0.1 | 0.0 | 0.0 | 0.0 | 0.0 | 0.1 | 0.0 | 0.0 | 0.0 | 0.3 | 0.3 | 0.8 | 0.0 | 102.5 |
| 1930.82.62c | colourless | raw glass | 61.8 | 1.8 | 6.6 | 5.2 | 17.3 | 3.0 | 0.6 | 0.1 | 0.0 | 0.0 | 0.0 | 0.0 | 0.0 | 0.0 | 0.0 | 0.1 | 0.0 | 0.0 | 0.0 | 0.2 | 0.2 | 0.8 | 0.0 | 68.4 |
| 1930.68.16 | green | bead | 64.1 | 0.8 | 5.6 | 3.8 | 15.3 | 2.2 | 4.7 | 0.0 | 0.0 | 0.0 | 2.5 | 0.1 | 0.1 | 0.0 | 0.0 | 0.1 | 0.0 | 0.0 | 0.1 | 0.2 | 0.3 | 0.9 | 0.0 | 100.6 |
| 1930.67.42 | green opaque | bead | 64.1 | 2.0 | 5.6 | 3.4 | 17.2 | 3.1 | 1.2 | 0.1 | 0.0 | 0.0 | 0.8 | 0.0 | 0.0 | 0.0 | 0.1 | 0.1 | 0.0 | 0.0 | 0.0 | 0.4 | 0.2 | 1.1 | 0.0 | 100.2 |

Table 12: 2nd millennium BC glass by colour

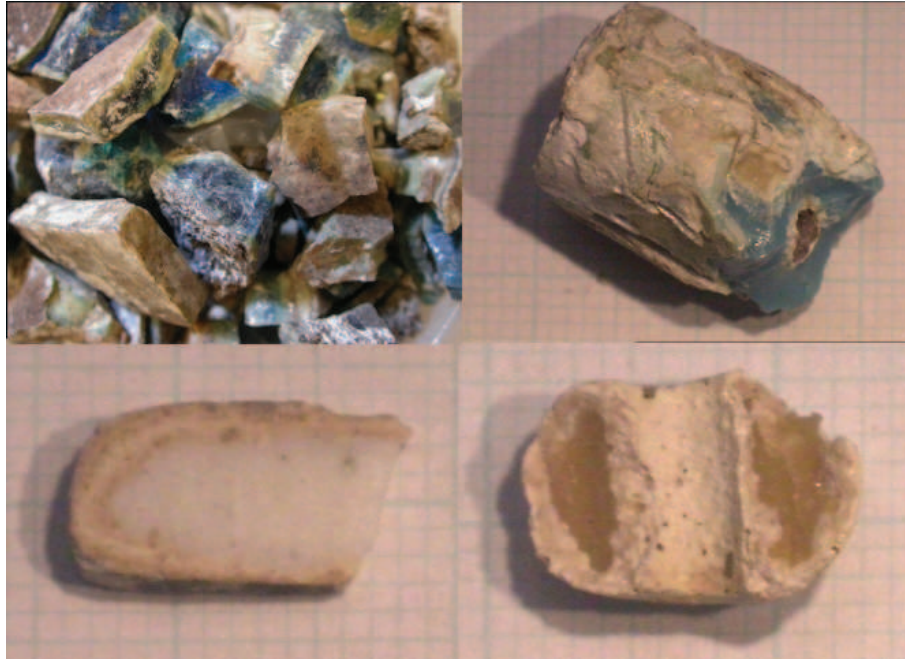


Figure 22: Examples of translucent blue, opaque blue, white and yellow glass

Translucent blue: The 2nd millennium BC translucent blue glasses were produced by the addition of copper as Cu^{2+} ions, acting as network modifiers (Weyl 1955:60). The depth of colour is determined by the number of oxygen ions around each Cu^{2+} ion and their distribution within the glass network (Weyl 1955:164). Lower melting temperatures favour the formation of a blue colour and at higher temperatures the glass becomes a greener colour as Cu^+ ions are also formed. The presence of magnesia within a glass melt also favours the production of bluer colours and sodium oxide alkali produces a better colour than potassium oxide (Weyl 1955:167).

Opaque turquoise: The opaque appearance of these glasses is caused by the addition of antimony oxide in the glass melt. From the liquid glass batch the antimony crystallises on cooling, taking up calcium oxide from the glass, and forms calcium antimonate crystals, usually in the form of $\text{Ca}_2\text{Sb}_2\text{O}_7$ (Shortland, 2002), these are clearly visible on SEM images, Figure 24a. These crystals scatter the light coming into the glass giving it its opaque appearance. The combination of copper (creating the blue colour) and calcium antimonate crystals produces the opaque turquoise colour observed.

White: White glass is produced by adding antimony oxide to colourless glass, again the formation of calcium antimonate crystals creates the opaque appearance. A single example of unaltered white glass has been analysed so far (1930.82.59) and was found to contain no colorant other than the antimony oxide used as an opacifier. A number of altered white glasses were also identified on SEM analysis from the presence of antimony oxide within the glass, the presence of calcium antimonate crystals being unaffected by post-depositional processes. For example, 1930.82.58 was from a group of fragments which are recorded as being a thin-walled vessel, although they lack the curve that would be expected and may come from

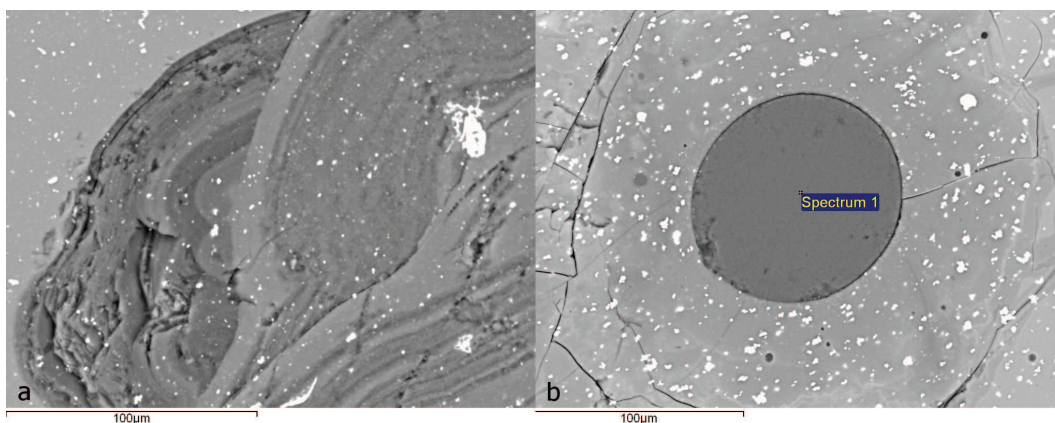


Figure 23: a: Calcium antimonate in opaque turquoise glass 1930.68.27c; b: Lead antimonate in yellow inlay 1930.82.15b

another type of object. No definite white glass beads have been found in the analyses carried out so far, although some beads may have had inlays or other decoration as white glass inlay has been noted in the vessel glasses. For example, 1930.82.7 has apparently opaque blue decoration which on closer examination with SEM was found to be a white inlay which had 'bled' into the blue translucent glass body of the vessel

Yellow: The yellow colour is produced by the presence of lead antimonate particles ($\text{Pb}_2\text{Sb}_2\text{O}_7$), which was also used as a yellow pigment, (Shortland 2002) in contrast to calcium antimonate, where the crystals are formed on cooling, lead antimonate is thought to have been added in that form to the liquid glass melt (Shortland 2002). However, in the only unaltered yellow bead analysed (1930.60.140a) antimony oxide is present at only 0.5%; this and the appearance of the unaltered portions of the bead suggest that it was a near translucent yellow. This is in contrast to the yellow inlays, and most of the altered yellow beads, which contain several weight percent of antimony oxide as well as lead suggesting that they were deliberately opacified with lead antimonate. A number of glasses coloured with lead antimonate that did not contain any unaltered glass are also known, these are detailed in Table 22, Section 6.1. The lead colorant is clearly visible on SEM images with compositional analysis confirming the presence of antimony and lead oxides, Figure 23b.

Green: A single opaque green cylindrical bead (1930.67.42) from a known Bronze Age context was analysed and was found to contain copper and lead as colorants, interestingly the antimony oxide levels are very low in this bead, 0.1% suggesting that lead antimonate crystals are not creating the yellow part of the colour observed. In contrast the only other example of a green glass from a Bronze Age context found within the museum assemblage is a translucent green eye bead (1930.68.18) which appears to have been coloured with a mixture of iron and copper as it contains high levels of both metals (4.7% FeO and 2.5% CuO). Iron is known to create a wide range of colours within glasses depending on the oxidising conditions within the glass melt (Weyl 1955:92-5). The green colour observed in this bead could have been created by iron oxide giving a green-brown colour and copper oxide the strong blue; experimental work has indicated that

mixing these oxides, in similar quantities, in faience glazes can create a strong greenish blue colour (Tite et al 2008a).

Colorant-free: Five amber-to-black coloured glasses were analysed. No colorant metals were found within these glasses and the brown-amber colour of the glass is probably caused by the creation of a chromophore from small quantities of iron and sulfur in the glass; under reducing conditions in the melt, from the addition of a reducing agent such as carbon, even very small quantities of these elements can create a strong colour (Weyl 1955:254-5; Beerkens 2003). For example, 1930.82.18, a black glass eye bead was found to contain no colorants, the black colour being produced solely by the small amounts of sulfur and iron oxides in the glass (0.3% of each).

Black altered glasses: The only possible other black glasses analysed were two very heavily altered eye beads 1930.63.59c and 1930.68.27b which contained small particles of copper sulfide (CuS) typically only a few microns across (Figure 24). A parallel for these glasses is noted from Hasanlu in Iran, where an assemblage of glass from the Early Iron Age (the assemblage dates from 11th to 9th century BC) has been extensively studied. The black glasses from Hasanlu are all coloured by copper sulfide particles, which are interpreted as being from smelting byproducts of sulfidic copper ores such as chalcopyrite (Stapleton and Swanson 2002). However, no unaltered black glasses of this type have been found in the Nuzi assemblage thus far.

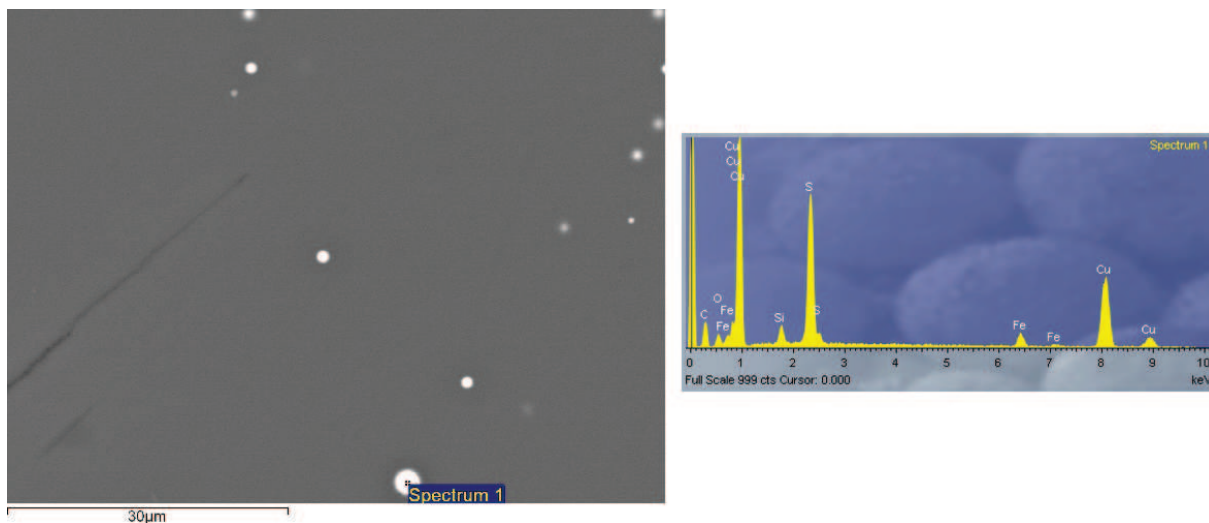


Figure 24: 1930.: SEM image altered black glass, CuS inclusions visible as bright white specks

Colourless: Two colourless fragments were analysed, 1930.82.62b and 1930.82.62c. They have similar levels of major and minor oxides as the rest of the LBA glasses apart from somewhat higher aluminium oxide levels than most of the other samples analysed (1.8% and 1.7%). 1930.82.62c also contained significant manganese oxide (0.6%) and both fragments had a light green-blue tint caused by the presence of iron oxide (0.8% and 0.6%).

5.2.2 Compositional variation within the 2nd millennium BC glasses

The opaque blue glasses are compositionally distinct from their translucent counterparts in being, on average, significantly lower in soda and higher in lime (13.8% Na₂O in the opaque glasses compared to 16.6% in the translucent glasses and 9.2% CaO compared to 5.8%), Figure 25. They are also slightly lower in potash and magnesia (2.4% K₂O in the opaque glasses compared to 3.1% in the translucent glasses and 3.4% MgO compared to 4.8%).

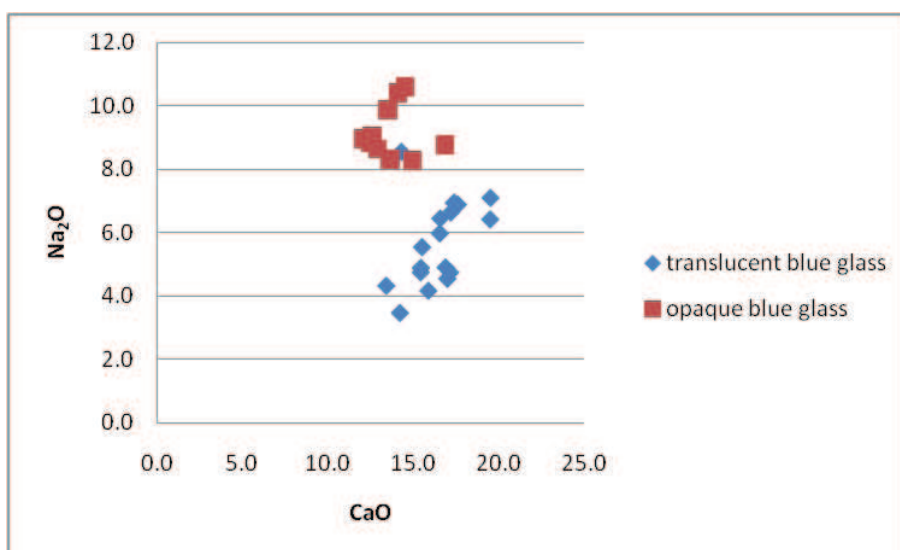


Figure 25: Compositional difference between translucent and opaque glasses Nuzi

A single example of unaltered white glass has been analysed so far and compositionally it sits well with the other glasses sampled containing slightly less soda and more lime than the translucent blue and colorant-free glasses but similar levels to the antimony-opacified turquoise glasses. 1930.82.59 also contains very low levels of aluminium and iron oxides consistent with the majority of the 2nd millennium BC glasses.

Only one unaltered yellow glass bead has been found so far in the Nuzi assemblage, it is comparable in composition to the other glasses with levels of potash and magnesia suggesting a plant ash glass. However, it is somewhat at the lower end of the scale in terms of lime and soda levels (3.1% CaO and 13.9% Na₂O) and also contains a high amount of lead oxide (8.2%), which may have affected the proportions of the other oxides present. The only unaltered yellow glass inlay contained significantly less silica than the other glasses (54.9% compared to the average of 64.6%) and also contained significant quantities of antimony and lead oxides (3.2% Sb₂O₅ and 10.9% PbO) which again may have affected the rest of the composition.

The solitary translucent green eye bead was found to be similar in composition to the translucent blue glasses for most major elements apart from iron; 1930.68.16 contained 4.7% iron oxide, compared to less than 1% in most of the blue glasses, alongside manganese, nickel and chromium oxides present at around 0.1%, which were not found in the translucent blue glasses. The opaque green bead (1930.67.42) contains

higher aluminium oxide than the majority of the LBA glasses analysed (1.9%) but otherwise resembles the translucent blue glasses in terms of its major oxide composition.

On analysis the colorant-free glasses were found to correspond well with the translucent blue glasses, containing similar amounts of the major elements, but no colorants. One of the amber glasses was found, however, to contain higher aluminium oxide (2%) and tin oxide at a level just above the detection limit (0.04%). On SEM imaging this inlaid bead was found to have areas of unknown composition alongside the glass which contained tin-rich inclusions (Figure 26).

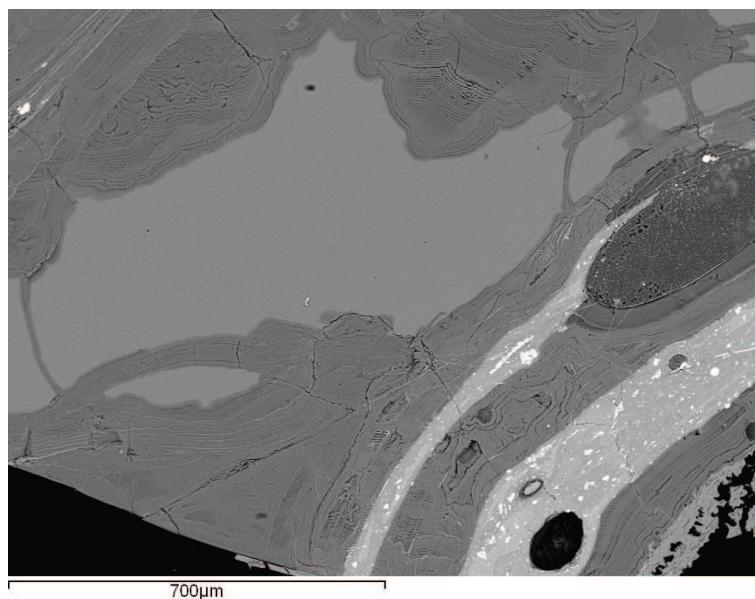


Figure 26: Colorant-free glass bead with tin-rich inclusions in inlay (1930.62.52)

5.3 Later glass

A number of glasses from a much later period than the Late Bronze Age examples discussed above were also analysed. These were considered to be later based on their composition, which is generally higher in aluminium and titanium oxides, the form of the object or an indication from the finds notebooks that the object came from a later context.

Table 13 details the Late period glasses analysed. The majority are colourless and split into three groups: the first group consists of plant ash alkali glasses, which contain significant potash and magnesia; the second, glasses that contain low levels of potash and magnesia, considered to be made with a mineral soda such as natron; and the third group which is a small number of coloured glasses.

The 20 colourless plant ash glasses have relatively wide ranges within their major oxide levels: silica ranges from 58.0% to 68.5% with an average of 63.4%; lime is present at 4.4% to 10.1%, average 7.8%; magnesia 2.8% to 7.4%, average 5.1%; soda 12.8% to 18.6%, average 15.4% and potash 1.2% to 4.1%, average

| Plant ash glasses | | SiO ₂ | Al ₂ O ₃ | CaO | MgO | Na ₂ O | K ₂ O | Fe ₂ O ₃ | TiO ₂ | CoO | CuO | MnO | NiO | ZnO | SnO | Sb ₂ O ₃ | BaO | PbO | Cl ₂ O ₃ | P ₂ O ₅ | SO ₃ | Cl | SrO | Total | |
|-------------------|--------------|------------------|--------------------------------|-----|------|-------------------|------------------|--------------------------------|------------------|-----|-----|-----|-----|-----|-----|--------------------------------|-----|-----|--------------------------------|-------------------------------|-----------------|-----|-----|-------|-------|
| Sample | Colour | Object type | 64.1 | 1.3 | 4.4 | 6.9 | 15.2 | 2.8 | 0.4 | 0.1 | 0.0 | 0.0 | 1.4 | 0.0 | 0.0 | 0.0 | 0.0 | 0.0 | 0.0 | 0.0 | 0.1 | 0.3 | 0.7 | 0.0 | 97.6 |
| 1930.43.38 | colourless | vessel | 61.2 | 1.8 | 8.5 | 5.4 | 17.7 | 3.0 | 0.7 | 0.2 | 0.0 | 0.0 | 0.0 | 0.0 | 0.0 | 0.0 | 0.0 | 0.0 | 0.0 | 0.0 | 0.2 | 0.5 | 0.7 | 0.0 | 99.9 |
| 1930.52.1a | colourless | vessel | 64.4 | 2.2 | 7.7 | 5.1 | 15.6 | 2.8 | 0.8 | 0.1 | 0.0 | 0.0 | 0.0 | 0.0 | 0.0 | 0.1 | 0.0 | 0.0 | 0.0 | 0.0 | 0.2 | 0.3 | 0.7 | 0.0 | 100.0 |
| 1930.67.45a | colourless | vessel | 63.0 | 2.2 | 5.9 | 5.1 | 14.6 | 3.0 | 0.8 | 0.1 | 0.0 | 0.0 | 1.3 | 0.0 | 0.0 | 0.0 | 0.0 | 0.0 | 0.0 | 0.0 | 0.2 | 0.2 | 0.6 | 0.0 | 97.2 |
| 1930.67.45b | colourless | vessel | 66.8 | 1.2 | 5.4 | 5.4 | 14.7 | 2.8 | 0.4 | 0.1 | 0.0 | 0.0 | 1.1 | 0.0 | 0.0 | 0.0 | 0.0 | 0.0 | 0.0 | 0.0 | 0.1 | 0.3 | 0.5 | 0.0 | 98.9 |
| 1930.82.28 | colourless | vessel | 59.8 | 3.9 | 9.9 | 4.6 | 14.5 | 2.7 | 1.4 | 0.2 | 0.0 | 0.0 | 0.4 | 0.0 | 0.0 | 0.0 | 0.0 | 0.0 | 0.0 | 0.0 | 0.4 | 0.3 | 0.5 | 0.0 | 98.6 |
| 1930.82.30 | colourless | vessel | 58.0 | 3.4 | 9.3 | 4.8 | 17.2 | 1.2 | 1.1 | 0.2 | 0.0 | 0.0 | 0.9 | 0.0 | 0.0 | 0.0 | 0.0 | 0.0 | 0.0 | 0.0 | 0.2 | 0.2 | 1.1 | 0.0 | 97.5 |
| 1930.82.31 | colourless | vessel | 61.2 | 3.8 | 10.1 | 4.7 | 15.0 | 2.6 | 1.4 | 0.2 | 0.0 | 0.0 | 0.4 | 0.0 | 0.0 | 0.0 | 0.0 | 0.0 | 0.0 | 0.0 | 0.4 | 0.3 | 0.5 | 0.0 | 100.6 |
| 1930.82.32 | colourless | vessel | 68.3 | 3.5 | 7.0 | 3.6 | 14.7 | 1.5 | 1.1 | 0.2 | 0.0 | 0.0 | 0.0 | 0.0 | 0.0 | 0.0 | 0.0 | 0.0 | 0.0 | 0.0 | 0.1 | 0.2 | 0.9 | 0.0 | 101.1 |
| 1930.82.33 | colourless | vessel | 66.4 | 1.4 | 7.7 | 4.5 | 14.0 | 2.6 | 0.9 | 0.2 | 0.0 | 0.1 | 0.1 | 0.0 | 0.0 | 0.0 | 0.1 | 0.0 | 0.0 | 0.0 | 0.2 | 0.3 | 0.6 | 0.0 | 98.8 |
| 1930.82.34 | colourless | vessel | 62.9 | 2.4 | 7.7 | 5.8 | 16.2 | 2.8 | 0.6 | 0.1 | 0.0 | 0.0 | 0.1 | 0.0 | 0.0 | 0.0 | 0.1 | 0.0 | 0.0 | 0.0 | 0.2 | 0.3 | 0.6 | 0.0 | 100.4 |
| 1930.82.35 | colourless | vessel | 68.5 | 1.5 | 7.1 | 2.8 | 13.6 | 3.1 | 0.7 | 0.1 | 0.0 | 0.0 | 0.0 | 0.0 | 0.0 | 0.0 | 0.1 | 0.0 | 0.0 | 0.0 | 0.3 | 0.3 | 0.7 | 0.0 | 98.7 |
| 1930.82.36 | colourless | vessel | 66.2 | 1.3 | 8.8 | 4.6 | 12.8 | 2.4 | 0.4 | 0.1 | 0.0 | 0.0 | 0.3 | 0.0 | 0.0 | 0.0 | 0.0 | 0.0 | 0.0 | 0.0 | 0.1 | 0.3 | 0.7 | 0.0 | 98.2 |
| 1930.82.37 | colourless | vessel | 61.7 | 1.3 | 7.7 | 6.6 | 17.2 | 3.2 | 0.5 | 0.1 | 0.0 | 0.0 | 0.3 | 0.0 | 0.0 | 0.0 | 0.1 | 0.0 | 0.0 | 0.0 | 0.2 | 0.3 | 0.7 | 0.0 | 99.9 |
| 1930.82.44 | colourless | vessel | 63.5 | 2.2 | 9.0 | 4.7 | 13.6 | 2.5 | 0.9 | 0.1 | 0.0 | 0.0 | 0.0 | 0.0 | 0.0 | 0.0 | 0.0 | 0.0 | 0.0 | 0.0 | 0.2 | 0.3 | 0.8 | 0.0 | 97.9 |
| 1930.82.45a | colourless | vessel | 62.5 | 1.1 | 7.7 | 7.4 | 16.2 | 2.9 | 0.4 | 0.1 | 0.0 | 0.0 | 0.4 | 0.0 | 0.0 | 0.0 | 0.1 | 0.0 | 0.0 | 0.0 | 0.2 | 0.2 | 0.8 | 0.0 | 99.8 |
| 1930.82.46 | colourless | vessel | 66.5 | 1.7 | 8.1 | 4.1 | 13.0 | 2.4 | 0.6 | 0.1 | 0.0 | 0.0 | 0.3 | 0.0 | 0.0 | 0.0 | 0.0 | 0.0 | 0.0 | 0.0 | 0.2 | 0.3 | 0.8 | 0.0 | 98.0 |
| 1930.82.6a | colourless | vessel | 66.3 | 0.7 | 8.3 | 5.0 | 16.7 | 2.2 | 0.4 | 0.0 | 0.0 | 0.0 | 0.0 | 0.0 | 0.0 | 0.0 | 0.1 | 0.0 | 0.0 | 0.0 | 0.1 | 0.4 | 0.9 | 0.0 | 101.1 |
| Average | | | 63.7 | 2.1 | 7.8 | 5.0 | 15.3 | 2.7 | 0.8 | 0.1 | 0.0 | 0.0 | 0.4 | 0.0 | 0.0 | 0.0 | 0.0 | 0.0 | 0.0 | 0.0 | 0.2 | 0.3 | 0.7 | 0.0 | |
| Natron glasses | | SiO ₂ | Al ₂ O ₃ | CaO | MgO | Na ₂ O | K ₂ O | Fe ₂ O ₃ | TiO ₂ | CoO | CuO | MnO | NiO | ZnO | SnO | Sb ₂ O ₃ | BaO | PbO | Cl ₂ O ₃ | P ₂ O ₅ | SO ₃ | Cl | SrO | Total | |
| 1930.69.33 | colourless | bead | 65.4 | 2.6 | 7.6 | 0.9 | 17.4 | 0.6 | 0.7 | 0.1 | 0.0 | 0.0 | 0.1 | 0.0 | 0.0 | 0.0 | 0.8 | 0.0 | 0.0 | 0.0 | 0.1 | 0.3 | 1.2 | 0.0 | 97.7 |
| 1930.82.12 | colourless | vessel | 71.8 | 2.0 | 5.8 | 0.4 | 16.8 | 0.4 | 0.3 | 0.1 | 0.0 | 0.0 | 0.0 | 0.0 | 0.0 | 0.0 | 0.6 | 0.0 | 0.0 | 0.0 | 0.0 | 1.3 | 0.0 | 0.0 | 99.6 |
| 1930.82.21 | colourless | vessel | 69.4 | 3.1 | 7.5 | 0.6 | 17.7 | 0.4 | 0.4 | 0.1 | 0.0 | 0.0 | 0.0 | 0.0 | 0.0 | 0.0 | 0.9 | 0.0 | 0.0 | 0.0 | 0.0 | 1.3 | 0.0 | 0.0 | 101.6 |
| 1930.82.6b | colourless | vessel | 68.6 | 3.1 | 7.5 | 0.6 | 17.5 | 0.4 | 0.3 | 0.1 | 0.0 | 0.0 | 0.0 | 0.0 | 0.0 | 0.0 | 0.9 | 0.0 | 0.0 | 0.0 | 0.0 | 1.3 | 0.0 | 0.0 | 100.5 |
| 1930.82.47 | green | raw glass | 67.4 | 3.5 | 8.6 | 0.7 | 14.7 | 0.7 | 0.5 | 0.1 | 0.0 | 0.0 | 0.2 | 0.0 | 0.0 | 0.0 | 0.0 | 0.0 | 0.0 | 0.0 | 0.2 | 0.1 | 0.9 | 0.0 | 97.5 |
| Average | | | 68.5 | 2.8 | 7.4 | 0.6 | 16.8 | 0.5 | 0.4 | 0.1 | 0.0 | 0.0 | 0.1 | 0.0 | 0.0 | 0.0 | 0.7 | 0.0 | 0.0 | 0.0 | 0.1 | 0.2 | 1.2 | 0.0 | |
| Coloured glasses | | SiO ₂ | Al ₂ O ₃ | CaO | MgO | Na ₂ O | K ₂ O | Fe ₂ O ₃ | TiO ₂ | CoO | CuO | MnO | NiO | ZnO | SnO | Sb ₂ O ₃ | BaO | PbO | Cl ₂ O ₃ | P ₂ O ₅ | SO ₃ | Cl | SrO | Total | |
| 1930.66.89a | yellow | bead | 55.6 | 3.0 | 10.2 | 4.1 | 15.6 | 1.9 | 1.1 | 0.2 | 0.0 | 0.0 | 0.0 | 0.0 | 0.0 | 0.0 | 0.0 | 6.3 | 0.0 | 0.0 | 0.3 | 0.3 | 0.7 | 0.0 | 101.0 |
| 1930.69.39 | green opaque | bead | 62.0 | 1.9 | 6.9 | 5.1 | 16.4 | 2.7 | 0.6 | 0.1 | 0.0 | 0.7 | 0.0 | 0.0 | 0.0 | 0.1 | 0.0 | 2.9 | 0.0 | 0.0 | 0.2 | 0.2 | 1.1 | 0.0 | 101.1 |
| 1930.60.56 | black | bead inlay | 64.6 | 2.7 | 6.5 | 3.9 | 16.4 | 2.7 | 1.3 | 0.1 | 0.1 | 0.1 | 0.1 | 0.0 | 0.0 | 0.0 | 0.1 | 0.0 | 0.1 | 0.0 | 0.3 | 0.2 | 0.9 | 0.0 | 100.1 |
| N124 | black | bracelet | 62.7 | 0.7 | 7.9 | 6.1 | 18.7 | 3.3 | 0.3 | 0.0 | 0.0 | 0.0 | 0.0 | 0.0 | 0.0 | 0.0 | 0.1 | 0.0 | 0.0 | 0.0 | 0.2 | 1.1 | 0.8 | 0.0 | 101.8 |
| 1930.82.11 | dark blue | fused to clear | 60.8 | 1.9 | 7.1 | 3.7 | 11.1 | 4.2 | 1.4 | 0.1 | 0.0 | 0.0 | 0.0 | 0.0 | 1.0 | 0.0 | 1.0 | 0.0 | 0.0 | 0.0 | 0.3 | 0.3 | 0.6 | 0.0 | 99.0 |
| 1930.82.38 | blue | vessel | 60.7 | 1.5 | 6.7 | 7.7 | 17.4 | 3.2 | 0.5 | 0.1 | 0.0 | 0.8 | 0.1 | 0.0 | 0.1 | 0.1 | 0.0 | 0.2 | 0.0 | 0.0 | 0.2 | 0.4 | 0.5 | 0.0 | 100.0 |

Table 13: Late period glass bulk compositions

2.7%. These glasses also contained much higher levels of aluminium oxide than the earlier glasses with levels ranging from 0.7% to 3.9%, and an average of 2.0%. Iron is also present in small quantities ranging from 0.3% to 1.5%, average 0.8% and it is this that gives these glasses their faint green to greenish-blue tints. These glasses split into two further groups the first containing manganese oxide at levels below 0.1% (eight samples) and those containing significant manganese oxide ranging from 0.14% to 1.4%. Manganese oxide was used as a decolorant in later periods to cancel out the effects of the iron oxide present (Shelby 2005: 215). These glasses also contain higher titanium dioxide levels than the Late Bronze Age glasses, 0.14% on average for the Late plant ash, colourless, glasses compared to 0.03% in the translucent blue LBA glasses.

The second group comprises of five samples and on analysis were found to contain: silica from 65.4% to 71.8%, average 68.5%; lime 5.8% to 8.6%, average 7.4%; magnesia 0.4% to 0.9%, average 0.6%, soda 14.7% to 17.6%, average 16.8%; and potash 0.4% to 0.7%, average 0.5%. Aluminium oxide levels range from 1.9% to 3.5%, average 2.8% with iron present from 0.3% to 0.7%, average 0.4%. The alkali source in these glasses is most probably natron, which is an evaporite mineral usually containing relatively pure soda (Shortland et al 2006). Natron glasses, or LMGs, are characterised by low levels of magnesium and potassium oxides (<1%) (Turner, 1956; Sayre and Smith, 1961). Natron was not used in Bronze Age glasses, the first examples dating from the early first millennium BC (Schlick-Nolte and Werthemann 2003; Reade et al 2005) and was the predominant source of alkali in Roman glasses. Four of the five natron type glasses also contain antimony oxide from 0.6% to 0.9%; antimony is added to glass as a fining agent and decolorant (Shelby 2005: 44). It is noticeable that these glasses were almost completely colourless whereas the other natron glass sample which does not contain any antimony (1930.82.47) is a pale green colour.

Several late coloured glasses were also found, the compositional analyses can be seen in Table 13. 1930.82.38 is a blue plant ash glass, which although similar to the LBA examples for most oxides contains much more aluminium oxide, 1.5% compared to the average of 0.6% in the LBA glasses. 1930.66.89a is an opaque bright yellow bead which has a somewhat different composition from the 2nd millennium BC glasses. This bead contains 55.6% silica, 10.2% lime, 4.1% magnesia, 15.6% soda and 1.9% potash, with the exception of the silica this is not significantly different from most of the LBA glasses, however, this bead also contains 3.0% aluminium oxide, 1.1% iron oxide and 0.2% titanium dioxide, much higher than most of the earlier glasses. In addition the colorant of this glass is lead-tin yellow (0.9% SnO and 6.3% PbO), which is only found from the late 1st millennium BC onwards (Tite et al, 2008b). For the opaque yellow bead, 1930.66.89a, a documented site location could not be found and it may come from the Parthian settlement, which overlay some parts of the site; the Sassanian period cemetery, or could even be a modern surface find. The opaque green bead, 1930.69.39, is from an apparent Bronze Age context (F24) but may be intrusive despite having a similar composition to the 2nd millennium BC glasses; again

significant amounts of tin and lead oxides are present (0.2% SnO and 2.9% PbO) alongside copper oxide at 0.7%, creating the green colour.

Two other probable late glasses are a dark blue glass fragment fused to a piece of ceramic (1930.82.11) and a black glass fragment found within a small yellowish bead of unknown composition (1930.60.56a). 1930.82.11 has an unusual composition with low soda (11.1%) and very high copper oxide and tin oxide levels (5.5% CuO and 1.0% SnO), it also contains significant lead oxide, 1.0%. The presence of tin and lead oxides alongside copper oxide suggest a later glass using bronze scale as colorant. No find location could be ascertained so the context of this glass remains ambiguous. The black glass fragment found within 1930.60.56 has a similar composition to the 2nd millennium BC glasses but contains significantly higher aluminium oxide (2.7%) and small quantities of copper, cobalt, manganese and lead oxides. Again there is no find location for this object so its date and context are unclear.

5.4 Glazed ceramics

The preservation of the glaze is in most cases very poor and very few unaltered glazes were found. From the 31 glaze samples analysed 12 had totals close to 100%, Table 14, suggesting that they had not been significantly altered by post-depositional processes. However, despite their high totals several of these samples had a visual appearance consistent with significant post depositional alteration, for example 1930.52.1f has a total of 100% but has clear alteration layers, Figure 28. All of these samples, apart from one (1930.16.3) contain aluminium oxide above 2.5% with several above 10% suggesting that the interaction layer, which was often visible on SEM imaging, between the glaze and ceramic body has affected the analysis, Figure 27. In addition, three of the glaze samples analysed appear to be from the Late period. Samples 1930.52.1g and 1930.52.1c contain tin and lead oxide in addition to copper suggesting that the copper source was bronze scale, they also have aluminium levels close to those seen in the late period glasses found at Nuzi. These samples also had tin-rich inclusions visible on SEM imaging (Figure 60 Section 6.4). Sample 1930.52.62b also contains some tin and lead oxide so was thought to be a late glaze as well.

1930.16.3 has a composition very close to the translucent blue glasses although it is slightly lower in soda (13.4% compared to 14% and above) when compared to most of the translucent blue glasses analysed, it also has lower magnesia compared to potash (4.0% MgO to 4.8% K₂O). Previous work has suggested that powdered glass, of a slightly different composition, was being used as the glazing agent of Bronze Age ceramics at Nuzi (Paynter 2009). For the remaining six glaze samples, although affected by an interaction layer, it was noted that three of them had lower magnesia levels than potash levels, similar to 1930.16.3; whereas the others followed the same pattern as the majority of the 2nd millennium BC glasses with higher magnesia than potash. No glasses were found with the low magnesia-high potash pattern seen in some of the glazes although several have very similar magnesia and potash levels: 1930.68.27h (2.6%

| Sample | Colour | Original colour | Object type | SiO ₂ | Al ₂ O ₃ | CaO | MgO | Na ₂ O | K ₂ O | Fe ₂ O ₃ | TiO ₂ | CoO | CuO | MnO | NiO | ZnO | SnO | Sh ₂ O ₃ | BaO | PhO | Cr ₂ O ₃ | P ₂ O ₅ | SO ₂ | Cl | SrO | Total | |
|-------------|--------------|-----------------|---|------------------|--------------------------------|-------|------|-------------------|------------------|--------------------------------|------------------|------|-------|------|------|------|------|--------------------------------|------|------|--------------------------------|-------------------------------|-----------------|------|------|--------|-------|
| 1930.138.3 | white | blue | glazed mudbrick | 42.87 | 4.06 | 3.90 | 2.56 | 0.50 | 2.89 | 1.55 | 0.21 | 0.00 | 0.32 | 0.00 | 0.00 | 0.00 | 0.01 | 0.07 | 0.00 | 0.00 | 0.00 | 0.12 | 0.27 | 0.58 | 0.05 | 59.95 | |
| 1930.14.10 | blue | blue | glaze sample | 46.13 | 3.47 | 1.69 | 0.71 | 0.12 | 0.71 | 0.93 | 0.18 | 0.00 | 30.97 | 0.00 | 0.00 | 0.00 | 0.00 | 0.00 | 0.05 | 0.00 | 0.00 | 0.07 | 0.11 | 0.18 | 0.53 | 0.04 | 85.86 |
| 1930.14.2 | blue/green | blue/green | glaze sample | 53.35 | 10.54 | 8.12 | 5.04 | 8.31 | 3.51 | 5.18 | 0.46 | 0.00 | 2.84 | 0.12 | 0.00 | 0.00 | 0.00 | 0.08 | 0.00 | 0.00 | 0.00 | 0.16 | 0.24 | 0.39 | 0.00 | 98.24 | |
| 1930.14.3 | blue | blue | glaze sample | 30.70 | 2.45 | 1.11 | 0.38 | 0.28 | 1.41 | 1.22 | 0.10 | 0.00 | 0.49 | 0.00 | 0.00 | 0.00 | 0.00 | 0.00 | 0.00 | 0.00 | 0.00 | 0.01 | 1.71 | 0.85 | 0.05 | 40.74 | |
| 1930.14.5 | blue | blue | glazed ceramic | 43.68 | 2.52 | 0.97 | 9.98 | 0.11 | 0.12 | 0.20 | 0.00 | 0.00 | 15.33 | 0.00 | 0.00 | 0.00 | 0.00 | 0.00 | 0.00 | 0.00 | 0.00 | 0.09 | 0.14 | 0.47 | 0.00 | 73.63 | |
| 1930.14.6a | white | blue | glazed ceramic (outer surface) | 58.79 | 5.97 | 5.61 | 4.04 | 7.40 | 3.83 | 3.34 | 0.37 | 0.00 | 1.44 | 0.08 | 0.00 | 0.00 | 0.00 | 0.08 | 0.00 | 0.00 | 0.02 | 0.21 | 0.18 | 0.69 | 0.00 | 91.97 | |
| 1930.14.6b | white | white | glazed ceramic (inner surface) | 68.42 | 0.99 | 0.49 | 0.13 | 0.07 | 0.28 | 0.17 | 0.00 | 0.00 | 0.00 | 0.00 | 0.00 | 0.00 | 0.00 | 1.45 | 0.00 | 0.00 | 0.00 | 0.00 | 0.17 | 0.45 | 0.12 | 72.13 | |
| 1930.14.9 | blue | blue | glaze sample | 59.66 | 1.16 | 1.24 | 0.21 | 0.06 | 0.48 | 0.27 | 0.05 | 0.00 | 0.46 | 0.00 | 0.00 | 0.00 | 0.00 | 0.07 | 0.00 | 0.00 | 0.00 | 0.00 | 1.07 | 0.69 | 0.03 | 65.38 | |
| 1930.16.1 | blue | blue | glaze sample | 68.65 | 0.27 | 0.27 | 0.19 | 0.12 | 0.39 | 0.17 | 0.03 | 0.00 | 0.26 | 0.00 | 0.00 | 0.00 | 0.00 | 0.00 | 0.00 | 0.00 | 0.00 | 0.00 | 0.00 | 0.05 | 0.00 | 90.39 | |
| 1930.16.3 | blue | white | glaze fragment | 64.97 | 0.53 | 5.93 | 3.99 | 13.99 | 4.81 | 0.27 | 0.05 | 0.00 | 2.20 | 0.00 | 0.00 | 0.00 | 0.00 | 0.09 | 0.00 | 0.00 | 0.00 | 0.12 | 0.21 | 0.81 | 0.00 | 97.92 | |
| 1930.16.8b | white | blue/green | glazed ceramic | 43.63 | 1.22 | 0.82 | 0.13 | 0.12 | 0.87 | 0.16 | 0.00 | 0.00 | 0.00 | 0.00 | 0.00 | 0.00 | 0.00 | 1.41 | 0.00 | 0.00 | 0.00 | 0.01 | 1.56 | 0.75 | 0.13 | 50.81 | |
| 1930.16.9 | blue | blue | glaze sample | 54.55 | 10.63 | 6.22 | 3.56 | 9.97 | 5.33 | 4.85 | 0.49 | 0.00 | 1.76 | 0.09 | 0.02 | 0.03 | 0.00 | 0.09 | 0.00 | 0.00 | 0.02 | 0.14 | 0.92 | 0.55 | 0.00 | 99.16 | |
| 1930.52.1c | blue | blue | glaze sample | 86.44 | 0.79 | 0.37 | 0.49 | 0.13 | 0.35 | 0.44 | 0.07 | 0.00 | 0.97 | 0.02 | 0.00 | 0.05 | 0.05 | 0.00 | 0.00 | 0.00 | 0.00 | 0.00 | 0.06 | 0.09 | 0.00 | 90.30 | |
| 1930.52.1d | yellow | blue/green | glaze fragment (glassy) | 55.37 | 3.02 | 6.96 | 4.10 | 15.05 | 3.86 | 1.36 | 0.12 | 0.00 | 2.72 | 0.00 | 0.00 | 0.00 | 0.33 | 0.09 | 0.00 | 1.58 | 0.00 | 0.31 | 0.38 | 0.66 | 0.00 | 99.93 | |
| 1930.52.1e | yellow | blue/green | glazed ceramic | 49.58 | 15.38 | 10.07 | 5.22 | 6.17 | 3.67 | 7.57 | 0.84 | 0.00 | 0.27 | 0.12 | 0.00 | 0.00 | 0.00 | 0.07 | 0.00 | 0.00 | 0.02 | 0.17 | 0.02 | 0.10 | 0.00 | 99.16 | |
| 1930.52.1f | white | blue/green | glazed ceramic | 43.28 | 8.15 | 13.22 | 8.20 | 5.16 | 2.22 | 5.04 | 0.43 | 0.00 | 0.37 | 0.07 | 0.04 | 0.00 | 0.00 | 0.05 | 0.00 | 0.00 | 0.10 | 0.14 | 0.20 | 0.09 | 0.00 | 86.75 | |
| 1930.52.1f | white | blue | glazed ceramic, glaze layer | 56.94 | 7.26 | 8.38 | 5.18 | 12.55 | 3.73 | 3.45 | 0.31 | 0.00 | 1.37 | 0.08 | 0.00 | 0.00 | 0.00 | 0.08 | 0.00 | 0.00 | 0.00 | 0.23 | 0.21 | 0.26 | 0.03 | 100.02 | |
| 1930.52.1g | green | blue | glazed ceramic, glaze layer | 68.21 | 2.49 | 7.68 | 3.18 | 7.16 | 5.14 | 1.20 | 0.16 | 0.00 | 1.98 | 0.04 | 0.00 | 0.00 | 0.00 | 0.48 | 0.10 | 0.00 | 0.17 | 0.00 | 0.48 | 0.37 | 0.46 | 99.35 | |
| 1930.52.1h1 | green | blue | glazed ceramic, glaze layer | 46.08 | 6.61 | 1.20 | 1.47 | 0.86 | 2.62 | 0.81 | 0.15 | 0.00 | 27.71 | 0.00 | 0.00 | 0.00 | 0.00 | 0.00 | 0.00 | 0.00 | 0.00 | 0.13 | 0.09 | 2.44 | 0.03 | 90.19 | |
| 1930.52.1h2 | green | blue | glazed ceramic, glaze/interaction layer | 54.57 | 10.68 | 6.90 | 3.64 | 11.82 | 4.32 | 4.14 | 0.68 | 0.00 | 2.34 | 0.08 | 0.00 | 0.00 | 0.00 | 0.09 | 0.00 | 0.00 | 0.00 | 0.21 | 0.29 | 0.40 | 0.00 | 100.11 | |
| 1930.52.2a | green | blue | glaze fragment | 86.81 | 0.52 | 0.35 | 0.18 | 0.05 | 0.28 | 0.22 | 0.05 | 0.00 | 0.44 | 0.00 | 0.00 | 0.00 | 0.00 | 0.00 | 0.00 | 0.00 | 0.00 | 0.00 | 0.00 | 0.03 | 0.00 | 88.91 | |
| 1930.52.2b | white | white | glazed ceramic, glaze layer | 87.42 | 0.77 | 0.66 | 0.29 | 0.06 | 0.36 | 0.47 | 0.07 | 0.00 | 0.84 | 0.00 | 0.00 | 0.00 | 0.00 | 0.00 | 0.00 | 0.00 | 0.00 | 0.00 | 0.00 | 0.03 | 0.03 | 90.98 | |
| 1930.52.6a | white | blue/green | glazed ceramic | 84.84 | 0.44 | 0.78 | 0.12 | 0.07 | 0.33 | 0.19 | 0.04 | 0.00 | 0.00 | 0.00 | 0.00 | 0.00 | 0.00 | 2.94 | 0.00 | 0.00 | 0.03 | 0.00 | 0.12 | 0.11 | 0.26 | 90.08 | |
| 1930.52.6b | bright green | blue | glazed ceramic | 63.48 | 4.29 | 6.84 | 3.75 | 11.31 | 4.33 | 1.95 | 0.26 | 0.00 | 1.94 | 0.09 | 0.00 | 0.00 | 0.00 | 0.07 | 0.09 | 0.00 | 0.09 | 0.03 | 0.31 | 0.40 | 0.05 | 99.43 | |
| 1930.52.6c | yellow | blue | glazed ceramic | 41.97 | 5.06 | 3.63 | 1.83 | 0.29 | 1.89 | 0.74 | 0.10 | 0.00 | 0.10 | 0.00 | 0.00 | 0.00 | 0.11 | 0.05 | 0.00 | 0.00 | 0.00 | 0.16 | 0.60 | 0.70 | 0.09 | 57.35 | |
| 1930.52.6d | green | blue | glazed ceramic | 62.47 | 5.14 | 7.98 | 2.91 | 9.62 | 4.72 | 2.05 | 0.30 | 0.00 | 1.27 | 0.24 | 0.00 | 0.23 | 0.00 | 0.10 | 0.00 | 0.00 | 0.00 | 0.32 | 0.29 | 0.38 | 0.06 | 98.08 | |
| 1930.52.6e | unknown | blue/green | striped glazed ceramic | 68.84 | 11.62 | 3.67 | 3.24 | 4.47 | 3.34 | 3.60 | 0.34 | 0.00 | 0.19 | 0.04 | 0.00 | 0.00 | 0.00 | 0.06 | 0.00 | 0.00 | 0.00 | 0.05 | 0.04 | 0.05 | 0.00 | 99.81 | |
| 1930.58.1a | yellow | blue/green | glazed ceramic (lion) | 35.15 | 3.80 | 0.95 | 0.50 | 0.28 | 2.47 | 3.10 | 0.17 | 0.00 | 0.84 | 0.00 | 0.00 | 0.00 | 0.00 | 0.08 | 0.00 | 0.00 | 0.01 | 0.02 | 0.29 | 0.81 | 0.05 | 46.47 | |
| 1930.58.1b | red | red | painted ceramic (lion) | 35.68 | 9.59 | 11.50 | 2.46 | 0.97 | 2.02 | 4.53 | 0.42 | 0.00 | 0.00 | 0.12 | 0.00 | 0.00 | 0.00 | 0.05 | 0.00 | 0.00 | 0.00 | 0.15 | 0.28 | 1.54 | 0.07 | 68.36 | |
| 1930.1C12 | green | blue/green | glaze sample | 57.58 | 12.01 | 5.09 | 3.32 | 12.74 | 2.82 | 3.82 | 0.36 | 0.00 | 1.25 | 0.04 | 0.00 | 0.00 | 0.00 | 0.00 | 0.04 | 0.00 | 0.00 | 0.40 | 0.55 | 1.18 | 0.00 | 101.36 | |
| 1930.1C15 | green | blue | glaze sample | 49.96 | 4.19 | 2.03 | 1.22 | 0.18 | 0.83 | 0.59 | 0.20 | 0.00 | 21.71 | 0.01 | 0.00 | 0.03 | 0.00 | 0.03 | 0.00 | 0.00 | 0.02 | 0.07 | 0.17 | 1.35 | 0.04 | 82.59 | |
| 1930.1C6 | turquoise | blue | glaze sample | 84.31 | 0.63 | 0.67 | 0.45 | 0.03 | 0.33 | 0.50 | 0.05 | 0.00 | 2.31 | 0.00 | 0.00 | 0.00 | 0.00 | 0.00 | 0.00 | 0.00 | 0.00 | 0.02 | 0.06 | 0.13 | 0.00 | 89.46 | |

Table 14: Glazed ceramics composition

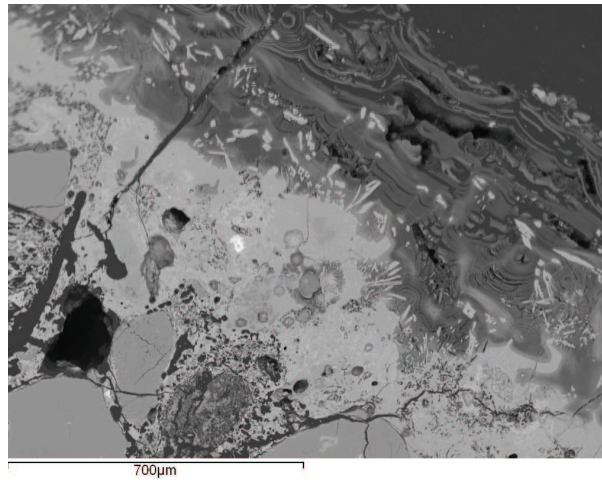


Figure 27: Glaze sample 1930.52.1f showing alteration layers and a clear interaction layer

MgO/2.7% K₂O), 1930.82.62b (4.0% MgO/3.6% K₂O), and 1930.82.7 (4.8% MgO/4.3% K₂O). The unusual composition glass 1930.82.11 has higher potash than magnesia (4.2% K₂O to 3.7% MgO) but as already noted its high aluminium levels suggest that it is a later glass.

Analysis of the glasses has indicated that the original colour of the glass can be extrapolated from the colorant metals present, even where no original glass remains. Twenty-seven of the glazes analysed contain copper suggesting that they were originally blue. However, 10 of the glaze samples also contain above 3% oxide weight of iron, perhaps indicating that they may have been green; although it is also possible that the iron oxide may be from interaction with the ceramic body. 1930.16.3, the only unaltered Late Bronze Age glaze sampled, contains almost no iron oxide and is clearly blue but there is a single translucent green glass eye bead (1930.68.18) which contains a mixture of copper and iron, Table 12. Three examples of white glazes were found: 1930.14.6b, 1930.16.7 and 1930.52.6a, these appear to have been opaque white originally as antimony oxide is present and there are no other colorants. The SEM images show calcium antimonate crystals present within the alteration layers, Figure 28.

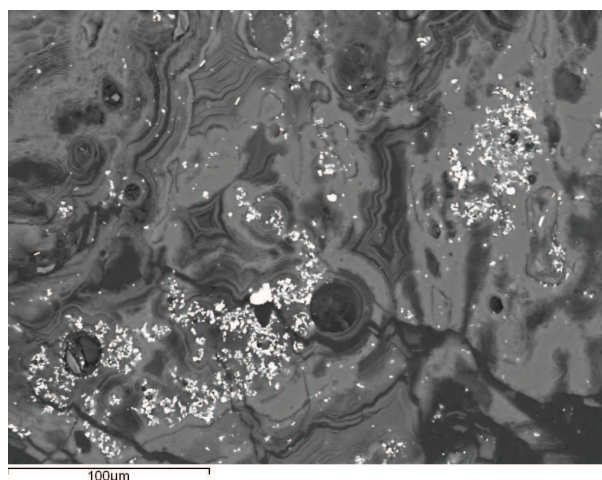


Figure 28: Altered white glaze, 1930.14.6b

One significant result from the analysis of the glazes was that the fragmentary yellow and red glazed lion (1930.5B.1), which is one half of a pair, the intact lion being on display in the museum, may actually have been originally blue, or green, copper was found in the sample of glaze analysed and there were no colorants associated with yellow glasses such as lead antimonate. In addition a fragment of glazed ceramic vessel and several apparently yellow glass beads were found to contain copper and no other colorants so were probably originally translucent blue in colour, Figure 29. The change in colour from translucent blue to a dirty yellow is most probably due to the weathering of the glass layer that forms the glaze. When glass devitrifies the silicate network that forms the glass breaks down so that the copper colorant is no longer present interstitially in the glass network and the original blue colour is lost. It was also found that the red paint on these lions is most probably iron oxide as a layer of pigment containing iron particles can be seen in the SEM images, Figure 30.



Figure 29: 'yellow' striped glazed vessel and 'yellow' bead

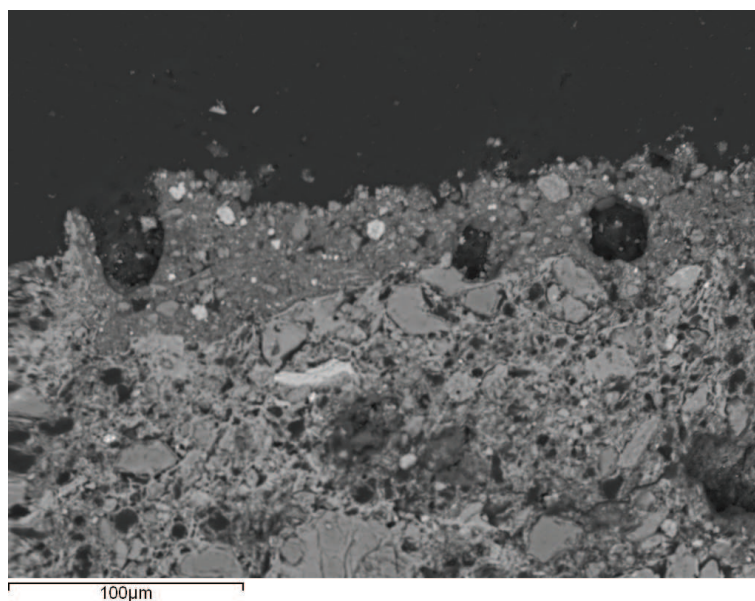


Figure 30: Red lion 1930.5B.1, SEM image of paint layer

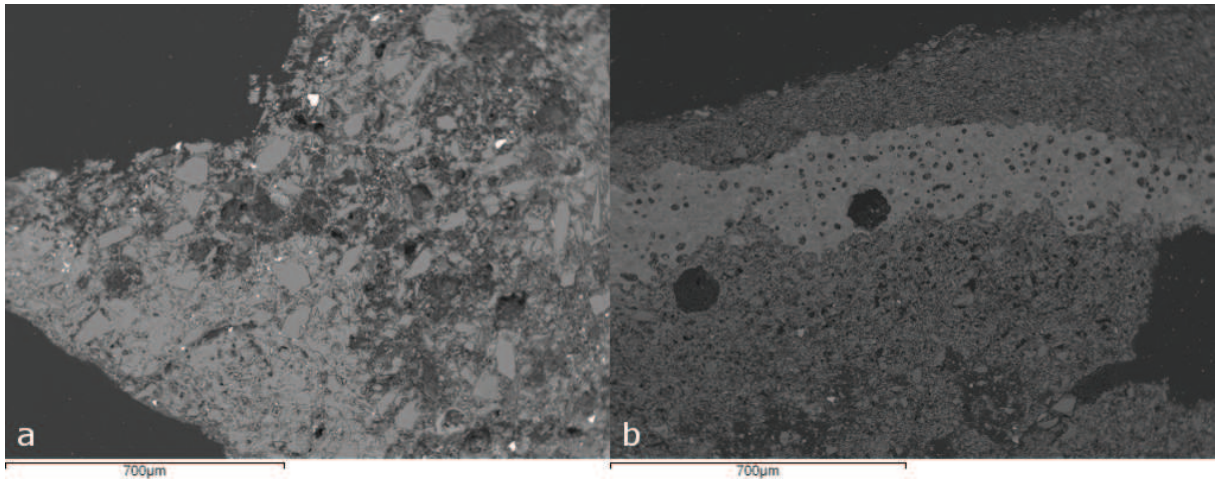


Figure 31: Marbleised faience sample 1930.82.1; glassy area in sample N25

5.5 Faience and related materials

The bulk compositional analyses of the faience and related materials is contained in Table 15. The majority of these are presented as individual points, rather than an average of several points from each object, due to the inhomogeneous nature of the material meaning that the composition at each point can vary considerably over even quite small areas.

5.5.1 Marbleised faience

SEM analysis of the marbled faience samples suggested that it consists of closely packed quartz grains surrounded by a glassy matrix (Figure 31a). A newly discovered sample of this material (N25) also contained some distinct glassy areas which on SEM imaging were found to contain partially fused quartz grains in an amorphous glassy matrix (Figure 31b). Compositional analysis of these areas has given enigmatic results. The glassy area is significantly lower in alkali and higher in silica than the true glasses sampled, with an average of 82.1% silica and 6.7% soda with 1.2% potash, 2.2% lime and 1.6% magnesia. The glassy areas also did not appear to be deliberately coloured, although iron oxide is present at 4.3%. It is therefore probable that these areas are simply over-fused faience rather than a deliberately produced glass. The red areas of all of the samples are coloured with iron oxide, in similar quantities to that seen in the glassy areas of N25; the yellow areas contain lead oxide as the colorant, interestingly no antimony oxide was noted in the analyses and lead antimonate crystals, the more usual form of yellow colorant, were not observed in the SEM images.

| Sample | Colour | Object type | SiO ₂ | Al ₂ O ₃ | CaO | MgO | Na ₂ O | K ₂ O | Fe ₂ O ₃ | TiO ₂ | CoO | CuO | MnO | NiO | ZnO | SmO | SrO | Sh ₂ O ₅ | BaO | PbO | Cr ₂ O ₃ | P ₂ O ₅ | SO ₃ | Cl | SrO | Total | |
|-----------------|------------|---------------------------|------------------|--------------------------------|------|------|-------------------|------------------|--------------------------------|------------------|-----|------|-----|-----|-----|-----|-----|--------------------------------|-----|-----|--------------------------------|-------------------------------|-----------------|-----|-----|-------|-------|
| 1930.47.14 | blue | Egyptian blue vessel | 62.5 | 0.4 | 13.7 | 0.3 | 0.6 | 0.3 | 0.4 | 0.0 | 0.0 | 17.8 | 0.0 | 0.0 | 0.0 | 0.0 | 0.0 | 0.0 | 0.0 | 0.0 | 0.0 | 0.0 | 0.1 | 0.1 | 0.1 | 0.1 | 96.5 |
| 1930.82.11 | various | marbelised faience vessel | 27.1 | 0.6 | 1.2 | 0.4 | 0.2 | 0.2 | 0.6 | 0.0 | 0.0 | 0.0 | 0.1 | 0.0 | 0.0 | 0.0 | 0.0 | 0.2 | 0.0 | 0.8 | 0.0 | 0.7 | 4.8 | 1.4 | 0.0 | 0.0 | 39.4 |
| 1930.82.11i | various | marbelised faience vessel | 84.4 | 0.1 | 2.8 | 1.3 | 0.1 | 0.1 | 0.3 | 0.0 | 0.0 | 0.0 | 0.0 | 0.0 | 0.0 | 0.0 | 0.0 | 0.0 | 0.0 | 0.0 | 0.0 | 0.0 | 0.3 | 0.1 | 0.1 | 0.1 | 89.6 |
| 1930.82.11ii | various | marbelised faience vessel | 98.5 | 0.0 | 0.0 | 0.0 | 0.0 | 0.0 | 0.0 | 0.0 | 0.0 | 0.0 | 0.0 | 0.0 | 0.0 | 0.0 | 0.0 | 0.0 | 0.0 | 0.0 | 0.0 | 0.0 | 0.0 | 0.0 | 0.0 | 0.0 | 98.5 |
| 1930.82.11iii | various | marbelised faience vessel | 68.4 | 0.6 | 0.7 | 2.9 | 0.3 | 0.2 | 0.8 | 0.1 | 0.0 | 0.0 | 0.0 | 0.0 | 0.0 | 0.0 | 0.0 | 0.0 | 0.0 | 0.3 | 0.0 | 0.1 | 0.6 | 0.3 | 0.0 | 0.0 | 76.3 |
| 1930.82.21 | various | marbelised faience vessel | 39.9 | 1.5 | 0.9 | 1.1 | 0.1 | 0.4 | 0.3 | 0.0 | 0.0 | 0.0 | 0.0 | 0.0 | 0.0 | 0.0 | 0.0 | 0.0 | 0.0 | 0.6 | 0.0 | 0.5 | 0.7 | 0.8 | 0.0 | 0.0 | 40.6 |
| 1930.82.21i | various | marbelised faience vessel | 18.9 | 0.6 | 2.7 | 1.6 | 0.1 | 0.2 | 0.4 | 0.2 | 0.0 | 0.0 | 1.2 | 0.0 | 0.0 | 0.0 | 0.0 | 0.0 | 0.0 | 5.4 | 0.0 | 1.4 | 1.7 | 1.9 | 1.2 | 0.1 | 36.3 |
| 1930.82.21ii | various | marbelised faience vessel | 42.1 | 1.6 | 2.0 | 3.7 | 0.2 | 0.4 | 0.5 | 0.0 | 0.0 | 0.0 | 0.0 | 0.0 | 0.0 | 0.0 | 0.0 | 0.0 | 0.0 | 2.6 | 0.0 | 0.0 | 0.0 | 0.0 | 0.0 | 0.0 | 56.1 |
| 1930.82.31 | various | marbelised faience vessel | 54.7 | 1.9 | 4.4 | 2.3 | 2.3 | 1.2 | 7.8 | 0.1 | 0.0 | 0.1 | 0.0 | 0.0 | 0.0 | 0.0 | 0.0 | 0.0 | 0.0 | 0.0 | 0.0 | 0.0 | 0.1 | 0.3 | 0.5 | 0.0 | 75.7 |
| 1930.82.31i | various | marbelised faience vessel | 72.6 | 0.8 | 1.0 | 0.7 | 0.5 | 0.8 | 3.7 | 0.2 | 0.0 | 0.2 | 0.0 | 0.0 | 0.0 | 0.0 | 0.0 | 0.0 | 0.0 | 0.1 | 0.1 | 0.1 | 0.4 | 0.2 | 0.0 | 0.0 | 81.2 |
| 1930.82.31ii | various | marbelised faience vessel | 91.1 | 0.1 | 0.1 | 0.2 | 0.1 | 0.1 | 1.0 | 0.0 | 0.0 | 0.0 | 0.0 | 0.0 | 0.0 | 0.0 | 0.0 | 0.0 | 0.0 | 0.0 | 0.0 | 0.0 | 0.0 | 0.0 | 0.0 | 0.0 | 92.6 |
| 1930.82.31iii | various | marbelised faience vessel | 63.2 | 0.3 | 0.9 | 0.6 | 0.4 | 0.3 | 3.9 | 0.0 | 0.0 | 0.2 | 0.0 | 0.0 | 0.0 | 0.0 | 0.0 | 0.0 | 0.0 | 0.0 | 0.0 | 0.0 | 0.1 | 0.6 | 0.4 | 0.0 | 71.0 |
| 1930.57.4 | unknown | faience cup (glaze layer) | 30.4 | 0.8 | 0.7 | 0.4 | 0.1 | 0.3 | 0.5 | 0.0 | 0.0 | 0.0 | 0.2 | 0.0 | 0.0 | 0.0 | 0.0 | 0.0 | 0.0 | 0.0 | 0.0 | 0.0 | 0.1 | 0.5 | 1.0 | 0.0 | 35.0 |
| N25 (area 1I) | unknown | marbelised faience vessel | 85.1 | 0.3 | 1.6 | 1.2 | 5.8 | 1.1 | 3.3 | 0.0 | 0.0 | 0.1 | 0.0 | 0.0 | 0.0 | 0.0 | 0.0 | 0.0 | 0.0 | 0.0 | 0.0 | 0.1 | 0.1 | 0.1 | 0.3 | 0.0 | 98.8 |
| N25 (area 1II) | unknown | marbelised faience vessel | 85.2 | 0.3 | 2.0 | 1.3 | 5.1 | 0.9 | 3.6 | 0.0 | 0.0 | 0.1 | 0.0 | 0.0 | 0.0 | 0.0 | 0.0 | 0.0 | 0.0 | 0.0 | 0.0 | 0.0 | 0.1 | 0.1 | 0.2 | 0.0 | 98.9 |
| N25 (area 1III) | unknown | marbelised faience vessel | 74.9 | 0.4 | 3.5 | 2.6 | 9.3 | 1.7 | 6.4 | 0.1 | 0.0 | 0.1 | 0.1 | 0.0 | 0.0 | 0.0 | 0.0 | 0.0 | 0.0 | 0.0 | 0.0 | 0.1 | 0.1 | 0.4 | 0.0 | 0.0 | 99.4 |
| N25 (area 2I) | unknown | marbelised faience vessel | 79.3 | 0.7 | 2.5 | 1.6 | 8.3 | 1.5 | 5.0 | 0.0 | 0.0 | 0.1 | 0.0 | 0.0 | 0.0 | 0.0 | 0.0 | 0.0 | 0.0 | 0.0 | 0.0 | 0.0 | 0.1 | 0.1 | 0.1 | 0.0 | 99.5 |
| N25 (area 2II) | unknown | marbelised faience vessel | 85.3 | 0.3 | 1.6 | 1.2 | 5.7 | 0.9 | 3.6 | 0.0 | 0.0 | 0.0 | 0.0 | 0.0 | 0.0 | 0.0 | 0.0 | 0.0 | 0.0 | 0.0 | 0.0 | 0.0 | 0.1 | 0.0 | 0.3 | 0.0 | 98.9 |
| N25 (area 2III) | unknown | marbelised faience vessel | 82.7 | 0.4 | 2.0 | 1.6 | 6.3 | 1.0 | 4.1 | 0.0 | 0.0 | 0.0 | 0.0 | 0.0 | 0.0 | 0.0 | 0.0 | 0.0 | 0.0 | 0.0 | 0.0 | 0.0 | 0.1 | 0.1 | 0.3 | 0.0 | 98.5 |
| N25 (area 3I) | various | marbelised faience vessel | 96.7 | 0.1 | 0.1 | 0.0 | 0.1 | 0.0 | 0.1 | 0.0 | 0.0 | 0.0 | 0.0 | 0.0 | 0.0 | 0.0 | 0.0 | 0.0 | 0.0 | 0.0 | 0.0 | 0.0 | 0.0 | 0.1 | 0.0 | 0.0 | 97.2 |
| N25 (area 3II) | various | marbelised faience vessel | 65.5 | 0.5 | 3.4 | 2.0 | 1.5 | 0.3 | 6.5 | 0.1 | 0.0 | 0.1 | 0.0 | 0.0 | 0.0 | 0.0 | 0.0 | 0.0 | 0.0 | 0.0 | 0.0 | 0.0 | 0.1 | 0.0 | 0.0 | 0.0 | 77.9 |
| N25 (area 3III) | various | marbelised faience vessel | 65.9 | 0.3 | 0.9 | 0.4 | 0.4 | 0.1 | 3.3 | 0.0 | 0.0 | 0.1 | 0.0 | 0.0 | 0.0 | 0.0 | 0.0 | 0.0 | 0.0 | 0.0 | 0.0 | 0.0 | 0.1 | 0.1 | 0.0 | 0.0 | 71.6 |
| 1930.61.123bi | blue/white | faience bead | 97.8 | 0.0 | 0.0 | 0.0 | 0.0 | 0.0 | 0.0 | 0.0 | 0.0 | 0.0 | 0.2 | 0.0 | 0.0 | 0.0 | 0.0 | 0.0 | 0.0 | 0.0 | 0.0 | 0.0 | 0.0 | 0.0 | 0.0 | 0.0 | 98.0 |
| 1930.61.123bi | blue/white | faience bead | 14.9 | 0.7 | 34.4 | 0.6 | 0.7 | 0.0 | 0.2 | 0.1 | 0.0 | 11.6 | 0.0 | 0.0 | 0.0 | 0.0 | 0.0 | 0.1 | 0.0 | 0.0 | 0.0 | 24.4 | 0.5 | 1.8 | 0.1 | 89.8 | |
| 1930.61.123bii | blue/white | faience bead | 65.6 | 0.2 | 0.6 | 0.3 | 0.0 | 0.0 | 0.1 | 0.0 | 0.0 | 2.7 | 0.0 | 0.0 | 0.0 | 0.0 | 0.0 | 0.0 | 0.0 | 0.0 | 0.0 | 0.0 | 0.3 | 0.2 | 0.4 | 0.0 | 70.4 |
| 1930.80.13i | white | cylinder seal | 33.7 | 6.8 | 5.3 | 3.5 | 0.1 | 0.8 | 3.2 | 0.4 | 0.0 | 10.5 | 0.0 | 0.0 | 0.0 | 0.0 | 0.0 | 0.0 | 0.0 | 0.0 | 0.0 | 0.1 | 0.1 | 0.6 | 0.4 | 0.0 | 65.7 |
| 1930.80.13ii | white | cylinder seal | 40.7 | 7.7 | 10.1 | 3.8 | 0.1 | 0.9 | 3.4 | 0.3 | 0.0 | 13.6 | 0.0 | 0.0 | 0.0 | 0.0 | 0.0 | 0.0 | 0.0 | 0.0 | 0.0 | 0.1 | 0.2 | 0.4 | 0.1 | 0.0 | 81.4 |
| 1930.80.13iii | white | cylinder seal | 39.1 | 7.9 | 9.1 | 2.4 | 0.1 | 1.3 | 2.9 | 0.2 | 0.0 | 12.6 | 0.0 | 0.0 | 0.0 | 0.0 | 0.0 | 0.0 | 0.0 | 0.0 | 0.0 | 0.1 | 0.1 | 0.4 | 0.1 | 0.1 | 76.5 |
| 1930.62.81bi | blue | faience bead | 90.8 | 0.6 | 1.1 | 0.1 | 0.2 | 0.1 | 0.5 | 0.0 | 0.0 | 3.5 | 0.0 | 0.0 | 0.0 | 0.0 | 0.0 | 0.0 | 0.0 | 0.0 | 0.0 | 0.0 | 0.0 | 0.0 | 0.1 | 0.0 | 96.8 |
| 1930.61.91ai | red | bead, unknown material | 31.1 | 4.4 | 1.6 | 0.3 | 0.2 | 1.3 | 2.5 | 0.1 | 0.0 | 0.0 | 0.0 | 0.0 | 0.0 | 0.0 | 0.0 | 0.0 | 0.0 | 0.0 | 0.0 | 0.6 | 0.3 | 0.6 | 0.1 | 43.0 | |
| 1930.61.91aii | red | bead, unknown material | 45.3 | 4.7 | 2.7 | 0.3 | 0.2 | 1.6 | 2.5 | 0.1 | 0.0 | 0.0 | 0.1 | 0.0 | 0.0 | 0.0 | 0.0 | 0.0 | 0.0 | 0.0 | 0.0 | 0.6 | 0.2 | 0.4 | 0.0 | 0.0 | 58.6 |
| 1930.61.91bi | blue | faience bead | 45.9 | 1.1 | 6.8 | 1.7 | 0.1 | 0.3 | 0.4 | 0.1 | 0.0 | 8.6 | 0.0 | 0.0 | 0.0 | 0.0 | 0.0 | 0.0 | 0.0 | 0.0 | 0.0 | 0.0 | 0.0 | 0.1 | 0.0 | 0.1 | 65.3 |
| 1930.61.91bii | blue | faience bead | 25.0 | 1.0 | 5.1 | 0.5 | 0.1 | 0.4 | 0.3 | 0.0 | 0.0 | 4.3 | 0.0 | 0.0 | 0.0 | 0.0 | 0.0 | 0.0 | 0.0 | 0.0 | 0.0 | 0.1 | 0.4 | 0.6 | 0.0 | 37.8 | |
| 1930.61.91biii | blue | faience bead | 25.5 | 1.9 | 1.9 | 1.8 | 0.1 | 0.4 | 0.8 | 0.1 | 0.0 | 2.3 | 0.0 | 0.0 | 0.0 | 0.0 | 0.0 | 0.0 | 0.0 | 0.0 | 0.0 | 0.0 | 0.2 | 0.3 | 0.1 | 35.4 | |
| 1930.61.91ci | blue | faience bead | 32.0 | 3.3 | 4.6 | 0.3 | 0.1 | 0.6 | 1.0 | 0.1 | 0.0 | 8.1 | 0.0 | 0.0 | 0.0 | 0.4 | 0.0 | 0.0 | 0.0 | 0.0 | 0.0 | 0.1 | 0.6 | 0.1 | 0.0 | 51.3 | |
| 1930.61.91cii | blue | faience bead | 87.4 | 0.9 | 1.4 | 0.1 | 0.2 | 0.4 | 0.0 | 0.0 | 0.0 | 2.0 | 0.0 | 0.0 | 0.0 | 0.0 | 0.0 | 0.0 | 0.0 | 0.0 | 0.0 | 0.0 | 0.1 | 0.0 | 0.0 | 0.0 | 92.5 |
| 1930.60.140ci | black | bead, unknown material | 3.2 | 0.1 | 0.1 | 0.0 | 0.0 | 0.0 | 0.1 | 0.0 | 0.0 | 0.0 | 0.0 | 0.1 | 0.0 | 0.0 | 0.0 | 0.0 | 0.0 | 0.0 | 0.0 | 0.0 | 0.1 | 0.3 | 1.3 | 0.0 | 5.3 |
| 1930.60.140cii | black | bead, unknown material | 75.9 | 0.4 | 0.4 | 0.1 | 0.1 | 0.1 | 1.0 | 0.0 | 0.0 | 0.0 | 0.0 | 0.3 | 0.0 | 0.0 | 0.0 | 0.0 | 0.0 | 0.0 | 0.0 | 0.4 | 0.1 | 0.0 | 0.0 | 78.9 | |
| 1930.60.140civ | black | bead, unknown material | 49.0 | 3.7 | 1.2 | 0.2 | 0.1 | 0.2 | 2.0 | 0.1 | 0.0 | 0.3 | 5.7 | 0.1 | 0.0 | 0.0 | 0.0 | 0.0 | 0.0 | 0.0 | 0.0 | 0.6 | 0.1 | 0.0 | 0.0 | 0.1 | 63.4 |
| 1930.60.140cvi | black | bead, unknown material | 83.4 | 0.0 | 0.0 | 0.0 | 0.0 | 0.0 | 0.0 | 0.0 | 0.0 | 0.0 | 0.0 | 0.1 | 0.0 | 0.0 | 0.0 | 0.0 | 0.0 | 0.0 | 0.0 | 0.0 | 0.0 | 0.0 | 0.0 | 0.0 | 83.5 |
| 1930.63.51i | black | bead, unknown material | 0.1 | 0.0 | 55.5 | 0.1 | 0.0 | 0.0 | 0.2 | 0.0 | 0.0 | 0.0 | 0.0 | 0.0 | 0.0 | 0.0 | 0.0 | 0.1 | 0.0 | 0.0 | 0.0 | 0.0 | 0.1 | 0.0 | 0.0 | 0.0 | 56.0 |
| 1930.63.51ii | black | bead, unknown material | 43.0 | 2.2 | 0.1 | 37.3 | 0.0 | 0.0 | 4.3 | 0.0 | 0.0 | 0.0 | 0.1 | 0.1 | 0.0 | 0.0 | 0.0 | 0.0 | 0.0 | 0.0 | 0.0 | 0.0 | 0.0 | 0.0 | 0.0 | 0.0 | 86.1 |
| 1930.63.51iii | black | bead, unknown material | 0.3 | 22.9 | 0.1 | 10.2 | 0.0 | 0.0 | 28.0 | 0.2 | 0.1 | 0.0 | 0.3 | 0.1 | 0.0 | 0.0 | 0.0 | 0.0 | 0.0 | 0.0 | 0.0 | 37.4 | 0.0 | 0.0 | 0.0 | 0.0 | 102.4 |

Table 15: Faience and other materials composition

5.5.2 Faience

A single sample of glazed faience, with the glaze still present, was analysed (1930.57.4). SEM imaging confirmed that this sample from a glazed faience cup consisted of a quartz core with a discrete glaze layer on both the inner and outer surfaces (Figure 32). The glaze layer appeared to be heavily altered by post-depositional changes and was also highly vesicular with some extremely large air bubbles being present. Compositional analysis of the glaze layer confirmed a heavily altered glaze which was most probably originally blue, as there was a small quantity of copper present, however, due to the significant post-depositional alteration direct comparison with the glass and glazed ceramics was not possible. Three faience beads, which had not retained their glaze layer were also analysed: 1930.63.40e, 1930.60.140c and 1930.61.123b. 1930.63.40e consisted of quartz grains in a glassy matrix with manganese and copper in the glassy phase on qualitative compositional analysis. 1930.60.140c is similar in appearance with less apparent glass, spectral analysis showed manganese and iron in the phase around the quartz grains – quantitative analysis indicated manganese oxide in one point at a level of 5.7%. 1930.61.123b also contained quartz grains with copper-rich areas between them, 11.5% copper oxide on quantitative analysis (Table 15).

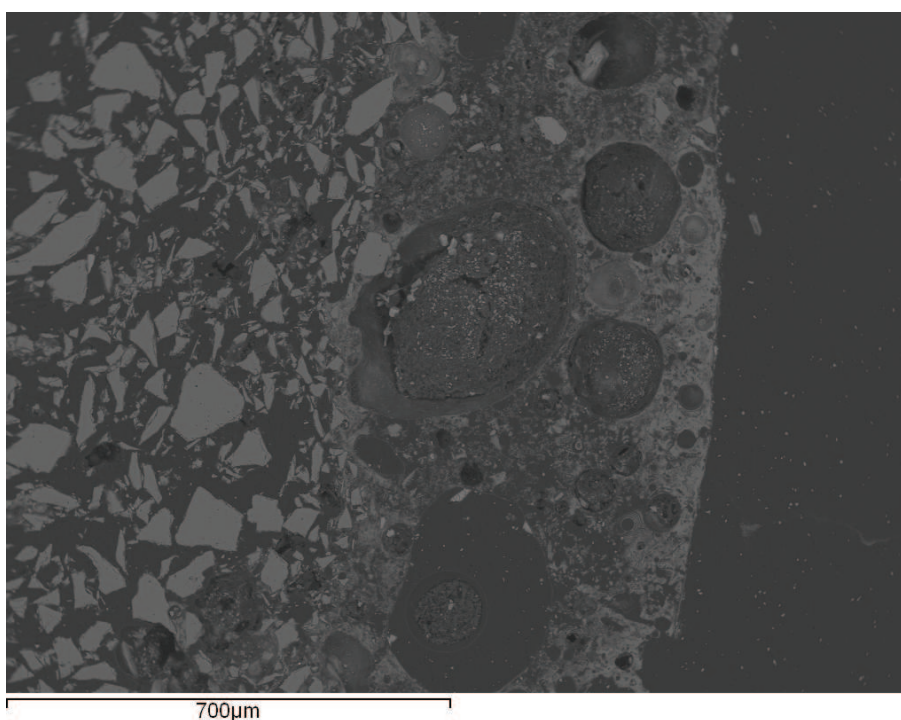


Figure 32: Faience vessel fragment; SEM image showing quartz body and heavily weathered glaze layer

5.5.3 Egyptian Blue

SEM imaging indicated that the moulded blue vessel fragment (1930.47.14) consisted of quartz particles in a paler glassy matrix with even lighter crystals in between (Figure 33). Initial spectra suggested that these were consistent with Egyptian Blue ($\text{CaCuSi}_4\text{O}_{10}$), a man-made pigment (Hatton et al 2008). Quantitative

analysis supported this as the fragment was found to consist of 62.5% of silica, 13.7% lime and 17.8% copper oxide, similar to analyses of similar objects from Egypt (Hatton et al 2008). SEM imaging has confirmed that the raw lump of pigment found is also Egyptian blue, albeit in an unconsolidated form (Figure 14; Section 4.2). Several beads thought to be of Egyptian blue were analysed, 1930.61.91b, 1930.61.91c and 1930.62.81b. SEM imaging showed that they were very similar to the vessel fragment above with clear quartz grains and cuprorivaite crystals visible. 1930.61.91b and 1930.62.81 also contain some glassy areas around the quartz grains and cuprorivaite crystals. Bulk compositional analysis confirmed the presence of silica, lime and copper oxides within these beads.

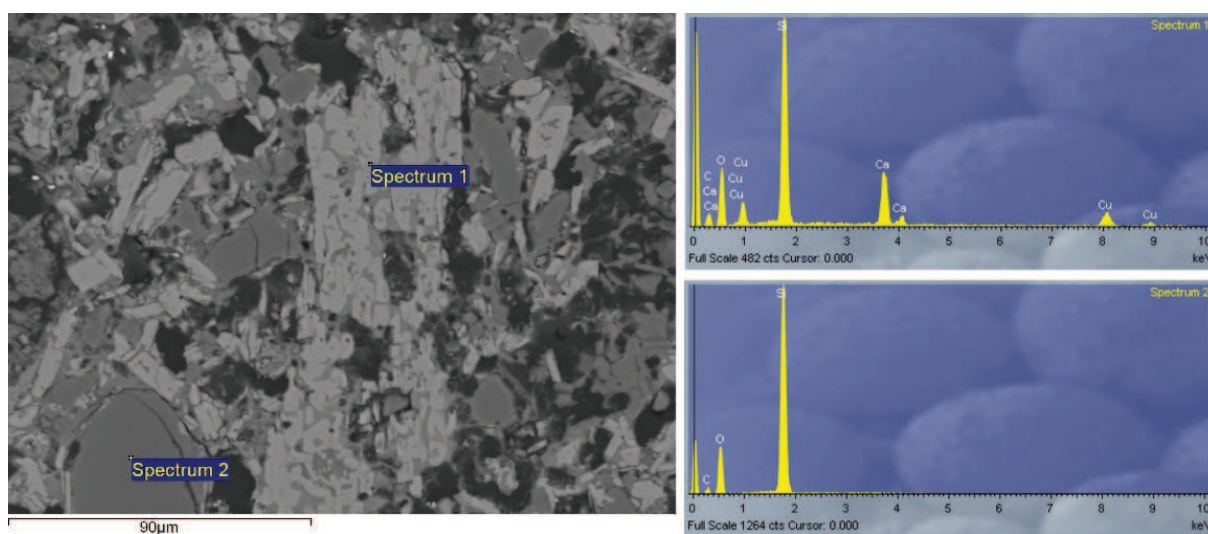


Figure 33: Egyptian blue vessel fragment SEM image and compositional spectrum

5.5.4 Cylinder seals

The SEM images of the sole sample that was taken for destructive analysis indicated that the seal was composed of tightly packed quartz grains with a small fragment of a possible glaze layer on one edge, although this appears to have a slightly odd texture on the SEM images, see Figure 34, with the glaze appearing to be not to be glassy, or devitrified or more crystalline, like the faience objects. Compositional analysis has indicated that the glaze on this seal (1930.80.13) has most probably suffered from post-depositional alteration as the soda level is extremely low (0.2%). The remnant composition, however, contains silica (37.8%), lime 8.2%, magnesia 3.2%, and potash 1.0%. It also contains very high amounts of aluminium oxide (7.5%) and copper oxide (12.2%) so may well be a specific type of material used only for cylinder seals, perhaps for practical reasons of carving and preservation or it may reflect post-depositional changes within the glaze layer.

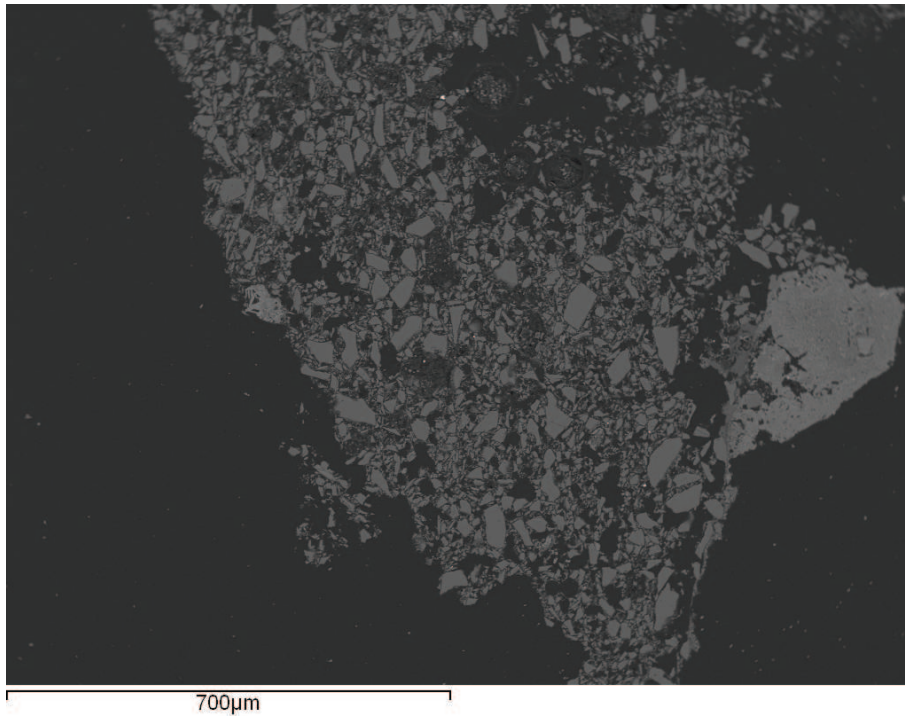


Figure 34: Cylinder seal fragment, SEM image - possible glaze fragment bottom right

5.6 Other materials

A few samples of other types of material were found on analysis. 1930.82.62d and 1930.68.26, which was blue-coloured, were found on SEM imaging to be of bone, with clear textures and bone microstructure (Figure 35). This was confirmed by X-ray analysis with calcium and phosphorous dominating the spectra. Two beads, 1930.60.140c and 1930.63.51 were most probably made of some kind of stone but their exact composition is ambiguous.

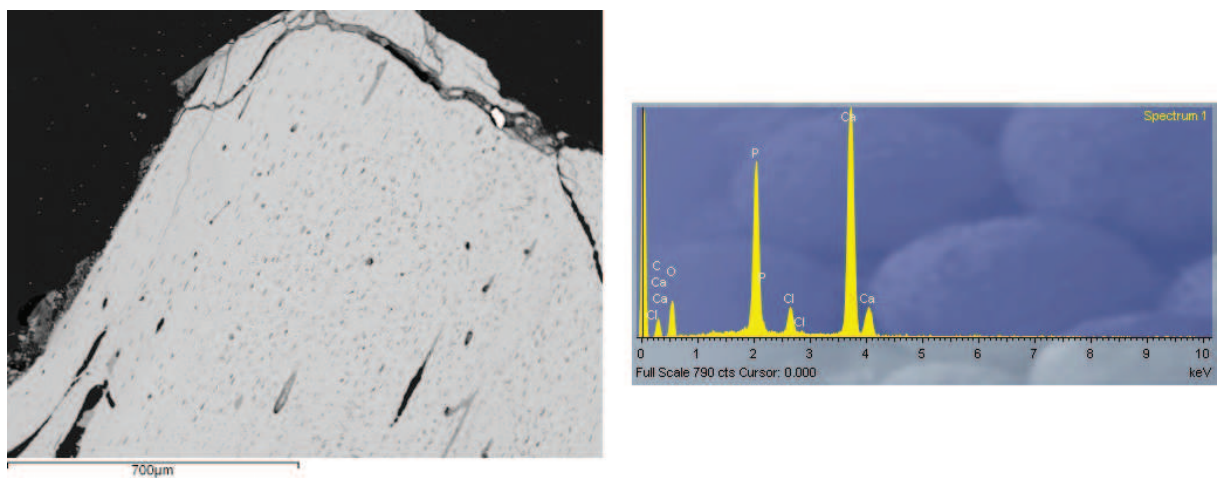


Figure 35: Bone bead 1930.68.26: SEM image and compositional spectrum

| Sample | 1930.82.62e | 1930.82.13 | 1930.63.37 | 1930.82.62 c | 1930.82.62 b | 1930.67.42 | 1930.62.103 | 1930.63.40 d | 1930.68.27 c | 1930.82.59 | 1930.60.140 a | 1930.82.7 |
|-------------|---------------|---------------|---------------|--------------|--------------|------------|-------------|--------------|--------------|------------|---------------|------------|
| Object type | pendant | vessel | eye bead | raw | raw | bead | bead | bead | bead | unknown | bead | inlay |
| Colour | colorant-free | colorant-free | colorant-free | colourless | colourless | green | turquoise | turquoise | turquoise | white | yellow | yellow |
| Sc | 19.20 | 33.66 | 47.65 | 11.11 | 9.54 | 11.55 | 20.23 | 8.36 | 13.37 | 9.05 | 11.76 | 287.27 |
| Ti | 515.96 | 172.80 | 275.54 | 558.24 | 434.28 | 592.59 | 160.49 | 80.99 | 156.25 | 118.03 | 284.90 | 159.87 |
| V | 308.21 | 7.02 | 7.89 | 307.61 | 239.26 | 303.19 | 4.19 | 61.99 | 90.74 | 74.02 | 160.17 | 9.67 |
| Cr | 49.55 | 22.92 | 16.68 | 49.58 | 41.42 | 16.00 | 17.93 | 18.95 | 24.58 | 27.42 | 26.75 | 23.70 |
| Mn | 309.08 | 195.00 | 197.75 | 4,370.81 | 250.44 | 405.60 | 151.08 | 103.02 | 139.49 | 180.52 | 264.26 | 273.24 |
| Fe | 8,080.67 | 2,166.40 | 2,027.77 | 4,381.92 | 4,891.04 | 7,540.80 | 1,788.46 | 1,257.43 | 1,704.85 | 1,386.53 | 3,628.47 | 6,545.13 |
| Co | 112.67 | 2.76 | 3.08 | 10.42 | 8.52 | 6.31 | 2.18 | 25.88 | 15.60 | 5.35 | 4.20 | 5.36 |
| Ni | 5.98 | 15.42 | 15.67 | 3.00 | 1.89 | 6.17 | 12.44 | 1.19 | 1.71 | 0.79 | 1.43 | 36.54 |
| Cu | 50.21 | 42.81 | 13.55 | 7.52 | 9.73 | 7,910.15 | 14,563.60 | 13,491.98 | 9,819.92 | 124.41 | 268.01 | 492.78 |
| Zn | 670.97 | 15.98 | 21.23 | 12.99 | 11.10 | 35.75 | 21.12 | 25.35 | 24.81 | 15.14 | 441.53 | 30.00 |
| Ga | 3.56 | 6.93 | 4.30 | 10.87 | 11.32 | 12.62 | 6.40 | 3.44 | 5.39 | 2.75 | 8.05 | 4.72 |
| As | 3.16 | 5.95 | 8.13 | 1.09 | 1.29 | 5.10 | 9.88 | 49.43 | 50.86 | 17.13 | 10.78 | 105.13 |
| Sr | 233.94 | 344.82 | 497.29 | 533.78 | 563.88 | 493.73 | 289.38 | 226.78 | 342.01 | 321.19 | 191.11 | 340.61 |
| Y | 3.38 | 2.87 | 2.96 | 3.35 | 2.44 | 3.67 | 1.25 | 0.87 | 1.23 | 1.18 | 2.34 | 2.89 |
| Zr | 13.43 | 7.89 | 11.78 | 51.78 | 14.54 | 33.66 | 5.88 | 2.57 | 4.86 | 4.08 | 13.93 | 9.20 |
| Ag | 0.05 | 0.49 | 0.13 | 0.03 | 0.02 | 3.16 | 0.78 | 1.85 | 1.02 | 0.13 | 16.75 | 18.08 |
| Sn | 20.93 | 0.83 | 2.81 | 0.27 | 0.17 | 1,533.13 | 2.52 | 9.90 | 12.79 | 9.20 | 5.01 | 8.02 |
| Sb | 13.35 | 51.13 | 1.74 | 0.18 | 1.60 | 4.32 | 31,673.41 | 19,185.94 | 20,831.52 | 29,749.83 | 7,839.15 | 27,782.05 |
| Cs | 0.16 | 0.19 | 0.42 | 0.12 | 0.11 | 0.43 | 0.60 | 0.31 | 0.28 | 0.42 | 0.53 | 2.17 |
| Ba | 9.76 | 47.32 | 34.90 | 83.21 | 92.44 | 97.42 | 40.64 | 18.31 | 38.81 | 21.84 | 57.88 | 40.04 |
| La | 3.25 | 1.76 | 1.89 | 3.28 | 2.19 | 6.12 | 1.37 | 0.59 | 1.02 | 0.92 | 2.04 | 3.26 |
| Ce | 6.26 | 3.16 | 5.75 | 5.68 | 3.70 | 10.75 | 1.96 | 0.96 | 1.64 | 1.64 | 3.74 | 5.16 |
| W | 0.06 | 0.00 | 0.20 | 0.07 | 0.09 | 0.11 | 0.04 | 0.02 | 0.03 | 0.03 | 0.18 | 31.14 |
| Au | 0.01 | 0.01 | 0.03 | 0.00 | 0.00 | 0.19 | 0.33 | 0.16 | 0.26 | 0.01 | 0.63 | 0.74 |
| Pb | 4.78 | 9.18 | 12.43 | 1.47 | 2.05 | 16,593.11 | 10.20 | 8.48 | 8.07 | 45.25 | 59,600.73 | 101,457.53 |
| Bi | 0.04 | 0.06 | 0.14 | 0.01 | 0.02 | 21.30 | 0.19 | 0.12 | 0.19 | 0.10 | 1,010.87 | 431.00 |
| Th | 0.48 | 0.51 | 1.95 | 1.02 | 0.44 | 1.86 | 0.26 | 0.08 | 0.17 | 0.43 | 0.85 | 5.15 |
| U | 0.62 | 0.16 | 0.30 | 0.30 | 0.18 | 0.31 | 0.08 | 0.04 | 0.07 | 0.04 | 0.22 | 2.09 |
| Cr/La | 15.25 | 12.99 | 8.83 | 15.12 | 18.88 | 2.61 | 13.08 | 31.87 | 24.08 | 29.92 | 13.12 | 7.28 |
| 1000Zr/Ti | 26.02 | 45.66 | 42.75 | 92.76 | 33.47 | 56.80 | 36.64 | 31.75 | 31.09 | 34.54 | 48.90 | 57.54 |

Table 16: Trace elemental analysis, results

5.7 Trace elemental compositional analysis

LA-ICPMS was used to examine the trace elemental composition of a selected sample of the glasses. Previous work had indicated that the blue glasses from Nuzi were distinct from contemporary Egyptian glasses from Amarna (Shortland et al 2007). However, it was decided to look at some of the other colours of glass from Nuzi, despite their much smaller numbers. The analysis was carried out at the Getty Conservation Institute in Los Angeles by Dr Marc Walton. The results are presented in Table 16.

The trace elemental analyses indicated that the coloured glasses differed from the blue glasses predominantly in the presence of metals such as lead which produces the yellow colour. When the ratios of elements that have been noted to produce discrimination between Near Eastern and Egyptian glasses are plotted, Figure 36, (Shortland et al 2007; Walton et al 2009) Two of the colorant-free examples, one of the three turquoise samples (1930.62.103) and the yellow glasses are close to the previously established Near Eastern group. The white glass (1930.82.59), two of the turquoise glasses, the other colorant-free glass, 1930.82.62e, and the two colourless examples all sit outside the known groups. A single green bead (1930.67.42) fits well with the Egyptian glasses so could represent an import, interestingly it is the only opaque green glass of Bronze Age date found in the assemblage from Nuzi. Unlike the translucent blue glasses, the colorant-free glasses, which are compositionally very similar in their major oxides (Table 12) show quite a wide scatter in their 1000Ti/Zr and Cr/La ratios; unfortunately there is no comparable data from Egyptian glasses of the same colour. It is unclear why this glass should be so different from the blue glasses, but the technology required to produce the amber colour, a reducing atmosphere, the use of different raw materials or the presence of reducing agents may have resulted in this being a specialist product. A colorant-free raw glass

ingot is noted from the contemporary Near Eastern site of Tell Brak (Oates et al 1997:85) suggesting that glass of this colour was being moved around in the Near East during this period.

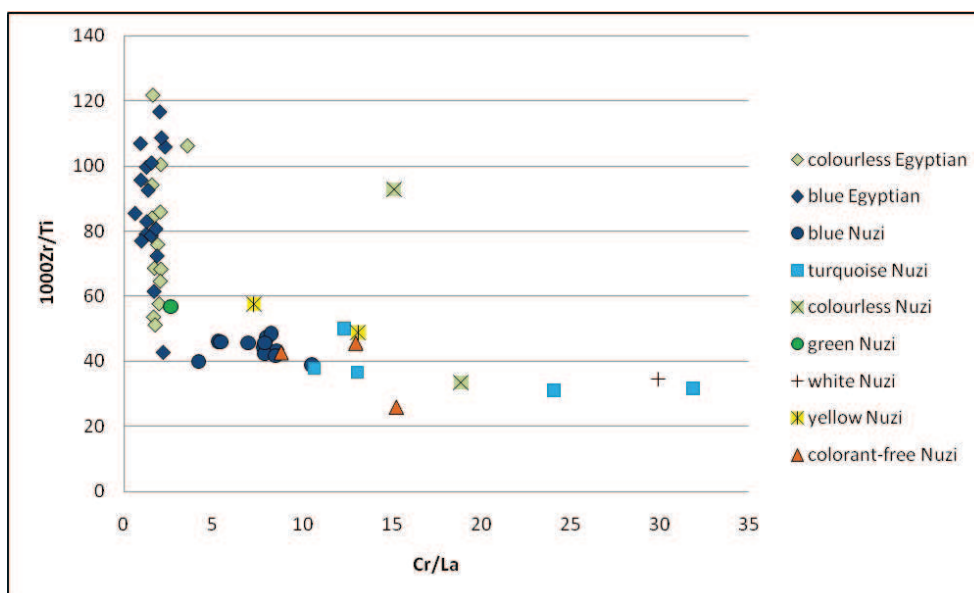


Figure 36: Scatterplot showing trace element groups for Egyptian and Near Eastern glass (from Shortland et al 2007) with additional data from the current project

The colourless glasses found at Nuzi are compositionally distinct in their major elements, for example they are higher in aluminium oxide than the other LBA glasses, and this is reflected in their trace element compositions as well. One appears similar to the outliers from the Near Eastern group (1930.82.62c) and the other is different from both groups (1930.82.62b). The outliers from Nuzi, excluding 1930.82.62b have similar $1000Zr/Ti$ ratios to the 'Near Eastern' group but different Cr/La . This could be an effect of the opacifier used, calcium antimonate, however, there are opaque examples, which fit well with the translucent glasses suggesting that the addition of antimony does not necessarily alter the overall ratios of the trace elements being used. The single unaltered white glass and the similar turquoise glasses may then represent the product of a further glassmaking centre; unfortunately there is very little white glass and colorant-free glass present within the assemblage for comparison. The outlying colorant-free glass is surprising as it an object type exclusive to Nuzi, a sun disk pendant, however it appears to be a unique object in this colour.

5.8 Summary

The bulk compositional analyses have indicated that the Nuzi glasses are a plant ash soda-lime silicate with various colorants used to create the range of colours seen. A distinction was noted between the opaque turquoise and translucent blue glasses, with the opaque glasses containing higher lime and lower soda than their translucent counterparts. A number of Late glasses were also analysed, these were found to have higher aluminium and titanium oxide levels than the LBA glasses. Several natron-based glasses were also

found. A yellow glass with lead stannate colorant was noted, this colour suggests a first rather than second millennium BC date for this object. A number of frit and faience objects were identified alongside two bone beads. The glazed ceramics were noted to be of slightly different composition to the glasses in some cases with a higher potash to magnesia level than the glasses. However, a few white-glazed objects were noted, coloured by calcium antimonate. The trace element analysis suggested that there several outliers from the Near Eastern group in the glasses analysed in this study, including a colorant-free pendant, two turquoise beads and the white glass object.

6 Results 3: Preservation and weathering

6.1 2nd millennium BC glass

6.1.1 Visual survey

The initial survey of the glass assemblage from Nuzi held within the Semitic Museum at Harvard University showed that the majority of the 2nd millennium BC glass was in a poor state of preservation. However there was considerable variation within this and several groups could be distinguished within the alteration states of the glass assemblage. The most obvious grouping was between objects with the original glass remaining and those where the object had completely devitrified. Of the 199 glass samples taken from the museum for analysis 76 still had glass remaining, i.e. retaining translucency and their original colour, and 123 did not; this does not include the samples of other vitreous materials. The glass assemblage was sampled to show the whole range of preservation present, this is detailed in Section 3.2. An exact survey of preservation within the museum materials could not be made as the presence, or absence, of glass was often not visible until an object was broken during sampling. Table 17 below shows the objects sampled by object type and presence of glass.

| Object type | Glass remaining | Devitrified |
|-------------------|-----------------|-------------|
| Vessel (fragment) | 8 | 26 |
| Beads | 32 | 96 |
| Pendant | 4 | 0 |
| Other | 5 | 1 |
| Late glasses | 27 | 0 |
| Total | 76 | 123 |

Table 17: Objects sampled by object type and presence of glass

Within these two groups several variations were present in terms of the degree of alteration. Several objects appeared almost completely unaltered (Figure 37a) whereas others had only a small area of unaltered glass

remaining. Within the devitrified samples there was some also variation with some remaining stable and glassy and others highly unstable and beginning to disintegrate, Figure 37b.

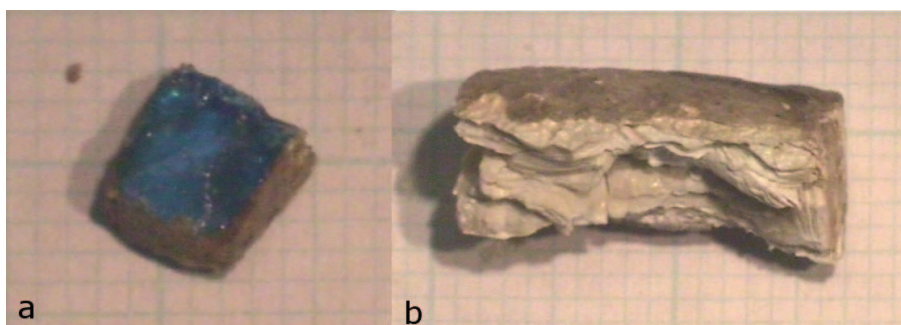


Figure 37: 1930.82.55, well preserved translucent blue glass; 1930.69.39e, devitrified glass bead.

The Bronze Age samples were then placed into a number of subgroups, outlined in Table 18. Within each of these groups there are variations in the type of alteration crust seen, some of the crusts are white and chalky (Figure 38a), others appear a darker colour and flaky (Figure 38b). There are also several beads that retain their translucency but have become highly fragile and tend to break easily. There are also a few examples with an iridescent appearance, for example 1930.66.90c and 1930.60.140d (Figure 38c).



Figure 38: a. 1930.63.40d, opaque turquoise glass with white weathering crust; b. 1930.63.37, colorant-free eye bead with beige weathering crust; c. 1930.66.90c, translucent blue glass with iridescent weathering crust.

| Group | Description | Number |
|-------|---|--------|
| a | No visible alteration | 17 |
| b | Thin alteration layers predominantly glass | 26 |
| c | Significant alteration layers | 22 |
| d | Predominant alteration layers, little glass | 11 |
| e | Devitrified, glassy | 15 |
| f | Devitrified, stable | 74 |
| g | Devitrified, unstable and flaking | 34 |
| | Total | 199 |

Table 18: Visual survey of preservation - subgroups

Some broad patterns were observed in the appearance of different colours of glasses. Many of the opaque

turquoise glasses and the single yellow glass bead and the white glass object appeared to alter to a chalky white consistency, often solid and retaining the original form of the object well. The translucent blue and colorant-free glasses tended to alter to a beige, somewhat more unstable material (groups c and d). Some of the translucent blue objects also had iridescent alteration layers (group c), which were not observed in any other colour of glass; illustrated in Figure 38c. However, there were also very many beads and vessel fragments where the original colour could not be visually assessed as there was no unaltered glass.

Analytical Scanning Electron Microscopy (SEM-EDS) was used to look at the weathering of the glasses and any alteration layers at a microscopic level, particularly in backscattered mode to provide information about compositional differences between the glasses and any secondary alteration layers. In addition, it was possible to get compositional information about the alteration layers, and any inclusions within the glasses, from the X-ray spectra generated. This analytical technique was also used to look at the change in composition between the original glass and the secondary alteration layers through line analysis and to create compositional maps.

6.1.2 Microstructure and morphology

SEM imaging was used to evaluate the condition and appearance of each sample in terms of its state of preservation and the morphology of any secondary alteration layers. The samples were then placed into groups which are similar to those in the visual summary but as a result of the greater detail available in the SEM images it was possible to refine the categories further, Table 19. The difference in numbers between the samples taken and those analysed is due to various reasons. A number of samples were not analysed, either due to their fragility making mounting them impossible, or analysis not being possible due to the sample 'plucking out' during polishing. A few samples lost their alteration layers during sampling, for example an opaque turquoise eye bead, 1930.67.67, meaning they could only be used for bulk analysis of the glass, and in one case a block (22) was broken during polishing, losing the five samples within it.

| Group | Description | Number |
|-------|---|--------|
| 1 | Glass with changes in backscattered signal only | 3 |
| 2 | Glass with secondary alteration layers less than 500µm thick | 8 |
| 3 | Glass with secondary alteration layers more than 500µm thick | 19 |
| 4 | Devitrified, but 'glassy' in appearance (absence of layers) | 9 |
| 5 | Devitrified, solid alteration layers | 23 |
| 6 | Devitrified, alteration layers beginning to separate | 20 |
| 7 | Devitrified, separated alteration layers, little material remaining | 8 |
| | Total | 90 |

Table 19: Altered glasses subgroups (after SEM imaging)

Ninety LBA samples were imaged with SEM; 100 had been planned but several proved to either be Late period examples, another vitreous material, or not glasses at all, for example samples 1930.82.62d and

sample 1930.68.26 were actually bone beads. An example from each alteration group is illustrated in Figure 39.

- Group 1: The few glasses in this group are almost pristine with the only weathering visible being a change in backscattered contrast at the edges of the samples, for example, 1930.67.42 a green opaque glass bead.
- Group 2: In this group the glasses showed thin secondary alteration layers at the edges of the sample. Several examples in this group also had backscatter coefficient changes extending along cracks in the glass, for example, 1930.82.15b, a translucent blue decorated vessel fragment.
- Group 3: This group has thick secondary alteration layers, in some cases these extend across much of the glass with only small areas of the original glass remaining, for example, 1930.82.17, a blue translucent monochrome vessel fragment.
- Group 4: The devitrified glasses in this group retain the appearance of the original glass despite no actual glass remaining – there are often the beginnings of layers and lamellar features, for example 1930.68.27a a bead.
- Group 5: This group consists of devitrified glasses consisting only of secondary alteration layers, generally the layers are clear but the object remains relatively solid in appearance, for example, 1930.82.58, a white glass possible vessel fragment.
- Group 6: The secondary layers which make up the devitrified glasses in this group are less stable and beginning to separate, however, more solid areas can still be observed, for example, 1930.82.70c a vessel fragment.
- Group 7: In this final group of devitrified glasses very little material remains and there is clear separation between the secondary alteration layers, for example, 1930.82.73d a vessel fragment.

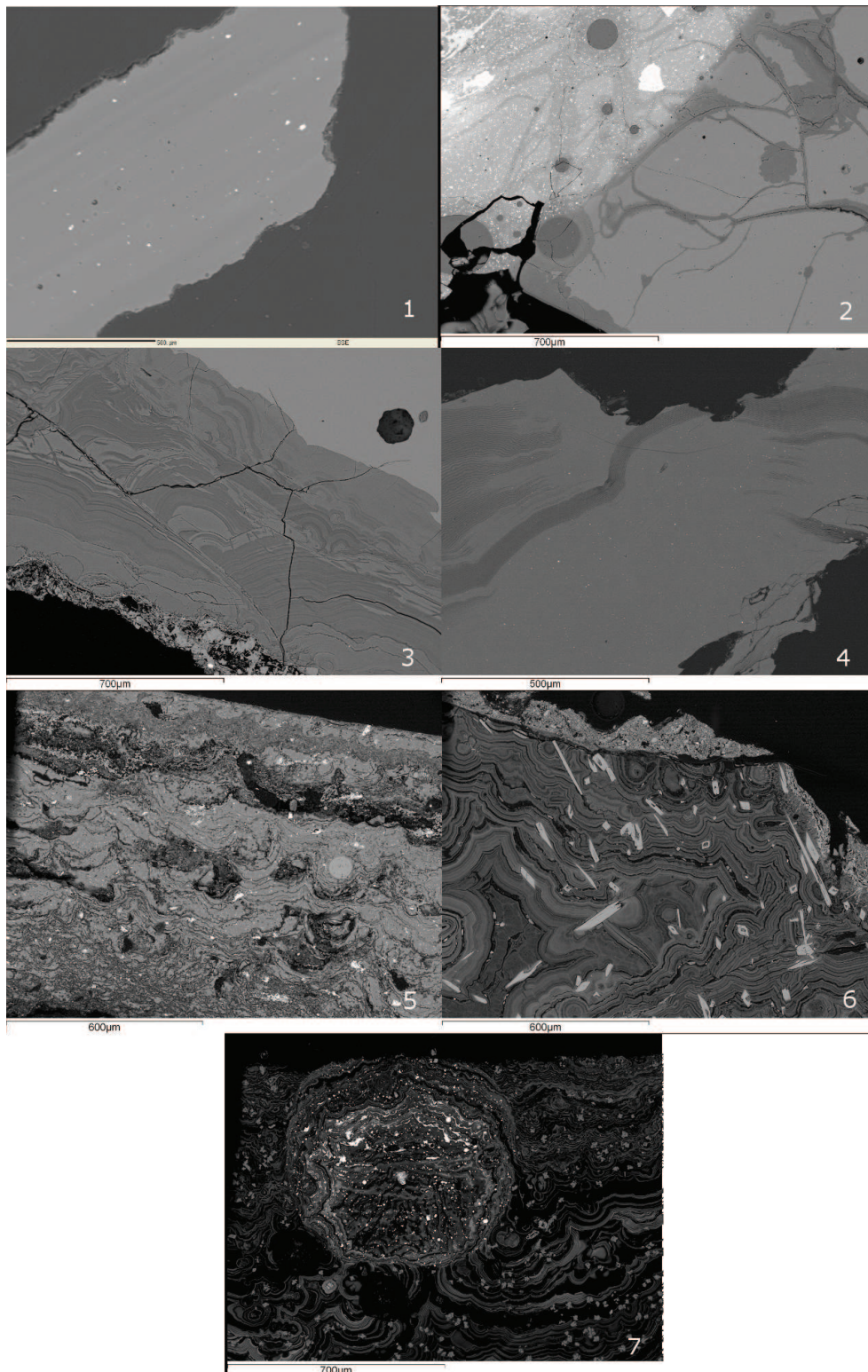


Figure 39: Examples of the preservation groups 1 to 7

Considerable variation was noted within the morphology of the secondary alteration layers seen in both the samples where glass remained and in devitrified examples. In some examples the secondary layers appeared smooth and almost swirled in appearance, for example, 1930.82.4 (Figure 40a). In others the layers were

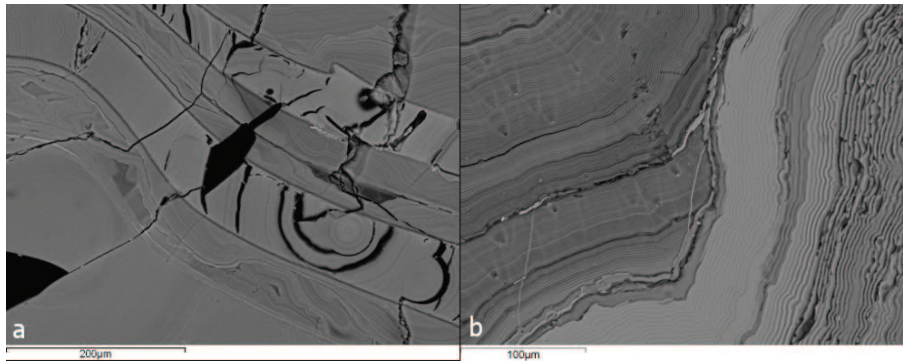


Figure 40: Morphology of alteration layers: a. 1930.82.4; b. 1930.63.37

well defined and more ordered, for example 1930.63.37 (Figure 40b). All of the examples where both glass and secondary alteration layers are present also showed considerable variation in the backscattered contrast in the images of the secondary layers, for example 1930.68.27c in figure 41. This was only observed in eight of the devitrified samples. Tables 20 and 21 show the detailed breakdown of all of the samples imaged and analysed for their preservation and weathering characteristics.

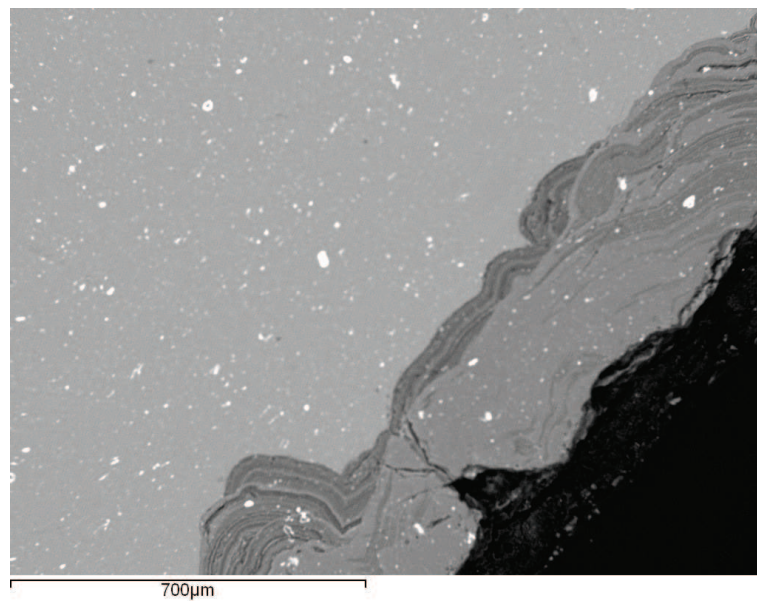


Figure 41: Variation in greyscale in BSE image of secondary alteration layers, 1930.68.27c

| Sample no. | Colour | Type | Location | Group | SEM | Line | Maps | WDS | Lameliae | L<1µm | L>1µm | L mix | L dir | Mg | Cu | Al ₂ O ₃ >1% | Ca | Mn/Fe | Pb | Inclusions | |
|--------------|------------|---------|----------|-------|-----|------|------|-----|----------|-------|-------|-------|-------|----|----|------------------------------------|----|-------|----|------------|--------------------|
| 1930.82.55 | blue | vessel | R87/M100 | 1 | x | | | x | | | | | | | | | | | | | |
| 1930.67.42 | green | bead | I2 | 1 | x | | | | | | | | | | | | | | | | |
| 1930.82.62b | colourless | lump | G50 | 1 | x | | | | | | | | | | | | | | | | |
| 1930.68.27c | turquoise | bead | G29 | 2 | x | | | x | x | | | | | | | | | | | | |
| 1930.82.15b | blue | vessel | M79 | 2 | x | | | x | | | | | | x | | | | | | | |
| 1930.82.7 | blue | vessel | none | 2 | x | | | x | | | | | | | | | | | | | |
| 1930.67.82 | turquoise | pendant | G53 | 2 | x | | | | | | | | | | | | | | | | |
| 1930.69.39d | blue | bead | F24 | 2 | x | | | | | | | | | | | | | | | | |
| 1930.82.13 | amber | vessel | Shil. 44 | 2 | x | | | | | | | | | | | | | | | | |
| 1930.82.50 | blue | ingot | K62 | 2 | x | | | | | | | | | | | | | | | | |
| 1930.82.62c | colourless | lump | G50 | 2 | x | | | | | | | | | | | | | | | | |
| 1930.60.140a | yellow | bead | G50 | 3 | x | x | | x | | | | | | x | | x | | | x | | |
| 1930.60.140b | turquoise | bead | G50 | 3 | x | | | x | | | | | | x | | x | | | | | |
| 1930.62.52 | amber | bead | C12 | 3 | x | | | x | x | x | | x | | | | | | | | | |
| 1930.63.40d | turquoise | bead | G50 | 3 | x | x | | x | x | | | | | | | | | | | | |
| 1930.66.90b | turquoise | bead | none | 3 | x | | | x | x | | | | | x | | | | | | | |
| 1930.66.90f | turquoise | bead | none | 3 | x | | | x | x | | | | | x | | | | | | | calcium/phosphorus |
| 1930.66.90g | blue | bead | none | 3 | x | | | x | x | | | | | x | | | | | | | |
| 1930.69.39f | blue | bead | F24 | 3 | x | x | | x | | | | | | x | | | | | | | |
| 1930.82.15a | blue | vessel | M79 | 3 | x | | | x | | | | | | x | | | x | | | | |
| 1930.82.17 | blue | vessel | L22 | 3 | x | | | x | x | | | | | x | | | x | | | | diopside/quartz |
| 1930.82.18 | black | bead | none | 3 | x | | | x | x | | | | | x | | | x | | | | |
| 1930.82.4 | blue | vessel | Shil. 15 | 3 | x | | | x | x | | | | | x | | x | | | | | |
| 1930.82.59 | white | bar | G50 | 3 | x | x | | x | x | | | | | x | | | | | | | quartz |
| 1930.62.31b | blue | bead | L11/20 | 3 | x | | | | x | x | | | | | | | x | | | | |
| 1930.63.37a | amber | bead | G50 | 3 | x | x | | x | x | | | | | | | | | | | | |
| 1930.66.90c | turquoise | bead | none | 3 | x | | | | x | x | | | | | | | | | | | |
| 1930.66.90h | blue | bead | none | 3 | x | | | | x | | | | | | | | | | | | |
| 1930.82.48 | blue | pendant | H33 | 3 | x | | | | x | | | | | | | | | | | | |
| 1930.82.62e | amber | pendant | G50 | 3 | x | | | | x | | | | | | | | | | | | |
| | | | | | 30 | 5 | 8 | 17 | 16 | 9 | 1 | 6 | 6 | 12 | 6 | 3 | 4 | 0 | | 1 | |

Table 20: Details of alteration: samples with glass present

| Sample no. | Colour | Type | Location | Group | SEM | Line | Maps | WDS | Lamellae | L<1µm | L>1µm | L, mik | L, dfr | Mg | Cu | Al ₂ O ₃ -% | Ca | Mn/Fc | Pb | Inclusions | |
|--------------|---------------|--------|----------|-------|-----|------|------|-----|----------|-------|-------|--------|--------|----|----|-----------------------------------|----|-------|----|------------|-----------------------|
| 1930.02.86 | blue | vessel | none | 4 | x | | | x | x | x | | | x | x | x | x | | | | x | diopside/chromspinel |
| 1930.01.123 | yellow | inlay | none | 4 | x | | | | | | | | | | | | | | | | albite |
| 1930.01.126 | blue | vessel | G29 | 4 | x | | | | | | | | | | | | | | | | diopside |
| 1930.08.27a | blue | bead | G29 | 4 | x | | | | | | | | | | | | x | | | | |
| 1930.02.271 | blue | bead | G29 | 4 | x | | | | | | | | | | | | | | | | |
| 1930.08.9 | blue | bead | Shil, 26 | 4 | x | | | | | | | | | | | | | | | | albite |
| 1930.09.39a | bead | F24 | | 4 | x | | | | | | | | | | | | | | | | |
| 1930.09.39c | turquoise | bead | F24 | 4 | x | | | | | | | | | | | | | | | | |
| 1930.02.62f | unknown | vessel | G50 | 4 | x | | | | | | | | | | | | | | | | |
| 1930.00.42 | blue | bead | 5416 | 5 | x | | | | | | | | | | | | | | | | albite |
| 1930.02.103 | yellow | bead | H8 | 5 | x | | | | | | | | | | | | | | | | albite |
| 1930.02.81 | yellow | bead | dheck | 5 | x | | | | | | | | | | | | | | | | none |
| 1930.02.70b | blue | vessel | G50 | 5 | x | | | | | | | | | | | | | | | | diopside |
| 1930.02.1E | yellow | vessel | none | 5 | x | | | | | | | | | | | | | | | | diopside |
| 1930.00.140f | yellow | bead | G50 | 5 | x | | | | | | | | | | | | | | | | albite |
| 1930.01.88d | turquoise | bead | G50 | 5 | x | | | | | | | | | | | | | | | | albite |
| 1930.01.91a | red | bead | G50 | 5 | x | | | | | | | | | | | | | | | | iron-rich |
| 1930.02.84b | blue | bead | G50 | 5 | x | | | | | | | | | | | | | | | | |
| 1930.02.84a | blue | bead | G50 | 5 | x | | | | | | | | | | | | | | | | |
| 1930.02.84c | blue | bead | G50 | 5 | x | | | | | | | | | | | | | | | | |
| 1930.02.84e | colorant-free | bead | G50 | 5 | x | | | | | | | | | | | | | | | | albite/feldspar |
| 1930.02.84f | colorant-free | bead | G50 | 5 | x | | | | | | | | | | | | | | | | calcium/phosphorus/ir |
| 1930.03.38 | unknown | bead | G50 | 5 | x | | | | | | | | | | | | | | | | |
| 1930.02.80a | colorant-free | bead | G50 | 5 | x | | | | | | | | | | | | | | | | |
| 1930.02.70b | yellow | bead | G50 | 5 | x | | | | | | | | | | | | | | | | |
| 1930.06.89 | unknown | bead | none | 5 | x | | | | | | | | | | | | | | | | bone fragment |
| 1930.06.89 | unknown | bead | none | 5 | x | | | | | | | | | | | | | | | | albite |
| 1930.09.39b | blue | bead | F24 | 5 | x | | | | | | | | | | | | | | | | |
| 1930.02.98 | white | vessel | L4 | 5 | x | | | | | | | | | | | | | | | | |
| 1930.02.65a | blue | vessel | G29 | 5 | x | | | | | | | | | | | | | | | | |
| 1930.02.65d | blue | vessel | G29 | 5 | x | | | | | | | | | | | | | | | | |
| 1930.02.67 | blue | vessel | G28 | 5 | x | | | | | | | | | | | | | | | | |
| 1930.02.73a | blue | vessel | G50 | 5 | x | | | | | | | | | | | | | | | | diopside |
| 1930.02.73c | blue | vessel | G50 | 5 | x | | | | | | | | | | | | | | | | |
| 1930.01.7 | blue | bead | 5111 | 6 | x | | | | | | | | | | | | | | | | diopside |
| 1930.01.88b | blue | bead | G50 | 6 | x | | | | | | | | | | | | | | | | diopside |
| 1930.02.84d | blue | bead | G50 | 6 | x | | | | | | | | | | | | | | | | albite |
| 1930.02.84e | blue | bead | G50 | 6 | x | | | | | | | | | | | | | | | | |
| 1930.02.84f | blue | bead | G50 | 6 | x | | | | | | | | | | | | | | | | |
| 1930.02.70a | blue | vessel | G50 | 6 | x | | | | | | | | | | | | | | | | diopside |
| 1930.02.70c | blue | vessel | G50 | 6 | x | | | | | | | | | | | | | | | | diopside |
| 1930.02.102 | yellow | bead | G29 | 6 | x | | | | | | | | | | | | | | | | |
| 1930.02.31a | turquoise | bead | L11/20 | 6 | x | | | | | | | | | | | | | | | | |
| 1930.02.82 | yellow | bead | G50 | 6 | x | | | | | | | | | | | | | | | | |
| 1930.02.84b | blue | vessel | G50 | 6 | x | | | | | | | | | | | | | | | | diopside |
| 1930.02.84c | blue | bead | G50 | 6 | x | | | | | | | | | | | | | | | | |
| 1930.02.29 | yellow | bead | G29 | 6 | x | | | | | | | | | | | | | | | | |
| 1930.03.37b | yellow | bead | G50 | 6 | x | | | | | | | | | | | | | | | | |
| 1930.03.59c | black | bead | G32 | 6 | x | | | | | | | | | | | | | | | | CuS |
| 1930.02.27b | black | bead | G29 | 6 | x | | | | | | | | | | | | | | | | CuS |
| 1930.02.15c | unknown | vessel | M79 | 6 | x | | | | | | | | | | | | | | | | |
| 1930.02.65c | blue | vessel | G29 | 6 | x | | | | | | | | | | | | | | | | |
| 1930.02.66 | blue | vessel | none | 6 | x | | | | | | | | | | | | | | | | albite |
| 1930.02.70b | blue | vessel | G50 | 6 | x | | | | | | | | | | | | | | | | |
| 1930.01.85 | blue | bead | G33 | 7 | x | | | | | | | | | | | | | | | | diopside |
| 1930.01.88a | colorant-free | bead | G50 | 7 | x | | | | | | | | | | | | | | | | |
| 1930.01.88c | blue | bead | G50 | 7 | x | | | | | | | | | | | | | | | | |
| 1930.02.73d | blue | vessel | G50 | 7 | x | | | | | | | | | | | | | | | | quartz |
| 1930.02.101 | check | bead | H14 | 7 | x | | | | | | | | | | | | | | | | |
| 1930.03.40f | check | bead | G50 | 7 | x | | | | | | | | | | | | | | | | |
| 1930.02.84f | colorant-free | bead | G50 | 7 | x | | | | | | | | | | | | | | | | |
| 1930.02.14 | unknown | vessel | G50 | 7 | x | | | | | | | | | | | | | | | | |

Table 21: Details of alteration: devitrified glasses

A notable feature of almost all of the samples with secondary precipitated layers was the presence of lamellar features; 69 out of 90 samples had clear lamellae. Of the ones that did not several did not have secondary layers and in the other cases it is possible that they were present but at a scale too small to be easily seen. These ranged in size from less than a micron across to several microns across (Figure 42a and b); in addition a change in scale within a single sample could also be seen in 32 of the samples imaged (Figure 42c). These lamellar features also showed a range of changes in direction within the samples from subtle shifts creating a ‘faceted’ appearance (Figure 40b) to almost right angles to one another, reminding one that the weathering processes are happening in three dimensions (Figure 42d). Another feature is the

'organisation' of the layers which in some cases is clear with the lamellae running in a single direction for most of the sample, for example as seen in 1930.69.39b (Figure 42e); in other cases they appear highly disorganised varying in thickness and direction, including the creation of circular forms (Figure 43f). These lamellar features appear to consist of smooth layers with disorganised, 'spongy' material in between these layers. However, it was only possible to observe this in a very few samples where the scale of the lamellae was large enough, such as 1930.62.84c (Figure 42b) and 1930.82.34, a later glass (Figure 61).

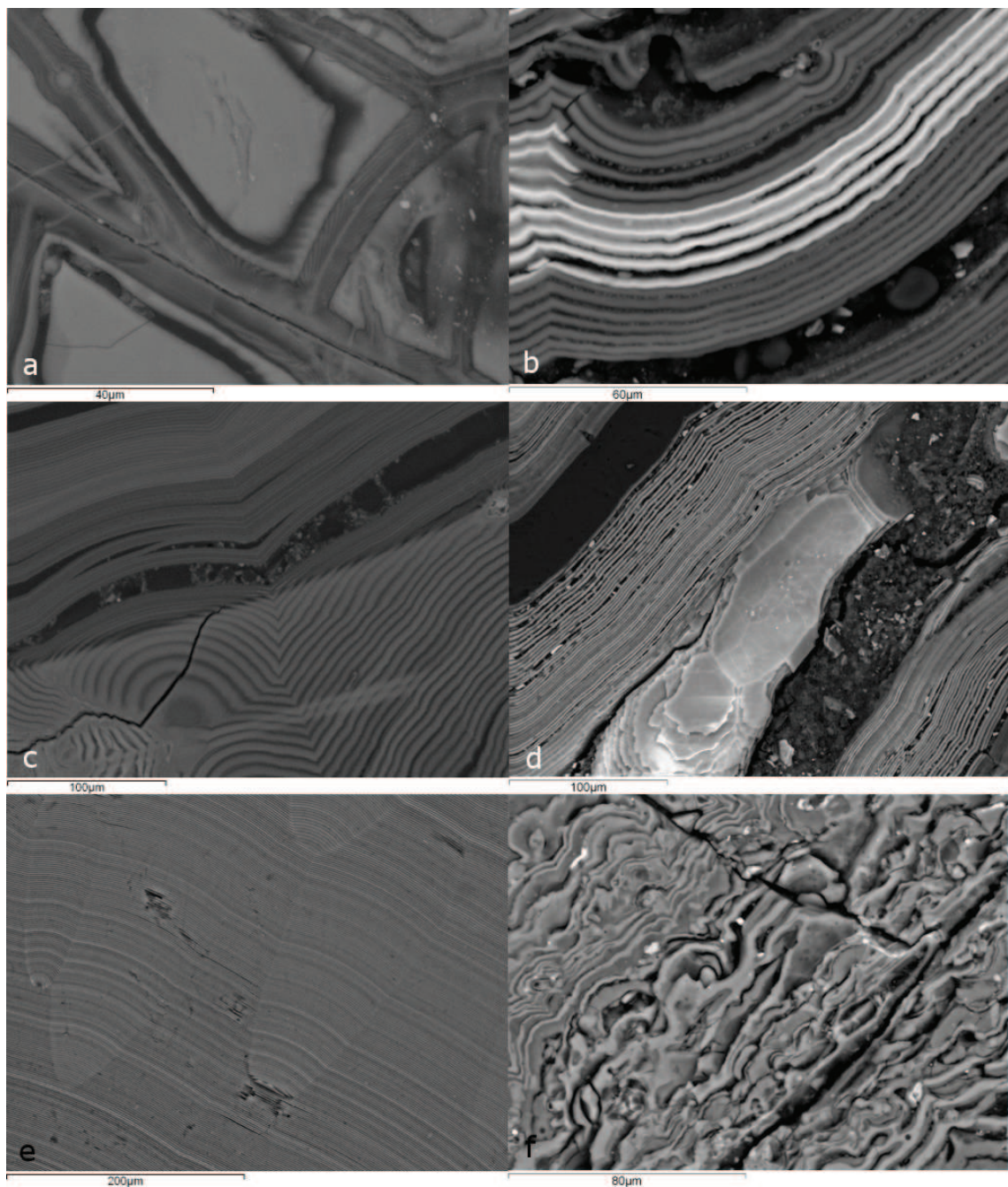


Figure 42: Lamellar features 1: a. 1930.60.42 fine lamellar features; b. 1930.62.84c larger lamellar features; c. 1930.63.40a changes in scale; d. changes in direction of reaction front; e. 1930.69.39b smooth well-organised lamellae; f. 1930.62.84e disorganised lamellae.

Several examples of the devitrified glasses also appeared to show signs of compression within the alteration layers, for example, 1930.82.66 (Figure 43a). Many of the samples were also fractured, such as 1930.68.27b (Figure 43b), although it is possible that mounting and polishing may have increased already existing weak points and fractures within the secondary alteration layers. Another occasional feature noted was lamellar features showing 'fault line' behaviour around cracks, also seen in 1930.68.27b (Figure 43b). In the samples where glass remained the alteration process was noted to run along cracks and other features, such as filled pores, with areas around these features often having been a darker colour indicating a change in composition, for example, 1930.82.15b (Figure 43c).

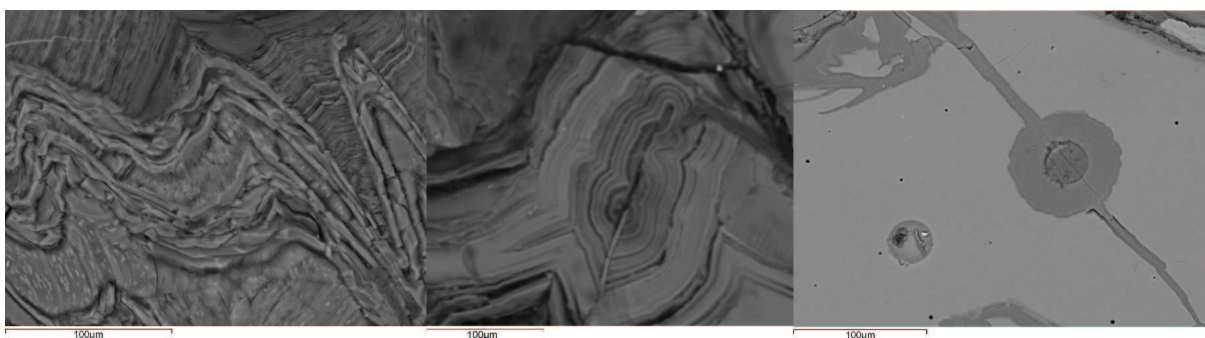


Figure 43: Features of secondary layers: 1930.82.66 with compressed layers; 1930.68.27b showing significant fractures and 'fault line' behaviour of lamellae around cracks; 1930.82.15b with the alteration process moving along cracks in otherwise pristine glass.

6.1.3 Line analyses

Line analyses were taken from eight samples: five with glass remaining, 1930.60.140a, 1930.63.37a, 1930.63.40d, 1930.69.39f and 1930.82.59; and three devitrified samples, 1930.69.39b, 1930.82.14 and 1930.82.73a. These were selected to cover each colour of glass and from each group of the devitrified glasses. In the samples where glass was retained the line analyses all showed a clear break between the glass and secondary alteration layers. In each case the counts for sodium and potassium reduced significantly with calcium also usually dropping. However, in all of the samples apart from 1930.60.140a there were sections of the line in the altered layers with increased counts of magnesium, as can be seen in Figure 44. These appeared to correspond with darker areas of the BSE images. In the devitrified examples there was less change across the line analysis, however, in sample 1930.82.14 (Figure 45) the areas where material had been lost had much lower counts of silicon. 1930.69.39b also showed the slight changes in composition across the lamellar features with a slight increase in silicon counts over the paler lines, Figure 46.

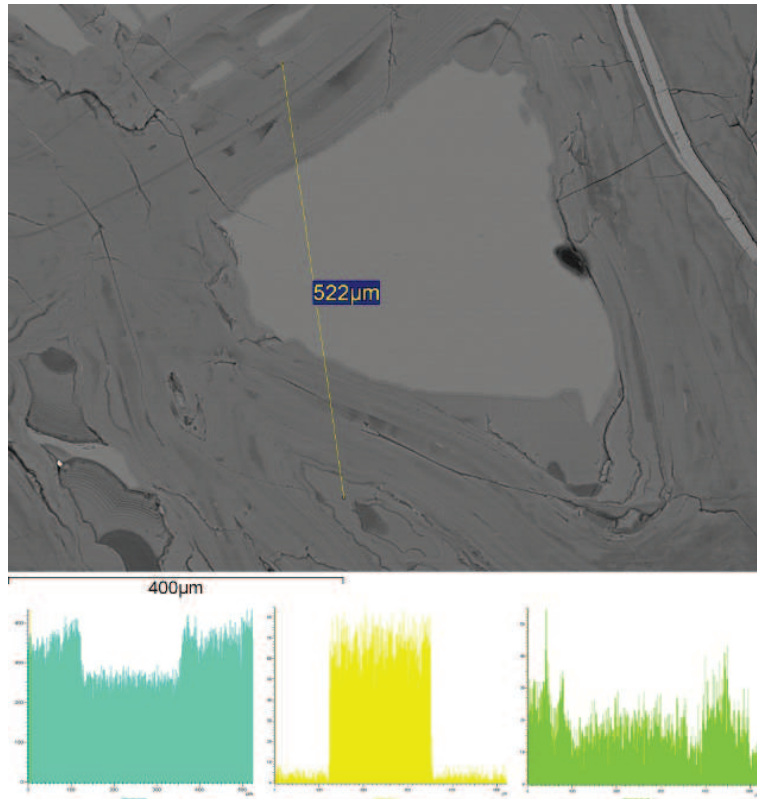


Figure 44: Line analysis of 1930.69.39f: silicon, sodium and magnesium maps

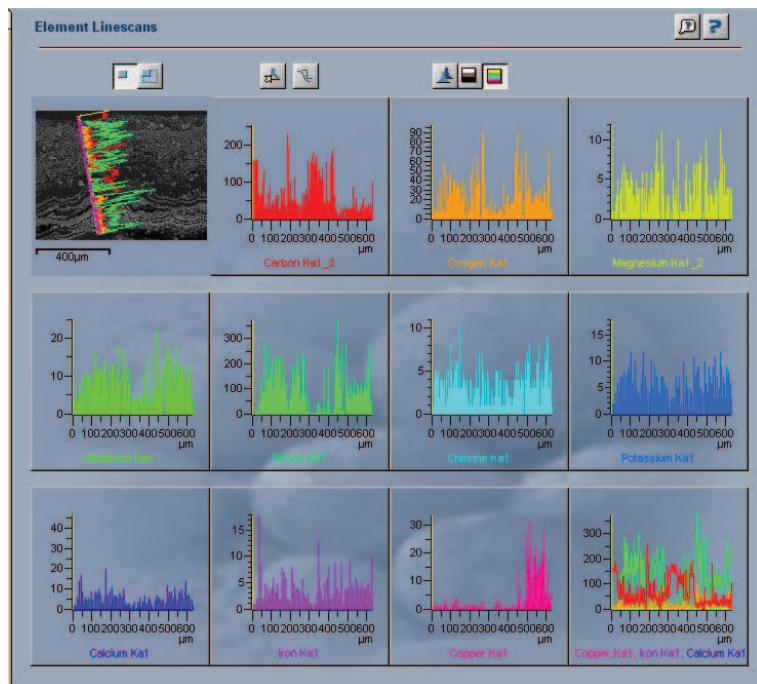


Figure 45: Line analysis 1930.82.14, screenshot

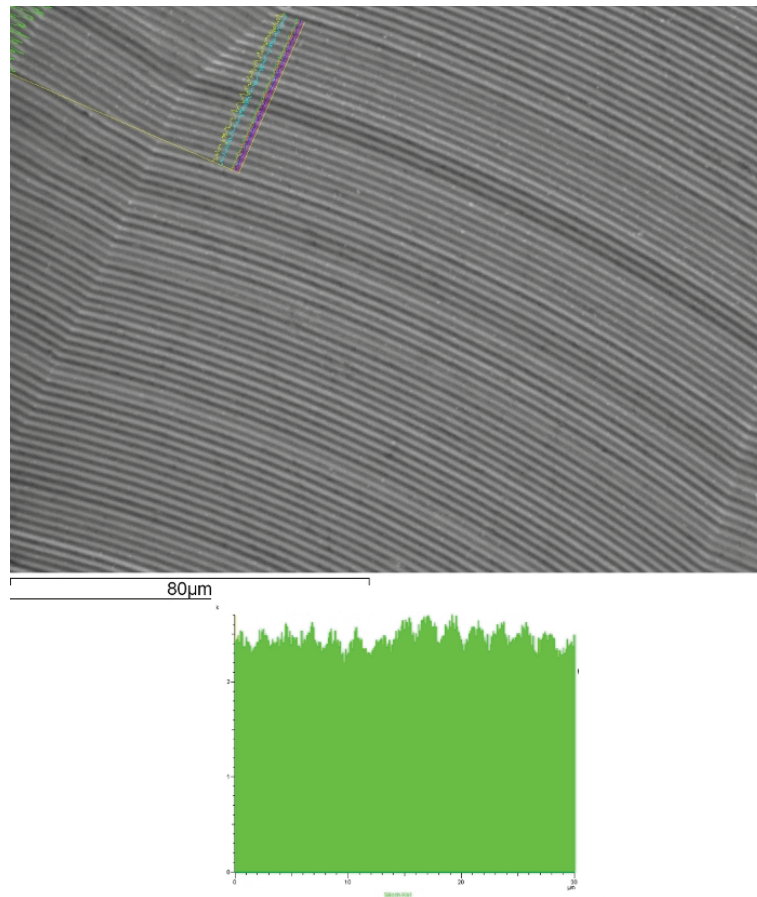


Figure 46: Line analysis 1930.69.39b, variation in silicon counts

6.1.4 Compositional maps

The line analyses had suggested that the composition of the altered layers varied, with magnesium in particular being higher in some areas than others; therefore, it was decided to run several compositional maps of the glasses with significant secondary alteration layers. Maps were run on the Cameca SX 100 using the SEM-EDS of all of the five samples mentioned above, except 1930.69.39f, and with the addition of samples 1930.82.4 and 1930.82.17, these were chosen as they all had interesting features in their alteration layers and were an example of each colour. A further three maps were run on SEM EDS where montages and maps of much larger areas could be analysed, including cross sections of two almost whole beads, 1930.66.90f and 1930.66.90g. A further map of 1930.82.4 was also produced on this machine to examine an odd area of the alteration layers; Figure 47 shows the BSE image, which appeared 'smeared' in areas of the layers, this was initially thought to be an artefact of the technique, perhaps caused by charging, but on reanalysis did seem to be actually present in the object.

The full series of images of 1930.82.59 (Figure 48) shows the elements mapped on the Cameca SX100, the relative brightness of each pixel analysed is related to the counts of each X-ray line sought over a set time. These maps show the complete loss of sodium and potassium, higher counts of calcium and magnesium in

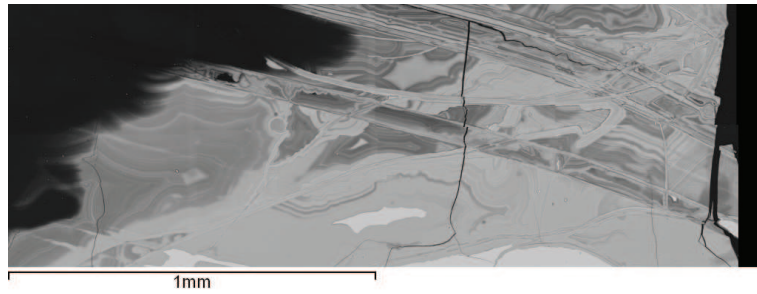


Figure 47: Montage of area of 1930.82.4 with 'smeared' areas in the secondary phases, BSE image

some areas of the alteration layers and the higher counts of silicon in the alteration layers compared to the original glass, the remnant quartz grains are clearly visible in this map as well. The high magnesium counts appear to correspond with lower counts in the silicon map, whilst the antimony map clearly shows that this element does not significantly change between the glass and alteration layers in this antimony-opacified white glass.

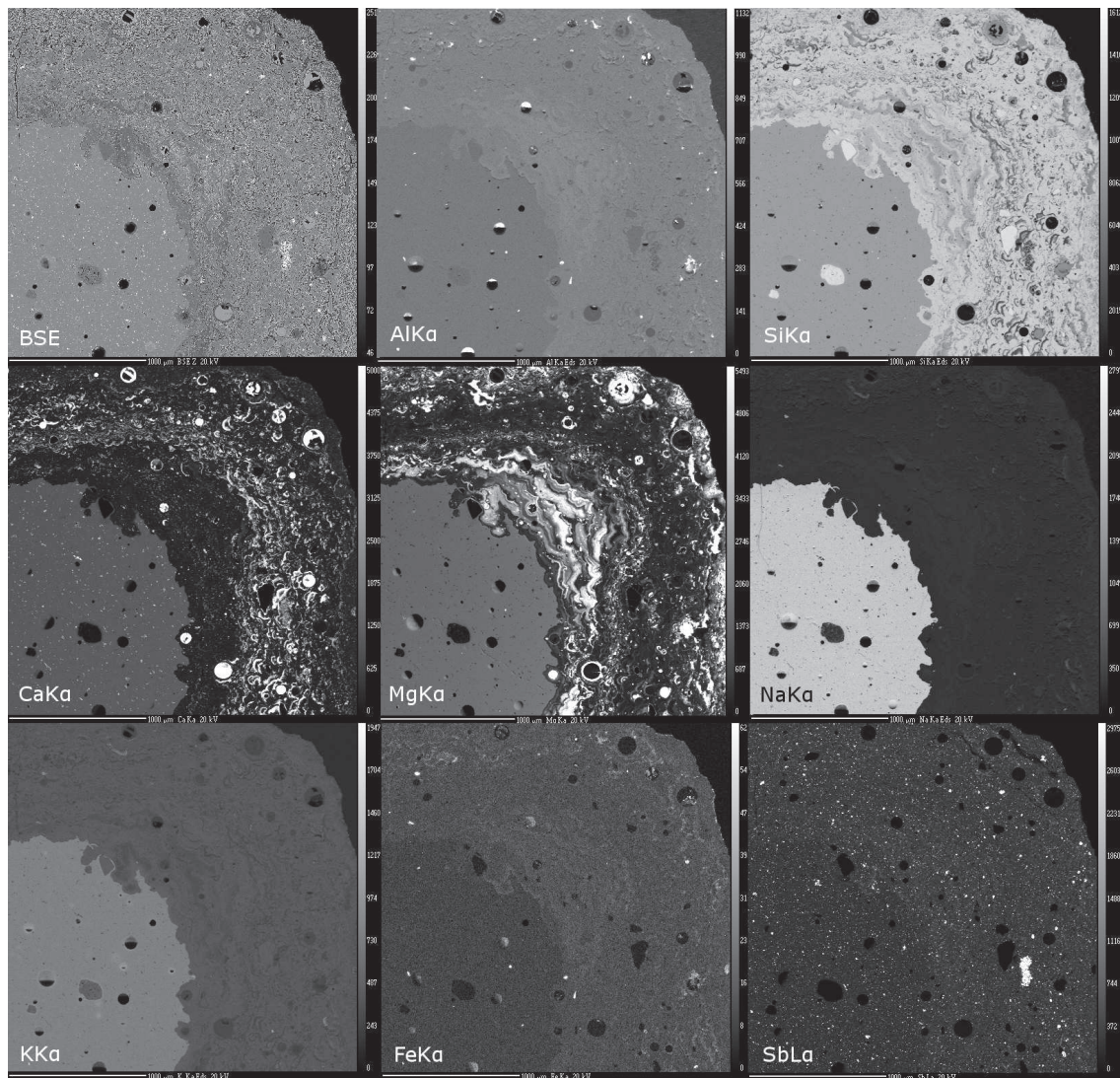


Figure 48: 1930.82.50, opaque white glass, compositional maps

This pattern is repeated in the other samples with copper maps in the blue glasses also showing areas of higher counts, in the same areas as the higher magnesium counts. This can clearly be seen in the maps for 1930.82.4, Figure 49. However, the pattern of high magnesium counts in areas of lower silicon counts can most clearly be seen in a false coloured image of 1930.66.90g, figure 50. The only map that did not follow a very similar pattern was 1930.60.140a. This yellow glass, with a lead-based colorant, did not have any increase in magnesium counts in the alteration layers. However, the maps of this sample show how inhomogeneous the composition of this glass is. Calcium, sodium, and lead all varied within the glass section of this sample giving it a streaky appearance as can be seen in Figure 51.

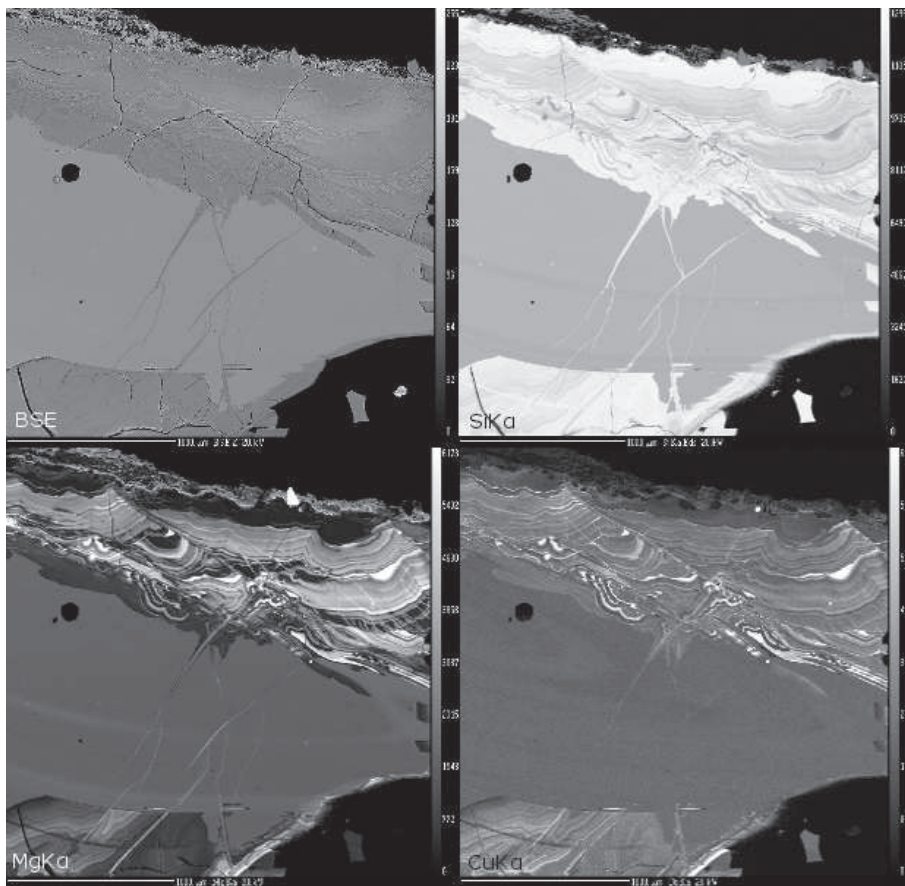


Figure 49: 1930.82.4 compositional maps

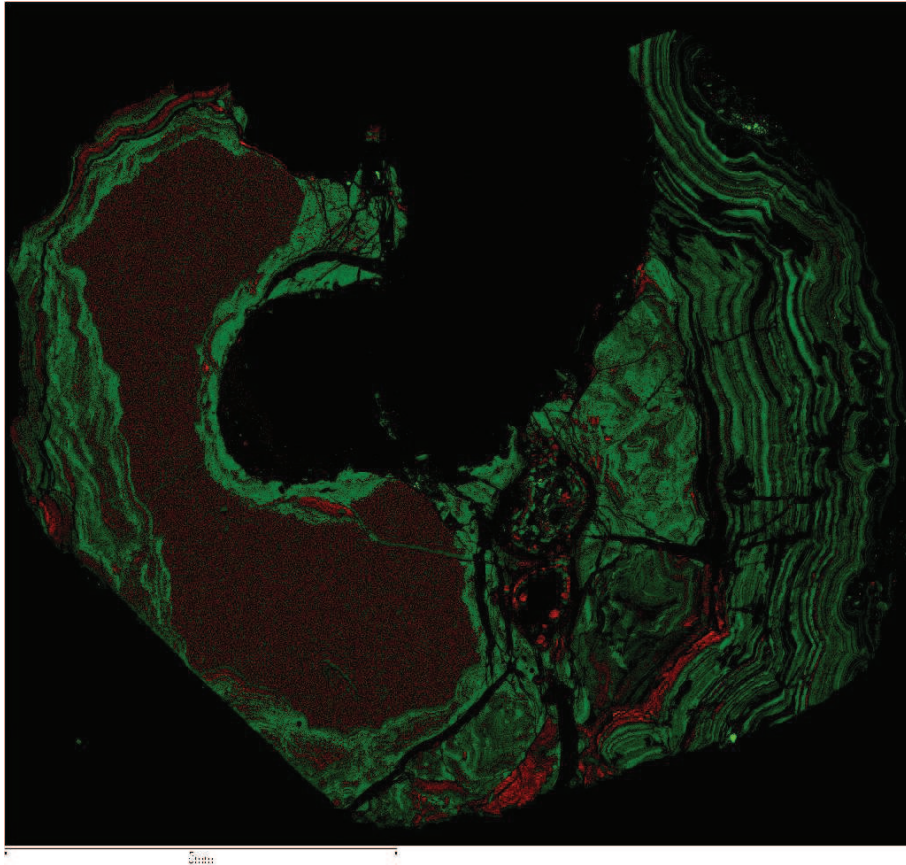


Figure 50: False coloured image of 1930.66.90g Si = green, Mg = red

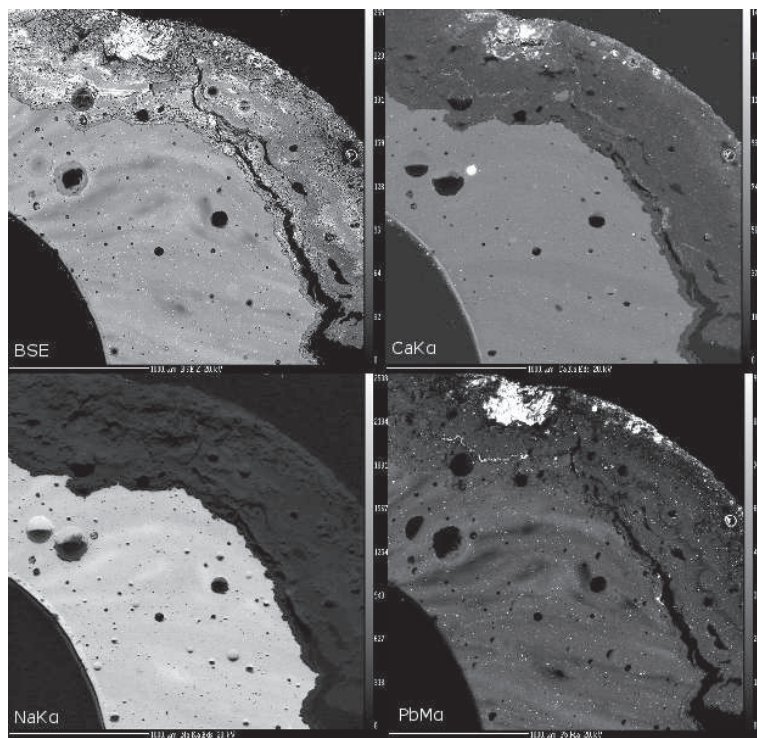


Figure 51: 1930.60.140a, yellow glass bead, compositional maps showing inhomogeneity of composition in unaltered glass

6.1.5 Infiltration and inclusions

Three samples showed infiltration by manganese and iron, as has been reported in other studies (Watkinson et al 2005; Gulmini et al 2009), for example, 1930.82.14 (Figure 52a) and 1930.63.38 contained small areas, bright on backscattered images, which appeared to have been infiltrated by these elements on spectral analysis. The most common type of infiltration along cracks was a calcium-rich substance, white on backscattered images, occurring in ten of the samples imaged, for example 1930.68.9 (Figure 52b). An interesting feature of the yellow glasses imaged is the apparent mobility of the lead colorant which appears to cluster in certain areas and/or migrate along the lamellar features or cracks; this was observed in all nine of the altered yellow glasses, for example 1930.60.140b (Figure 52c).

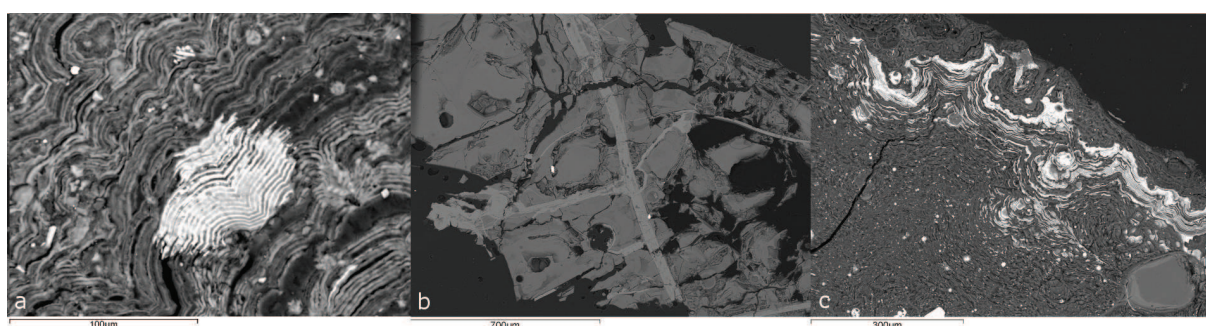


Figure 52: 1930.82.14, manganese and iron-rich area; 1930.68.9, calcium-rich substance infiltrating along cracks; 1930.60.140b, clustering of lead colorant.

The SEM images also showed a variety of inclusions in a number of the glasses, these were analysed using the EDS for identification. The most common is diopside crystals which were observed within 12 of the Bronze Age glasses (Figure 53a); these crystals varied in size from very fine needle-like examples to large well-formed crystals. Diopside are a pyroxene mineral consisting of magnesium, calcium and silicon and are formed at high temperatures, crystallising from a melt at around 1270°C, most usually found in igneous rocks (Walther 2009: 289). They are a relatively common inclusion in ancient glasses as a result of the raw materials used and the melting temperatures (Rehren 2008; Artioli et al 2008). More rarely albite crystals were noted, in seven samples (Figure 53b), these alkali feldspars contain aluminium, silicon and either sodium or potassium, crystallisation temperatures are lower than for pyroxenes at around 600°C (Walther 2009:171-2). Calcium and phosphate rich inclusions were found in two examples, 1930.66.90b (Figure 53c) and 1930.62.84e. Small iron-rich inclusions were noted in 1930.61.91a (Figure 53e), which was thought to be a red frit bead but appears to be an altered glass in the SEM images. Remnant quartz grains were observed in the white glass 1930.82.59 (Figure 48) and a possible chromspinel in 1930.82.66 (Figure 53d). Another unique inclusion was a small bone fragment in 1930.66.89 (Figure 53f).

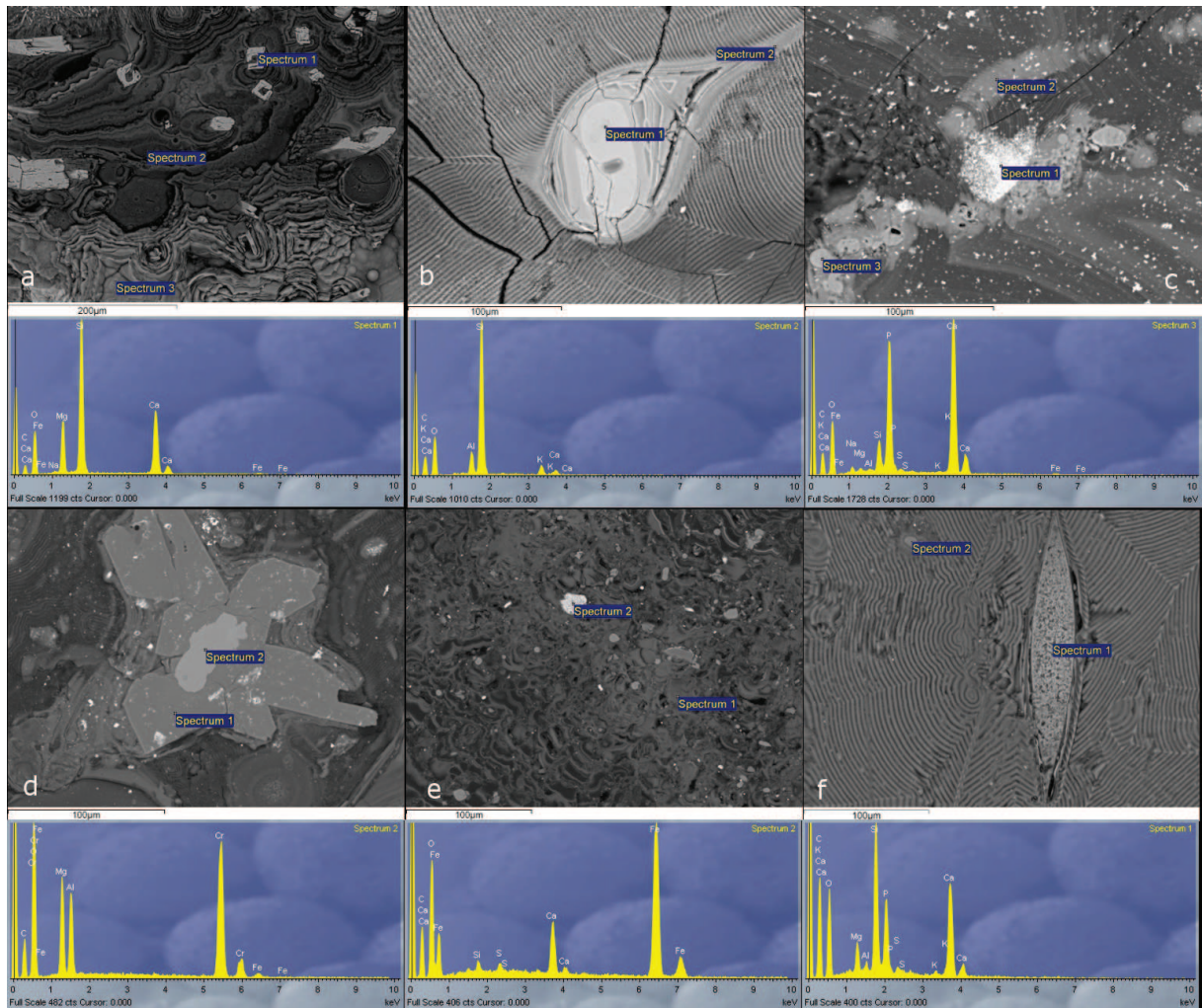


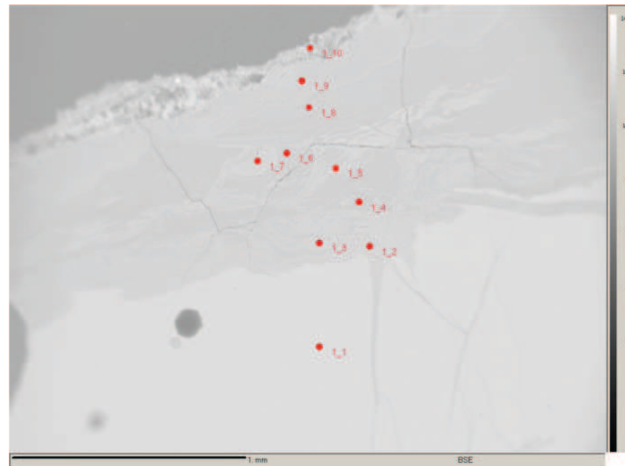
Figure 53: Various inclusions found in the glasses: a. diopsides (1930.82.70a); b. albite inclusion (1930.61.129a); calcium-phosphorus-rich (1930.66.90b); d. possible chromspinel, within diopside (1930.82.66); e. iron-rich inclusion (1930.61.91a); f. bone fragment (1930.66.89)

6.1.6 SEM-WDS

The compositional maps had confirmed the compositional variation seen in the line analyses and it was then decided to quantify these variations by using SEM-WDS to look at specific points in the alteration layers of samples containing glass and devitrified glasses; as well as bulk compositions from a range of completely devitrified glasses.

A number of point analyses were also carried out on samples where glass remained and completely devitrified examples with the number of points taken ranging from two to thirteen, a very low number of points were generally only used if the sample began to charge. Seventeen samples with glass remaining were analysed in this way alongside 18 devitrified glasses. These were selected to cover a range of colours, preservation groups and site locations. All of the detailed points analyses with their accompanying images are contained within Appendix 2.

In the examples where glass remained the point analyses indicated that the secondary layers contained more silica than the original glass, usually between 70 and 80%. Eleven out of the 17 samples analysed had layers high in magnesia such as 1930.66.90f where several layers contain above 10% magnesia (10.2 to 12.1%), the original glass containing 4.5% were noted. This enrichment in magnesia appears to come at the expense of silica, in the three points with higher magnesia the silica had dropped from over 70% to 55-59%; confirming the findings from the compositional maps discussed in the section above. The point analyses also showed six of the thirteen blue glasses showed an increase in copper oxide in some of their alteration layers; this is usually a small rise just above that seen in the original glass, for example, 1930.66.90g where copper oxide levels increase from 1.2% to between 1.6 and 2.0% in the alteration layers. However, in one example, 1930.60.140d, the levels of copper oxide in the alteration layers were extremely high, ranging from 7.5% to 25.6%, the original glass containing only 2.0%. 1930.82.4, Figure 54, is fairly typical, however, the complete analyses are contained in Appendix 2.



| Sample | Original col. | Object type | Location | SiO ₂ | Al ₂ O ₃ | CaO | MgO | Na ₂ O | K ₂ O | Fe ₂ O ₃ | TiO ₂ | CuO | Sb ₂ O ₃ | P ₂ O ₅ | SO ₃ | Cl | Total |
|----------------|---------------|-------------|----------|------------------|--------------------------------|-----|-----|-------------------|------------------|--------------------------------|------------------|-----|--------------------------------|-------------------------------|-----------------|-----|-------|
| 1930.82.4 (1) | trans. blue | vessel | Shil. 15 | 62.0 | 0.6 | 7.0 | 4.6 | 16.3 | 2.5 | 0.6 | 0.0 | 0.9 | 0.1 | 0.1 | 0.3 | 0.9 | 96.1 |
| 1930.82.4 (2) | trans. blue | vessel | Shil. 15 | 83.7 | 0.9 | 0.4 | 1.6 | 0.1 | 0.2 | 0.9 | 0.1 | 1.1 | 0.0 | 0.0 | 0.1 | 0.1 | 89.1 |
| 1930.82.4 (3) | trans. blue | vessel | Shil. 15 | 83.2 | 1.0 | 0.4 | 1.6 | 0.1 | 0.2 | 1.0 | 0.1 | 1.1 | 0.0 | 0.0 | 0.1 | 0.1 | 88.6 |
| 1930.82.4 (4) | trans. blue | vessel | Shil. 15 | 75.0 | 1.3 | 0.4 | 5.1 | 0.1 | 0.4 | 1.2 | 0.1 | 1.3 | 0.0 | 0.2 | 0.2 | 0.4 | 85.5 |
| 1930.82.4 (5) | trans. blue | vessel | Shil. 15 | 72.7 | 1.1 | 0.5 | 4.9 | 0.1 | 0.3 | 1.2 | 0.1 | 1.4 | 0.0 | 0.3 | 0.2 | 0.3 | 83.1 |
| 1930.82.4 (6) | trans. blue | vessel | Shil. 15 | 72.3 | 1.2 | 0.6 | 6.4 | 0.1 | 0.4 | 1.0 | 0.1 | 1.8 | 0.0 | 0.2 | 0.1 | 0.2 | 84.1 |
| 1930.82.4 (7) | trans. blue | vessel | Shil. 15 | 72.6 | 1.1 | 0.6 | 7.0 | 0.1 | 0.4 | 1.1 | 0.1 | 1.9 | 0.0 | 0.2 | 0.1 | 0.2 | 85.3 |
| 1930.82.4 (8) | trans. blue | vessel | Shil. 15 | 76.9 | 1.2 | 0.5 | 4.9 | 0.1 | 0.4 | 1.1 | 0.1 | 1.3 | 0.0 | 0.2 | 0.1 | 0.2 | 87.0 |
| 1930.82.4 (9) | trans. blue | vessel | Shil. 15 | 83.7 | 0.8 | 0.4 | 0.3 | 0.2 | 0.4 | 0.9 | 0.1 | 0.1 | 0.0 | 0.0 | 0.0 | 0.0 | 86.8 |
| 1930.82.4 (10) | trans. blue | vessel | Shil. 15 | 26.2 | 7.4 | 8.8 | 3.8 | 1.1 | 1.5 | 2.9 | 0.2 | 0.1 | 0.1 | 0.1 | 0.3 | 0.0 | 52.3 |

Figure 54: 1930.82.4 points analysis and BSE image

The devitrified glasses showed alteration layers with somewhat different compositions to the examples where glass remained. In general the analytical totals are lower than the samples with glass remaining, many below 60%; this is may to be due to material being 'plucked' out of the more fragile glasses during sample preparation, the rough surface affecting detection of the X-rays or may be due to the material itself. All 18 of the samples analysed by this method had aluminium oxide levels above 1% oxide weight in at least one point analysed, ranging from 1% to 7.9%, with 10 samples above 3%; the 2nd millennium BC glasses typically had aluminium oxide levels below 0.5%. Seven of the 18 samples also had copper-rich alteration layers with levels ranging from 3% to 26.6% oxide weight. Seven samples were also noted where the levels of potash were higher than would have been expected in an apparently completely devitrified glass, ranging from 1.2% to 3.8%. For example, 1930.82.70a (Figure 55), which is completely devitrified in appearance and on SEM images, contains between 2.6% and 3.0% potash on analysis, similar to levels in the unaltered glasses; seven of the 21 samples analysed has potash levels above 2%.

Table 22 shows the bulk compositional analyses that were taken from devitrified glasses. It can be seen that in each case the total of the analysis has fallen, it is probable that this is related to either hydration of the devitrified glass, or surface roughness on some of the samples, which could affect the geometry of the X-rays in relation to the spectrometer and thus the results achieved. Soda, lime and magnesia are not present in significant quantities and silica is the dominant oxide present in all of the samples analysed. 21 of the samples contain aluminium oxide at levels above 1% oxide weight suggesting that an increase in this oxide may be related to the alteration process. It was also noted that potash was present at levels above 1% oxide weight in 16 of the samples analysed with iron, at above 1%, in 11 of the samples. Copper oxide

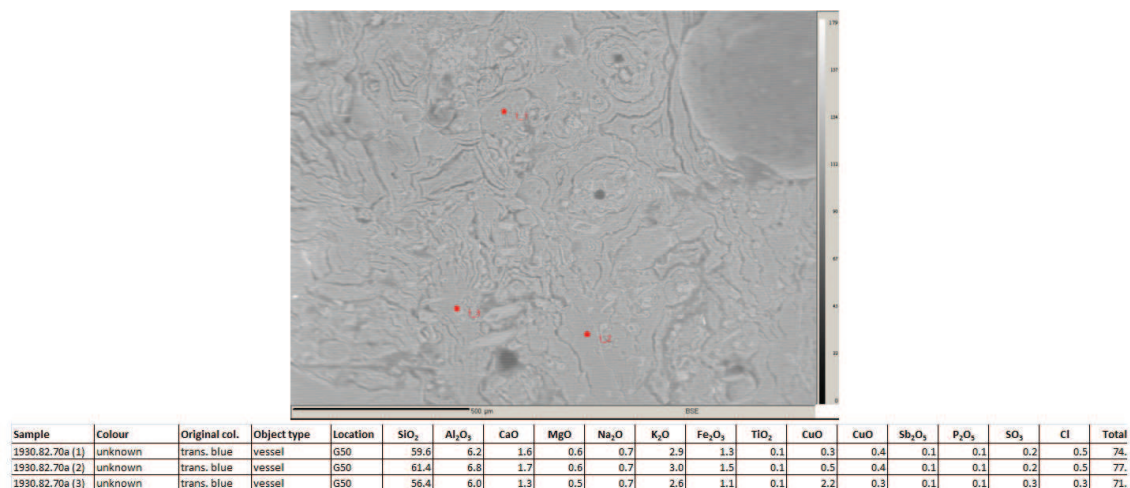


Figure 55: 1930.82.70a, quantified points and BSE image

was present above 0.2% oxide weight in 16 of the samples antimony oxide in five samples and lead oxide in two samples. From this it was possible to ascertain that 13 of the glasses sampled had been translucent blue in colour, two opaque turquoise, seven yellow and one opaque white; another three or four may also have been translucent blue, but copper was present at levels below 0.2% due to the alteration processes.

6.1.7 XRD

Five samples were analysed by X-ray powder diffraction (XRPD) of crushed secondary layers and 23 by point XRD analysis of the secondary layers on mounted samples. The samples analysed by XRPD produced better diffraction patterns than the point analyses. The peaks identified by XRPD analysis of the weathering crusts were matched to a number of substances using SearchMatch software looking at both the height of the peaks and their relative heights and positions to other peaks. This information was then used to identify the materials present in the mounted samples which were analysed by point XRD, identification had been problematic in these samples as the background was very high due to the large proportion of amorphous material. The XRD analysis of the powdered weathering crusts and point analysis of the mounted samples showed that they contain several crystalline materials, Table 23 shows the distribution of the materials observed. However, six of the mounted samples analysed by point XRD did not have any clear peaks and are considered to consist of amorphous material. The most common materials found are hydrated silicate, quartz and calcite, found in ten, nine and eight samples respectively; calcium antimonate was noted in five samples and pyroxenes (augite or diopside) inclusions were also noted in four samples. However, in 17 samples a peak was noticed in position 21.4, which could not be matched with any inorganic substance present in the chemical analysis of the objects. This is thought to possibly be a crystallised organic acid. The exact type of acid was not found as the SearchMatch software gave a variety of results for different samples, however, they were all noted to have the same ratio of C to H. Figures 56 and 57 show the

| Sample | Colour | Original col. | Object type | SiO ₂ | Al ₂ O ₃ | CaO | MgO | Na ₂ O | K ₂ O | Fe ₂ O ₃ | TiO ₂ | CoO | CuO | MnO | NiO | ZnO | SnO | Sb ₂ O ₃ | BaO | PbO | Cr ₂ O ₃ | P ₂ O ₅ | SO ₃ | Cl | SiO | Total | | |
|--------------|--------|----------------|-------------|------------------|--------------------------------|------|-----|-------------------|------------------|--------------------------------|------------------|-----|-----|-----|-----|-----|-----|--------------------------------|-----|------|--------------------------------|-------------------------------|-----------------|-----|-----|-------|------|------|
| 1930.60.140b | white | yellow | bead | 47.8 | 5.5 | 1.0 | 0.3 | 0.7 | 3.2 | 0.9 | 0.2 | 0.0 | 0.1 | 0.0 | 0.0 | 0.0 | 0.0 | 0.4 | 0.0 | 0.0 | 0.0 | 0.0 | 0.1 | 0.1 | 0.2 | 0.1 | 60.8 | |
| 1930.60.42 | blue | blue | bead | 85.7 | 1.5 | 0.5 | 0.7 | 0.2 | 0.6 | 0.6 | 0.1 | 0.0 | 0.0 | 1.3 | 0.0 | 0.0 | 0.0 | 0.0 | 0.0 | 0.0 | 0.0 | 0.0 | 0.0 | 0.1 | 0.1 | 0.4 | 0.0 | 91.4 |
| 1930.61.123a | yellow | yellow | inlay | 12.5 | 0.9 | 3.8 | 0.7 | 0.3 | 0.6 | 2.2 | 0.1 | 0.0 | 0.0 | 0.3 | 0.0 | 0.0 | 0.0 | 5.8 | 0.0 | 28.5 | 0.0 | 4.5 | 0.0 | 1.6 | 0.3 | 62.6 | | |
| 1930.62.102 | yellow | yellow | bead | 9.2 | 1.0 | 3.7 | 0.2 | 0.2 | 0.7 | 0.5 | 0.1 | 0.0 | 0.0 | 0.0 | 0.0 | 0.0 | 0.0 | 2.1 | 0.0 | 18.5 | 0.0 | 4.2 | 1.3 | 1.8 | 0.5 | 45.9 | | |
| 1930.62.31a | green | turquoise | bead | 46.2 | 3.1 | 1.1 | 1.3 | 0.5 | 1.7 | 1.3 | 0.2 | 0.0 | 0.0 | 5.2 | 0.0 | 0.0 | 0.0 | 0.1 | 0.8 | 0.0 | 0.0 | 0.0 | 0.1 | 0.1 | 0.4 | 0.1 | 62.2 | |
| 1930.62.82 | yellow | colorant-free? | bead | 16.6 | 0.9 | 0.3 | 0.1 | 0.1 | 0.6 | 0.3 | 0.0 | 0.0 | 0.0 | 0.0 | 0.0 | 0.0 | 0.0 | 0.0 | 0.0 | 0.0 | 0.0 | 0.0 | 0.0 | 0.2 | 0.1 | 0.0 | 19.1 | |
| 1930.62.82a | yellow | colorant-free? | bead | 33.6 | 3.6 | 0.7 | 0.4 | 0.2 | 1.5 | 1.2 | 0.1 | 0.0 | 0.0 | 0.0 | 0.0 | 0.0 | 0.0 | 0.0 | 0.0 | 0.0 | 0.0 | 0.0 | 0.0 | 0.2 | 0.6 | 0.0 | 42.1 | |
| 1930.62.82c | white | blue | bead | 9.5 | 0.2 | 24.0 | 0.1 | 0.1 | 0.1 | 0.1 | 0.0 | 0.0 | 0.1 | 0.0 | 0.0 | 0.0 | 0.0 | 0.0 | 0.0 | 0.0 | 0.0 | 0.0 | 0.0 | 0.0 | 0.0 | 0.0 | 10.5 | |
| 1930.62.84a | white | blue | bead | 42.2 | 4.9 | 0.9 | 0.4 | 0.7 | 3.3 | 1.5 | 0.2 | 0.0 | 0.0 | 0.4 | 0.0 | 0.0 | 0.0 | 0.1 | 0.0 | 0.0 | 0.0 | 0.0 | 0.0 | 0.0 | 0.2 | 0.1 | 54.8 | |
| 1930.62.84c | yellow | blue | bead | 16.0 | 1.0 | 1.7 | 0.6 | 0.3 | 0.7 | 3.0 | 0.1 | 0.0 | 0.0 | 0.5 | 0.0 | 0.0 | 0.0 | 8.9 | 0.0 | 25.6 | 0.0 | 2.0 | 0.4 | 1.0 | 0.6 | 62.4 | | |
| 1930.63.29 | yellow | yellow | bead | 17.2 | 1.7 | 6.3 | 0.1 | 0.1 | 0.7 | 0.4 | 0.1 | 0.0 | 0.0 | 0.8 | 0.0 | 0.0 | 0.0 | 0.5 | 0.0 | 6.2 | 0.0 | 0.0 | 0.7 | 0.6 | 1.5 | 0.1 | 36.3 | |
| 1930.63.37 | yellow | yellow | bead | 52.6 | 1.3 | 0.5 | 0.2 | 0.2 | 0.2 | 0.7 | 0.8 | 0.1 | 0.0 | 0.0 | 0.0 | 0.0 | 0.0 | 2.4 | 0.0 | 8.7 | 0.0 | 0.0 | 0.1 | 0.2 | 0.5 | 0.1 | 68.4 | |
| 1930.63.40a | white | colorant-free? | bead | 65.3 | 8.8 | 1.8 | 0.4 | 0.7 | 4.7 | 1.5 | 0.2 | 0.0 | 0.0 | 0.0 | 0.0 | 0.0 | 0.0 | 0.1 | 0.0 | 0.0 | 0.0 | 0.0 | 0.1 | 0.1 | 0.3 | 0.2 | 84.0 | |
| 1930.63.40c | white | unknown | bead | 15.6 | 0.2 | 0.2 | 0.0 | 0.1 | 0.1 | 0.1 | 0.0 | 0.0 | 0.0 | 0.0 | 0.0 | 0.0 | 0.0 | 0.0 | 0.0 | 0.0 | 0.0 | 0.0 | 0.0 | 0.1 | 0.0 | 0.0 | 16.4 | |
| 1930.63.59c | white | unknown | bead | 38.5 | 0.9 | 0.4 | 0.2 | 0.2 | 0.3 | 0.2 | 0.0 | 0.0 | 0.0 | 0.0 | 0.0 | 0.0 | 0.0 | 0.1 | 0.0 | 0.0 | 0.0 | 0.0 | 0.0 | 0.1 | 0.1 | 0.0 | 40.8 | |
| 1930.66.89 | white | colorant-free? | bead | 65.7 | 2.3 | 1.0 | 0.5 | 0.4 | 6.8 | 0.4 | 0.1 | 0.0 | 0.0 | 0.0 | 0.0 | 0.0 | 0.0 | 0.1 | 0.0 | 0.0 | 0.0 | 0.0 | 0.1 | 0.1 | 0.1 | 0.0 | 71.1 | |
| 1930.66.90 | white | unknown | bead | 34.2 | 0.4 | 1.2 | 0.1 | 0.1 | 0.1 | 0.1 | 0.0 | 0.0 | 0.1 | 0.0 | 0.0 | 0.0 | 0.0 | 0.0 | 0.0 | 0.0 | 0.0 | 0.0 | 0.0 | 0.0 | 0.0 | 0.0 | 36.5 | |
| 1930.68.27a | green | blue | bead | 84.7 | 0.9 | 0.7 | 0.3 | 0.1 | 0.4 | 0.5 | 0.1 | 0.0 | 0.0 | 0.9 | 0.0 | 0.0 | 0.1 | 0.0 | 0.0 | 0.0 | 0.0 | 0.0 | 0.0 | 0.0 | 0.0 | 0.0 | 88.5 | |
| 1930.68.27b | white | unknown | bead | 14.0 | 0.3 | 0.0 | 0.1 | 0.0 | 0.0 | 0.0 | 0.0 | 0.0 | 0.0 | 0.0 | 0.0 | 0.0 | 0.0 | 0.0 | 0.0 | 0.0 | 0.0 | 0.0 | 0.0 | 0.0 | 0.0 | 0.0 | 14.4 | |
| 1930.68.9 | blue | blue | bead | 83.0 | 0.3 | 1.3 | 1.6 | 0.1 | 0.2 | 0.1 | 0.0 | 0.0 | 2.6 | 0.0 | 0.0 | 0.0 | 0.0 | 0.0 | 0.0 | 0.0 | 0.0 | 0.0 | 0.1 | 0.4 | 0.1 | 0.0 | 89.3 | |
| 1930.69.39a | white | unknown | bead | 60.4 | 21.6 | 2.7 | 0.1 | 5.7 | 1.2 | 0.1 | 0.0 | 0.0 | 0.0 | 0.1 | 0.0 | 0.0 | 0.0 | 0.0 | 0.0 | 0.0 | 0.0 | 0.0 | 0.0 | 0.0 | 0.1 | 0.0 | 96.0 | |
| 1930.69.39b | white | blue | bead | 70.6 | 3.9 | 0.4 | 0.9 | 1.2 | 2.9 | 1.3 | 0.2 | 0.0 | 3.0 | 0.1 | 0.0 | 0.0 | 0.0 | 0.0 | 0.0 | 0.0 | 0.0 | 0.0 | 0.0 | 0.1 | 0.9 | 0.0 | 85.3 | |
| 1930.69.39c | white | turquoise | bead | 57.7 | 1.6 | 1.2 | 1.1 | 0.3 | 0.8 | 0.6 | 0.1 | 0.0 | 0.5 | 0.0 | 0.0 | 0.0 | 0.0 | 1.7 | 0.0 | 0.0 | 0.0 | 0.0 | 0.3 | 0.1 | 0.2 | 0.1 | 66.1 | |
| 1930.82.14a | white | blue | vessel | 26.9 | 1.0 | 0.6 | 0.3 | 0.1 | 0.5 | 1.1 | 0.1 | 0.0 | 0.3 | 0.0 | 0.0 | 0.0 | 0.0 | 0.0 | 0.0 | 0.0 | 0.0 | 0.0 | 0.0 | 0.1 | 0.1 | 0.0 | 31.0 | |
| 1930.82.14b | pink | yellow | inlay | 51.1 | 2.0 | 1.2 | 0.3 | 0.1 | 0.9 | 0.9 | 0.1 | 0.0 | 0.0 | 0.3 | 0.0 | 0.0 | 0.0 | 0.0 | 0.0 | 0.0 | 0.0 | 0.0 | 0.0 | 0.2 | 0.2 | 0.0 | 60.4 | |
| 1930.82.15a | yellow | yellow | inlay | 67.5 | 0.4 | 1.3 | 5.1 | 0.1 | 0.3 | 0.9 | 0.0 | 0.0 | 1.1 | 0.0 | 0.0 | 0.0 | 0.0 | 1.9 | 0.0 | 8.2 | 0.0 | 0.0 | 0.1 | 0.2 | 0.2 | 0.1 | 87.5 | |
| 1930.82.15c | white | blue | vessel | 33.1 | 3.8 | 0.8 | 0.3 | 0.4 | 1.8 | 0.5 | 0.1 | 0.0 | 0.1 | 0.0 | 0.0 | 0.0 | 0.0 | 0.0 | 0.0 | 0.0 | 0.0 | 0.0 | 0.0 | 0.1 | 0.2 | 0.0 | 41.4 | |
| 1930.82.58 | white | white | vessel | 54.4 | 0.7 | 3.1 | 1.1 | 0.1 | 0.2 | 0.2 | 0.0 | 0.0 | 0.0 | 0.1 | 0.0 | 0.0 | 0.0 | 5.8 | 0.0 | 0.0 | 0.0 | 0.0 | 0.1 | 0.1 | 0.1 | 0.5 | 66.6 | |
| 1930.82.65a | white | blue | vessel | 64.9 | 0.9 | 0.5 | 3.2 | 0.3 | 0.3 | 0.4 | 0.1 | 0.0 | 4.7 | 0.0 | 0.0 | 0.0 | 0.0 | 0.1 | 0.0 | 0.2 | 0.0 | 0.0 | 0.1 | 0.1 | 0.3 | 0.0 | 75.9 | |
| 1930.82.65d | white | blue | vessel | 79.2 | 4.2 | 1.1 | 1.0 | 0.3 | 1.7 | 0.9 | 0.1 | 0.0 | 1.5 | 0.0 | 0.0 | 0.0 | 0.0 | 0.1 | 0.0 | 0.0 | 0.0 | 0.0 | 0.1 | 0.1 | 0.1 | 0.0 | 90.4 | |
| 1930.82.67 | white | blue | vessel | 49.1 | 6.8 | 1.7 | 0.6 | 0.9 | 3.2 | 1.4 | 0.1 | 0.0 | 0.3 | 0.0 | 0.0 | 0.0 | 0.0 | 0.1 | 0.0 | 0.1 | 0.0 | 0.0 | 0.2 | 0.2 | 0.4 | 0.1 | 65.1 | |
| 1930.82.68 | white | blue | vessel | 66.4 | 6.9 | 1.8 | 0.9 | 0.9 | 4.0 | 2.6 | 0.2 | 0.0 | 1.2 | 0.0 | 0.0 | 0.0 | 0.0 | 0.1 | 0.0 | 0.0 | 0.0 | 0.0 | 0.1 | 0.4 | 0.5 | 0.1 | 85.9 | |
| 1930.82.72 | white | blue | vessel | 53.9 | 7.0 | 1.2 | 0.8 | 0.7 | 2.4 | 0.6 | 0.1 | 0.0 | 0.5 | 0.1 | 0.0 | 0.0 | 0.0 | 0.1 | 0.0 | 0.0 | 0.0 | 0.0 | 0.1 | 0.2 | 0.5 | 0.1 | 68.2 | |
| 1930.82.73a | white | blue | vessel | 71.1 | 7.4 | 1.7 | 0.5 | 0.9 | 3.9 | 1.0 | 0.1 | 0.0 | 0.4 | 0.0 | 0.0 | 0.0 | 0.0 | 0.1 | 0.0 | 0.0 | 0.0 | 0.0 | 0.0 | 0.3 | 0.7 | 0.0 | 88.1 | |

Table 22: Altered glasses, bulk composition

diffraction patterns for 1930.82.70 and 1930.60.140 with the identified materials below.

| Sample | No peaks | H Si | CaCO3 | qtz | aug | diop | 21.4 | other |
|--------------|----------|------|-------|-----|-----|------|------|--------------------|
| 1930.60.140 | | x | x | x | | | x | |
| 1930.63.29 | | x | | x | | | x | calcium antimonate |
| 1930.66.72 | | x | | x | x | | x | gypsum |
| 1930.69.39a | | x | x | | | | x | |
| 1930.82.70 | | | x | x | x | | | |
| 1930.82.65a | | | | | | | x | |
| 1930.82.67 | x | | | | | | | |
| 1930.82.15c | x | | | | | | | |
| 1930.82.72 | | | | ? | | x | | |
| 1930.62.84b | | x | ? | ? | | | x | calcium antimonate |
| 1930.62.84f | | x | ? | ? | | | x | |
| 1930.62.84c | x | | | | | | | |
| 1930.62.84a | | | | | | | x | |
| 1930.62.84e | | | x | | | | x | |
| 1930.69.39b | x | | | | | | | |
| 1930.63.39a | | | | | | | x | |
| 1930.69.31a | | | ? | | ? | | x | calcium antimonate |
| 1930.68.27a | | x | | | | | | |
| 1930.82.65d | x | | | | | | | |
| 1930.52.1e | | x | | | | | | calcium antimonate |
| 1930.61.129a | | | | | | | x | |
| 1930.62.84b | x | | | | | | | |
| 1930.62.84a | | x | x | | | | x | |
| 1930.62.31b | | | | x | | | | |
| 1930.82.48 | | | | | | | x | |
| 1930.63.40a | | x | x | | | | x | |
| 1930.61.88b | | | | | | | x | calcium antimonate |
| 1930.62.42 | | | | | | | x | |
| | 6 | 10 | 9 | 8 | 3 | 1 | 17 | |

Table 23: Table showing phases identified by XRD

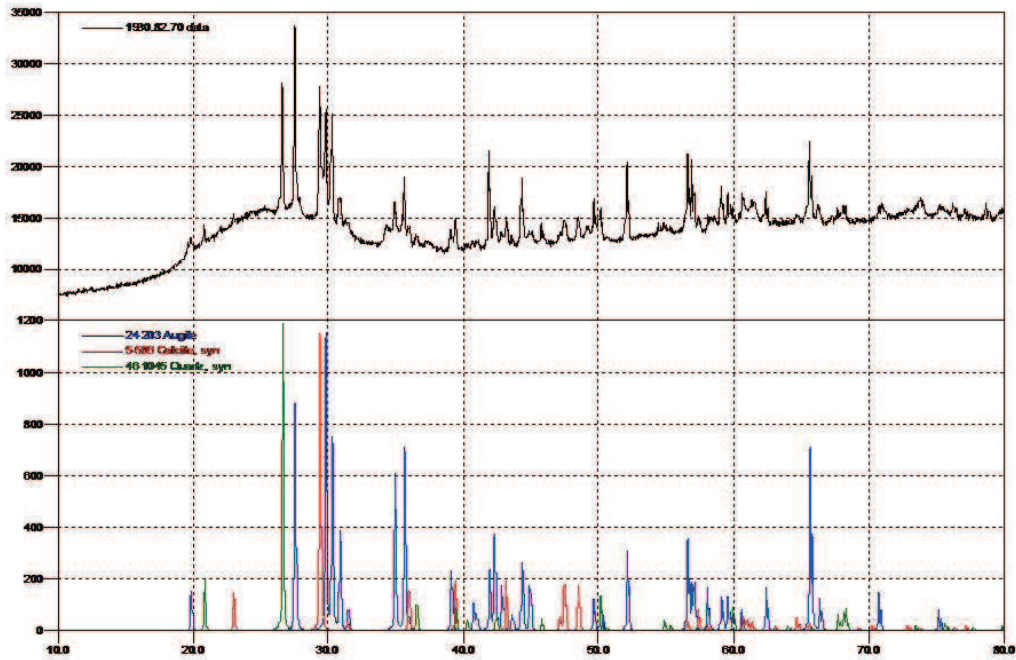


Figure 56: Diffraction pattern for 1930.82.70 (2 Theta on x axis)

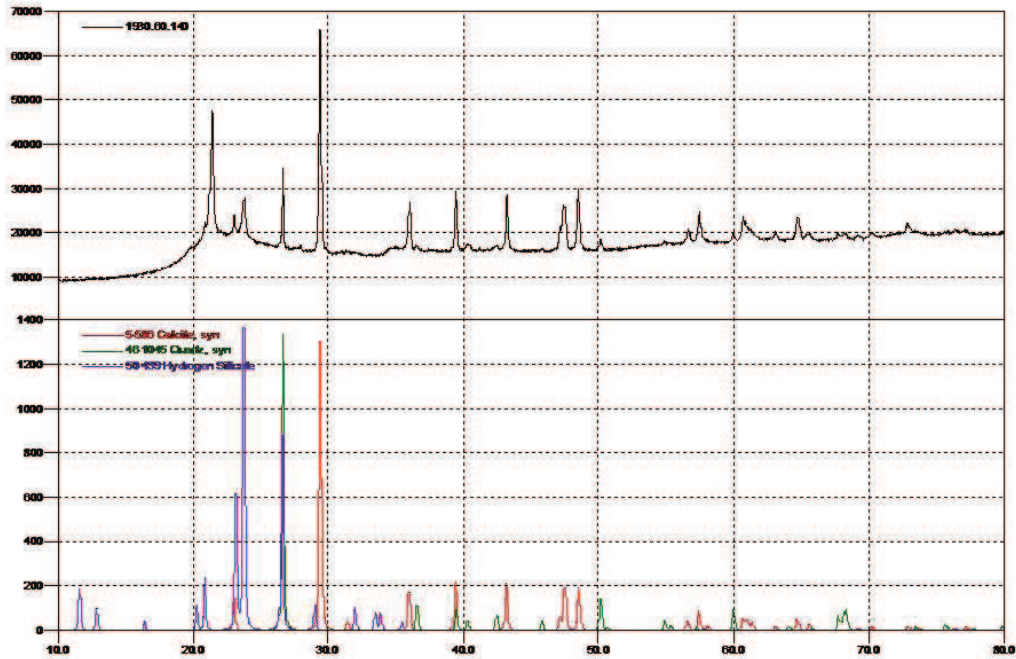


Figure 57: Diffraction pattern for 1930.60.140 (2 Theta on x axis)

6.2 Variation in alteration

6.2.1 Location on site

All of the samples with glass remaining are from the northwestern half of the site, or from the palace complex, no objects with glass remaining were found from the northeastern or southwestern residential areas. However, glass objects are much rarer from these areas. Seven of the 30 samples retaining glass are from the palace complex; three are from the northwestern residential area; six have no specific location recorded and the remaining 14 are from the temple and attached courtyards and buildings. No clear correlation between the state of preservation of an object and its location on the site was noted. Indeed several groups were noted where the preservation of objects from a single room varied widely; for example, 1930.82.15 from room M79, in the palace complex, contained decorated vessel fragments ranging in preservation from 1930.82.15a and b (Group 3 and 2 respectively) and 1930.82.15c which was in group 6 (completely devitrified and becoming unstable). Groups 1930.60.140, 1930.63.37, 1930.63.40 and 1930.82.62 from G50, the temple courtyard, all contain samples with glass remaining and devitrified examples. Groups 1930.68.27 and 1930.69.39 from G29, the cella of the Ishtar temple, and F24, in the northwestern residential area, respectively, also contain glass-bearing and devitrified samples. Even in groups with only devitrified samples there is still variation in the degree of preservation, for example, groups 1930.82.73 and 1930.61.88, both from G50, have samples from more than one preservation group.

6.2.2 Colour

Some possible variation was noted in the alteration of glasses of different colours. In the SEM images the opaque glasses have slightly more disordered alteration layers and a greater presence of filled pores/air bubbles, figure 58. This difference is clearly seen in several examples where an inlay of a different colour was present, (Figure 78, Section 8.3). The composition of the alteration layers does not appear to vary between the different colours of glass, as was seen in the compositional maps, although layers with very high concentrations of copper were only seen in the translucent blue glasses, Figure 59.

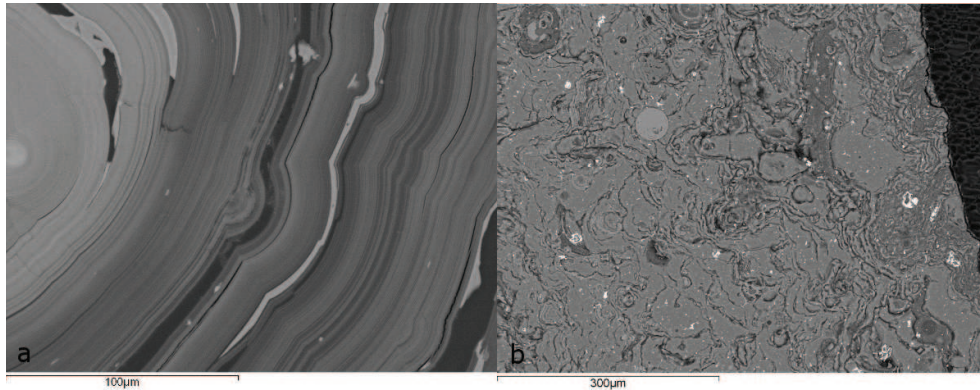


Figure 58: Translucent vs opaque glass secondary alteration layers; a. 1930.66.90a (translucent blue); b. 1930.82.59 (opaque white)

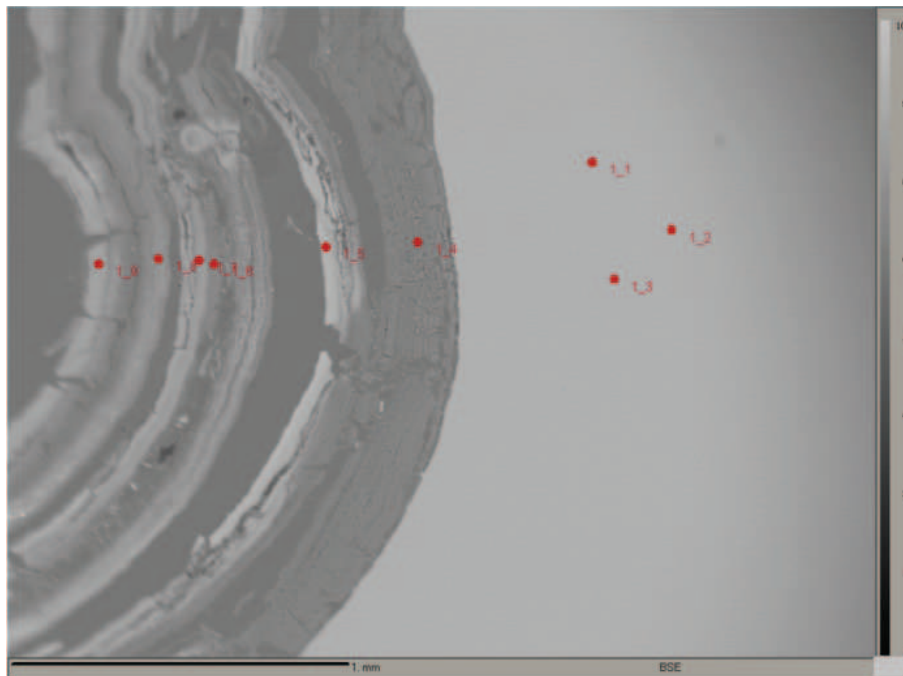


Figure 59: 1930.60.140d with copper-rich alteration layers; point 5: 25.6%, point 6: 7.5%, point 7 13.2% and point 9 on 14.2% CuO on analysis with SEM-WDS, compared to 2.0% in the unaltered glass.

6.2.3 Object type

Again little correlation was observed between the type of object and its preservation with examples of beads and vessels in all of the preservation groups, Tables 20 and 21. However, all of the pendant and ingot fragments found still contained glass, although only three pendants were sampled and two possible ingot fragments.

6.3 Glazed ceramics

The glazed ceramic samples were analysed in the same way as the glass samples. Twenty six samples were analysed using SEM-EDS and 30 with SEM-WDS to obtain bulk compositions. The samples were grouped according to their appearance on SEM using the same criteria as the glasses. Only four samples contained unaltered glaze and, unfortunately, three of these are likely to be from the Late period based on their composition; particularly the presence of tin and lead in the glaze which is not seen in the Bronze Age glazes; samples 1930.52.1c, 1930.52.1g and 1930.52.6b all contain tin and lead alongside copper in their glaze. SEM images of these samples suggest that they also do not have such a distinct interaction layer between the glaze and the ceramic body compared to many of the Bronze Age glazes and 1930.52.1g also has several tin inclusions within its glaze layer, the white area in Figure 60a. The only unaltered LBA glaze, 1930.16.3, has thin alteration layers and no lamellar features were noted (Figure 60b). However, lamellae similar to those seen in the alteration layers of the glasses were observed in 16 of the 27 glaze samples. Some differences were noted with the lamellae in the glazes being at a smaller scale and appearing to have softer edges than those noted in the glasses, as can be seen in 1930.52.1f and 1930.52.1h (Figure 60 c and d). Bulk compositional data from altered glazes was obtained from 30 LBA glaze and glazed ceramic samples. Compositionally the altered glazes are very similar to the devitrified glasses with lowered analytical totals, increased silica, and loss of alkalis and alkaline earths, although most have very high levels of aluminium, up to 15%. Seven of the glaze samples also contained high levels of copper oxide similar to some of the altered glasses, ranging from 2.3% to 30.9% (Table 14). The glazed ceramics also contain an interaction layer which may well have affected the analyses taken. For example, in sample, 1930.52.1h (Figure 60f), a visually clear distinction could be made between the glaze layer and an interaction layer, both layers were then analysed separately. The interaction layer was in a much better state of preservation than the glaze layer (certainly in terms of the alkali and alkaline earth oxides) but contained considerably more alumina, Table 24.

| Sample no. | Alt group | Key features | Lamellae | Scale change | Direction change | Inclusions |
|-------------|-----------|--|------------|--------------|------------------|----------------------------------|
| 1930.13B.3 | 5 | thin interaction layer; soft edges on lamellae | sub micron | N | N | diopsides |
| 1930.14.10 | 6 | thin interaction layer; very large air bubbles; many fine crystals; soft edges to lamellae | sub micron | N | N | diopsides |
| 1930.14.2 | 4 | smooth alteration | N | N | N | Ti-rich |
| 1930.14.3b | 6 | many large inclusions; very soft edges to lamellae | sub micron | N | N | quartz |
| 1930.14.5 | 7 | little material remaining; very disorganised; almost non-glassy; Ca infiltration in places | | | | |
| 1930.14.6a | 4 | thin interaction layer; disorganised 'smooth' layers; variable BS; large inclusions | N | N | N | quartz |
| 1930.14.6b | 6 | clear interaction layer; soft edges to lamellae | sub micron | N | N | |
| 1930.14.9 | 7 | very little material left; very soft edges to lamellae | sub micron | N | Y | |
| 1930.16.1 | 4 | smooth areas; lamellae very fine with soft edges only visible in places | sub micron | N | Y | none |
| 1930.16.3 | 2 | smooth alteration layers | N | N | N | none |
| 1930.16.7 | 6 | thin glaze layer; circular forms; soft edges on lamellae | mix | Y | N | none |
| 1930.16.8a | 6 | very disorganised; large inclusions | sub micron | N | N | quartz |
| 1930.16.9a | 4 | Mn-rich interaction layer; fine crystals; Ca-rich encrustation at one edge | none | N | N | diopsides |
| 1930.52.1g | 1 | well preserved glaze; no interaction layer | N | N | N | wollastonite and Sn-rich |
| 1930.52.1h | 6 | clear interaction layer; variable thickness of glaze layer | sub micron | N | N | diopsides |
| 1930.52.1d | 7 | separated layers; faceted 'soft' lamellae | sub micron | N | N | diopsides |
| 1930.52.2b | 5 | very disorganised layers; very large filled pores; variable BS; some Cu-rich areas; 'compressed' areas | sub micron | Y | Y | diopsides |
| 1930.52.6 b | 1 | well preserved glaze; no interaction layer | sub micron | N | N | none |
| 1930.52.6a | 6 | layers beginning to separate; | N | N | N | wollastonite/diopside |
| 1930.52.6b | 3 | glaze and alteration layers; no interaction layer | N | N | N | none |
| 1930.52.c | 7 | very altered glaze; clear interaction layer; lamellae visible in places | sub micron | N | N | diopsides and Sn-rich inclusions |
| 1930.5B1a | 6 | clear interaction layer; soft edges to lamellae | sub micron | N | N | diopsides |
| 1930.IC.12 | 6 | very soft edges to lamellae | sub micron | N | N | diopsides |
| 1930.IC.15 | 6 | circular forms; very soft edges to lamellae | sub micron | N | N | diopsides |
| 1930.IC.6 | 4 | smooth devitrified glaze; clear interaction layer; large air bubbles; faint and 'soft' lamellae | sub micron | N | Y | diopsides |
| 1930.52.2a | 4 | Cu-rich areas; faint lamellae in some areas | Y | N | N | diopsides |
| | | | | | | none |

Table 24: Alteration groups and details: glazed ceramics

The glaze samples also contain numerous crystalline inclusions as was seen in the glasses. Ten samples contain diopside crystals, three have unreacted quartz grains and two of the later samples contain wollastonite inclusions. In some cases the diopsides appear linked to the interaction between the ceramic and the glaze layer in others they are within the glaze and appear very similar to those seen in the glasses, for example, 1930.52.1f, illustrated in Figure 61e, shows both types of these. It was not possible to carry out point analyses or XRD of the glazed ceramics due to the thinness of the glaze layer.

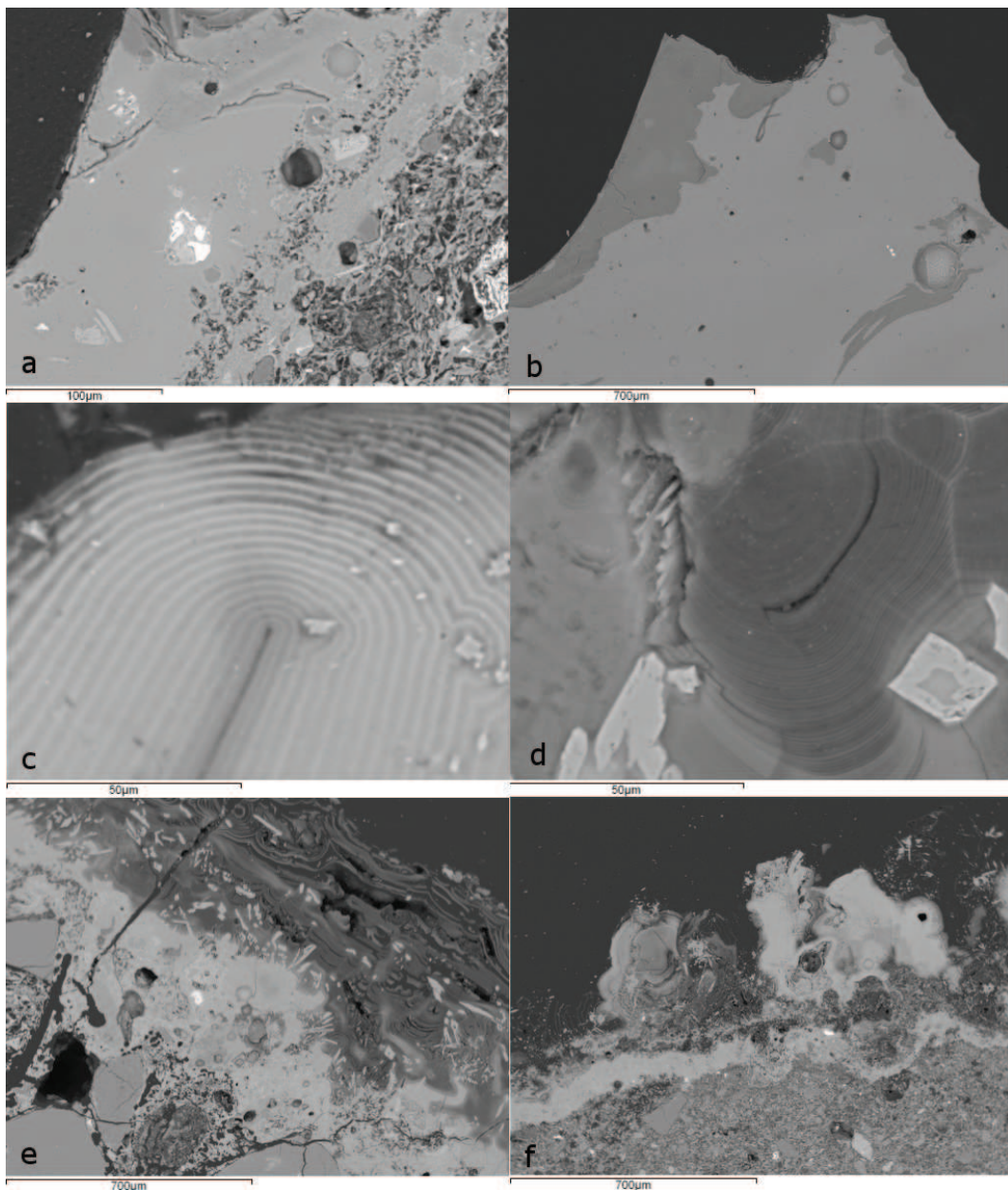


Figure 60: Glazed ceramics: a.1930.52.1g Late glaze with tin-rich inclusion (white) and wollastonite inclusions (grey); b.1930.16.3 well preserved LBA glaze; c. 1930.52.1h fine 'soft' lamellar features; d. 1930.52.1f fine lamellar features, diopside inclusions; e. 1930.52.1f interaction layer with diopside inclusions radiating from interaction layer; 1930.52.1h interaction layer between glaze and ceramic body.

6.4 Late period glass

Several late period glasses were examined in terms of their preservation and alteration in order to compare this to the earlier glass objects. In general these glasses were in a better state of preservation than the Bronze Age glass, unsurprisingly as they are around 1500 years younger. A compositional difference was noted between the natron-based and plant ash-based glasses in this assemblage, Table 13, Section 5; and this distinction was maintained in their state of preservation. The natron-based glasses were almost completely unaltered or only showed signs of minimal alteration products at their surface. The plant ash glasses on the other hand tended to have a visible thin alteration crust of varying colour and thickness.

SEM images were obtained for nine late period glasses and six samples were examined in detail using SEM imaging; five of these are plant ash glasses and 1930.82.21 which is a natron glass. 1930.82.31, 1930.82.32 and 1930.82.21 (Figure 61a) showed very minimal alteration with only a slight change in the backscattered signal at their edges. The other three glasses analysed, however, showed significant alteration layers on the SEM images, alongside some more unusual features, these are illustrated in Figure 61. All three samples had secondary phases that were clearly visible on the SEM images as can be seen in 1930.82.37 (Figure 61b). In some places these appeared very irregular and disorganised and in others much more regular and layered. The most significant feature of these samples, compared to the Bronze Age glasses, was the presence of an irregular 'wavy' interaction edge between the glass and the alteration layers (Figure 61c), this was seen in all three samples, although it was less marked in 1930.82.34. Samples 1930.82.34 and 1930.82.6a (Figure 61d) also have small areas appear to have altered at a slower rate than the rest of the surface. All of the samples with secondary layers there is a definite change of scale in the lamellar features observed within a small area, from very fine, sub-micron scale to layers several microns across, most clearly observed in 1930.82.34 (Figure 61e). These much larger lamellar features clearly show the different composition of the layers with a smooth layer alternating with a 'spongy' layer (Figure 61f).

Point analyses using SEM-WDS were obtained from four of the above samples to get quantified information on the alteration layers; samples 1930.82.21, the natron glass and 1930.82.6a, 1930.82.34 and 1930.82.37, the plant ash glasses. 1930.82.21 did not provide usable results as the altered area was too narrow for the point size and edge effects caused low analytical totals. 1930.82.34 and 1930.82.37 displayed similar characteristics to the LBA glasses with increases in silica and loss of alkalis and alkaline earths, however, the increased magnesia was not observed in any of the analysed points. 1930.82.6a did have several layers where magnesia had not been completely lost, indeed point 6 contained 7.6% MgO compared to 4.8% in the glass. The detailed results are contained in Appendix 2.

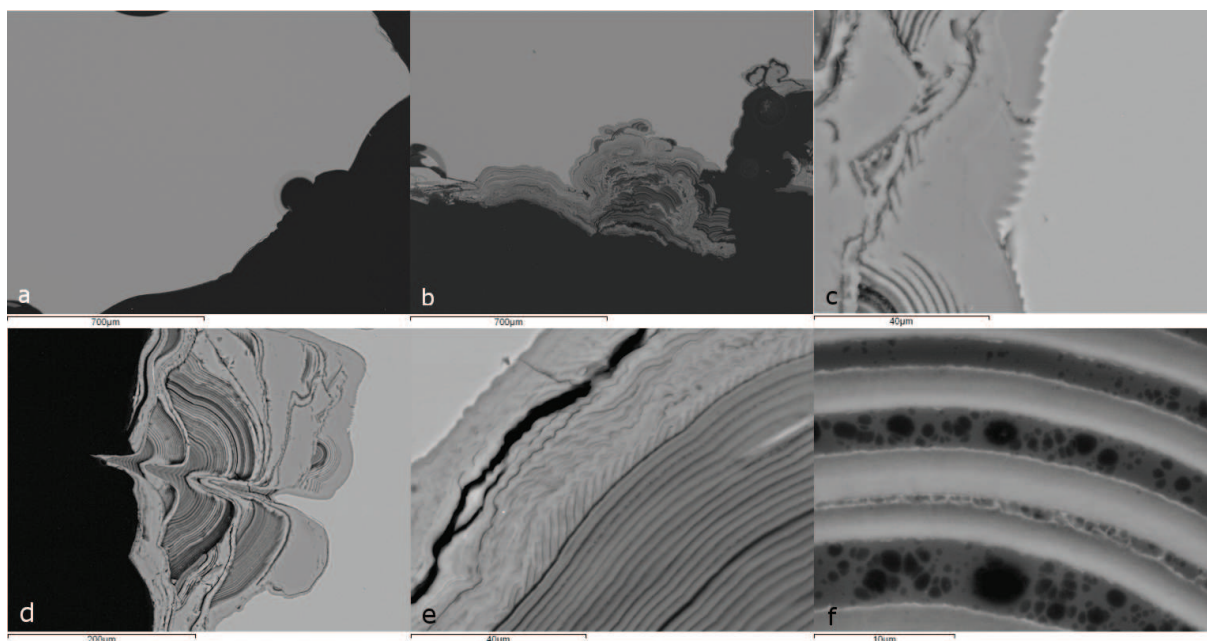


Figure 61: Late glasses: a. 1930.82.21 natron glass with minimal weathering at edge; b. 1930.82.37 glass with significant secondary layers; c. 1930.82.6a 'wavy' interaction layer between glass and secondary phases; d. 1930.82.6a are of slower weathering; e. 1930.82.34 change of scale/organisation in lamellar features; f. 1930.82.34 large lamellae showing difference in structures.

6.5 Other vitreous materials

Lamellar features similar to those observed in the altered glasses were also observed in some of the frit and faience objects in the assemblage, for example in an Egyptian blue bead, 1930.61.91b (Figure 62). These features suggest that parts of these objects would originally have been much more glassy and that their glassy areas have weathered in a similar fashion to the glasses. Similarly to the glazed ceramics the lamellae appear to be at a smaller scale and have softer edges than those seen in the glasses.

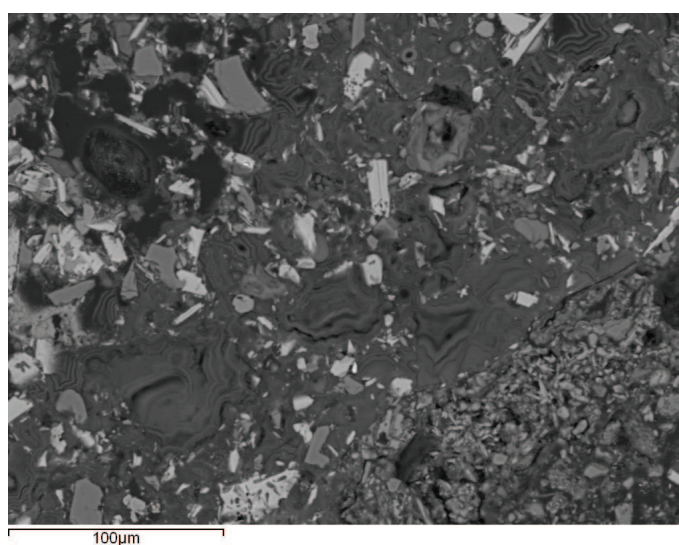


Figure 62: 1930.61.91: Egyptian blue bead with devitrified glassy areas with distinct lamellar features in places.

6.6 Summary

The altered glasses have shown that there is a very wide variation in the degree of preservation within the Nuzi assemblage, which can be seen at both the macro and micro-scale. The secondary alteration layers in particular show considerable variation in their morphology, scale and composition including magnesia and copper-rich layers in the secondary alteration products. The devitrified glasses have a distinct composition, compared to the examples with glass remaining, with higher aluminium oxide levels. The observed variation, in both glass-retaining and devitrified samples, does not correlate with the location of an object on the site, its colour or the type of object. A range of crystalline inclusions, particularly diopsides or other plagioclase minerals were identified in many of the altered glasses. The alteration of the glazed ceramics appears very similar to that of the glasses with only minor variations. However, the Late period glasses analysed show some different features in their alteration, such as the uneven interaction line between the glass and secondary alteration layers and the great differences in scale seen in the lamellae, which may be related to the shorter burial period or to their differences in their composition, specifically their higher aluminium oxide and lack of colorants.

7 Results 4: Experiments (replication and dissolution)

7.1 Glass dissolution and alteration experiments

A number of experiments were carried out to look at the dissolution and alteration behaviour of replica Bronze Age composition glasses. An initial experiment was carried out to look at the difference between monoliths and powders as it was unclear whether monoliths would alter enough over short-term experiments. The results after 7 days at 90 °C are presented in Table 25 below, see Section 3.5 for methods. This experiment showed that a monolith did show an increase in pH, despite the short time period. Therefore it was decided that monoliths could be used in the further dissolution and alteration experiments.

| | Powder | Monolith |
|----------|--------|----------|
| Start pH | 6.73 | 6.73 |
| End pH | 9.57 | 8.65 |

Table 25: Powder vs monolith: initial experiment

7.1.1 Dissolution experiments

A set of simple experiments were carried out to look at the rates of alkali and silica loss during short-term dissolution of replica glass monoliths, see Section 3.5 for methods. These experiments were carried out

for 7 days and 28 days on replica Bronze Age composition glass monoliths as well as a small number of archaeological glasses for comparison. Table 26 below details the start and end weights of each sample and the start and end pH of the solution. these show that there was little or no weight lost in the seven-day experiments but that the small replica glass monoliths lost on average 0.004g (2%) in weight over the 28 day experiments. The larger fragments of archaeological glass lost relatively more weight over the 28 day experiments, most probably due to their larger starting size and surface area, Table 26. There was also a measurable rise in pH in all of the samples, most probably associated with the loss of alkalis and alkaline earths from the glass into the solution. However, the rise in pH in the blank samples is unexpected and suggests that the pH increases noted could be lower than the figures suggest if the overall pH of the solution has risen without input from the glasses. The pH difference in the blank samples is most likely to be an artefact of the pH checking as it was difficult at times to get the checker to stabilise in the solutions, despite regular calibration.

The solutions from these experiments were analysed by ICP-AES to look at the loss of silicon, magnesium, sodium, potassium and copper from the replica glasses. Table 26 below outlines these results. All the results are in ppm with “<” denoting “element below detection limit”. It was not possible to get results for calcium as the presence of some calcium in the dissolution solution masked the signal from the calcium released from the glass. It is clear that the larger samples lost more of each element, due to their greater initial weight and larger surface area. However, there are some differences in monoliths of similar size, weight and surface area, Figure 63. Copper was not released into solution at levels above the detection limit, which is very low; this is not completely unexpected as copper was at the lowest concentration in the original glass compared to the other elements (1.6% CuO). The studies into the composition of the altered glasses had also suggested that copper is less mobile than the other elements. The lack of sodium in all of the seven day results and in one of the 28 day results (28_90_1) is unexpected as this element had been noted to be the most mobile in the compositional analysis of the altered glasses.

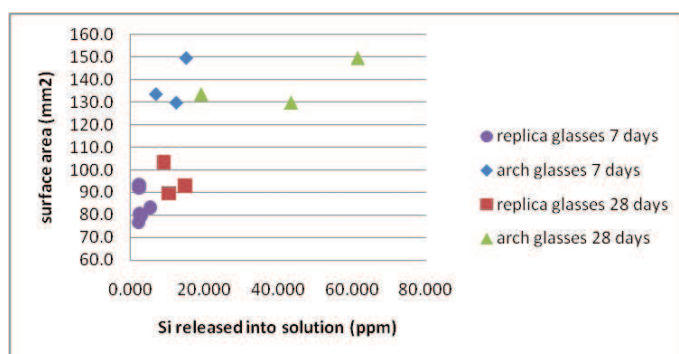


Figure 63: Scatterplot showing loss of silicon into solution versus surface area, dissolution experiments

| Sample | Early stages | Secondary phases | Congruent dissolution |
|----------|--------------|------------------|-----------------------|
| 60 14 | yes | no | no |
| 60 28 | yes | no | no |
| 60 56 | yes | yes | no |
| 60 84 | no | no | yes |
| RT 14 | no | no | no |
| RT 28 | yes | no | no |
| RT 56 | yes | yes | no |
| RT 84 | yes | yes | no |
| PV 60 14 | yes | no | no |
| PV 60 28 | yes | no | no |
| PV 60 56 | yes | no | no |
| PV 60 84 | yes | yes | no |
| PV RT 14 | no | no | no |
| PV RT 28 | yes | no | no |
| PV RT 56 | yes | no | no |
| PV RT 84 | yes | no | no |

Table 27: Experimental samples, clay solution and 100% RH

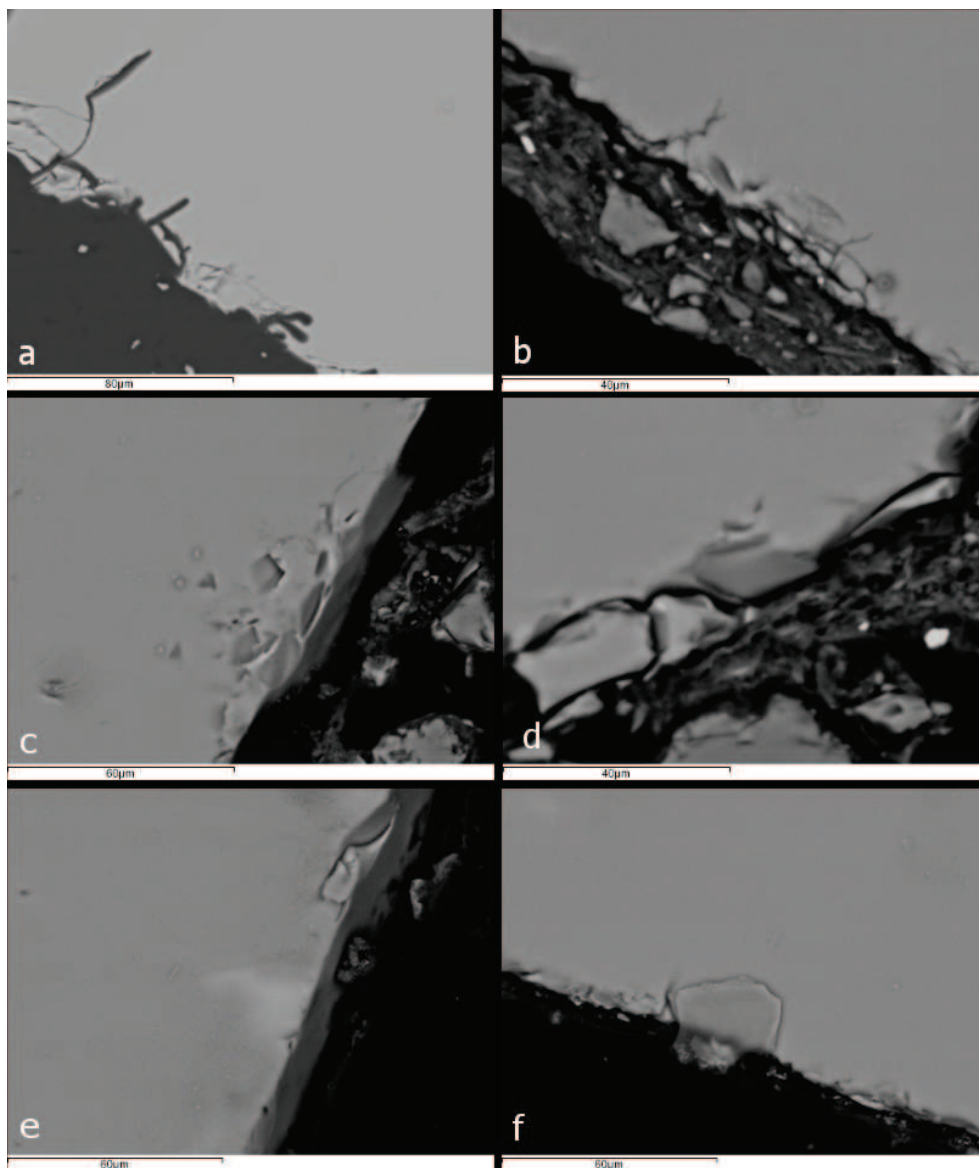


Figure 64: a: congruent dissolution attacking along cracks; b and d: typical appearance of experimental glasses after 28 and 56 days in solution at 60 degrees Celsius; c, e and f possible secondary phases (c - 60-28 e/f RT-56);

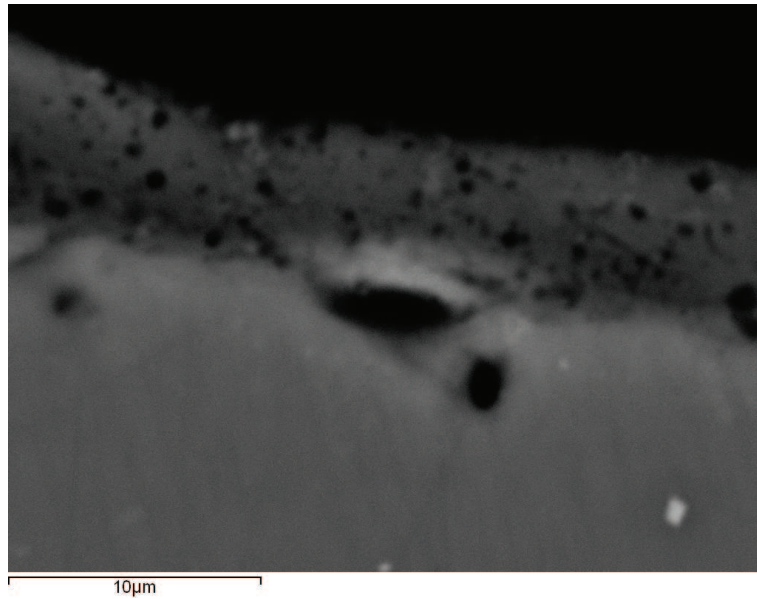


Figure 65: Secondary alteration phases on 84 day sample 100% RH experiments

The experiments at 60 °C with a clay solution did, however, produce some initial alteration phases comparable to the archaeological glasses. Areas of alkali loss are visible on backscattered electron images (Figure 77, Section 8.3) as well as surface changes with 'steps' appearing at the edges of the samples, Figure 66b). This is seen in some of the archaeological glasses, particularly the later glasses, for example 1930.82.21 (Figure 66a). Interestingly the longest-term experiment (60 °C for 84 days) appears to have reverted to congruent dissolution with the solution attacking along cracks and fissures in the glass surface (Figure 67a), as was noted in the dissolution experiments. The room temperature experiments (from 28 days onwards) in the clay solution showed similar early stages to those in the clay solution at 60 °C, Figure 67b, with possible secondary phases in the two longest experiments.

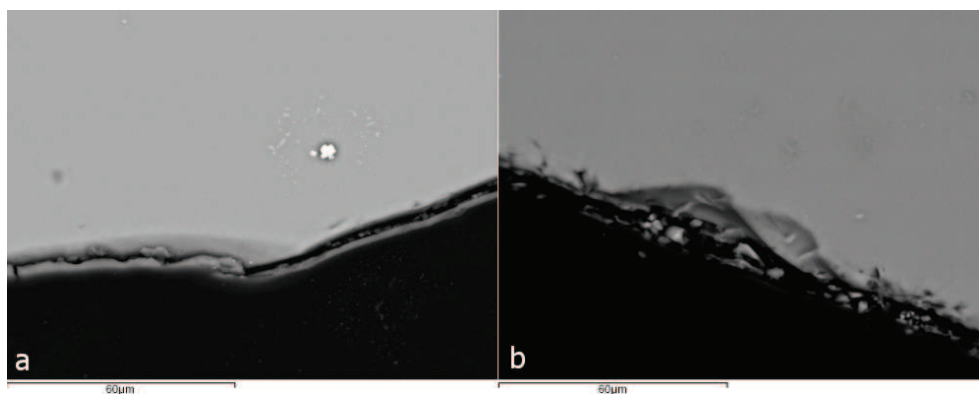


Figure 66: Early alteration stages: a. archaeological glass 1930.82.21; b. experimental glass RT 56

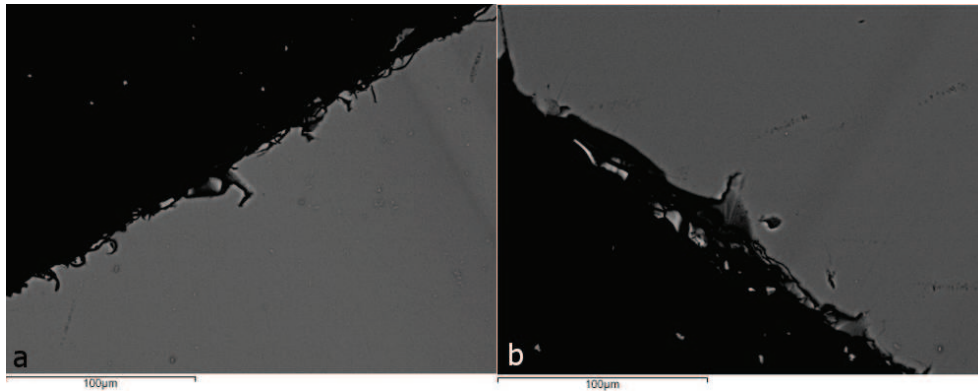


Figure 67: a. 60 84, congruent dissolution; b. RT 84, early stages

7.2 Replication of glasses

7.2.1 Replication of antimonate glasses

Table 28 summarises the results of the experimental glasses that were made to replicate LBA antimony-opacified glasses. The first experimental glass batches, containing antimony, fired at 1050 °C (glasses A2-A4) produced a highly vesicular ‘frothy’ glass, part of which had bubbled over the top of the crucible, leaving little glass present once cooled (Figure 68). This did not happen with glass A1 which did not contain any antimony oxide and produced a colourless translucent glass with few air bubbles. Glass batch C2, which contained cullet and antimony oxide, also produced a good glass although it had a slight yellowish colour and appeared slightly patchy (Figure 69). This was despite very careful mixing of the crushed glass and antimony oxide. In contrast to the first experiments, the glass batches fired at 1150 °C produced solid opaque white glasses with few air bubbles, glasses B2 to B4. No difference was observed in the appearance of these glasses, as can be seen in Figure 70. B1 is the translucent colourless glass fired at 1150 °C and there was no visible difference between it and glass A1.

| | Experimental glasses | Result |
|----|---|------------------------------|
| A1 | colourless glass batch | well-fused colourless glass |
| A2 | 3% Sb ₂ O ₃ | ‘frothy’ white glass |
| A3 | 3% Sb ₂ O ₃ , 3% CaO | ‘frothy’ white glass |
| A4 | pre-roasted Sb ₂ O ₃ +CaCO ₃ | ‘frothy’ white glass |
| B1 | colourless glass batch | well-fused colourless glass |
| B2 | 3% Sb ₂ O ₃ | well-fused white glass |
| B3 | 3% Sb ₂ O ₃ +3% CaO | well-fused white glass |
| B4 | pre-roasted Sb ₂ O ₃ +CaCO ₃ | well-fused white glass |
| C1 | cullet | colourless glass, green tint |
| C2 | cullet +3% Sb ₂ O ₃ | patchy yellowish-white glass |

Table 28: Replica antimonate glasses



Figure 68: 'Frothy' replica antimonate glass (1050°C)



Figure 69: Experimental replica glasses B2-B4 and C2 (from left to right top); close-up of B4 (left) and C2 (right)

7.2.2 SEM-EDS

SEM-EDS images of the replicate glasses confirmed the visual similarity between the replica experimental glasses, despite their different compositions. Each of the experimental glasses has a similar distribution of calcium antimonate crystals in addition to numerous agglomerations which are also comparable in terms of size and form (Figure 71). By contrast glass C2, the cullet + antimony oxide glass, showed large clusters of calcium antimonate which may follow the original form of cullet fragments – despite the crushed glass

being sieved to remove very large particles (Figure 70).

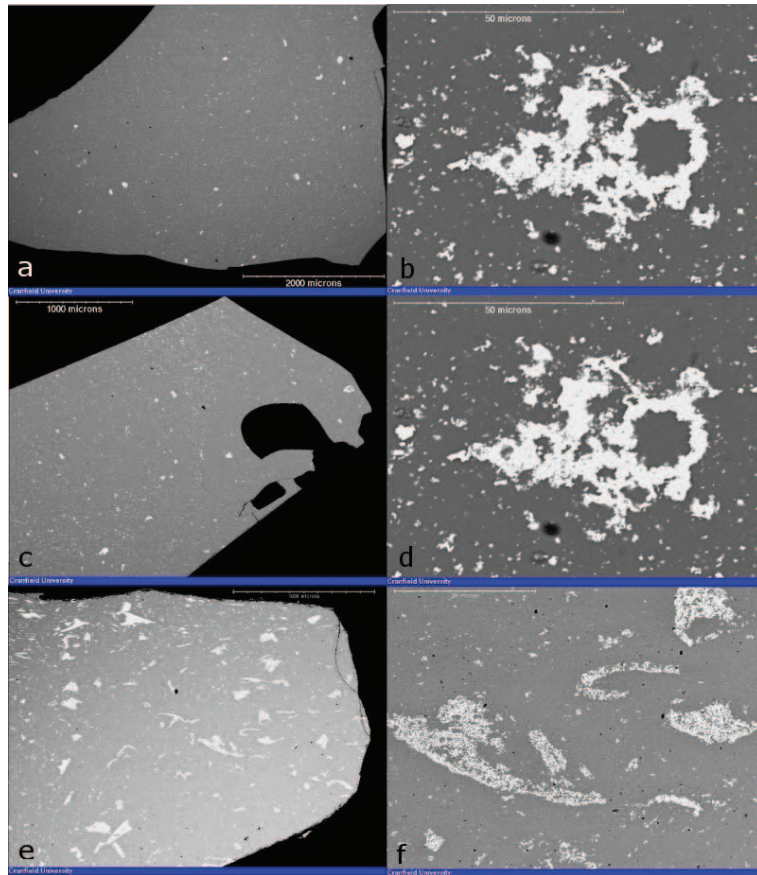


Figure 70: Experimental antimonate glasses: a. and b. glass B2, 3% Sb_2O_3 ; c. and d. glass B3 (3% Sb_2O_3 + 3% CaO); e. and f. glass C2 (cullet + 3% Sb_2O_3)

The SEM-EDS images were compared to opaque LBA glasses from Nuzi and were found to be virtually indistinguishable from the experimental replicates, in terms of the size, frequency and morphology of the calcium antimonate inclusions; suggesting that they had undergone similar processes, Figure 71 shows glass 1930.62.103.

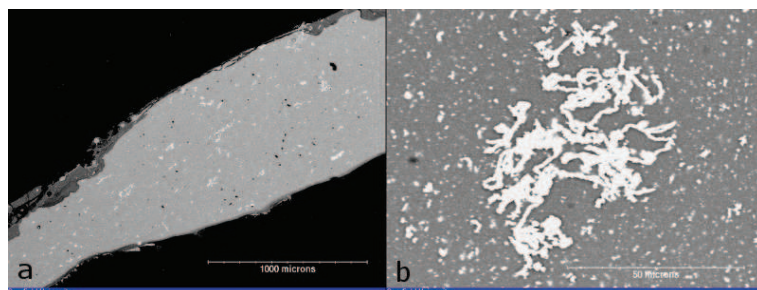


Figure 71: Nuzi antimonate glass 1930.62.103

7.2.3 SEM-WDS

Bulk analysis of the replicate glasses was carried out to check their composition compared to the original recipes, the results are presented in Table 29. There was generally a good match and the composition of the replica glasses reflected the original batch recipes. However, there are some differences, Table 30 below shows the recipe alongside the bulk compositions of the 1150°C replica glasses. Soda levels have dropped in all of the glasses with added antimony and silica levels have dropped in the two glasses containing additional lime as well as antimony, most probably as a result of the additional material in the recipe.

| Sample | Colour | SiO ₂ | Al ₂ O ₃ | CaO | MgO | Na ₂ O | K ₂ O | Fe ₂ O ₃ | Sb ₂ O ₃ | Total |
|--------|---------------------------|------------------|--------------------------------|------|-----|-------------------|------------------|--------------------------------|--------------------------------|-------|
| A1 | colourless (1050) | 68.4 | 0.4 | 6.9 | 4.3 | 17.7 | 3.4 | 0.3 | 0.0 | 101.4 |
| A2 | white (+3%Sb) | 63.6 | 0.4 | 6.4 | 4.4 | 14.9 | 3.0 | 0.1 | 2.4 | 95.1 |
| A3 | white (+3%Sb + 3%Ca) | 58.8 | 0.5 | 9.9 | 4.4 | 16.0 | 2.6 | 0.1 | 3.3 | 95.5 |
| B1 | colourless (1150) | 68.5 | 0.4 | 6.8 | 4.2 | 17.5 | 3.5 | 0.0 | 0.0 | 101.1 |
| B2 | white (+3%Sb) | 69.8 | 0.4 | 6.0 | 4.3 | 14.8 | 2.5 | 0.2 | 3.0 | 101.0 |
| B3 | white (+3%Sb + 3%Ca) | 66.6 | 0.4 | 9.5 | 4.1 | 14.6 | 2.3 | 0.2 | 2.2 | 99.8 |
| B4 | white (+ preroasted SbCa) | 66.0 | 0.4 | 10.1 | 4.0 | 15.5 | 3.5 | 0.0 | 1.9 | 101.4 |
| C1 | colourless | 62.8 | 1.1 | 8.7 | 8.0 | 17.1 | 2.4 | 0.4 | 0.1 | 100.4 |
| C2 | white | 62.9 | 1.1 | 7.8 | 7.7 | 16.1 | 2.5 | 0.4 | 1.4 | 99.9 |

Table 29: Bulk compositional analysis experimental antimonate glasses

| Sample | Colour | SiO ₂ | Al ₂ O ₃ | CaO | MgO | Na ₂ O | K ₂ O | Fe ₂ O ₃ | Sb ₂ O ₃ | Total |
|--------|---------------------------|------------------|--------------------------------|------|-----|-------------------|------------------|--------------------------------|--------------------------------|-------|
| Recipe | | 68.0 | 0.5 | 6.0 | 5.0 | 17.0 | 3.0 | 0.5 | 0.0 | |
| B1 | colourless (1150) | 68.5 | 0.4 | 6.8 | 4.2 | 17.5 | 3.5 | 0.0 | 0.0 | 101.1 |
| Recipe | | 68.0 | 0.5 | 6.0 | 5.0 | 17.0 | 3.0 | 0.5 | 3.0 | |
| B2 | white (+3%Sb) | 69.8 | 0.4 | 6.0 | 4.3 | 14.8 | 2.5 | 0.2 | 3.0 | 101.0 |
| Recipe | | 68.0 | 0.5 | 9.0 | 5.0 | 17.0 | 3.0 | 0.5 | 3.0 | |
| B3 | white (+3%Sb + 3%Ca) | 66.6 | 0.4 | 9.5 | 4.1 | 14.6 | 2.3 | 0.2 | 2.2 | 99.8 |
| B4 | white (+ preroasted SbCa) | 66.0 | 0.4 | 10.1 | 4.0 | 15.5 | 3.5 | 0.0 | 1.9 | 101.4 |

Table 30: Recipes compared to analyses replica antimonate glasses

7.2.4 XRD

XRD point analysis was carried out on all of the experimental replicates. The translucent glasses did not produce any diffraction patterns, as would be expected from amorphous material. The results are summarised in Table 31 which shows that all of the antimony-opacified glasses analysed contained calcium antimonate in the form of Ca₂Sb₂O₇ (Figure 72). However, the XRD analysis of the replica glasses show that for glass B2, which contained antimony oxide and no added lime; the diffraction patterns are consistent with a mixture of two forms of calcium antimonate Ca₂Sb₂O₇ and CaSb₂O₆ (Figure 72). XRD analyses were also done several archaeological antimony-opacified glasses from Nuzi (Table 31). The results show that some samples only have Ca₂Sb₂O₇, whereas others contain both phases of calcium antimonate.

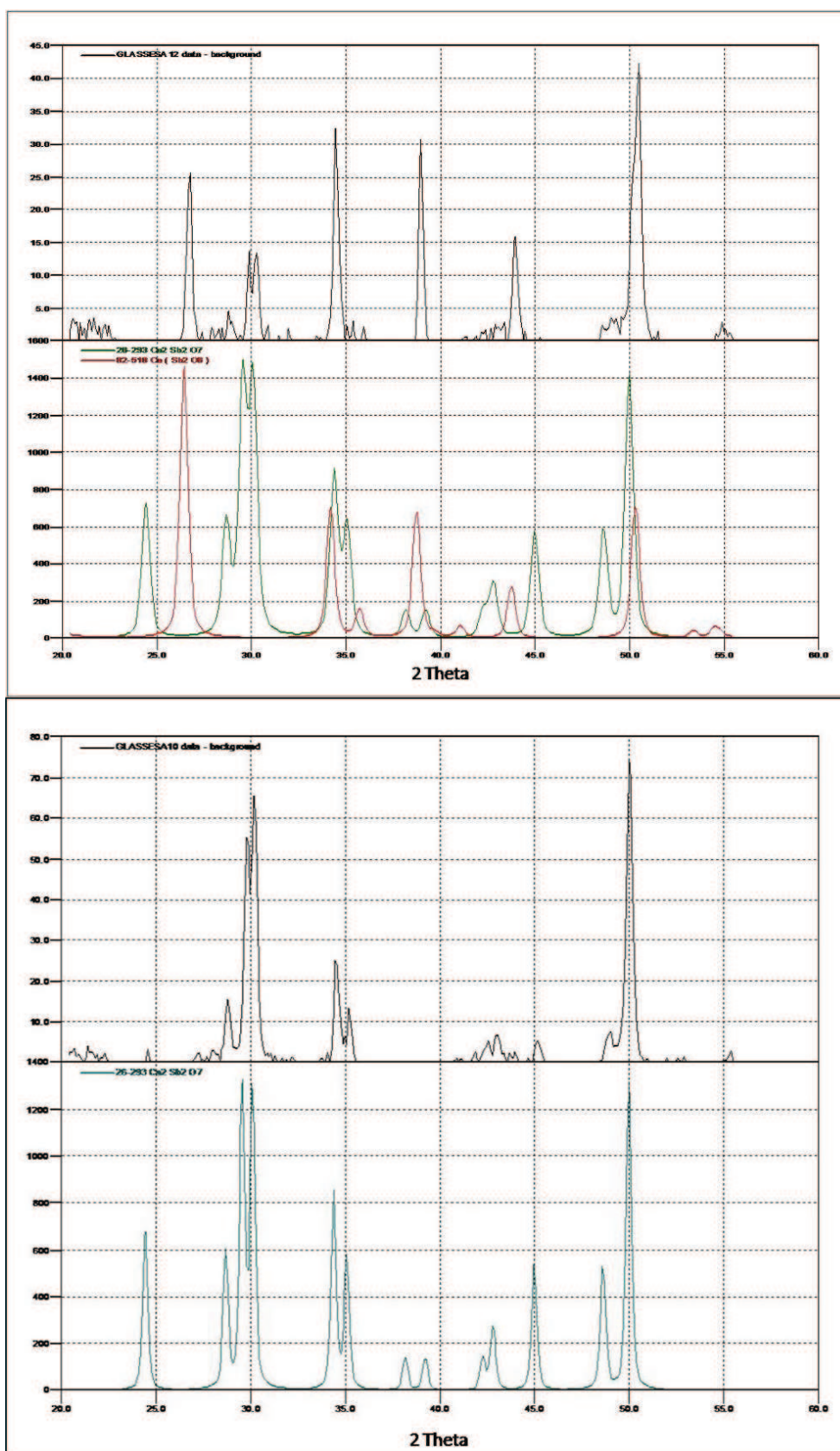


Figure 72: Diffraction patterns for experimental antimonate glasses: glass B2 top and B3 bottom

| Sample | Colour | XRD result |
|-------------|-----------|---|
| B2 | white | CaSb ₂ O ₈ and Ca ₂ Sb ₂ O ₇ |
| B3 | white | Ca ₂ Sb ₂ O ₇ only |
| B4 | white | Ca ₂ Sb ₂ O ₇ only |
| 1930.62.103 | turquoise | Ca ₂ Sb ₂ O ₇ only |
| 1930.66.90c | turquoise | Ca ₂ Sb ₂ O ₇ only |
| 1930.66.90d | turquoise | Ca ₂ Sb ₂ O ₇ only |
| 1930.67.45 | turquoise | CaSb ₂ O ₈ and Ca ₂ Sb ₂ O ₇ |
| 1930.68.82 | turquoise | CaSb ₂ O ₈ and Ca ₂ Sb ₂ O ₇ |
| 1930.67.67 | turquoise | Ca ₂ Sb ₂ O ₇ only |
| 1930.68.27 | turquoise | Ca ₂ Sb ₂ O ₇ only |
| 1930.82.59 | white | CaSb ₂ O ₈ and Ca ₂ Sb ₂ O ₇ |

Table 31: XRD results of experimental and archaeological antimonate glasses

7.3 Summary

The results of the alteration experiments provided only ambiguous traces of secondary alteration layer precipitation. However, they did show similar early stage alteration to some of the archaeological glasses. The dissolution experiments provided information about the behaviour of the glasses at a higher temperature and without the effects of a burial environment present. All of the monoliths released several elements into solution, however, copper was not released, even after 28 days and the presence of significant silicon suggesting that the glass network was beginning to break down. The original mass and surface area of the monoliths appeared to have less of an effect than had been expected, however, the only opaque blue glass in the experiments, the archaeological glass 1930.66.90b appeared to be breaking down faster in solution than the other archaeological glasses.

The replication experiments of the antimonate glasses indicated that the addition of antimony to a glass melt produced significant degassing during melting and that a temperature of 1150°C was required to produce a good quality glass in a single step. SEM imaging indicated that the experimental glasses made from raw glass batch, regardless of composition, were very similar to the antimony-opacified glasses from Nuzi. However the use of crushed glass cullet with added antimony produced an appearance which had not been observed in the ancient glasses. The XRD results also showed that the experimental glasses were very similar to the ancient glasses with a mixture of both phases of calcium antimonate in some examples and Ca₂Sb₂O₇ in the rest, with this phase being more common.

8 Discussion

8.1 Archaeological results

8.1.1 Survey of vitreous materials

The survey of vitreous materials from Nuzi has indicated that a large number of objects of glass, glazed ceramics, frit and faience remain within the assemblage held at the Semitic Museum at Harvard University. Similar objects are noted from several other contemporary sites in the Near East including Tell Brak, Alalakh and Tell al Rimah; Tell Brak was part of the Mitanni kingdom in northeast Syria (Oates et al 1997:xvii); Tell al Rimah was an Assyrian town in northern Iraq (Oates 1965) and Alalakh a major trading centre in Syria (Gates 1981), which was only part of the Mitanni kingdom at certain points of the Late Bronze Age. A major difference, however, noted between these other sites and Nuzi is the sheer quantity of beads found at Nuzi, particularly from the northwestern temple. Beads are reported in significant quantities from Tell al Rimah where hundreds of glass and frit beads are noted from the Mitanni period temple and palace (Oates 1965; 1968; 1970). Woolley (1955:64, 66, 120) also reports a number of glass beads from several levels of the temple at Alalakh and a few from the Level IV palace. However, the majority of the beads are reported from grave sites across the city (Woolley 1955:268). Small numbers of beads, including glass and frit examples are reported from Tell Brak, with the majority of the glass beads coming from a large reception room in the palace (McDonald 1997:101). The number of beads reported from all of these sites, however, is much smaller than the many thousands recovered from Nuzi. The types of beads found at Tell al Rimah are not recorded in the excavation reports. However, similar types of beads to those found at Nuzi are recorded at both Alalakh and Tell al Rimah. These include, spherical, cylindrical, inlaid, polychrome eye beads and zoomorphic frog and fly-shaped beads from Alalakh (Woolley, 1955:269-70) and similar types, excluding zoomorphic beads but including moulded glass and frit spacer beads, from Tell Brak (Oates et al 1997:243-251).

The difference in the numbers of beads recorded from these sites may be due to the use of beads as decorative motifs in the Ishtar temple at Nuzi, with the beads being hung in strings around the temple or set into the mud-brick walls (Starr 1939:92-3). Another possibility is that because Stratum II at Nuzi is a catastrophic destruction layer, which was not intensively rebuilt afterwards, little material was removed before the sacking and destruction of the city, compared to the other sites where later occupation has removed earlier traces. Indeed Oates et al (1997:21) note that the inhabitants of Tell Brak were extremely tidy, removing all traces of themselves from many areas of the site. However, far fewer beads, compared to Nuzi, were found in Phase 2 of the temple at Tell al Rimah which is also a destruction layer, considered to be approximately contemporary with the destruction of Nuzi, and also potentially dedicated to Ishtar (Oates 1965). The use of beads as decoration within the Ishtar temple at Nuzi, coupled to the destruction

and near abandonment of the site at the end of Stratum II, appears to be the most likely explanation of the sheer number of beads found during the excavation. There is, however, another possibility, many of the beads from Nuzi are extremely small and it is possible that the level of recovery during excavation was higher at Nuzi than at other sites in the region. It is clear from the finds notebooks that the number of objects found in the early years of the excavations was fairly low, only increasing significantly once the temple complex was found, and many small objects were recorded in more detail than would have been expected from an excavation of this period. However, the excavation reports from the other sites suggest that the level of recovery of small objects from these sites was also high so the number of beads at Nuzi seems to be a genuine difference in the use of these objects and that a combination of all of the above factors is most likely explanation for the differences seen.

Decorated glass vessels are reported in significant numbers from all three contemporary sites, with similar types of decoration and colours being recorded as at Nuzi, although opaque white and cream glass vessels are recorded from Alalakh and Tell Brak (Woolley 1955:298; Oates et al 1997:83,85; Oates; 1965, 1966), whereas almost all of the vessels from Nuzi are translucent blue. However, the moulded and plain pendants noted from Nuzi are not reported from either Alalakh or Tell al Rimah and only plain pendants were found at Tell Brak (Oates et al 1997:244). A number of other types of small objects noted from Nuzi were also found at other sites with amulets, similar to those at Nuzi, being recorded from Alalakh (Woolley 1955:271) and gaming pieces from Tell Brak (Oates et al 1997:86). Woolley (1955:302) also reports a glass figurines similar to the moulded Ishtar figurines from Nuzi (Starr 1939:451). Mosaic glass vessels are recorded from both Tell Brak and Tell al Rimah with a single fragment of glass with granulated decoration from Tell Brak, neither type was recorded from Nuzi (Oates et al 1997:83-4; Oates 1966).

Nineteen glass ingots and ingot fragments, including 12 found in association with a workshop area in the palace, are reported from Tell Brak (Oates et al 1997:88). Three small fragments, possibly from an ingot were found in the Nuzi assemblage; but no examples are reported from Alalakh or Tell al Rimah. These objects are evidence of secondary glass working rather than glass production and the location of primary glassmaking sites in the Near East remains ambiguous.

The vitreous assemblage from Nuzi also contained several examples of frit and faience vessels, including Egyptian blue vessels, glazed faience vessels and marbled faience vessels. Similar vessels are reported from Alalakh including an Egyptian faience vase and dark blue 'paste' vessels which, from their description, appear similar to the blue frit vessel fragment found in the Nuzi assemblage (Woolley 1955:71, 81, 297). A blue frit bowl, thought to be made from Egyptian blue, yellow frit vessels and other objects such as a faience mace-head and gaming pieces are noted from Tell Brak (Oates et al 1997:25, 27, 87). No frit or faience vessels are reported from Tell al Rimah, however, a 'glazed frit' mask was found in the Phase 1 temple (Oates 1966). The best known example of the marbled faience outside of Nuzi is from the tomb

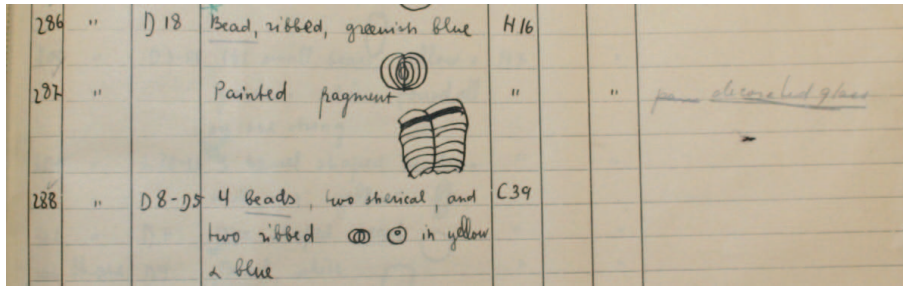


Figure 73: Extract from notebook showing decorated glass fragment recorded as 'painted fragment'

of the foreign wives of Thutmosis III, this appears very similar to the most complete fragment from Nuzi, although the Nuzi examples lack the gilding seen on the example from Egypt. This object is generally thought to be of Near Eastern origin (Lilyquist and Brill 1993:10).

Glazed ceramic vessels, figurines and wall nails are relatively common within the Nuzi assemblage. However, no glazed ceramics are recorded from Tell al Rimah and only glazed ceramic vessels from Alalakh (Woolley 1955:292,299). Around 70 glazed ceramic vessel sherds are noted from Tell Brak with no mention of any figurines or other types of object (Oates et al 1997:72). There do not appear to be any parallels of the blue-glazed lion (and other) figurines found at Nuzi in contemporary Near Eastern sites. In addition to the more unusual glazed objects such as the white-glazed socket from the temple, 1930.14.6.

8.1.2 Comparison of the assemblage to the finds notebooks

Around half the number of objects recorded in the finds notebooks were noted within the assemblage. This is most probably due to the division of finds carried out at the end of each excavation season with many of the finds going to the Baghdad museum. It was also clear from the finds notebooks that some of the objects in the museum assemblage were never recorded in the notebooks, for example, 1930.82.17, a group of monochrome translucent blue vessel fragments from room L22 in the palace. This may have been due to the misidentification of objects, several of the glass vessels are recorded as 'painted fragments' in the finds books, for example, a decorated glass fragment from H16 which was recorded as a painted fragment, later corrected as being decorated glass, Figure 73. There are also vitreous objects in the museum assemblage, for example, the moulded blue frit vessel fragment 1930.47.14 found in the assemblage also does not have a record in the finds notebooks. There are also a few objects described in the excavation report which are neither in the museum assemblage nor in the finds notebooks, for example a yellow glass vessel described by Starr (1939:459).

8.1.3 Find locations

Overall almost 70% of the objects surveyed in the assemblage were found to have a known location. This was either based on the field number, then by cross referencing the finds notebooks, or a location number written on the object itself. Where all of these matched this was straightforward, however, there were a few examples where the field number did not match up to the object with that number, for example the Late glass vessel with the field number of a ceramic object noted in Section 4.4. And there were numerous objects where the field number did not have a location attached to it (Table c Appendix 1). In addition several objects only had a field or room number on the packaging associated with them rather than directly linked to a particular object. There were also a large number of objects which had neither a field number nor a room number associated with them. It is possible that this is due to the collection being moved from one area of the museum to another during the early 1970s (Armstrong, 2008 pers comm) when some of the field numbers may have become detached from their objects or were not recorded on the objects' accession into the museum. There may also have been considerable disruption of some of the collection when one of the early shipments had to be unpacked prior to entry into the USA as they had been packed in straw, which was not allowed into the country (Armstrong, 2008 pers comm).

8.1.4 Distribution of vitreous materials

The majority of the vitreous materials from Nuzi are from either religious or high status contexts (see Section 4.5). This suggested that glass and other vitreous materials at Nuzi were a luxury or otherwise significant type of object. The exception to this is the beads which are found across the site in all types of building, although the vast majority are from the temple complex. The contemporary Near Eastern sites of Alalakh, Tell Brak and Tell al Rimah show a broadly similar pattern of distribution with vitreous materials being found in the palaces and temples of these sites (Woolley 1955:297-302; Oates et al 81-95; Oates 1966,1967). However, many of the glass vessels, and other objects, found at Alalakh and Tell al Rimah are from burial contexts (Woolley 1955:203-223) whereas no burials (apart from infant burials) are known from Nuzi.

Much of the vitreous material from Nuzi is connected with areas of the city connected to religion both in the temple and in private 'chapels' in the residential areas. This could suggest that this type of material was connected to the worship of particular gods at Nuzi, especially Ishtar; very little vitreous material was found in the southwestern temple of the religious complex which is thought to have been dedicated to Teshub. The preponderance of glazed ceramics, in particular the glazed lions an animal associated with Ishtar (Starr 1930), the glass beads used as decorative elements and other vitreous materials, such as the blue frit vessels, suggest that these materials could have been highly significant in the ritual practice surrounding this temple and the worship of Ishtar. This may be related to contemporary ideas about the

importance of the colour and luminosity of certain materials (Feldman 2006:121). The glass vessels from Nuzi, however, are more commonly associated with high status areas such as the palace and suburban dwellings with glass as an indicator of status rather than a ritual object, although there are some decorated glass vessels associated with the temple complex, not unexpectedly for such high status objects.

Tell al Rimah shows a relatively even distribution of vitreous materials between the temple, tentatively ascribed to the worship of Ishtar, and palace, although exact numbers of objects are not always reported (Oates 1965,1966,1967,1968,1970, 1972). However, several of the glass objects recorded from the palace are noted to have been in association with a shrine (Oates 1968; 1970). Tell al Rimah is in Assyria rather than Mesopotamia so the differences with Nuzi may be related to regional variations in ritual practice despite the gods being in the same pantheon. At Alalakh again most categories of vitreous materials are noted from the temple, palace and from graves (Woolley, 1955:297-302). However, similar to Nuzi, glazed ceramics are only noted in the temple, and in some graves, and not from the palace (Woolley 1955:299). At Tell Brak, however, glass and other vitreous materials are found in both the palace and temple, including glazed ceramics (Oates et al 1997:72-3). The majority of the glass ingots and cullet found at Tell Brak were in association with a probable workshop in the palace complex (Oates et al 1997:28,85), perhaps suggesting royal control over this industry. Only one of the possible ingot fragments from Nuzi could be assigned a location, which was in the palace complex again tentatively suggesting some royal or high-status control over the production of glass objects.

The distribution of vitreous materials from Nuzi suggests that these objects had a strong religious significance, particularly the blue-glazed ceramics. However, glass objects were also found in 'high status' areas and decorated glass vessels were found in both high status and religious contexts. There are a number of differences between the distribution of vitreous materials at Nuzi and at other contemporary sites, including the use of glass beads and architectural elements within the Ishtar temple and the presence of glazed ceramic figurines and other objects. However, each of these sites have their own histories in terms of their occupation, destruction and abandonment. they are also in different geographical and political regions at various times as well as covering relatively long timescales and periods of occupation. Therefore, drawing any strong conclusions about the use of vitreous materials in the Near East during the Late Bronze Age on anything other than a site by site basis is difficult.

8.1.5 Intrusion into SII

It was also found that considerable intrusion into the Stratum II layers had occurred at various times, 40 rooms or areas within Stratum II had been potentially affected by the late period cemetery with around another 30 rooms or areas affected by later occupation across the rest of the site. This does mean that there is the potential for later objects to have been mixed in with Stratum II material. However, in many

cases the late objects are sufficiently different that distinguishing between them is straightforward, such as the silver coins dated to the Parthian period by a particular king (Starr, 1939:294). The finds notebooks also occasionally note that an object is late period or found in a disturbed area, again often allowing the later and earlier material to be separated, such as 29-12-135, recorded as a light blue glass vase from Grave 25. However, in many cases further analysis is required to distinguish between 2nd millennium and later objects, for example, a few of the yellow and green beads (section 5.3).

8.2 Bulk compositions

8.2.1 2nd millennium BC glasses

The translucent blue glasses from Nuzi are very similar in composition to contemporary glasses of the same colour from Tell Brak and are distinguished from Egyptian glasses of the same date only by somewhat lower lime levels, for example the translucent blue glasses from Amarna and Malkata analysed by Shortland and Eremin (2006) have an average lime level of 8.7% compared to 5.7% for the Nuzi glasses. The Nuzi glasses have similar average lime values to those noted for Tell Brak, although Henderson (1997:96) notes slightly lower lime levels for translucent blue glasses from Tell Brak. It is possible that this difference is related to the raw materials used in the manufacture of the glass. Plant ashes can vary considerably in composition depending on both plant species and geographical location (Tite et al 2006; Barkoudah and Henderson 2006) and those used to manufacture the Nuzi glasses may have contained somewhat less calcium. The colorant-free amber glasses from Nuzi also show slightly lower levels of lime than the Egyptian examples of the same colour (Shortland and Eremin 2006), an average of 6.3% compared to 7.8%, with the other major oxides being similar to one another. In contrast the deliberately opacified glasses containing calcium antimonate have considerably higher calcium oxide levels than the translucent glasses. This may be due to a number of factors such as: different raw materials, contamination from a calcium-rich parting layer or different firing and cooling regimes, this is discussed in more detail in Section 8.4.

All of the blue glasses from Nuzi contain copper as their colorant with no tin or lead being present. Tin and lead oxides, alongside copper, suggests the use of bronze scale as a colorant, which is suggested as having been used in the manufacture of Egyptian vitreous materials (Tite et al 2007; Hatton et al 2008). In addition, a number of copper-blue glasses from Amarna and Malkata have tin present, 20 of the 29 analysed have tin at levels above 0.05% (average 0.12%) (Shortland and Eremin 2006). The lack of tin and lead in the Nuzi glasses suggest that bronze scale was being used as a colorant here. Analysis of the metal objects found at Nuzi has suggested that copper and bronze were the most common metals found with smaller quantities of leaded bronzes, brass and silver-copper alloys (Shortland et al 2008). It is possible, therefore, that copper scale was being used, however, given that bronze appears to have been as common

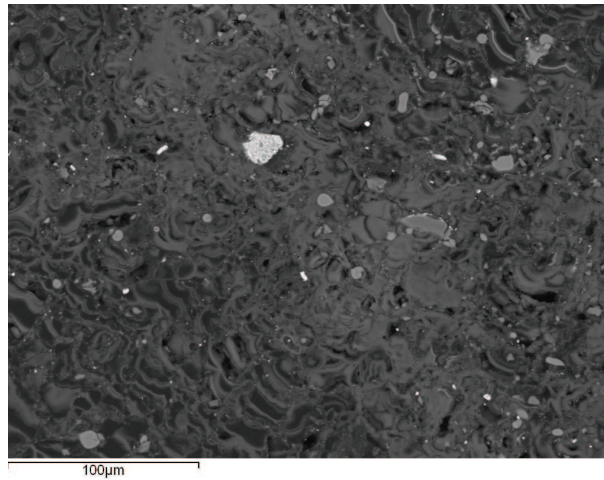


Figure 74: Possible altered red glass bead 1930.61.91a

as copper another type of copper mineral, such as malachite (copper carbonate), may have been used to colour the blue glasses at Nuzi.

Interestingly no cobalt-coloured glasses were found in the assemblage, although glass of this colour is common in Egyptian glasses from the same period (Shortland and Eremin). Relatively few cobalt-coloured glasses are reported from the Near East: two examples from Tell Brak have been analysed, a single purplish-blue bead, thought to have been coloured by Egyptian cobalt (Henderson, 1997:96-7) and a translucent blue vessel coloured by cobalt and copper (Brill 1999b:39) again probably coloured by Egyptian cobalt. In addition, a collection of cobalt- and copper-coloured glass axes are known from Nippur, which appear to have a non-Egyptian cobalt source (Shortland et al, in preparation).

There were also no purple or black manganese-coloured glasses and no red, cuprite-coloured, glasses in the 2nd millennium BC assemblage, again these are found in Egyptian glasses of a similar date (Shortland and Eremin 2006). A single possible red glass was found but this did not contain any copper and no unaltered examples were found. Sample 1930.69.91a which was thought to be red frit bead, however, on imaging with SEM it appeared to have more of an altered glass morphology with iron-rich inclusions giving the colour, Figure 74. Interestingly Vandiver (1983) notes that the red frit from Nuzi is coloured by iron oxide so this bead could be overfired frit that has become glassy. A single green opaque bead, from a Bronze Age context, was analysed and was found to be coloured by copper and lead antimonate, however, trace elemental analysis suggested that it may be an import from Egypt, Section 5.7.

Several examples of black glass are known from Nuzi but these are caused by either a very deep iron-sulfur chromophore, i.e. colorant-free glass, or small particles of copper sulfide, although no unaltered examples of glasses with this colorant type were found. Glasses containing copper sulfide as a black colorant are known from the ninth century BC Iranian site of Hasanlu (Stapleton and Swanson 2002) but glasses with this colorant have not been recorded from any other Near Eastern site so far.

Two small colourless raw glass lumps from Nuzi were analysed, 1930.82.62b and 1930.82.62c. No other colourless glass has been found in the Bronze Age assemblage and there is a possibility that these fragments represent imports, perhaps from Egypt where colourless glasses are more common and higher aluminium oxide levels have been reported (Shortland and Eremin 2006). However, the presence of manganese oxide at 0.6% in 1930.82.62c could suggest a later date than thought for these glasses, although a colorant-free glass with 0.33% manganese oxide is reported from Lisht and several glasses with unexpectedly high manganese, ranging from 0.5% to 1.4%, were found in other colours of Egyptian glass in Shortland and Eremin's study (2006). The location of these glasses would suggest a definite 2nd millennium BC date, they are recorded as having come from the bottom of the well in G50, the courtyard of the temple, some 9 metres below the level of Stratum II, large quantities of material from the temple appears to have been thrown down this well during the destruction of the city (Starr 1939:104).

8.2.2 Late glasses

Five examples of mineral soda-based glasses were analysed, these glasses contain very little magnesia and potash compared to plant-ash based glasses and are thought to have been made from natron and sand. Natron glasses are found from the ninth century BC onwards, becoming the dominant composition of glass during the Roman period (Shortland et al 2006), Section . Therefore, these glasses are clearly of a later date. However, most of the late glasses analysed have a typical plant-ash based composition similar to the Bronze Age glasses in terms of potash and magnesia levels. Fortunately there are some differences between these glasses and the earlier examples. Aluminium oxide levels are typically much higher; usually well above 1% oxide weight and over 3% in some cases. Titanium dioxide is also present at levels well above the detection limits with an average of 0.13% compared to 0.03% for the translucent blue Bronze age glasses. Of the 20 colourless plant-ash based glasses 13 contain manganese oxide, several above 1% oxide weight, which is not seen in the earlier glasses. Manganese was extensively used in later periods as a decolorant; under reducing conditions the brown/yellow colour created by manganese can cancel out the blues and greens from iron. The later plant ash glasses from Nuzi also appear similar to other Sassanian glasses from Iraq analysed by Brill (1999b:152-155), although there are some overlaps between the earlier and later glasses, particularly the colourless Egyptian glasses (Shortland and Eremin 2006), Figure 75. In the late opaque green and yellow glasses analysed the presence of tin as an opacifier alongside lead to create the yellow colour identifies these glasses as being later, the use of lead stannate as an opacifier not being found until the 1st millennium BC (Tite et al 2008b).

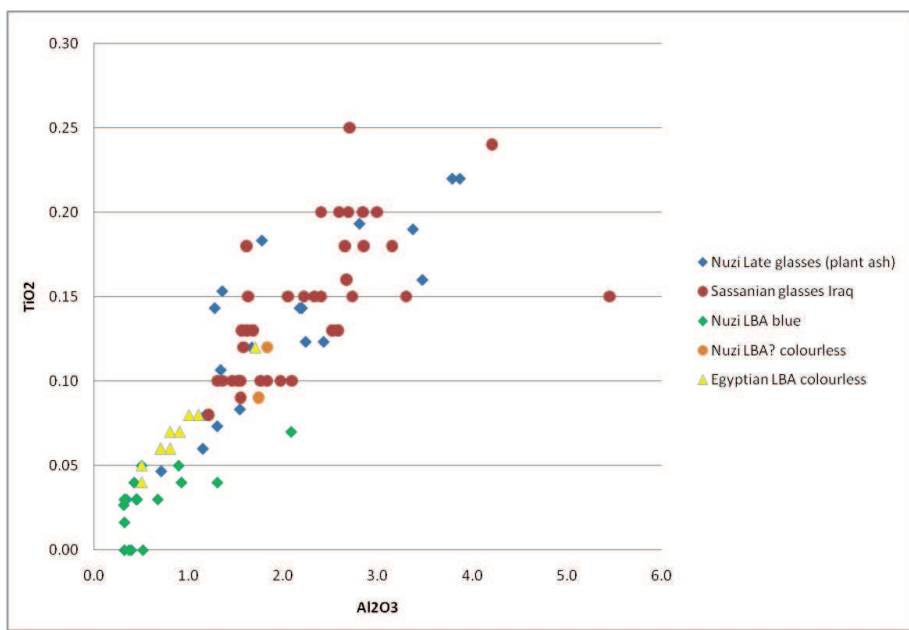


Figure 75: Scatterplot of Late period glasses compared to LBA glasses: Sassanian glasses from Brill 1999b (152-156) and Egyptian data from Shortland and Eremin 2006

8.2.3 Glazed ceramics

The SEM-WDS analyses of the glazed ceramics, where it was possible to get a reasonable bulk composition of the glazes (close to 100% total), have suggested that they are very similar to the translucent blue glasses. The only difference is that several of the glazes have higher potash levels compared to magnesia levels whereas the glasses are the other way round, as was noted by Paynter (2009) on a single unaltered sample from Nuzi. Paynter (2009) suggested that powdered glass may have been the method used to apply the glaze to the ceramics during this period, the potash levels being affected by potassium present in fuel ash becoming incorporated during the firing. Recent work has suggested that the ceramics from Nuzi are all made from local clays, regardless of the object type (Erb-Satullo et al, in prep.). There is also no difference between the clays used to make the glazed and unglazed ceramics, including statues and figurines as well as vessels. This suggests that, although there is no archaeological evidence as yet, the manufacture of these ceramics was taking place close to the city. Given the overlap between the glaze and glass compositions it could also indicate that glassmaking was also a local activity. Alternatively the technique of glazing, that of using powdered glass, could suggest that the glass may have been imported from some distance, powdered and then used in the glazing of ceramics.

8.2.4 Other vitreous materials

A number of objects of vitreous material were also analysed as part of this project, including four marbled faience fragments, a fragment of a faience vessel, and an Egyptian blue frit vessel fragment. The Egyptian

blue vessel has a very similar composition to contemporary Egyptian blue objects from Amarna it is also different to other Mesopotamian Egyptian blue objects, being lower in silica and higher in copper and lime (Hatton et al 2008). However, the Nuzi vessel is also somewhat different to the Amarna objects in that it lacks the tin and lead oxides thought to result from the use of bronze scale as the copper colorant in the Egyptian examples (Hatton et al 2008). Unfortunately the other Egyptian blue objects from Nuzi were too weathered to allow comparative quantitative analysis. The SEM images of the faience vessel suggested that it was made by application glazing rather than the more common efflorescence glazing technology due to the lack of interparticle glass (Tite et al 2007). The marbled faience samples produced very similar results to previous work on these object, having a highly crystalline structure and the colours being produced by iron oxide in the case of the red and lead in the yellow areas, although the lead antimonate colorant noted by Liliquist and Brill (1993:10) was not seen, lead alone being present.

8.2.5 Trace elemental composition

Recent work on trace elements and isotopes have indicated that Egyptian and Near Eastern glasses can be distinguished from one another on the basis of ratios of certain trace elements (Shortland et al, 2007) and into Egyptian, Nuzi and Tell Brak groups on the basis of isotopic ratios (Degryse et al, 2009). The trace element data from the glasses analysed by LA-ICPMS as part of this project has indicated that most of the objects fall within the Near Eastern trace elemental group (see Section 5.7 for details). However, several of the samples analysed are somewhat different. Sample 1930.67.42 a green opaque bead appears closer to the Egyptian material in its trace elemental composition, Figure 36. In addition, one of the colorant-free glasses from Nuzi (1930.82.62e), the white glass (1930.82.59) and two of the turquoise glasses, 1930.63.40d and 1930.68.27c, are also rather different, having much higher Cr/La ratios than the other Nuzi glasses, Figure 36, which could suggest that they were made in a different region or manufactured using a different technology. Shortland et al (2007) suggest that the Cr/La ratio is affected by the crucibles used in the manufacture of glass and it is possible that higher ratios could indicate a greater contribution from the crucible walls, or could arise from contamination of the raw materials during processing.

8.3 Alteration of glasses

The results of the analysis of the 2nd millennium BC glasses have shown that all of the samples analysed are weathered or otherwise altered to one degree or another. There is considerable variation in the degree of preservation of the glasses, despite bulk analyses of the unaltered areas of the glasses indicating that they have a relatively narrow compositional range. A clear distinction was noted between examples where glass was still present and completely devitrified examples. From the samples taken for analysis, which were selected to be a representative sample of the glass assemblage held at the Semitic Museum at

Harvard University, the devitrified glasses were in the majority with almost twice as many devitrified examples compared to those with glass remaining suggesting that either the burial conditions or the original compositions of the glasses were not conducive to good preservation. It is also possible that there may have been other examples that have not survived at all, the glass dissolving completely prior to excavation, this has been suggested by several authors as biasing the study of ancient glass towards the objects that survived with an unknown fraction that existed in the past no longer being extant in the archaeological record (Vandiver 1993; Freestone 2001). In the Nuzi assemblage it is unclear whether the variation in preservation seen is based upon differences in the composition of the glass or the burial environment, which contained it; a combination of these factors is also possible.

8.3.1 2nd millennium BC glasses

The 2nd millennium BC samples were grouped into seven groups based on their appearance on SEM images. Groups 1 and 2 had a change in the backscattered electron image contrast was noted at the glass surface, Group 2 also had a thin crust of secondary alteration layers (<500µm). Group 3 had a much thicker crust of secondary alteration layers (>500µm) and groups 4-7 were completely devitrified; differentiated on the basis of their SEM appearance and stability.

Early stages of alteration: The samples in groups 1 and 2, the glasses where a change in the backscattered electron image was noted, are compositionally consistent with the process of ion exchange suggested to be the initial stage of glass weathering (see section 2.3 for details and references). Hydrogen ions in water react with the alkali ions within the glass network creating an alkali depleted, silicon enriched, and hydrated layer. However, it is generally suggested that this layer is very thin, tens of nanometres thick, before becoming a completely altered layer, very different to the original glass in structure (Grambow 2006). However, in the examples from Nuzi, this change in backscattered electron greyscale can extend for some distance into the glass and along cracks or other weak points. In example 1930.82.55 the alkali depleted layer extends into the glass surface for several hundred microns and in the case of 1930.82.15b has moved deep into the glass along cracks, Figure 76 shows 1930.82.55 and 1930.82.15b is Figure 43 in Section 6.1. It is not completely clear that the changes seen can all have occurred during the burial of the glass and there is the possibility that some of this apparent early stage alteration seen may have occurred since the excavation of the objects. Indeed Starr noted that many of the glazed objects rapidly deteriorated after excavation (1939:442) and Vandiver (1992) has also noticed significant post-excavation changes in very early glasses from the Near East. In addition, experimental work carried out within this project has suggested that this initial stage of glass weathering can happen over very short time periods, in just 28 days an area with a change in backscattered signal suggestive of an hydrated layer was noted in one of the replica glass samples, RT 28 (a monolith aged for 28 days in a clay solution at room temperature),

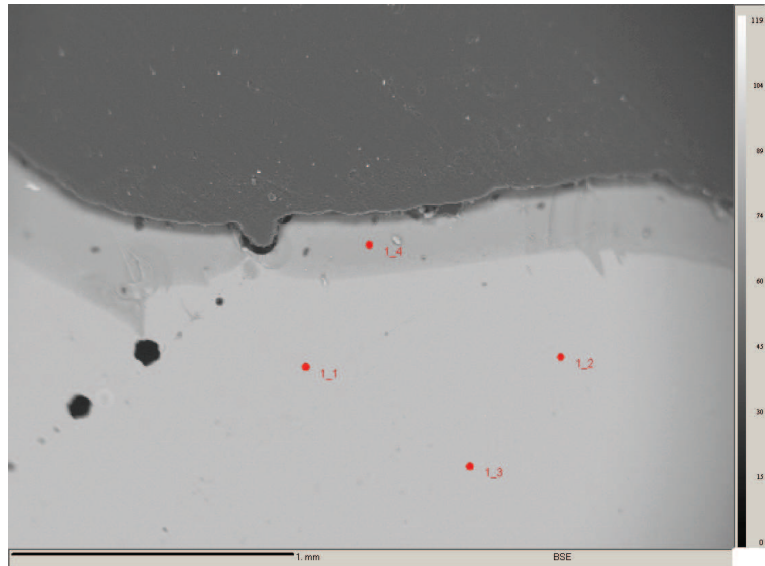


Figure 76: Early stages of alteration, 1930.82.55

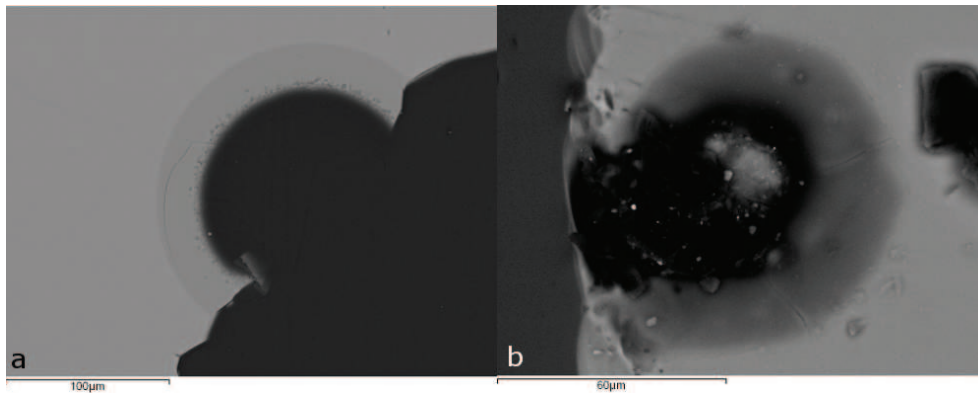


Figure 77: a. 1930.82.21, Late period vessel fragment; b. Experimental replica alteration experiment RT 28

which was similar to a feature in one of the Late period glasses 1930.82.21, Figure 77. This layer does not extend deeply into the glass but does show that this stage of weathering is rapid and could conceivably take place in the time period between excavation and analysis, 70-80 years. Vandiver (1993) has also noted an Egyptian core-formed vessel from Amarna, contemporary with the glasses from Nuzi that has a similar depleted layer at the surface, on SEM imaging, thought to be the result of atmospheric weathering rather than during burial. This type of information can be useful when looking at the future storage and conservation of the materials.

Secondary alteration layers (composition): The largest group of samples where any unaltered glass remains is group 3 where there are significant secondary layers around a core of unaltered glass. Previous work has suggested that these layers are formed by the silica network breaking down via hydrolysis reactions, releasing all of the elements present in the glass into solution at the glass surface some of these then reprecipitate from this saturated solution forming the layers observed (Salviulo et al 2004; Grambow 2006).

Hydrogen ions and molecular water, which have entered the glass network via ion exchange with alkali ions and diffusion reactions, create new reaction sites within the glass network for hydrolysis reactions which then break down the silica network, once silica has reached saturation point in solution it starts reprecipitating at the glass surface. Previous work has suggested that these layers are dominated by silica with occasional contributions from other elements from the glass and the surrounding soils, such as aluminium and a loss of alkalis and alkaline earths (Cox and Ford 1989; Jantzen et al 2008). Analysis of the secondary alteration layers showed that they had much lower totals than the unaltered glasses, which was thought to indicate hydration of these layers. However, it has also been suggested that the secondary layers are much more porous than the original glass containing a large number of voids reducing the analytical total (Gulmini et al 2009). Magnesium-rich layers were noted in a number of the samples, appearing to substitute for silicon in the alteration layers, as was observed in several of the compositional maps prepared. This has been noted by several authors as occurring in both archaeological and nuclear waste glasses, which contained significant magnesia (Salviulo et al 2004; Van Iseghem, 2001), and also in glasses that did not, Vandiver (1993) suggests that magnesia-rich layers can be formed both from magnesia within the glass and within the burial environment. Calcium-rich material infiltrating along cracks were also noted, this appeared to be coming from the calcium-rich soils as it appeared to be completely separate from the glass and alteration layers. One difference observed between the Nuzi glasses and previously published studies of both archaeological and nuclear waste glasses is the presence of copper-rich areas in the secondary layers, at levels well above that seen in the original glass, in some cases this is as much as a factor of 10. This may well be due to these very early glasses containing high levels of copper as colorant, which is not as common in later periods, where considerably more work has been carried out. The presence of copper at such high levels is puzzling as there is no copper in the surrounding soil (Table 5), unlike magnesium, aluminium and potassium where the presence of these elements in the soil could be affecting the quantities present in the secondary alteration layers. This could suggest that copper is less mobile than the other elements present in the glass, becoming part of the secondary phases rather than going into the surrounding burial environment. This was also suggested by the dissolution experiments carried out as part of this project where copper was not found in the attacking solution used, even after 28 days at a high temperature when ICP-AES analysis indicated that silicon was being released into the solution at this point, meaning that the network was breaking down and should have released all of the other elements contained in the glass into solution. Another difference between the Nuzi glasses and other studies was the lack of manganese and iron infiltration into the secondary alteration layers, which is commonly reported for archaeological glasses (Gulmini et al 2009) but only observed in a very few examples from Nuzi. This is most probably due to the low levels of these elements in the surrounding soil. Previous work has noted that manganese can easily migrate into alteration crusts (Watkinson et al 2005).

The groupings in the devitrified glasses (4-7) are based largely on the structural integrity of the samples which now consist completely of secondary precipitated layers, formed in the same processes as noted above. The composition of these samples was fairly consistent but slightly different to that seen in the groups with glass remaining. Again the analytical totals are low, suggesting significant hydration, and silica is the dominant oxide within the layers. Almost all of the samples analysed quantitatively indicated that aluminium was significantly increased in the secondary layers compared to the expected amount that would have been in the glasses. It is possible that the devitrified glasses were originally higher in aluminium, although some of the higher values are significantly outside what would normally be expected in glasses of this period, for example, 1930.60.140b with levels above 5% oxide weight, see Table 22 for more details. It would also generally be expected for glasses containing higher levels of aluminium oxide to be more durable than those containing less than 1% oxide weight, as is the case in the majority of the Nuzi glasses where the original composition could be analysed. This suggests that the aluminium oxide is coming from the soil fraction of the glass/environment interface becoming incorporated into the secondary precipitated layers on their formation. This could indicate that the devitrified glasses were in an environment more conducive to this than the less altered glasses. However, it is also possible that the aluminium oxide present at relatively low levels in the glasses is becoming enriched at certain points in the layers due to the nature of the reactions forming the layers. The presence of potassium at levels which would not usually be expected in devitrified glasses was also observed in a number of the devitrified glasses, this has been noted in previous studies as coming from the burial environment as it was noted in glasses which did not originally contain any potassium (Van Iseghem, 2001). The variation in compositions of the secondary alteration layers could suggest that burial conditions are not stable across the site in terms of their environment and composition.

Secondary alteration layers (morphology): The secondary precipitated layers observed in groups 2 to 7 vary in their morphology as well as their composition. The morphologies of the secondary precipitated layers vary considerably in their scale, direction, and behaviour around inclusions. In a few examples smooth layers proceed across the glass object suggesting a reaction front unaffected by changes in glass composition, environment or inclusions in the glass. All of these factors appear to have affected a number of other examples. Many examples appear to consist of highly disorganised layers, suggesting that the reaction front has not proceeded smoothly from the glass surface into the body of the glass but has been affected by several possible factors. The first is these is inhomogeneities in the glass composition, with the reaction front being accelerated or decreased by less or more durable areas within a single object. It is not absolutely clear how much variation would be required in order to effect changes of this magnitude, although relatively minor variations in the quantities of several oxides are known to significantly affect the durability of glass. For example, aluminium oxide at levels of above 1% is known to increase the durability of glasses due to the configuration of this oxide in the glass network. Aluminium oxide forms network forming

tetrahedra with three oxygens and immobilises an alkali ion to balance the charge (Shelby 2005:90), this fixes an alkali in the network meaning that there are fewer reaction sites to be attacked by hydrolysis reactions. Apart from elements such as aluminium the most critical element within a glass in terms of its durability is silicon, in the form of silica (El-Shamy 1973). It has been noted that glasses containing less than 62mol% silica are more susceptible to weathering than those with higher silica levels, this is due to the fact that at this point each silica tetrahedron within the network has a shared oxygen with at least one other network former tetrahedron, therefore the network is continuous with fewer reaction sites open for hydrolysis (El-Shamy 1973). Within the samples where glass remains all of the silica levels are above this critical point. However, the compositional maps created as part of the analysis of the glasses from Nuzi have indicated that there was relatively little compositional variation within the unaltered glasses, example and figure. The one exception to this (1930.60.140a) was highlighted in Section 6.1, Figure 51 where several elements were seen to vary significantly in composition across the unaltered glass area. In addition to the compositional maps the SEM-WDS data from the bulk compositional analyses of the glasses also showed that there was little variation in the composition of a single object. Each object was analysed in three areas with the average being taken, and very little variation was noted between the analyses in most cases.

The presence of regular lamellar feature was noted in a large number of the samples analysed. These features are common in archaeological glasses, being reported from a range of glass compositions, locations and time periods, for example, Cox and Ford (1989), glasses on the seabed; Janssens et al 1996, for Roman glasses in Jordan and Gulmini et al in Sasanian glasses in Iraq. The lamellae consist of alternating bands of smooth silicon-rich layers with a spongy material in between, Figure 61f. An SEM-EDS line analysis across a devitrified sample (1930.69.39b), Figure 46 showed the silicon levels rising and falling in pattern with the layers, the darker spongy material being lower in silicon. However, the exact method of formation of these layers remains somewhat ambiguous. It has been suggested that they indicate regular cycles of changing environmental conditions at the glass/water interface (Cox and Ford 1989). McLoughlin (2003:226) has also suggested that they are formed by regular saturation events in the solution at the glass surface, changing direction due to variations in the glass composition and irregularities such as air bubbles. However, none of these explanations covers all of the variation seen in these features from samples from the site of Nuzi. Significant changes in the scale of the lamellae are noted both between objects and within single objects, for example, 1930.82.18 and 1939.63.40a. Figure 42c with the lamellae ranging from sub-micron in scale to several microns across; suggesting that the processes which create the lamellae can be subject to change in the same object in the same burial conditions. Examples with lamellae moving in several directions are also noted, for example 1930.60.42, Figure 42a, suggesting that the reaction front is attacking at different times and areas of the object.

One area where significant variation in the organisation and scale of the secondary precipitated layers was noted was in samples where decorative inlays of glass were present and had also devitrified, for example 1930.52.1e, Figure 78. It would appear that differences in composition of the glass and inlay would be responsible for this difference as this is on a single object, which has been subjected to identical environment conditions. In addition the decorative inlays are generally white or yellow glasses containing calcium or lead antimonate as a colorant and it has been noted that the turquoise, white and yellow glasses did appear to weather slightly differently to the translucent glasses, forming a more 'chalky' textured weathering crust, with generally a more disorganised precipitated secondary layer structure, Figure 58. This suggests that there the opacifiers cause these glasses to alter differently to the translucent glasses, this was also indicated in the experimental results where the opaque glass dissolved at a much faster rate than the translucent examples, Table 26 and Section 8.4.

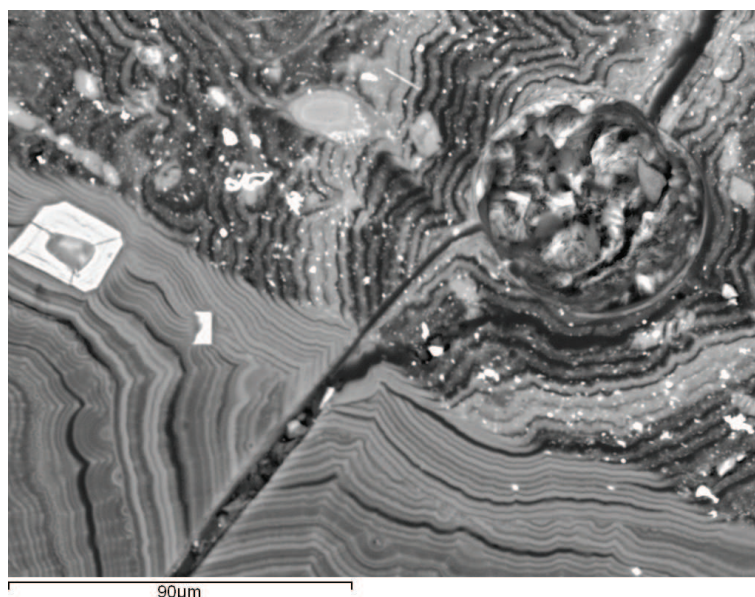


Figure 78: Altered glass 1930.52.1e inlay and body glass

However, examples were also noted where a single object, of the same type of glass, had weathered differently in different areas. For example, 1930.66.90g is a large translucent blue cylindrical bead around 20mm in diameter and originally around 50mm in length. This bead was sampled to reveal the entire cross section which was analysed by SEM-WDS and imaged and mapped on SEM-EDS. It can clearly be seen that this bead has weathered significantly more on one side than on the other with glass still remaining in a small area on a single side. In these larger beads the reaction appears to be two-fronted proceeding both from the surface and from the central hole of the bead, Figure 79. This example could indicate that different environmental conditions were present on different sides of the beads, millimetres apart; this could be due to the object being in contact with another object or in an area where the soil conditions were more varied due to burning or the decomposition of organic materials from the destruction layer. Within

the temple there were many thousands of beads and it is probable that many were in close contact with one another. A photograph from the excavation suggests that this may well have been the case, Figure 80 and again highlights the significance of burial environmental conditions in the alteration of these glasses.

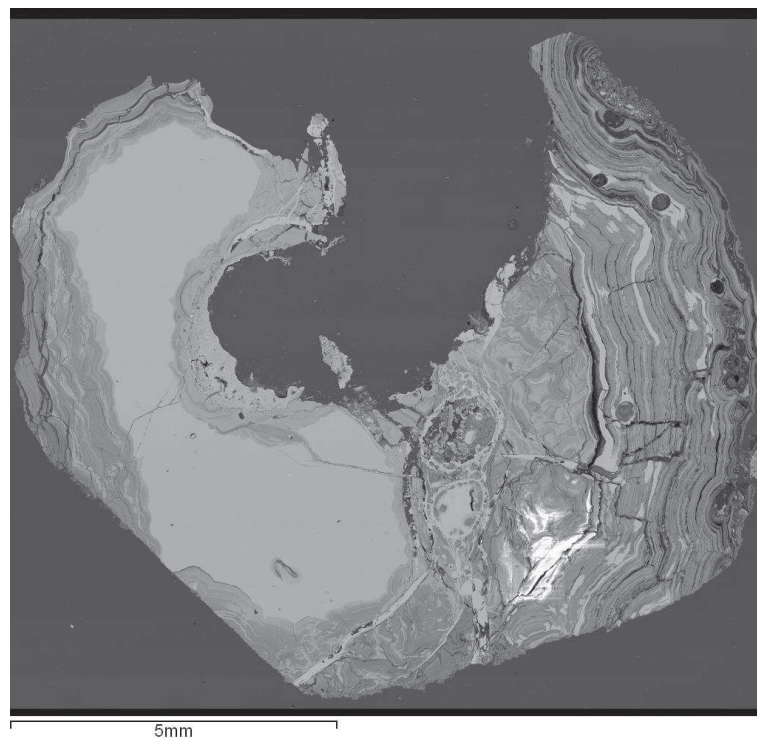


Figure 79: Bead 1930.66.90g, significantly more altered on one side than the other



Figure 80: Excavation photograph, showing beads very close together

Opacifiers: Leading on from the observed difference in behaviour of the opacified glasses a difference was noted between the calcium antimonate opacified glasses and those containing lead antimonate. Lead antimonate had a tendency to cluster within the secondary layers, occasionally apparently moving between individual layers (Figure 81a). However, calcium antimonate did not appear to move within the secondary

layers with its distribution apparently unchanged between the original glass and secondary layers (Figure 81b). This suggests that the opacifiers have different degrees of mobility within the secondary phases, perhaps connected to how the crystals are bonded, or not, to the silica network of the original glass.

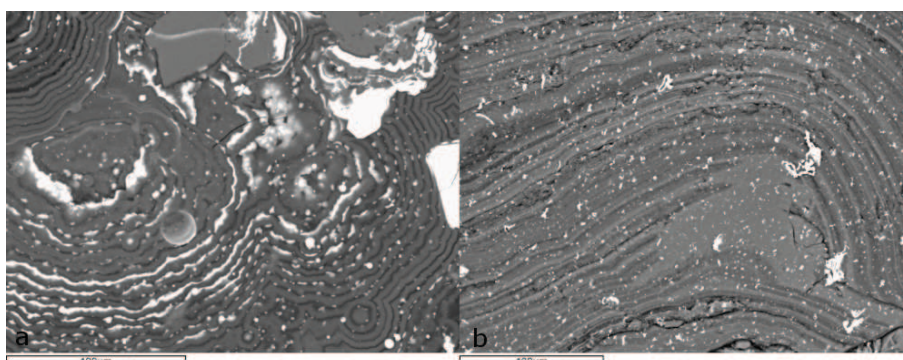


Figure 81: a. lead antimonate in alteration layers (1930.62.81); b. calcium antimonate in alteration layers (1930.66.90b)

Possible explanations: The complexities of mineral precipitation from solution as a result of silicate mineral weathering has been highlighted by Fritz and Noguera (2009:371) who note that saturated solution composition is not fixed but is derived from its parent minerals; that the secondary minerals formed also vary in their composition and that it is an open system with the possibility of the movement of elements within the solution. Once saturation within the aqueous solution has been reached it is thermodynamically possible for precipitation to take place, small nuclei form which can then cluster into 'embryos' of the secondary minerals, at this stage they can still dissociate back into solution, with variations in the clustering and dissociation of nucleated material being closely related to energy changes within the reactions taking place; however, eventually a steady state of nucleation is achieved and the secondary mineral layers form (Fritz and Noguera, 2009: 374). Therefore the reactions that created the secondary alteration phases result from energy changes, dependent on the composition of the glass and the burial environment, affecting the composition of the secondary layers and also on the movement of elements in solution within the burial environment. The complexity of the reactions required to create these secondary layers is the most probable explanation for the variation seen in the composition and morphology of the secondary layers seen in the Nuzi glasses.

Variation in burial environment across the site is more difficult to assess due to the lack of soil samples, such samples were not taken routinely at the time of excavation of this site and it was not possible to collect samples at the present time. However, some data on the soil composition was obtained through analysis of various objects of unfired clay from the site, such as the mudbricks used in the architecture of the city. A number of these were analysed by solution ICP-AES, alongside a number of fired ceramics, as part of a project looking at the provenance of the ceramic assemblage (Erb-Satullo et al, in preparation). It was found that the clay samples contained magnesium, potassium, iron, and manganese in addition to

aluminium and silicon (Table 5). There appeared to be little variation observed between the mudbricks and other clay objects analysed, suggesting that soils do not vary to a great degree in this region. Another possible factor is the depth of burial with this ranging from over 10 metres below the surface in the case of objects from the well in G50 to just over a metre for objects from parts of the northeastern residential area. A floor level was recorded for many rooms in the city on Plan 13 of Stratum II (Starr, 1937) with the objects from that room considered to have come from at, or close to, that level. However, few vitreous objects are noted to have come from this shallowly buried region of the city and very few could be found within the assemblage. It was noted that all of the objects analysed from this region are devitrified but it cannot be ruled out that better preserved items were found there which are either not in the Harvard assemblage or did not retain their original location information. In addition a small group of objects from the G50 well (1930.82.62) contains glasses with a range of preservation states from groups 2 to 6. There are also potential variables within the original burial environment which it is impossible to assess but are suggested by some of the results such as compression and stress from burial, hinted at by the 'compressed' appearance of some alteration layers and the presence of many cracks and 'fault lines' in a number of samples, Figure 43. Such stresses can have an effect on the alteration of glasses with external stress being a factor that can speed up breakdown of the silicate network (Bunker 1994).

8.3.2 Differences between LBA and Late period glasses

The Late glasses showed somewhat different weathering patterns to the 2nd millennium BC examples. They are generally in a better state of preservation with a thin weathering crust extending only a short distance into the body of the glass. The weathering crusts observed in the Late period Nuzi glasses are very similar to those noted in (Gulmini et al 2009) looking at Sassanian glasses from central Iraq, although, as noted in the LBA glasses, there are few examples of manganese- and iron-rich areas within the crust of the Nuzi glasses, presumably related to the concentration of these elements within the soil profile, compared to further south in Iraq. Another difference noted is the 'saw-tooth' reaction front at the interface between the weathering crust and the pristine glass, Figure 61. This echoes the 'stepped' dissolution with etch pits caused by weak points of the surface of silicate minerals during weathering noted by Taylor and Eggleton (2001:148) suggesting that the reaction is targeting weaknesses at the glass/water interface, although this does not explain the regularity of their profile. The late glasses are a compositionally distinct group from the Nuzi glasses (Table 21, Section 5.3) and this coupled with their much shorter burial period is the most probable reason for their differences compared to the LBA glasses.

8.3.3 Comparison with glazed ceramics

The main difference noted between the weathering of the glasses and the glaze layer of the glazed ceramics was the scale and appearance of the lamellar features of the glazes. These layers appeared smaller and 'softer' at the edges than those seen in the glasses (Figure 60). It is not absolutely clear what is causing these differences but they suggest that the process by which the lamellae are created does not switch between the creation of each layer type as swiftly or completely in the glazes as it does in the glasses, which could create a softer appearance. It is also possible that the effects of any interaction layer and ceramic body in close proximity to the glaze could have affected how the glass phase has weathered by adding different elements to the attacking solution, altering the local burial environment.

8.3.4 XRD results

The XRD results of the secondary alteration layers of the Nuzi samples have shown that many of these crusts consist of amorphous material to a greater or lesser extent. Previous work has indicated that these crusts are generally poorly crystalline usually consisting of clay minerals (Cox and Ford 1989; Curti et al 2006). However, identification of these minerals is usually difficult and some studies have not found any crystalline material in the weathering crusts, for example, Gulmini et al's (2009) study on Sasanian glasses. No clay minerals were identified in the analyses carried out in this project, however, the hydrated silicate found in ten samples has been found in a number of other studies (Ziemath 1998; Salviulo et al 2005). The quartz noted in eight samples may well be remnant material from the glass batch, large remnant quartz grains were noted in the SEM images and silicon map of sample 1930.82.59 discussed in Section 6.1, Figure 48, or the quartz may be reprecipitation from solution, as this can occur even at lower temperatures (Brehm et al 2005). Calcium-rich material infiltrating along cracks in the glass and weathering crust was also noted in a number of the samples imaged using SEM and the calcite identified in the XRD analysis of nine samples may be coming from this. Calcium antimonate was deliberately used to opacify blue glasses and inlays of white glass were found in a number of the samples analysed using other techniques. Other inclusions formed by high temperature processes were also noted in a number of the samples analysed by SEM. These were thought to be diopsides, however, the XRD analysis has suggested that some of these inclusions may be augites instead. Augite and diopside are closely related, they are both pyroxenes, have similar chemical composition, are formed at similar temperatures, and have relatively similar crystal habits. For example, 1930.82.70 was noted to have augite inclusions on XRD, however, SEM images of several fragments of this sample showed square cross section crystals which appeared to be diopsides on spectral analysis (Figure 53a, Section 6.1).

The presence of possible crystallised organic acids, however, is extremely interesting. Several studies have examined the effects of microbial action and organic acids on mineral weathering and the role of

microorganisms on the weathering of glasses has also been examined (Krumbein 1993; Brehm et al 2005), although most previous studies have been concerned with the atmospheric weathering of stained glass windows. The detrimental effects of organic acids in vapour form on glasses in museum collections has also been studied (Robinet et al 2006). The presence of organic acids in the alteration layers of the glasses from Nuzi suggest that these acids were in the soil at the point that these crusts were formed and may have had an effect on the dissolution and reprecipitation process. Particularly as the soil at Nuzi may well have contained a large organic fraction from the mudbricks used to build the houses; the remains of which form the soil the glasses were buried in. It is also possible that these acids are a result of contact with organic acids during the storage of these materials post-excavation. However, detailed analysis of the effects of such acids on the preservation and weathering of these glasses was beyond the scope of this project, it is noted as being of potential importance in the behaviour of buried glasses and future work is recommended.

8.4 Experimental results

8.4.1 Dissolution experiments

The results of the experiments carried out to look at the weathering and dissolution of replica Bronze Age composition glasses have indicated that dissolution can occur over very short timescales at elevated temperatures and that creation of stepped profiles and hydrated layers may occur again at short timescales at a lower temperature. The ICP-AES results have shown that silicon was released from the glass network during the dissolution experiments at a rate which appears to be related to the surface area and mass of the original monolith. Silicon-release from the glass network is considered by several authors to be the rate-limiting step of glass dissolution (Oelkers 2001; Grambow 2006) as once the network is broken down the glass no longer exists in its original form and is no longer structurally a glass. The dissolution experiments were carried out to determine a basic dissolution rate, not affected by environmental variables, for glass of Late Bronze Age composition; and to compare a simplified replica composition to some actual archaeological glasses. The initial stage of this was to calculate the normalised elemental mass loss for the silicon released into solution by these experiments. this was done by applying equation 4, from Jégou et al (2000).

$$NL_i = 10^{-2} \frac{C_i}{X_i \frac{S}{V}} \text{ (Equation 5)}$$

Where NL_i equals normalised elemental mass loss ($\text{g}\cdot\text{m}^{-2}$), C_i equals concentration of element in solution (mg/l), X_i equals the mass fraction of the element in the glass, S/V equals surface area to volume ratio of the glass (cm^{-1}). These ranged from 4.34×10^{-4} to 3.36×10^{-3} (Table 32). For both the 7-day and 28-day experiments the values are in good agreement to one another, despite their different initial sizes and surface

| Sample | Surface area | Volume | SA/V | NL _i | g/m-2 per s-1 (90) | g/m-2 per s-1 (20) | Rate per year |
|---------|--------------|--------|------|-----------------|--------------------|--------------------|---------------|
| 7_90_1 | 76.7 | 49.2 | 1.56 | 4.34(10-4) | 7.18(10-10) | 2.87(10-13) | 9.06(10-6) |
| 7_90_2 | 80.5 | 53.3 | 1.51 | 5.13(10-4) | 8.48(10-10) | 3.39(10-13) | 1.07(10-5) |
| 7_90_3 | 93.6 | 65.1 | 1.44 | 4.93(10-4) | 8.15(10-10) | 3.26(10-13) | 1.03(10-5) |
| 7_90_4 | 83.3 | 56.3 | 1.48 | 1.16(10-3) | 1.91(10-9) | 7.64(10-13) | 2.41(10-5) |
| 7_90_5 | 79.6 | 52.3 | 1.52 | 4.88(10-4) | 8.06(10-10) | 3.22(10-13) | 1.01(10-5) |
| 7_90_6 | 92.0 | 63.5 | 1.45 | 4.89(10-4) | 8.08(10-10) | 3.23(10-13) | 1.02(10-5) |
| 28_90_1 | 89.6 | 61.8 | 1.45 | 2.29(10-3) | 9.46(10-10) | 3.78(10-13) | 1.19(10-5) |
| 28_90_2 | 92.9 | 65.2 | 1.42 | 3.36(10-3) | 1.39(10-9) | 5.56(10-13) | 1.75(10-5) |
| 28_90_3 | 103.4 | 76.0 | 1.36 | 2.13(10-3) | 8.80(10-10) | 3.52(10-13) | 1.11(10-5) |

Table 32: Normalised elemental mass loss and dissolution rates of replica glasses

areas. The only exception to this is the replica glass 7_90_4 which had a normalised elemental mass loss of 1.16×10^{-3} , more than twice as high as the other replica glasses in the 7-day experiment, the reason for this is unclear as this monolith was no different than the others in terms of its size and shape. It is possible that it had an invisible crack or other surface damage which advanced the dissolution of this monolith compared to the others.

The masses lost were then used to calculate a rate per second which could then be applied across longer timescales. The next stage was then to look at the temperature of the reaction and the Arrhenius equation was applied to work out the reaction sites available at 20°C compared to 90°C as the Nuzi glasses were not buried in temperatures as high as 90 degrees. It had previously been noted that most oxides in glasses follow Arrhenius kinetics for their reaction rates (Ojovan et al 2006).

$$k = A_e^{-\frac{E_A}{RT}} \text{ (Equation 6)}$$

Where k equals the sites available for reaction, e is the exponential, E_A is the activation energy in j/mol, R is the gas constant and T is the temperature in Kelvin. The activation energy is that required to break the silica-oxygen bonds by hydrolysis reactions in water and has been calculated as being 23.6kcal/mol (98742 j/mol) (Ref). Applying the Arrhenius equation at 90°C (363K) and 20°C (293K) gave results of 6.177×10^{-15} at 363K and 2.489×10^{-18} at 293K. The next problem was to relate this to the reaction rates previously calculated and to find out what they would be at the lower temperature. It was calculated that the available reaction sites at 293K represented 0.04% of those available at 363K, suggesting that the reactions at the lower temperature would only be significantly slower. This percentage was then used to calculate the reaction rates at 293K. If this reaction rate is then expanded over a longer period then it would take over 10,000 years for these monoliths to completely dissolve in water at 20°C.

It was hoped then to extend these rates into the archaeological glasses, however, assessing the SA/V ration for the archaeological glasses was difficult as they did not have a regular shape to calculate their volume from. Therefore it was decided to use an alternative normalised mass loss equation to look the overall mass lost: m_i = total leached mass of compound in g; f_i = fraction of element in glass composition; S = surface

| Sample | Loss (g) | rate (g/m ² per s-1) 90 | rate (g/m ² per s-1) 20 | rate per year (g/m ²) |
|---------|----------|------------------------------------|------------------------------------|-----------------------------------|
| 28_90_1 | 0.003 | 1.37(10 ⁻¹⁰) | 5.48(10 ⁻¹⁴) | 1.73(10 ⁻⁶) |
| 28_90_2 | 0.004 | 1.84(10 ⁻¹⁰) | 7.36(10 ⁻¹⁴) | 2.32(10 ⁻⁶) |
| 28_90_3 | 0.004 | 1.65(10 ⁻¹⁰) | 6.60(10 ⁻¹⁴) | 2.06(10 ⁻⁶) |
| 28_90_4 | 0.005 | 1.48(10 ⁻¹⁰) | 5.92(10 ⁻¹⁴) | 1.87(10 ⁻⁶) |
| 28_90_5 | 0.030 | 8.27(10 ⁻¹⁰) | 3.31(10 ⁻¹³) | 1.04(10 ⁻⁵) |
| 28_90_6 | 0.007 | 2.22(10 ⁻¹⁰) | 8.89(10 ⁻¹⁴) | 2.81(10 ⁻⁶) |

Table 33: Comparison of normalised mass loss into solution from archaeological and replica glasses

area in m² (Ojovan et al 2006). The normalised mass loss for the archaeological and replica glasses in the 28-day experiments converted into a rate per second. The correction for temperature was performed again and then a rate per year calculated. Again this rate suggested that it would take around many thousands of years for the replica monoliths to dissolve.

$$NL = \frac{m_i}{f_i S} \text{ (Equation 7)}$$

Two of the archaeological glasses have a higher dissolution rate than the replica glasses, although this is less marked in the translucent blue glass, however, archaeological sample 28_90_4 had a dissolution rate very close to the replica glasses. The only opaque blue glass studied in this experiment (28_90_5, 1930.66.90b) had a much higher dissolution rate than any of the other glasses studied, despite not being significantly larger or having a larger surface area than the other archaeological glasses. Similarly to 7_90_5, the replica glass with a much higher rate, this could be due to unseen cracks or other surface effects. The high rate for this glass was particularly surprising as this glass would be expected to be more durable than the translucent glasses, having significantly lower alkali and higher lime (Table 12). The only main difference is the presence of antimony oxide and calcium antimonate crystals, which sit outside the glass network and appear unaffected by glass alteration (see Sb map in Figure 48). It is possible that antimony may have an effect on the glass network, facilitating dissolution reactions; or the presence of the calcium antimonate crystals could potentially be affecting the porosity of the glass network, again encouraging the movement of water and speeding up dissolution. Further work on the durability of different colours and compositions of Late Bronze Age glasses would be extremely interesting, particularly as differences in the secondary alteration layers formed by the opaque glasses compared to the translucent glasses have already been noted (Figure 78).

The durability of the archaeological and replica glasses was also assessed using the free energy of hydration model outlined by Jantzen (1992a). To calculate the free energy of hydration of the replica glass the moles of each oxide considered to create non-bridging oxygens was added together with those oxides which create bridging oxygens (aluminium and iron) subtracted; only the translucent blue glass was used for this as the replica glass was also translucent blue.

$$NBOs = 2(CaO + MgO + Na_2O + K_2O + CuO) - (Al_2O_3 + Fe_2O_3) / \text{oxide mole sum} \text{ (Equation 8)}$$

The free energy of hydration was calculated by the regression of ΔG_{hyd} against NBO, verified experimentally by Jantzen (1984;1992a).

$$\Delta G_{hyd} = -19.23 \text{ NBO} + 4.77$$

This indicated that the LBA glass had a free energy of hydration of -7.80 and the replica glass -7.67; this is similar to other archaeological glasses in terms of their durability, according to this model with the Nuzi glasses being less durable than Roman glasses (around -1) and more durable than some medieval glasses (-10 to -12) (Jantzen, 1992a). It is interesting, however, that they are so close given the compositional differences between the archaeological and replica glasses and the slight difference in dissolution rates observed above.

8.4.2 Secondary alteration layers

The experiments which were set up to try and create secondary precipitated layers were for the most part unsuccessful both for the experiments within a clay-rich environment and for the phase vapour hydration experiments. This may have been for several reasons: it is possible that not enough time elapsed during the experiments for these layers to form; in the case of the clay-rich solution the environment at the glass/solution interface may have been at too high a pH for layers to form or the temperature may have favoured network breakdown rather than reprecipitation of secondary layers. The most probable solution is that the experiments were carried out for insufficient time periods to allow secondary layers to form as pH levels were checked in the clay solutions at the start and end of the experiments and at both points were not high enough to trigger dominant network dissolution, the exception being the 84 day experiment which, despite the pH readings being below 9 had signs of congruent dissolution and attacks along cracks and weak points at the glass surface, Figure 67. In addition the phase vapour hydration tests were carried out with no solution in contact with the glass surface to try to discourage congruent dissolution and encourage the growth of secondary layers, secondary phases were only noted in the 84 day sample, suggesting that longer timescales are required to produce these phases in this type of experiment (Figure 65).

However, some early stages of glass weathering were noted within the experimental samples, including the formation of what appeared to be a hydrated layer in a room temperature experiment; some possible beginnings of secondary layers and the uneven 'attack' front; noted as being an early stage of mineral weathering (Taylor and Eggleton 2001:148). The hydrated layer seen in RT 28 has already been discussed in Section 8.3. Samples 60 56, RT 56 and RT 84 did show some possible secondary crystals forming at the glass surface, unfortunately it was not possible to analyse these features as they were too small and at the edge of the sample (Figure 64).

8.4.3 Antimonate glasses

A significant finding of the experimental replications carried out was that a higher temperature than had been anticipated was required to produce a good quality white glass in a single stage. At the lower temperature (1050 °C) a highly vesicular 'frothy' glass was produced (Figure 68). This is almost certainly due to the intrinsic properties of antimony oxides, which are utilised extensively as fining agents in modern commercial glassmaking. Antimony oxide releases large amounts of gas during the melt creating large air bubbles which in the fining process rise to the top of the melt and are released, degassing the glass (Shelby 2005:43). The high viscosity of the ancient glass compositions used in these experiments, however, makes it more difficult for this gas to escape; an increased amount of antimony is present within the ancient composition as well which would increase the gas present within the glass. The replicates produced from cullet and additional antimony had a distinctive microstructure which did not resemble any of the ancient samples (Figure 70e and f) suggesting that this method was not used to produce the opacified glasses from Nuzi.

Rehren (2000) has suggested that an increase in temperature can significantly increase the amount of lime available within a glass melt at the expense of the sodium oxide so this could explain the compositional difference seen between the translucent and opacified glasses from Nuzi. This increased firing temperature could also have increased any contamination of the glass, from a calcium-rich parting layer in the crucibles used. An increase of around 100-150 °C could potentially cause more lime to be dissolved into the glass melt from the parting layer, depending on the size of the crucible and volume of the glass batch (Rehren 2008). In addition the turquoise colour of the glasses compared to the bluer translucent glasses could also suggest that the melting temperature for the opaque glasses is higher; Weyl (1955:167) suggests that higher temperatures favour the creation of greener colours from the Cu^{2+} transition metal colorant used to create blue colours, whereas lower temperatures create a bluer colour in the glass and this difference is visible in the translucent and opaque blue glasses from Nuzi (Figure 22).

8.5 Summary

The work carried out during this project has produced a wide of range of information regarding the vitreous materials from Nuzi. The survey of the assemblage allowed careful and representative sampling of the material, the assignment of locations for as many objects as possible, information about the distribution and possible perceptions of glass in the LBA city; and where later material may have intruded into the 2nd millennium BC contexts. In addition this work formed the basis of looking at variability in the preservation of the vitreous materials, without this it would have been impossible to look at differences between objects from different parts of the site. The compositional analysis and identification of materials allowed the

technology of the vitreous materials to be examined, with strong indications of a technological difference between the opaque and translucent blue glasses being found; and objects made from non-vitreous materials to be excluded; the provenance of the glass was also studied with some colours appearing to be from different production sources. The bulk compositional analysis was also related to the preservation study in that it provided information about the original composition of the glasses which again could be used to look at variability in preservation. The detailed characterisation of the weathering products of the glasses provided considerable information about their composition and morphology. The devitrified glasses were also studied in detail and some differences were found between objects where glass remained and those which were completely devitrified. No link could be found between an object's state of preservation and its original location could be found, however, indications of localised variation in burial environment were found in some examples. Some differences between colours of glass were noted; although there appeared to be little difference between types of objects that could not be ascribed to overall size. The mineralogy of the weathering crusts was also examined with a number of crystalline phases being found including hydrated silicates and calcite. The experiments carried out to look at the dissolution and precipitation of secondary phases in replica LBA composition glasses indicated that early stages of weathering can be recreated within a short-term experiment; however, they were of limited use in recreating the secondary phases so prevalent in the Nuzi glasses. The recreation of the opaque antimonate glasses shed further light on technical aspects of producing these glasses which may have created a different production technology in comparison to the more common translucent glasses.

9 Conclusions and Future work

9.1 Conclusions

9.1.1 Distribution

The main conclusions from this project are that the vitreous materials from Nuzi have provided a great deal of information about the distribution, composition, technology, and preservation of these materials from this site from an early stage in the widespread use of glass. The survey of the museum assemblage and finds notebooks allowed the distribution of vitreous materials at this site to be studied. Vitreous materials at Nuzi are concentrated in religious and high-status areas across the city suggesting that these materials not only have a high perceived value but are also closely linked to religious practice, in particular the worship of Ishtar. This is particularly true for the glazed ceramics, the majority of which are from either the northwestern temple complex or from rooms which were thought to be associated with religion or some kind of ritual practice. Some differences were noted between the vitreous materials at Nuzi and at other

contemporary sites, including the use of beads and glazed wall nails as architectural elements within the Ishtar temple and the presence of glazed ceramic figurines, which are not recorded from the other sites. The work on the museum assemblage and excavation archive also indicated that there had been significant intrusion in Stratum II, the Late Bronze Age layers, from Later periods in many areas and that there were some later examples of glass and glazed ceramics mixed in with the earlier material. The areas most likely to have been affected were highlighted and this information was used in the later phases of the project, with some samples being removed or examined in a different part of the project.

The composition and technology of the vitreous materials was also examined in some detail. The bulk compositional information gained from the SEM-WDS analyses provided detailed information about the composition of both the LBA and Late period glasses studied. These analyses have shown that the Late period glasses contain higher levels of aluminium and titanium oxides than the Late Bronze Age examples, although there is some overlap. The LBA glasses are all plant ash based soda-lime-silicates with a variety of colorants and opacifiers. Translucent blue coloured by copper is the most common colour with opaque turquoise, opacified with calcium antimonate, also being relatively common. Yellow glasses are rare apart from decorative inlays which are more frequent, and only single example of unaltered white glass was found. Several colorant-free glasses were found in the analyses, including a very rare colorant-free glass vessel and a unique colorant-free sun-disk pendant fragment. In general the analyses fit well with previous studies of similar material from the Near East. Although the Nuzi material differs from contemporary Egyptian glasses in terms of the colour range with cobalt blue, manganese purple and black and cuprite red glasses all being absent from the Nuzi assemblage. One major finding of the bulk compositional analyses was a difference in composition between translucent and opaque blue glasses with the opaque glasses being significantly higher in lime and lower in soda than the translucent blues, despite their trace elemental and isotopic compositions suggesting that they were made from very similar raw materials. Experimental work on the manufacture of antimonate glasses carried out as part of this study indicated that a higher temperature (1150°C) is required to produce antimonate glasses in a single step, without the glass becoming highly vesicular and boiling over the top of the crucible. XRD analysis of the opaque glasses also found the higher temperature form of calcium antimonate in several samples and this in addition to the greener colour of the opaque glasses suggests that the opaque glasses may have been manufactured at a higher temperature than the translucent blue glasses, although considerably more work would be required to verify this.

The trace elemental analysis indicated that almost all of the blue and turquoise Nuzi glasses plot with the Near Eastern trace elemental group, along with the yellow glasses analysed in this study. A single green glass appears to be an Egyptian import and the white, yellow and some of the colorant-free glasses do not plot with either the Egyptian or current Near Eastern group, which could suggest a number of manufacturing sites, or the use of different raw materials; in the case of the colorant-free glasses the

differences could be related to the technology required to produce this colour, which involved the use of reducing agent such as carbon.

Extensive SEM imaging provided identification of ambiguous materials, particularly in the more weathered samples, finding Egyptian blue and faience beads and vessels and even two bone beads. SEM images also allowed the identification of colorants in completely altered glasses and glazes, including a few white-glazed ceramics, containing calcium antimonate as an opacifier, which have not been reported from any other contemporary sites in the region. The single cylinder seal analysed was found to be made from a vitreous material, although its exact nature could not be established due to its state of preservation.

The characterisation of the alteration layers of the glasses and the devitrified glasses and glazes provided a great deal of information about the composition and morphology of these phases. In both the samples where glass remained and completely devitrified examples the secondary alteration layers were found to be predominantly amorphous silica with low analytical totals suggesting significant hydration of these materials. A number of the devitrified glasses also had increased levels of aluminium and potash in the secondary phases, which were thought to have become fixed from the burial environment during the precipitation of these phases. Many of the examples where glass remained had high levels of magnesia in the secondary layers, well above the levels in the original glass, based on the compositional maps, these appeared to be substituting for silica in some regions of the layers suggesting that the magnesia from the glass, alongside a contribution from the burial environment, was becoming incorporated into the secondary phases due to local environmental conditions at particular periods during the burial of these objects. Uniquely, very high levels of copper oxide were noted in several altered translucent blue glass samples, up to 10 times higher than in the original glass, where that could be measured. This was thought to suggest that copper is much less mobile than many of the other elements in the glasses, becoming fixed into the secondary phases rather than diffusing into the surrounding soils. This was supported by the dissolution experiments where no copper was found in the ICP analyses of the solutions even after 28 days at a high temperature and despite very low detection limits for this element in the analysis used.

The morphologies of the secondary alteration layers and devitrified glasses showed a very wide range of structures, degrees of organisation, directions of the reaction front and scale of the layers produced. Some differences were noted between the samples with glass remaining and those that were devitrified. In general the alteration layers appeared to be at a smaller scale in the devitrified glasses, with more samples having lamellae and layers at a sub-micron scale. The devitrified glasses also did not appear to have the compositional differences, within the same sample, seen in the examples with glass remaining. Some differences were also seen between different colours of glass with the translucent and opaque glasses producing secondary phases with different textures. This was particularly apparent in samples where inlays of opaque glass and bodies of translucent glass in the same object could be compared; the translucent

glasses tended to produce more organised, 'smoother' layers than the opaque glasses.

The X-ray diffraction analyses indicated that the majority of the secondary alteration layers had a high amorphous component, based on the high backgrounds seen on the diffraction patterns obtained. However, several secondary mineral phases were found including a hydrated silicate and secondary quartz. The other mineral phases found were from infiltration in the case of calcite and from high temperature processes in the case of pyroxene inclusions. The only other crystalline phases found were the deliberately added opacifiers, such as calcium antimonate. There was also the possibility that there may be an organic acid crystallised into the alteration layers, however, this could not be verified and considerable further work would be required.

One major finding of the study was that there appeared to be no correlation between the location on site and the degree of preservation, with a number of groups of objects recorded as being from the same location having widely varying states of preservation, even where the original glass (when it could be analysed) appeared to have a very similar composition. This could indicate that the burial environment also varies across the site, despite most of the glass being buried at a similar level within the mound and the relatively small size of the city (around 200m²). This variation in preservation could even be seen within single objects with several beads showing significantly more alteration on one side than the other. Previous work on silicate minerals has suggested that relatively small changes in the activation energies of solutions in open systems can significantly affect the precipitation of secondary phases and it is possible that this is what is happening at Nuzi with minor variations in the burial environment affecting the reactions that govern the alteration of glass. This highlights one of the problems with using archaeological glasses as analogues for the long-term disposal of nuclear waste, which are generally deposited in as close to a closed system as possible. However, it does indicate that the burial environment is as important, or even more important than composition in the alteration of similar glass types.

The glazed ceramics and other vitreous materials were found to alter in a very similar way to the glasses, with complex morphologies of secondary alteration layers and lamellar features being found in many examples. However, the alteration layers appeared to be at a smaller scale and had softer edges than was seen in most of the glasses, the exact reasons for this are unclear.

A number of experiments were carried out to compare the dissolution rates (i.e. the breaking of the silica-oxygen bonds in the glass network) for replica and archaeological glasses. It was found that the dissolution rates could be compared between glasses of the same colour, despite the slight compositional differences between the replica and archaeological glasses. However, the opaque turquoise glass behaved differently, appearing to react more quickly and release more silica into solution than the translucent blue glasses. This was unexpected based on the compositions of this glass, the opaque blue glass being higher in lime and lower in alkalis than the translucent glasses and would be expected to be more durable. However, it

is possible that the presence of an opacifier, calcium antimonate in this case, could be affecting the glass network, such as its porosity, thus speeding up the network-breaking reactions within the glass. These rates were extrapolated to a lower temperature and across wider timescales and suggested that it would take several thousand years for the small monoliths used to completely dissolve, this seems plausible based on the scale and preservation of many examples of surviving glass objects from Nuzi. However, considerably further modelling work would be required to verify these data.

A number of experiments were carried out to try and reproduce the secondary alteration layers seen in almost all of the Nuzi glasses, the exceptions being the best preserved examples. These experiments were largely unsuccessful with only the very earliest stages of glass alteration being produced with some possible secondary phases in a few examples. One of the main problems with these experiments was the the dominant mechanism of alteration appeared to change, despite measures to address being taken. In the room temperature and the shorter-term experiments at 60°C, hydration and ion exchange appeared to be the dominant mechanism with only limited network dissolution. However, in the longer-term 60°C, which was only 84 days, the mechanism switched to network dissolution between 56 and 84 days, despite the pH being checked and the temperature remaining constant. This work highlighted the difficulties of reproducing long-term behaviours in the laboratory over short timescales and it is possible that longer-term experiments could produce more usable results.

The work on the alteration of the Nuzi glasses and the experiments on glasses of a similar composition have suggested that, although simplified composition replica glasses can be good analogues for archaeological examples, and reasonable theoretical dissolution rates can be obtained from experiments, there are significant limitations in modelling the alteration of glasses in an open system. The Nuzi glasses show an incredible variety in the morphology and composition of the secondary alteration layers and minor variations in the burial environment across very small regions appears to be the most likely reason for this variation. This is extremely difficult to recreate in a laboratory experiment, particularly in the case of Nuzi where there are some unknown variables in the burial environment. There is also the difficulty of making sure that the mechanism of alteration remains constant throughout the experiment, as was found in the experiments looking at secondary phases.

The use of archaeological glasses as analogues for long-term disposal of nuclear waste glasses has been extensively discussed in the literature and despite the differences in composition natural and archaeological glasses remain the only way to examine very long-term processes in a natural burial environment, particularly regarding the potential problems of accelerated tests noted above. This study has indicated that the burial environment is as important as glass composition in the alteration of glasses. Suggesting that differences in composition between nuclear waste glasses and archaeological glasses may be less significant than the difference between the open systems of archaeological burial environments and the closed, more controlled,

burial environments of nuclear waste glasses. The use of data from archaeological glasses in studies looking at the long-term effects of burial of nuclear waste glasses therefore has to be carefully applied.

9.2 Future work

A number of areas for further study were highlighted in this study including the need for more work on distinguishing between Late Bronze Age and later period plant ash glasses, as some overlap was noted within this project. The trace element and isotopic composition of the Late glasses would be very interesting to establish as it could give an indication of local production or imported glasses and how they related to the earlier examples.

In terms of the compositional differences between opaque and translucent glasses further work on the effects of a parting layer would be required to look at this in more detail. In addition further experiments using a wider range of melting temperatures and timings would be useful to establish possible reasons for the difference observed. Quantifying the effects of temperature and composition on the copper colorant in Late Bronze Age glasses would also be beneficial. A range of trace element compositions were noted in the opaque turquoise, and other colour, glasses from Nuzi and further research on further samples would be useful.

The studies of the alteration of the Nuzi glasses indicated that this is a highly complex and variable process. A great deal of potential experimental work has been indicated by the current study including looking at the behaviour of oxides such as aluminium, potash, magnesia and copper both in the glass and in the burial environment solution in the composition of secondary alteration layers. For example, do magnesia-rich secondary layers require magnesia in the glass, in solution or both? However, as already noted producing the secondary layers can be problematic and much longer-term experiments, particularly simulating the burial environment would be required. Another aspect highlighted by this study is the behaviour of opacified glasses. They appeared to have slightly different secondary alteration layers to the other colours of glasses and the opaque turquoise glass had a faster dissolution rate than the translucent blue glasses. Further experiments on all colours of glass would be useful to see if this is always the case, or if the opaque glass in this study was unusual in some way.

10 References

- Aagard P and Helgeson H. 1982. Thermodynamic and kinetic constraints on reaction rates among minerals and aqueous solutions. I. Theoretical considerations. *American Journal of Science* 282: 237-285.
- Akkermans PMMG and Schwartz GM. 2003. *The archaeology of Syria: from complex hunter-gatherers to early urban societies (ca. 16,000 to 300 BC)*. Cambridge:Cambridge University Press.
- Artioli G, Angelini I and Polla A. 2008. Crystals and phase transitions in protohistoric glass materials. *Phase Transitions* 81(2-3): 233-252.
- Barag D. 1970. Mesopotamian Core-formed Vessels (1500-50BC). In: *Glass and Glassmaking in Ancient Mesopotamia: An Edition of the Cuneiform Texts which contain Instructions for Glassmakers with a Catalogue of Surviving Objects*. New York: Corning Museum of Glass Press. 131-197.
- Barkoudah J and Henderson J. 2006. Plant ashes from Syria and the manufacture of a glass: ethnographic and scientific aspects. *The Journal of Glass Studies* 48: 297-321.
- Beerkens RGC. 2003. Amber chromophore formation in sulphur- and iron-containing soda-lime-silica glasses. *Glass Science and Technology* 76(4): 166-175.
- Beerkens RGC. 2003. Amber chromophore formation in sulphur- and iron-containing soda-lime-silica glasses. *Glass Science and Technology* 76(4): 166-175.
- Bergoffen C. 2005. *The Cypriot Bronze Age Pottery from Sir Leonard Woolley's Excavations at Alalakh (Tell Atchana)*. Contributions to the Chronology of the Eastern Mediterranean, Volume V. Wien: Verlag der Österreichischen Akademie der Wissenschaften.
- Bernhardsson MT. 2005. *Reclaiming a Plundered Past: Archaeology and Nation Building in Modern Iraq*. Austin:University of Texas Press.
- Bildstein O, Trotignon C, Pozo M and Jullien M. 2007. Modelling glass alteration in an altered argillaceous environment. *Journal of Nuclear Materials* 362: 493-501.
- Bimson M and Freestone IC. 1988. Some Egyptian Glass dated by Royal inscription. *Journal of Glass Studies* 30:11-15.
- Brehm U, Gorbushina A and Mottershead D. 2005. The role of microorganisms and biofilms in the breakdown of quartz and glass. *Palaeography, Palaeoclimatology, Palaeoecology* 219: 117-129.
- Brill, R.H., 1970, The Chemical interpretation of the Texts, in: Oppenheim, A.L., *Glass and Glassmaking in Ancient Mesopotamia: An Edition of the Cuneiform Texts Which Contain Instructions for Glassmakers With a Catalogue of Surviving Objects*, Corning: The Corning Museum of Glass Press, 105-124.
- Brill RH. 1999a. *Chemical analyses of early glasses, volumes 1 (Catalogues)*. Corning, New York: Corning Museum of Glass.

- Brill RH. 1999b. Chemical analyses of early glasses, volumes 2 (Tables), Corning, New York: Corning Museum of Glass.
- Bryce T. 2003. Letters of the Great Kings of the ancient Near East: The Royal Correspondence of the Late Bronze Age. Routledge: London.
- Buckwalter CQ, Pederson LR and McVay GL. 1982. The effects of surface area to solution volume ratio and surface roughness on glass leaching. *Journal of Non-Crystalline Solids* 49: 397-412.
- Bunker BC. 1994. Molecular mechanisms for corrosion of silicate and silicate glasses. *Journal of Non-Crystalline Solids* 179: 300-308.
- Buringh P. 1960. Soils and soil conditions in Iraq. Baghdad: Ministry of Agriculture.
- Butler KH, Bergin MJ, Hannaford VMB. 1950. Calcium Antimonates. *Electrochemical Society Journal* 97(4): 117-122.
- Cailleteau C, Angeli F, Devreux F, Gin S, Jestin J, Jollivet P and Spalla O. 2008. Insight into silicate-glass corrosion mechanisms. *Nature Materials* 7: 978-983.
- Carmona N, Villegas MA and Fernandez Navarro JM. 2006. Characterisation of an intermediate decay phenomenon of historical glasses. *Journal of Materials Science* 41 2339-2346.
- Chave T, Frugier P, Ayrat A and Gin S. 2007. Solid state diffusion during nuclear glass residual alteration in solution. *Journal of Nuclear Materials* 362: 466-473.
- Chiera E and Speiser EA. 1924-1925. A New Factor in the History of the Ancient East. *The Annual of the American Schools of Oriental Research* 6: 75-92.
- Cochrane et al. The infant remains from Nuzi, in preparation.
- Cox GA and Ford BA. 1989. The corrosion of glass on the sea bed. *Journal of Materials Science* 24: 3146-3153.
- Crow P. 2008. Mineral weathering in forest soils and its relevance to the preservation of the buried archaeological resource. *Journal of Archaeological Science* 35: 2262-2273.
- Cullity BD. 1978. Elements of X-ray diffraction. Second edition. Reading: Addison-Wesley.
- Curti E, Crovisier JL, Morvan G and Karpoff AM. 2006. Long-term corrosion of two nuclear waste reference glasses (MW and SON68): a kinetic and mineral alteration study. *Applied Geochemistry* 21: 1152-1168.
- Dal Bianco B, Bertonecello R, Milanese L and Barison S. 2004. Glasses on the seabed: surface study of chemical corrosion in sunken Roman glasses. *Journal of Non-Crystalline Solids* 343: 91-100.
- Dal Bianco B, Bertonecello R, Milanese L and Barison S. 2005. Glass corrosion across the Alps: A surface study of chemical corrosion of glasses found in marine and ground environments. *Archaeometry* 47(2): 351-360.

- Dean JR. 2005. Practical inductively coupled plasma spectroscopy. Chichester:Wiley.
- Degryse P, Boyce A, Erb-Satullo N, Eremin K, Kirk S, Scott R, Shortland A, Schneider J and Walton M. 2009. Isotopic discriminants between Late Bronze Age glass from Egypt and the Near East. *Archaeometry*, in press.
- De Martino S. 2004. A Tentative Chronology of the Kingdom of the Mittani from its rise to the Reign of Tušratta. In: H Hunger and R Pruzsinszky (eds) *Mesopotamian Dark Age Revisited. Proceedings of an International Conference of SCIEEM 2000 (Vienna 8th – 9th November 2002). Contributions to the Chronology of the Eastern Mediterranean Volume VI*. Vienna: Verlag der Österreichischen Akademie der Wissenschaften. 35-42.
- Domenich-Carbo M-T, Domenich-Carbo A, Osete-Cortina L and Sauri-Peris M-C. 2006. A Study on Corrosion Processes of Archaeological Glass from the Valencian Region (Spain) and its Consolidation Treatment. *Microchimica Acta* 154: 123-142.
- Doremus RH. 1994. *Glass Science*. Second edition. London: John Wiley & Sons
- Egerton RF. 2005. *Physical principles of electron microscopy: an introduction to TEM, SEM and AEM*. New York:Springer Science + business media.
- Ehrich RW. 1939. The Later Cultures at Yorgan Tepe. In: Starr RFS. 1939. *Nuzi: report on the excavations at Yorgan Tepe and Kirkuk, Iraq: conducted by Harvard University in conjunction with the American Schools of Oriental Research and the University Museum of Philadelphia, 1927-1931 Volume I Text*. Cambridge MA: Harvard University Press. 545-569.
- El-Shamy TM, Lewins J, Douglas RW. 1972. The dependence on the pH of the decomposition of glasses by aqueous solutions. *Glass Technology* 13(3): 81-87.
- El-Shamy TM. 1973. The chemical durability of K₂O-CaO-MgO-SiO₂ glasses. *Physics and chemistry of glasses* 14(1): 1-5.
- Environmental Protection Agency. 2002. *Methods for Measuring the Acute Toxicity of Effluents and Receiving Waters to Freshwater and Marine Organisms*. Fifth edition.
- Erb-Satullo N, Shortland AJ and Eremin K. A chemical and mineralogical study of Nuzi Ware and other Late Bronze Age ceramics. In preparation.
- Ernsberger FM. 1980. The role of molecular water in the diffusive transport of protons in glasses. *Physics and Chemistry of Glasses* 21(4): 146-149.
- Fearn S, McPhail DS and Oakley V. 2004. Room temperature corrosion of museum glass: an investigation using low-energy SIMS. *Applied Surface Science* 231-232: 510-514.

- Fearn S, McPhail DS, Hagenhoff B and Tallarek E. 2006. TOF-SIMS analysis of corroding museum glass. *Applied Surface Science* 252: 7136-7139.
- Feldman MH. 2006. *Diplomacy by Design: Luxury Arts and an "International Style" in the Ancient Near East, 1400-1200 BCE*. Chicago and London: University of Chicago Press.
- Ferrand K, Abdelouas A and Grambow B. 2006. Water diffusion in the simulated French nuclear waste glass SON 68 contacting silica rich solutions: Experimental and modelling. *Journal of Nuclear Materials* 355: 54-67.
- Freestone IC. 2001. Post-depositional Changes in Archaeological Ceramics and Glasses. In D Brothwell and AM Pollard (eds) *Handbook of Archaeological Sciences*. London: John Wiley and Sons Ltd. 615-625.
- Friedmann AH. 1987. Towards a relative chronology at Nuzi. In *Studies on the Civilization and Culture of Nuzi and the Hurrians*. Volume 2. General studies and excavations at Nuzi 9/1. 101-130.
- Freidman I, Trembour FW and Hughes RE. 1997. Obsidian Hydration Dating. In: RE Taylor and MJ Aitken (eds) *Chronometric dating in archaeology*. New York: Plenum. 297-322.
- Fritz B and Noguera C. 2009. Mineral Precipitation Kinetics. In: EH Oelkers and J Schott (eds) *Thermodynamics and Kinetics of water-rock interactions*. *Reviews in Mineralogy and Geochemistry*, Vol 70: 371-410.
- Frugier P, Gin S, Minet Y, Chave T, Bonin B, Godon N, Lartigue J-E, Jollivet P, Ayrat A, De Windt L and Santarini G. 2008. SON68 nuclear glass dissolution kinetics: Current state of knowledge and basis of the new GRAAL model. *Journal of Nuclear Materials* 380: 8-21.
- Gates M-HC. 1981. Alalakh Levels VI and V: A Re-examination of a mid-Second Millenium BC: A Chronological Reassessment. *Monographic Journals of the Near East. Syro-Mesopotamian Studies* 4/2.
- Gettens RG. 1939. *Chemical and Microscopic Examination of the Green Glaze Objects found at Nuzi*. In: Starr RFS. 1939. *Nuzi: report on the excavations at Yorgan Tapa and Kirkuk, Iraq: conducted by Harvard University in conjunction with the American Schools of Oriental Research and the University Museum of Philadelphia, 1927-1931 Volume I Text*. Cambridge MA: Harvard University Press. 523-525.
- Gillies KJS and Cox A. 1988. Decay of medieval stained glass at York, Canterbury and Carlisle. *Glastechnische Berichte* 61(3): 75-84.
- Gin S, Jégou C, Frugier P and Minet Y. 2008. Theoretical consideration on the application of the Aagaard-Helgeson rate law to the dissolution of silicate minerals and glasses. *Chemical Geology* 355: 14-24.
- Goldstein SM. 1979. *Pre-Roman and early Roman glass in the Corning Museum of Glass*. Corning: Corning Museum of Glass.

- Goldstein J, Newbury D, Joy D, Lyman C, Echlin P, Lifshin E, Sawyer L and Michael J. 2003. Scanning electron microscopy and X-ray microanalysis. New York:Plenum Press.
- Goodhew PJ, Humphreys J and Beanland R. 2001. Electron microscopy and analysis. London: Taylor and Francis.
- Grambow B. 1992. Geochemical Approach to Glass Dissolution. In: DE Clark and BK Zaitos (eds) Corrosion of Glass, Ceramics and Ceramic Superconductors. Noyes: William Andrew Publishing. 124-152.
- Grambow B. 2006. Nuclear Waste Glasses – How Durable? Elements 2: 357-364.
- Grambow B and Müller R. 2001. First-order dissolution rate law and the role of surface layers in glass performance assessment. Journal of Nuclear Materials 298: 112-124.
- Grambow B and Giffaut E. 2006. Coupling of Chemical Processes in the Near Field. Materials Research Society Symposium Proceedings 932: 55-66.
- Greaves GN, Gurman SJ, Catlows CRA, Chadwick AV, House-Walter S, Henderson CMB and Dobson BR. 1991. A structural basis for ionic diffusion in oxide glasses. Philosophical Magazine A 64(5): 1059-1072.
- Gulmini M, Pace M, Ivaldi G, Negro Ponzi M and Mirti P. 2009. Morphological and chemical characterization of weathering products on buried Sasanian glass from central Iraq. Journal of Non-Crystalline Solids 355: 1613-1621.
- Harbet CJ and Bateman LA. 1943. US Patent no. 2329161, Manufacture of calcium antimonate.
- Hatton GD, Shortland AJ and Tite MS. 2008. The production technology of Egyptian blue and green frits from second millennium BC Egypt and Mesopotamia. Journal of Archaeological Science in press.
- Helebrant A, Jirica A and Jirickova J. 2004. Corrosion of glass. Glass Science and Technology 77 C: 85-94.
- Hench LL and Clark DE. 1978. Physical chemistry of glass surfaces. Journal of Non-Crystalline Solids 28: 82-105.
- Henderson J. 1997. Analyses of Tell Brak glass, In: Oates, D., Oates, J., and McDonald, H. (eds), 1999, Excavations at Tell Brak: Vol I: The Mitanni and Old Babylonian Periods, Cambridge: McDonald Institute Monographs, London, British School of Archaeology in Iraq, 95-98.
- Icenhower PJ, McGrail BP, Shaw WJ, Pierce EM, Nachimutu P, Shuh DK, Rodriguez EA and Steele JL. 2008. Experimentally determined dissolution kinetics of Na-rich borosilicate glass at far from equilibrium conditions: Implications for Transition State Theory. Geochimica et Cosmochimica Acta 72: 2767-2788.
- Janssens K, Aerts A, Vincze L, Adams F, Yang C, Utui R, Malmqvist L, Jones KW, Radtke M, Garbe S, Lechtenberg F, Knochel A and Wouters H. 1996. Corrosion phenomena in electron, proton and synchrotron X-Ray microprobe analysis of Roman glass from Qumran, Jordan. Nuclear Instruments and Methods in Physics Research B 109/110: 690-695.

- Jackson CM. 2005. Glassmaking in Bronze Age Egypt. *Science* 308: 1750-1752.
- Jackson CM, Nicholson PT, Gneisinger W. 1998. Glassmaking at Tell el-Amarna: an integrated approach. *Journal of Glass Studies* 40: 11-24.
- Jantzen CM. 1992a. Nuclear Waste Glass Durability: I, Predicting Environmental Response from Thermodynamic (Pourbaix) Diagrams. *Journal of the American Ceramic Society* 75(9): 2433-2448.
- Jantzen CM. 1992b. Thermodynamic Approach to Glass Corrosion. In: DE Clark and BK Zaitos (eds) *Corrosion of Glass, Ceramics and Ceramic Superconductors*. Noyes: William Andrew Publishing.
- Jantzen CM and Plodinec MJ. 1984. Thermodynamic model of natural, medieval and nuclear waste glass durability. *Journal of Non-Crystalline Solids* 67: 207-223.
- Jantzen CM, Kaplan DI, Bibler NE, Peeler DK and Plodinec MJ. 2008. Performance of a buried radioactive high level waste (HLW) glass after 24 years. *Journal of Nuclear Materials* 378: 244-256.
- Jégou C, Gin S and Larché F. 2000. Alteration kinetics of a simplified nuclear glass in an aqueous medium: effects of solution chemistry and of protective gel properties on diminishing the alteration rate. *Journal of Nuclear Materials* 280: 216-229.
- Krumbein WE, Urzi CE and Gehrmann C. 1991. Biocorrosion and Biodeterioration of Antique and Medieval Glass. *Geomicrobiology Journal* 9: 139-160.
- Kuisma-Kursala P. 2000. Accuracy, Precision and Detection Limits of SEM-WDS, SEM-EDS and PIXE in the Multi-Elemental Analysis of Medieval Glass. *X-Ray Spectrometry* 29: 111-118.
- Kuhrt A. 1995. *The Ancient Near East c3000 -300 BC: Volume 1*. London:Routledge.
- Le Bourhis E. 2007. *Glass: Mechanics and Technology*. Weinheim:Wiley-VCH.
- Lilyquist C. 1993. Granulation and Glass: Chronological and Stylistic Investigations at Selected Sites, ca 2500-1400 B.C.E. *Bulletin of the American Schools of Oriental Studies* 290/291: 29-94.
- Lilyquist C and Brill RH. 1993. *Studies in Early Egyptian Glass*. New York: Metropolitan Museum of Art.
- Lombardo T, Chaba A, Lefevre R-A, Verita M and Geotti-Bianchini F. 2005. Weathering of float glass exposed outdoors in an urban area. *Glass Technology* 46(3): 271-276.
- McDonald H. 1997. The Beads. In: Oates, D., Oates, J., and McDonald, H. (eds), 1999, *Excavations at Tell Brak: Vol I: The Mitanni and Old Babylonian Periods*, Cambridge: McDonald Institute Monographs, London, British School of Archaeology in Iraq, 101-104.
- McLoughlin SD. 2003. *The Characterisation of Archaeological Glasses Using Advanced Analytical Techniques*. PhD Thesis, Imperial College, London.

- McLoughlin SD, Hand RJ, Hyatt NC, Lee WE, Notingher I and McPhail DS. 2006. The long-term corrosion of glasses: analytical results after 32 years of burial at Ballidon. *European Journal of Glass Science and Technology Part A Glass Technology* 47(3): 59-67.
- Macquet C and Thomassin JH. 1992. Archaeological glasses as modelling the behavior of buried nuclear waste glass. *Applied Clay Science* 7 17-31.
- Moorey PRS, 1994. *Ancient Mesopotamian Materials and Industries*. Oxford: Clarendon Press.
- Morgenstein ME, Wickert C and Barkatt A. 1999. Consideration of Hydration-rind Dating of Glass Artefacts: Alteration Morphologies and Experimental Evidence of Hydrogeochemical Soil-zone Pore Water Control. *Journal of Archaeological Science* 26: 1193-1210.
- Newton RG. 1975. The weathering of medieval window glass. *Journal of Glass Studies* 17: 161-168.
- Newton RG and Davidson S. 1996. *The conservation of glass*. Oxford: Butterworth-Heinemann.
- Nicholson PT, Jackson CM, Trott KM. 1997. The Ulu-Burun glass ingots, cylindrical vessels and Egyptian glass. *Journal of Egyptian Archaeology* 83: 143-153.
- Nicholson PT and Henderson J. 2000. Glass. In: PT Nicholson and I Sham (eds) *Ancient Egyptian Materials and Technology*. Cambridge: Cambridge University Press. 195-226.
- Oates D. 1965. The excavations at Tell al Rimah, 1964. *Iraq* 27:62-80.
- Oates D. 1966. The excavations at Tell al Rimah, 1965. *Iraq* 28: 122-139.
- Oates D. 1967. The excavations at Tell al Rimah, 1966. *Iraq* 29: 70-96.
- Oates D. 1968. The excavations at Tell al Rimah, 1967. *Iraq* 30: 115-138.
- Oates D. 1970. The excavations at Tell al Rimah, 1968. *Iraq* 32: 1-26.
- Oates D. 1972. The excavations at Tell al Rimah, 1971. *Iraq* 34: 77-86.
- Oates D, Oates J and McDonald H. 1997. *Excavations at Tell Brak: Vol I: The Mitanni and Old Bablylonian Periods*. Cambridge: McDonald Institute Monographs. London: British School of Archaeology in Iraq.
- Oelkers EH. 2001. General kinetic description of multioxide silicate mineral and glass dissolution. *Geochimica et Cosmochimica Acta* 65(21): 3703-3719.
- Ojovan MI, Pankov A and Lee WL. 2006. The ion exchange phase in corrosion of nuclear waste glasses. *Journal of Nuclear Materials* 358: 57-68.
- Ojovan MI, Hand RJ, Ojovan NV and Lee WE. 2005. Corrosion of alkali-borosilicate waste glass K-26 in non-saturated conditions. *Journal of Nuclear Materials* 340: 12-24.

- Oppenheim AL. 1970. *Glass and Glassmaking in Ancient Mesopotamia: An Edition of the Cuneiform Texts Which Contain Instructions for Glassmakers With a Catalogue of Surviving Objects*. Corning: The Corning Museum of Glass Press.
- Paul A. 1990. *Chemistry of glasses*. 2nd edition. London: Chapman and Hall.
- Paynter S and Tite M. 2001. *The Evolution of Glazing Technologies in the Ancient Near East and Egypt*. In: AJ Shortland (ed) *The Social context of Technological Change: Egypt and the Near East, 1650-1550 BC*. Oxford: Oxbow. 239-254.
- Paynter S. 2009. *Links between glazes and glass in mid-2nd millennium BC Mesopotamia and Egypt*. In: AJ Shortland, Th. Rhren and IC Freestone (eds) *From mine to microscope*. Oxford:Oxbow Books.
- Peltenberg EJ. 1987. *Early faience: recent studies, origins and relations with glass*. In: M Bimson and IC Freestone (eds) *Early Vitreous Materials*. British Museum Occasional Paper No. 56. London: British Museum Publications. 5-30.
- Perret D, Crovoisier J-L, Stille P, Shields G, Mader U, Advocat T, Schenk K and Chardonnens M. 2003. *Thermodynamic stability of waste glasses compared to leaching behaviour*. *Applied Geochemistry* 18: 1165-1184.
- Peuget S, Broudie V, Jégou C, Frugier D, Roudil , Deschanel X, Rabiller H and Noel PY. 2007. *Effect of alpha radiation on the leaching behaviour of nuclear glass*. *Journal of Nuclear Materials* 362: 474-479.
- Pfeiffer RH. 1931. *The Excavations at Nuzi: Preliminary Report of the Fourth Campaign*. *Bulletin of the American Schools of Oriental Research* 42:1-7.
- Pierce EM, Rodriguez EA, Calligan LJ, Shaw WJ and McGrail BP. 2008. *An experimental study of the dissolution rate of simulated aluminoborosilicate waste glasses as a function of pH and temperature under dilute conditions*. *Applied Geochemistry* 23(9): 2559-2573.
- Rao KJ. 2002. *Structural chemistry of glass*. Oxford:Elsevier Science.
- Reade W, Freestone IC and Simpson S. 2005. *Innovation or continuity? Early first millennium BCE glass in the Near East: The cobalt blue glasses from Assyrian Nimrud*. *Annales du 16e Congres. Association pour l'Histoire du Verre* 2003: 23-27.
- Rebiscoul D, Van der Leer A, Rjeutord F, Né F, Spalla O, El-Mansouri A, Frugier P, Ayrat A and Gin S. 2004. *Morphological evolution of alteration layers formed during nuclear glass alteration: new evidence of a gel as a diffusive barrier*. *Journal of Nuclear Materials* 326: 9-18.
- Redford DB. 2003. *The Wars in Syria and Palestine of Thutmose III*. Leiden: Brill.
- Reed SJB. 2005. *Electron Microprobe Analysis and Scanning Electron Microscopy*. Cambridge:Cambridge University Press.

- Rehren Th. 2000. Rationales in Old World Base Glass Compositions. *Journal of Archaeological Science* 27: 1225-1234.
- Rehren Th. 2008. A review of factors affecting the composition of early Egyptian glasses and faience: alkali and alkali earth oxides. *Journal of Archaeological Science*. In press.
- Rehren Th. and Pusch EB. 1997. New Kingdom Glass-Melting Crucibles from Qantir-Piramesses. *Journal of Egyptian Archaeology* 83: 127-141.
- Rehren Th. and Pusch EB. 2005. Late Bronze Age Glass Production at Qantir-Piramesses, Egypt. *Science* 308: 1756-1758.
- Reimer L. 1998. *Scanning electron microscopy: Physics of image formation and microanalysis*. New York: Springer Verlag.
- Robinet L, Eremin K, Cobo del Arco B and Gibson LT. 2004. A Raman spectroscopic study of pollution-induced glass deterioration. *Journal of Raman Spectroscopy* 35: 662-670.
- Robinet L, Coupry C, Eremin K and Hall C. The use of Raman spectrometry to predict the stability of historic glasses. *Journal of Raman Spectroscopy* 37: 789-797.
- Robson E. 2001. *Technology in Society: Three Textual Case Studies for Late Bronze Age Mesopotamia*. In: AJ Shortland (ed) *The Social context of Technological Change: Egypt and the Near East, 1650-1550 BC*. Oxford: Oxbow. 39-58.
- Römich H. 2003. Studies of ancient glass and their application to nuclear waste. *MRS Bulletin* 28(7): 500-505.
- Salviulo G, Silvestri A, Molin G and Bertocello R. 2004. An archaeometric study of the bulk and surface weathering characteristics of Early Medieval (5th to 7th century) glass from the Po valley, northern Italy. *Journal of Archaeological Science* 31: 295-306.
- Sayre EV and Smith RW. 1961. Compositional Categories of Ancient Glass. *Science* 133:1824-1826.
- Schlick-Nolte B. and Werthmann R. 2003. Glass vessels from the burial of Nesikhons. *Journal of Glass Studies* 45: 11-34.
- Scholze H. 1991. *Glass: Nature, Structure and Properties*. Translated by Michael J Lakin. London: Springer Verlag.
- Shelby JE. 2005. *Introduction to Glass Science and Technology* (2nd edition). Cambridge: Royal Society of Chemistry.
- Shortland AJ. 2002. The use and origin of antimonate colorants in early Egyptian glass. *Archaeometry* 44(4): 517-530.

- Shortland AJ. 2007. Who were the glassmakers? Status, theory and method in mid-second millennium glass production. *Oxford Journal of Archaeology* 26(3): 261-247.
- Shortland A, Nicholson P and Jackson C. 2001. Glass and faience at Amarna: different methods of both supply for production, subsequent distribution. In: AJ Shortland (ed) *The Social context of Technological Change: Egypt and the Near East, 1650-1550 BC*. Oxford: Oxbow. 147-160.
- Shortland AJ and Eremin K. 2006. The analysis of second millennium glass from Egypt and Mesopotamia, Part 1: new WDS analyses. *Archaeometry* 48(4): 581-603.
- Shortland A, Schachner L, Freestone I and Tite M. 2006. Natron as a flux in the early vitreous materials industry: sources, beginnings and reasons for decline. *Journal of Archaeological Science* 33(4):521-530.
- Shortland A, Rogers N and Eremin K. 2007. Trace element discriminants between Egyptian and Mesopotamian Late Bronze Age glasses. *Journal of Archaeological Science* 34: 781-789.
- Shortland A, Eremin K, Kirk S and Armstrong J. 2008. Reassessing Bronze Age Manufacturing Technologies at Nuzi. In: PB Vandiver, B McCarthy, RH Tykot, JL Ruvalcaba-Sil and F Casadio *Materials Issues in Art and Archaeology VIII, Materials Research Society Symposium Proceedings 1047*. Warrendale, PA, 2008.
- Shortland et al, A possible new source of cobalt in Near Eastern glasses, in preparation
- Silvestri A, Molin G and Salviulo G. 2005. Archaeological glass alteration products in marine and land-based environments: morphological, chemical and microtextural characterization. *Journal of Non-Crystalline Solids* 351: 1338-1349.
- Sinton CW and LaCourse WC. 2001. Experimental survey of the chemical durability of commercial soda-lime-silicate glasses. *Materials Research Bulletin* 36: 2471-2479.
- Speiser EA. 1929. A Letter of Saustatar and the date of the Kirkuk tablets. *Journal of the American Oriental Society* 49:269-275.
- Stapelton CP and Swanson SS. 2002. Batch material processing and glassmaking technology of 9th century BC artifacts excavated from the site of Hasanlu, northwest Iran. *Materials Research Society Symposium Proceedings* 712: 117.4.1-117.4.7.
- Starr RFS. 1930. Kirkuk Expedition. Notes (Fogg Arts Museum) 2(5): 182-197.
- Starr RFS. 1931. Excavations in Iraq. *Bulletin of the Fogg Art Museum* 1:6-14.
- Starr RFS. 1935. Notes of the Tracing of Mud-Brick Walls. *Bulletin of the American Schools of Oriental Research* 58:18-27.

- Starr RFS. 1937. Nuzi: report on the excavations at Yorgan Tapa and Kirkuk, Iraq: conducted by Harvard University in conjunction with the American Schools of Oriental Research and the University Museum of Philadelphia, 1927-1931 Volume II Plates and Plans. Cambridge MA: Harvard University Press.
- Starr RFS. 1939. Nuzi: report on the excavations at Yorgan Tapa and Kirkuk, Iraq: conducted by Harvard University in conjunction with the American Schools of Oriental Research and the University Museum of Philadelphia, 1927-1931 Volume I Text. Cambridge MA: Harvard University Press.
- Strachan DM. 2001. Glass dissolution: testing and modelling for long-term behaviour. *Journal of Nuclear Materials* 298: 69-77.
- Stein DL. 1989. A Reappraisal of the "Sauštatar Letter" from Nuzi. *Zeitschrift für Assyriologie und Vorderasiatische Archäologie* 79(1): 36-60.
- Sterpenich J and Libourel G. 2006. Water diffusion in silicate glasses under natural weathering conditions: evidence from buried medieval stained glasses. *Journal of Non-Crystalline Solids* 352: 5446-5451.
- Stevenson CM, Wheeler D, Novak SW, Speakman RJ and Glascock MD. 2007. A new dating method for high-calcium glasses based upon surface-water diffusion: preliminary calibrations and procedures. *Archaeometry* 49(1): 153-177.
- Taylor G and Eggleton RA. 2001. *Regolith geology and geomorphology*. Chichester: John Wiley & Sons.
- Thornton CP and Ehlers C. 2003. Early brass in the ancient Near East. *IAMS* 23:3-8
- Tite MS, Shortland A and Maniatis Y. 2006. The composition of the soda-rich and mixed alkali plant ashes used in the production of glass. *Journal of Archaeological Science* 33 (9): 1284-1292.
- Tite MS, Manti P and Shortland AJ. 2007. A technological study of ancient faience from Egypt. *Journal of Archaeological Science* 34: 1568-1583.
- Tite MS, Maniatis Y, Kavoussanaki D, Panagiotaki M, Shortland AJ and Kirk SF. 2008a. Colour in Minoan Faience. *Journal of Archaeological Science* 36:370-378.
- Tite M, Pradell T and Shortland A. 2008b. Discovery, production and use of tin-based opacifiers in glasses, enamels and glazes from the late Iron Age onwards: a reassessment. *Archaeometry* 50: 67-84.
- Turner WES. 1956. *Studies in Ancient Glasses and Glassmaking Processes*. Part V. Raw materials and melting processes. *Journal of the Society of Glass Technology* 40: 277T-300T.
- White Art F. Weathering characteristics of natural glass and influences on associated water chemistry. *Journal of Non-Crystalline Solids* 67: 225-244.
- Van Iseghem P, Valcke E and Lodding A. 2001. In situ testing for the chemical durability of vitrified high-level waste in a Boom Clay formation in Belgium: discussion of recent data and concept of a new test. *Journal of Nuclear Materials* 298: 86-94.

- Vandiver P. 1983. Glass technology at the mid-second millennium BC Hurrian site of Nuzi. *Journal of Glass Studies* 25: 239-47.
- Vandiver PB. 1992. Corrosion and Conservation of Ancient Glass and Ceramics. In: DE Clark and BK Zaitos (eds) *Corrosion of Glass, Ceramics and Ceramic Superconductors*. Noyes: William Andrew Publishing. 393-430.
- Vandiver PB. 1993. Corrosion of synthesized glasses and glazes as analogs for nuclear waste glass degradation. *Materials Research Society Symposium Proceedings* 333: 969-982.
- Vernaz E, Gin S, Jégou C and Ribet I. 2001. Present understanding of R7T7 glass alteration kinetics and their impact on long-term behaviour modelling. *Journal of Nuclear Materials* 298: 27-36.
- Verney-Carron A, Gin S and Libourel G. 2008. A fractured Roman glass block altered for 1800 years in seawater : Analogy with nuclear waste glass in a deep geological repository. *Geochimica et Cosmochimica Acta* 72: 5372-5385.
- Vilarigues M and da Silva RC. 2006. Characterization of potash-glass corrosion in aqueous solution by ion beam and IR spectroscopy. *Journal of Non-Crystalline Solids* 352: 5368-5375.
- Walther JV. 2009. *Essentials of Geochemistry*. London: Jones and Bartlett.
- Walton MS, Shortland A, Kirk S and Degryse P. 2009. Evidence for trade of Mesopotamian and Egyptian glasses to Mycenaean Greece. *Journal of Archaeological Science* 36: 1496-1503.
- Watkinson D, Weber L and Anheuser K. 2005. Staining of archaeological glass from manganese-rich environments. *Archaeometry* 47: 69-82.
- Weyl WA. 1955. *Coloured glasses*. Sheffield: Society of Glass Production.
- White AF. 1984. Weathering characteristics of natural glass and influences on associated water chemistry. *Journal of Non-Crystalline Solids* 67: 225-244.
- White AF and Brantley SL. 1995. Chemical weathering rates of silicate minerals: an overview. In: AF White and SL Brantley (eds) *Chemical weathering rates of silicate minerals*. *Reviews in Mineralogy* volume 31. 1-22.
- White AF and Brantley SL. 2003. The effect of time on the weathering of silicate minerals: why do weathering rates differ in the laboratory and field? *Chemical Geology* 202: 479-506.
- Wicks GG. 1992. Nuclear Waste Glasses: Corrosion Behaviour and Field Tests. In: DE Clark and BK Zaitos (eds) *Corrosion of Glass, Ceramics and Ceramic Superconductors*. Noyes: William Andrew Publishing. 218-268.

Woolley L. 1955. Alalakh: An Account of the Excavations at Tell Atchana in the Hatay, 1937-1949. Reports of the Research Committee of the Society of Antiquaries of London. Oxford: The Society of Antiquaries.

Zachariasen WH. 1932. The atomic arrangement in glass. Journal of the American Chemistry Society 54 (10): 3841-3851.

Ziemath EC. Degradation of the surface of a metasilicate glass due to atmosphere moisture. Quimica Nova 21(3): 356-360.

Appendix 1

Standard data for SEM-WDS

Standard composition :

JAD3 STD048 = O : 47.6%, Na : 11.28%, Mg : 0.05%, Al : 13.33%, Si : 27.79%, Ca : 0.08%, Fe : 0.0%

WOL4 STD097 = O : 41.04%, Si : 23.8%, Ca : 34.16%, Fe : 0.6%, Mn : 0.05%

FOR STD277 = O : 45.48%, Mg : 34.55%, Si : 19.98%

COR4 STD028 = Al : 52.9242%, O : 47.0758%

APA2 STD217 = O : 38.94%, F : 1.75%, Si : 0.1%, P : 18.34%, S : 0.06%, Ca : 37.04%, Cl : 1.94%, Sr : 0.47%, Ce : 0.32%, Na : 0.13%

KBR3 STD075 = K : 32.8551%, Br : 67.1449%

WOL STD097 = O : 41.04%, Si : 23.8%, Ca : 34.16%, Fe : 0.6%, Mn : 0.05%

MNT STDIC = Mn : 36.4219%, Ti : 31.756%, O : 31.8221%

CRO2 STDIC = Cr : 68.4195%, O : 31.5805%

FEO STDIC = O : 30.07%, Fe : 69.93%

PCO STD121 = Co : 100.0%

NIO2 STDIC = Ni : 78.5839%, O : 21.4161%

CU2 STD123 = Cu : 100.0%

ZNS2 STDIC = Zn : 67.1%, S : 32.9%

GAA STD208 = Ga : 48.208%, As : 51.792%

CEL3 STD026 = O : 34.84%, S : 17.45%, Sr : 47.7%

CAS STD024 = Sn : 78.7644%, O : 21.2356%

PSB STD109 = Sb : 100.0%

BAR2 = Ba : 58.8415%, S : 13.7367%, O : 27.4218%

VAN STDIC = O : 13.55%, Cl : 2.55%, V : 10.78%, Pb : 73.12%

Table a – detection limit data (ppm, wt%) for SEM-WDS analysis (run 13 Jul 2009)

Detection limit data (ppm, wt %) for SEM-WDS (run 13 Jul 2009)

| Point | Na | Si | Mg | Al | P | K | Ca | Ti | Cr | Mn | Fe | Co | Ni | Cu | Zn | Sr | Sn | Sb | Ba | S | Cl | Pb |
|----------|-----|-----|-----|-----|-----|-----|-----|-----|-----|-----|-----|-----|-----|-----|-----|-----|-----|-----|-----|-----|-----|-----|
| 1 / 1 . | 204 | 130 | 94 | 86 | 245 | 221 | 245 | 162 | 146 | 507 | 486 | 219 | 221 | 279 | 710 | 459 | 343 | 358 | 506 | 164 | 159 | 457 |
| 1 / 2 . | 189 | 124 | 94 | 84 | 242 | 224 | 245 | 166 | 143 | 517 | 531 | 224 | 221 | 277 | 770 | 455 | 335 | 355 | 506 | 172 | 155 | 434 |
| 1 / 3 . | 194 | 125 | 95 | 84 | 239 | 233 | 238 | 158 | 144 | 514 | 549 | 216 | 225 | 275 | 780 | 453 | 346 | 348 | 493 | 162 | 140 | 428 |
| 1 / 4 . | 375 | 131 | 105 | 93 | 238 | 239 | 265 | 167 | 150 | 513 | 561 | 227 | 235 | 294 | 737 | 463 | 357 | 382 | 533 | 174 | 164 | 460 |
| 1 / 5 . | 405 | 134 | 105 | 94 | 224 | 246 | 268 | 165 | 148 | 565 | 553 | 233 | 238 | 291 | 815 | 473 | 360 | 380 | 512 | 169 | 165 | 459 |
| 1 / 6 . | 411 | 132 | 107 | 95 | 239 | 214 | 258 | 162 | 150 | 587 | 566 | 227 | 232 | 296 | 725 | 472 | 356 | 374 | 526 | 183 | 155 | 468 |
| 1 / 7 . | 409 | 131 | 109 | 94 | 243 | 240 | 272 | 161 | 150 | 480 | 555 | 233 | 230 | 288 | 814 | 478 | 346 | 389 | 522 | 158 | 155 | 480 |
| 1 / 8 . | 417 | 131 | 105 | 94 | 231 | 209 | 266 | 163 | 146 | 458 | 559 | 228 | 234 | 283 | 757 | 475 | 361 | 368 | 539 | 148 | 155 | 454 |
| 1 / 9 . | 201 | 128 | 94 | 85 | 234 | 226 | 260 | 163 | 146 | 478 | 533 | 216 | 230 | 282 | 740 | 458 | 347 | 361 | 504 | 145 | 160 | 461 |
| 1 / 10 . | 289 | 131 | 103 | 89 | 295 | 244 | 288 | 166 | 149 | 569 | 544 | 232 | 236 | 293 | 821 | 468 | 338 | 377 | 527 | 168 | 146 | 467 |
| 1 / 11 . | 428 | 129 | 108 | 93 | 257 | 238 | 280 | 167 | 151 | 503 | 562 | 229 | 248 | 283 | 776 | 466 | 348 | 376 | 531 | 165 | 151 | 466 |
| 1 / 12 . | 424 | 135 | 107 | 94 | 253 | 227 | 264 | 164 | 151 | 532 | 518 | 230 | 228 | 291 | 808 | 482 | 357 | 370 | 534 | 158 | 151 | 464 |
| 1 / 13 . | 419 | 133 | 106 | 95 | 224 | 232 | 281 | 160 | 149 | 546 | 593 | 229 | 237 | 280 | 817 | 482 | 349 | 393 | 524 | 163 | 151 | 463 |
| 1 / 14 . | 425 | 132 | 107 | 94 | 229 | 236 | 272 | 167 | 151 | 510 | 507 | 235 | 236 | 287 | 803 | 462 | 339 | 386 | 530 | 173 | 154 | 462 |
| 1 / 15 . | 422 | 130 | 110 | 92 | 246 | 230 | 272 | 165 | 151 | 500 | 535 | 229 | 233 | 301 | 800 | 461 | 351 | 384 | 550 | 162 | 155 | 459 |
| 1 / 16 . | 421 | 134 | 107 | 94 | 210 | 239 | 269 | 169 | 150 | 488 | 524 | 230 | 238 | 292 | 769 | 479 | 356 | 379 | 528 | 161 | 169 | 458 |
| 1 / 17 . | 413 | 133 | 108 | 95 | 236 | 219 | 264 | 165 | 149 | 477 | 590 | 232 | 233 | 297 | 791 | 479 | 356 | 386 | 533 | 165 | 152 | 476 |
| 1 / 18 . | 431 | 133 | 110 | 94 | 199 | 248 | 280 | 162 | 149 | 576 | 604 | 219 | 241 | 306 | 829 | 469 | 358 | 387 | 535 | 166 | 152 | 469 |
| 1 / 19 . | 402 | 132 | 107 | 96 | 252 | 245 | 229 | 166 | 152 | 518 | 612 | 226 | 234 | 298 | 783 | 472 | 354 | 373 | 518 | 176 | 167 | 477 |
| 1 / 20 . | 402 | 137 | 106 | 95 | 242 | 225 | 259 | 162 | 151 | 513 | 598 | 219 | 236 | 300 | 809 | 474 | 358 | 379 | 537 | 194 | 157 | 485 |
| 1 / 21 . | 414 | 133 | 108 | 96 | 233 | 258 | 260 | 162 | 151 | 513 | 554 | 227 | 238 | 296 | 821 | 477 | 354 | 376 | 538 | 149 | 156 | 466 |
| 1 / 22 . | 221 | 130 | 97 | 101 | 241 | 190 | 360 | 162 | 151 | 567 | 511 | 234 | 241 | 297 | 838 | 475 | 352 | 388 | 530 | 148 | 158 | 424 |
| 1 / 23 . | 266 | 135 | 124 | 108 | 211 | 249 | 616 | 175 | 158 | 570 | 533 | 257 | 260 | 337 | 926 | 444 | 362 | 480 | 550 | 166 | 151 | 431 |
| 1 / 24 . | 210 | 131 | 90 | 101 | 222 | 219 | 353 | 169 | 153 | 545 | 494 | 231 | 235 | 308 | 837 | 468 | 354 | 383 | 544 | 158 | 143 | 437 |
| 1 / 25 . | 188 | 136 | 82 | 78 | 235 | 201 | 232 | 162 | 147 | 491 | 483 | 216 | 234 | 278 | 762 | 504 | 342 | 339 | 500 | 142 | 146 | 444 |
| 1 / 26 . | 283 | 134 | 90 | 85 | 248 | 240 | 238 | 160 | 149 | 574 | 549 | 221 | 237 | 304 | 799 | 498 | 334 | 350 | 533 | 156 | 160 | 463 |
| 1 / 27 . | 188 | 138 | 82 | 76 | 220 | 215 | 226 | 161 | 145 | 589 | 516 | 222 | 227 | 285 | 738 | 501 | 341 | 354 | 506 | 154 | 150 | 444 |
| 1 / 28 . | 394 | 131 | 106 | 93 | 213 | 205 | 232 | 164 | 147 | 562 | 533 | 232 | 234 | 303 | 793 | 484 | 381 | 374 | 511 | 186 | 153 | 461 |
| 1 / 29 . | 403 | 132 | 99 | 94 | 247 | 213 | 215 | 165 | 149 | 534 | 606 | 232 | 247 | 287 | 807 | 485 | 400 | 366 | 504 | 174 | 148 | 440 |
| 1 / 30 . | 400 | 133 | 102 | 93 | 232 | 218 | 246 | 167 | 148 | 548 | 546 | 243 | 242 | 292 | 819 | 483 | 383 | 376 | 524 | 160 | 158 | 454 |
| 1 / 31 . | 407 | 132 | 102 | 94 | 273 | 230 | 218 | 164 | 147 | 547 | 624 | 230 | 239 | 294 | 785 | 490 | 378 | 359 | 526 | 162 | 138 | 437 |
| 1 / 32 . | 412 | 130 | 100 | 94 | 236 | 222 | 233 | 157 | 148 | 556 | 548 | 235 | 235 | 295 | 759 | 495 | 385 | 356 | 510 | 154 | 142 | 451 |
| 1 / 33 . | 407 | 131 | 102 | 96 | 239 | 210 | 246 | 165 | 147 | 503 | 585 | 229 | 240 | 282 | 799 | 489 | 369 | 367 | 511 | 165 | 153 | 452 |
| 1 / 34 . | 425 | 130 | 103 | 95 | 209 | 210 | 262 | 170 | 150 | 537 | 595 | 226 | 237 | 282 | 761 | 491 | 359 | 375 | 519 | 171 | 153 | 457 |

| | | | | | | | | | | | | | | | | | | | | | | |
|----------|-----|-----|-----|-----|-----|-----|-----|-----|-----|-----|-----|-----|-----|-----|-----|-----|-----|-----|-----|-----|-----|-----|
| 1 / 35 . | 421 | 131 | 106 | 96 | 240 | 222 | 243 | 164 | 149 | 547 | 533 | 234 | 241 | 289 | 791 | 488 | 350 | 378 | 535 | 174 | 145 | 443 |
| 1 / 36 . | 425 | 133 | 107 | 92 | 211 | 224 | 248 | 163 | 148 | 486 | 510 | 227 | 241 | 287 | 774 | 488 | 351 | 377 | 522 | 161 | 158 | 452 |
| 1 / 37 . | 374 | 130 | 108 | 93 | 228 | 246 | 247 | 181 | 169 | 541 | 577 | 255 | 262 | 319 | 855 | 456 | 385 | 407 | 573 | 183 | 174 | 681 |
| 1 / 38 . | 383 | 131 | 108 | 91 | 214 | 257 | 271 | 182 | 167 | 619 | 581 | 248 | 260 | 323 | 846 | 459 | 397 | 414 | 580 | 180 | 173 | 652 |
| 1 / 39 . | 387 | 132 | 108 | 94 | 256 | 260 | 254 | 187 | 166 | 622 | 614 | 260 | 256 | 315 | 837 | 458 | 394 | 398 | 580 | 163 | 170 | 669 |
| 1 / 40 . | 410 | 129 | 106 | 99 | 283 | 242 | 242 | 161 | 148 | 543 | 547 | 224 | 234 | 286 | 796 | 456 | 360 | 401 | 519 | 159 | 153 | 462 |
| 1 / 41 . | 395 | 129 | 106 | 104 | 246 | 249 | 249 | 167 | 149 | 498 | 552 | 229 | 230 | 294 | 815 | 446 | 348 | 386 | 524 | 160 | 159 | 459 |
| 1 / 42 . | 417 | 132 | 109 | 101 | 232 | 211 | 245 | 167 | 151 | 611 | 507 | 222 | 237 | 287 | 841 | 461 | 360 | 388 | 513 | 157 | 150 | 453 |
| 1 / 43 . | 211 | 130 | 85 | 95 | 213 | 235 | 241 | 161 | 144 | 473 | 576 | 219 | 231 | 279 | 779 | 456 | 364 | 378 | 515 | 163 | 159 | 457 |
| 1 / 44 . | 233 | 129 | 89 | 95 | 243 | 258 | 240 | 165 | 149 | 467 | 528 | 224 | 221 | 276 | 760 | 456 | 363 | 378 | 512 | 179 | 158 | 449 |
| 1 / 45 . | 233 | 129 | 86 | 99 | 240 | 252 | 232 | 159 | 148 | 550 | 551 | 231 | 226 | 284 | 789 | 464 | 361 | 360 | 514 | 164 | 148 | 444 |
| 1 / 46 . | 218 | 135 | 86 | 89 | 195 | 237 | 235 | 163 | 148 | 511 | 617 | 217 | 236 | 278 | 789 | 493 | 349 | 351 | 537 | 166 | 145 | 460 |
| 1 / 47 . | 209 | 134 | 86 | 88 | 275 | 229 | 270 | 161 | 152 | 520 | 527 | 230 | 232 | 288 | 774 | 481 | 348 | 375 | 504 | 158 | 167 | 486 |
| 1 / 48 . | 215 | 131 | 87 | 87 | 215 | 221 | 254 | 168 | 150 | 528 | 576 | 232 | 230 | 283 | 798 | 476 | 355 | 370 | 514 | 168 | 168 | 523 |
| 1 / 49 . | 391 | 131 | 101 | 96 | 246 | 243 | 284 | 164 | 150 | 539 | 521 | 230 | 233 | 286 | 802 | 468 | 360 | 392 | 514 | 172 | 155 | 441 |
| 1 / 50 . | 386 | 131 | 105 | 96 | 238 | 253 | 247 | 166 | 153 | 483 | 581 | 223 | 243 | 292 | 808 | 468 | 361 | 383 | 503 | 172 | 166 | 442 |
| 1 / 51 . | 387 | 131 | 104 | 95 | 213 | 249 | 278 | 169 | 150 | 572 | 512 | 237 | 235 | 291 | 797 | 469 | 345 | 376 | 514 | 161 | 152 | 466 |
| 1 / 52 . | 384 | 133 | 108 | 93 | 231 | 241 | 311 | 166 | 153 | 575 | 594 | 232 | 244 | 296 | 840 | 468 | 358 | 404 | 544 | 162 | 154 | 461 |
| 1 / 53 . | 408 | 132 | 102 | 99 | 249 | 225 | 252 | 166 | 149 | 524 | 522 | 225 | 225 | 288 | 763 | 490 | 332 | 359 | 521 | 173 | 166 | 437 |
| 1 / 54 . | 407 | 130 | 103 | 98 | 258 | 216 | 223 | 160 | 150 | 540 | 540 | 224 | 235 | 278 | 834 | 491 | 346 | 348 | 505 | 160 | 157 | 443 |
| 1 / 55 . | 426 | 131 | 103 | 98 | 263 | 235 | 234 | 162 | 149 | 535 | 540 | 225 | 235 | 282 | 800 | 489 | 341 | 367 | 509 | 173 | 157 | 467 |
| 1 / 56 . | 429 | 131 | 100 | 98 | 204 | 223 | 258 | 166 | 148 | 460 | 606 | 223 | 233 | 278 | 865 | 487 | 340 | 364 | 519 | 168 | 163 | 460 |
| 1 / 57 . | 440 | 129 | 102 | 98 | 242 | 206 | 230 | 160 | 151 | 535 | 480 | 229 | 236 | 285 | 764 | 486 | 345 | 366 | 526 | 171 | 167 | 453 |
| 1 / 58 . | 432 | 129 | 106 | 98 | 248 | 215 | 248 | 166 | 150 | 472 | 531 | 233 | 232 | 275 | 776 | 485 | 340 | 354 | 533 | 143 | 151 | 454 |
| 1 / 59 . | 423 | 130 | 102 | 97 | 251 | 222 | 239 | 161 | 148 | 484 | 563 | 218 | 232 | 283 | 796 | 499 | 344 | 359 | 515 | 179 | 155 | 447 |
| 1 / 60 . | 422 | 131 | 102 | 95 | 248 | 214 | 244 | 160 | 148 | 489 | 567 | 221 | 233 | 287 | 818 | 498 | 333 | 365 | 509 | 158 | 149 | 450 |
| 1 / 61 . | 423 | 127 | 104 | 98 | 236 | 207 | 255 | 164 | 150 | 484 | 514 | 234 | 229 | 281 | 791 | 495 | 354 | 366 | 502 | 144 | 142 | 431 |
| 1 / 62 . | 421 | 129 | 99 | 99 | 230 | 217 | 246 | 159 | 153 | 546 | 528 | 238 | 247 | 295 | 783 | 487 | 351 | 367 | 507 | 163 | 148 | 452 |
| 1 / 63 . | 419 | 129 | 106 | 97 | 267 | 224 | 248 | 160 | 149 | 484 | 500 | 224 | 241 | 291 | 775 | 487 | 338 | 368 | 514 | 157 | 149 | 444 |
| 1 / 64 . | 405 | 127 | 103 | 98 | 267 | 236 | 254 | 166 | 148 | 521 | 567 | 227 | 234 | 288 | 790 | 488 | 341 | 360 | 498 | 138 | 159 | 459 |
| 1 / 65 . | 419 | 130 | 103 | 96 | 264 | 193 | 228 | 158 | 149 | 489 | 550 | 222 | 301 | 270 | 799 | 497 | 347 | 371 | 510 | 158 | 146 | 438 |
| 1 / 66 . | 421 | 132 | 99 | 96 | 188 | 230 | 243 | 160 | 148 | 545 | 470 | 221 | 311 | 286 | 786 | 497 | 337 | 367 | 530 | 158 | 154 | 456 |
| 1 / 67 . | 406 | 132 | 102 | 94 | 245 | 134 | 134 | 161 | 148 | 483 | 549 | 228 | 320 | 283 | 790 | 497 | 348 | 358 | 521 | 168 | 167 | 492 |
| 1 / 68 . | 421 | 129 | 102 | 100 | 263 | 225 | 249 | 164 | 148 | 454 | 639 | 236 | 235 | 292 | 777 | 485 | 350 | 363 | 515 | 175 | 146 | 445 |
| 1 / 69 . | 419 | 131 | 103 | 98 | 218 | 229 | 252 | 159 | 147 | 518 | 564 | 238 | 244 | 285 | 829 | 487 | 351 | 355 | 512 | 146 | 159 | 424 |
| 1 / 70 . | 427 | 133 | 103 | 100 | 251 | 223 | 241 | 161 | 148 | 528 | 568 | 227 | 232 | 289 | 866 | 484 | 358 | 350 | 507 | 171 | 153 | 434 |
| 1 / 71 . | 419 | 129 | 103 | 101 | 252 | 233 | 246 | 163 | 148 | 558 | 540 | 231 | 223 | 279 | 762 | 492 | 349 | 370 | 513 | 157 | 157 | 450 |
| 1 / 72 . | 407 | 131 | 101 | 101 | 238 | 203 | 250 | 165 | 149 | 504 | 499 | 234 | 235 | 291 | 806 | 492 | 346 | 349 | 522 | 173 | 155 | 429 |

| | | | | | | | | | | | | | | | | | | | | | | |
|-----------|-----|-----|-----|-----|-----|-----|-----|-----|-----|-----|-----|-----|-----|-----|-----|-----|-----|-----|-----|-----|-----|----------------|
| 1 / 73 . | 418 | 130 | 104 | 101 | 261 | 224 | 232 | 168 | 148 | 520 | 587 | 231 | 236 | 279 | 836 | 500 | 333 | 361 | 521 | 155 | 161 | 454 |
| 1 / 74 . | 410 | 131 | 96 | 93 | 232 | 226 | 245 | 164 | 146 | 610 | 534 | 222 | 223 | 283 | 757 | 506 | 335 | 351 | 509 | 161 | 154 | 441 |
| 1 / 75 . | 406 | 131 | 101 | 95 | 222 | 214 | 245 | 158 | 146 | 439 | 501 | 223 | 237 | 286 | 747 | 503 | 338 | 370 | 503 | 149 | 158 | 447 |
| 1 / 76 . | 396 | 131 | 99 | 94 | 219 | 216 | 245 | 161 | 147 | 560 | 466 | 223 | 224 | 289 | 767 | 504 | 330 | 365 | 493 | 145 | 165 | 440 |
| 1 / 77 . | 390 | 129 | 97 | 96 | 251 | 233 | 228 | 167 | 149 | 551 | 537 | 232 | 234 | 285 | 764 | 496 | 351 | 354 | 520 | 170 | 157 | 462 |
| 1 / 78 . | 399 | 129 | 100 | 95 | 251 | 215 | 227 | 164 | 151 | 556 | 568 | 230 | 235 | 287 | 795 | 495 | 339 | 354 | 510 | 156 | 144 | 447 |
| 1 / 79 . | 403 | 130 | 98 | 97 | 203 | 227 | 241 | 165 | 149 | 506 | 514 | 216 | 235 | 281 | 828 | 497 | 352 | 370 | 517 | 179 | 161 | 455 |
| 1 / 80 . | 370 | 131 | 100 | 98 | 256 | 216 | 251 | 165 | 148 | 579 | 596 | 229 | 227 | 276 | 778 | 486 | 353 | 355 | 527 | 169 | 154 | 451 |
| 1 / 81 . | 374 | 130 | 97 | 97 | 262 | 210 | 237 | 163 | 151 | 522 | 616 | 217 | 239 | 297 | 808 | 489 | 343 | 362 | 501 | 152 | 160 | 460 |
| 1 / 82 . | 375 | 130 | 97 | 96 | 239 | 236 | 243 | 159 | 150 | 541 | 576 | 220 | 226 | 296 | 761 | 488 | 336 | 364 | 540 | 170 | 154 | 444 |
| 1 / 83 . | 415 | 129 | 100 | 96 | 246 | 232 | 271 | 164 | 148 | 570 | 491 | 227 | 225 | 284 | 812 | 501 | 339 | 362 | 488 | 160 | 155 | 454 |
| 1 / 84 . | 420 | 130 | 98 | 94 | 234 | 216 | 241 | 161 | 147 | 561 | 551 | 219 | 233 | 283 | 761 | 507 | 336 | 356 | 519 | 160 | 158 | 458 |
| 1 / 85 . | 413 | 132 | 99 | 95 | 231 | 209 | 255 | 163 | 148 | 501 | 538 | 231 | 232 | 284 | 773 | 501 | 347 | 368 | 516 | 153 | 157 | 447 |
| 1 / 86 . | 396 | 130 | 100 | 97 | 224 | 220 | 287 | 168 | 149 | 515 | 518 | 240 | 232 | 305 | 799 | 489 | 339 | 375 | 523 | 179 | 159 | 439 |
| 1 / 87 . | 403 | 131 | 98 | 96 | 218 | 221 | 306 | 166 | 152 | 545 | 545 | 232 | 234 | 283 | 805 | 488 | 357 | 378 | 517 | 170 | 153 | 469 |
| 1 / 88 . | 401 | 128 | 101 | 96 | 234 | 226 | 296 | 165 | 151 | 550 | 595 | 224 | 234 | 291 | 754 | 489 | 353 | 389 | 529 | 175 | 164 | 456 |
| 1 / 89 . | 422 | 131 | 98 | 96 | 222 | 200 | 256 | 161 | 148 | 512 | 585 | 221 | 233 | 290 | 814 | 491 | 345 | 350 | 516 | 165 | 163 | 441 |
| 1 / 90 . | 406 | 131 | 102 | 99 | 237 | 232 | 259 | 165 | 152 | 480 | 552 | 227 | 233 | 292 | 740 | 491 | 340 | 358 | 512 | 161 | 153 | 452 |
| 1 / 91 . | 419 | 131 | 102 | 97 | 225 | 228 | 245 | 162 | 148 | 551 | 572 | 231 | 228 | 279 | 800 | 492 | 336 | 359 | 515 | 157 | 162 | 454 |
| 1 / 92 . | 413 | 127 | 98 | 98 | 252 | 231 | 242 | 165 | 148 | 530 | 562 | 229 | 241 | 286 | 778 | 485 | 348 | 374 | 518 | 159 | 159 | 449 |
| 1 / 93 . | 411 | 126 | 99 | 100 | 199 | 236 | 254 | 161 | 150 | 582 | 523 | 234 | 236 | 285 | 815 | 487 | 345 | 361 | 512 | 164 | 159 | 427 |
| 1 / 94 . | 412 | 128 | 98 | 97 | 216 | 229 | 256 | 159 | 146 | 539 | 544 | 222 | 241 | 276 | 848 | 487 | 343 | 358 | 507 | 165 | 167 | 444 |
| 1 / 95 . | 382 | 133 | 103 | 86 | 228 | 238 | 299 | 163 | 151 | 450 | 535 | 224 | 228 | 297 | 802 | 482 | 351 | 384 | 517 | 154 | 139 | 427 |
| 1 / 96 . | 379 | 135 | 102 | 88 | 246 | 247 | 298 | 169 | 153 | 515 | 565 | 229 | 237 | 292 | 796 | 479 | 361 | 392 | 520 | 150 | 160 | 434 |
| 1 / 97 . | 370 | 133 | 105 | 89 | 238 | 261 | 316 | 164 | 150 | 595 | 544 | 224 | 236 | 288 | 877 | 485 | 347 | 382 | 525 | 174 | 150 | <u>-381307</u> |
| 1 / 98 . | 396 | 131 | 108 | 89 | 247 | 242 | 316 | 171 | 150 | 540 | 586 | 237 | 248 | 298 | 819 | 464 | 350 | 402 | 535 | 172 | 160 | 429 |
| 1 / 99 . | 398 | 132 | 108 | 86 | 261 | 224 | 308 | 163 | 150 | 510 | 553 | 229 | 238 | 289 | 892 | 469 | 351 | 399 | 541 | 158 | 136 | 445 |
| 1 / 100 . | 404 | 134 | 111 | 89 | 211 | 234 | 330 | 168 | 152 | 489 | 544 | 231 | 236 | 291 | 851 | 464 | 358 | 416 | 528 | 150 | 139 | 443 |
| 1 / 101 . | 394 | 128 | 110 | 90 | 239 | 236 | 243 | 170 | 147 | 559 | 586 | 224 | 230 | 289 | 759 | 481 | 341 | 378 | 513 | 156 | 139 | 432 |
| 1 / 102 . | 394 | 129 | 106 | 92 | 239 | 214 | 256 | 162 | 147 | 504 | 543 | 226 | 231 | 276 | 796 | 484 | 333 | 375 | 525 | 169 | 140 | <u>2254750</u> |
| 1 / 103 . | 401 | 134 | 108 | 92 | 219 | 232 | 267 | 161 | 148 | 548 | 556 | 225 | 224 | 276 | 779 | 478 | 352 | 378 | 522 | 142 | 133 | 436 |
| 1 / 104 . | 390 | 136 | 102 | 89 | 209 | 228 | 296 | 161 | 153 | 545 | 574 | 222 | 237 | 297 | 825 | 489 | 346 | 397 | 532 | 153 | 133 | 460 |
| 1 / 105 . | 393 | 133 | 102 | 89 | 202 | 217 | 282 | 166 | 153 | 554 | 594 | 229 | 234 | 291 | 772 | 491 | 356 | 396 | 514 | 163 | 147 | 448 |
| 1 / 106 . | 407 | 132 | 106 | 88 | 278 | 247 | 294 | 164 | 153 | 520 | 570 | 233 | 233 | 302 | 808 | 484 | 354 | 386 | 523 | 155 | 138 | 433 |
| 1 / 107 . | 377 | 133 | 103 | 88 | 235 | 228 | 305 | 169 | 149 | 590 | 512 | 231 | 241 | 291 | 796 | 495 | 349 | 386 | 531 | 160 | 155 | 436 |
| 1 / 108 . | 380 | 131 | 104 | 89 | 235 | 242 | 284 | 160 | 149 | 572 | 569 | 219 | 227 | 292 | 805 | 492 | 346 | 381 | 515 | 158 | 138 | 447 |
| 1 / 109 . | 387 | 133 | 103 | 89 | 220 | 226 | 308 | 161 | 148 | 544 | 590 | 220 | 231 | 285 | 775 | 492 | 344 | 385 | 531 | 168 | 157 | 431 |
| 1 / 110 . | 376 | 130 | 96 | 98 | 208 | 228 | 257 | 165 | 150 | 566 | 568 | 217 | 226 | 293 | 767 | 495 | 342 | 368 | 519 | 162 | 139 | 442 |

| | | | | | | | | | | | | | | | | | | | | | | |
|----------------|------------|------------|------------|-----------|------------|------------|------------|------------|------------|------------|------------|------------|------------|------------|------------|------------|------------|------------|------------|------------|------------|------------|
| 1 / 111 . | 378 | 128 | 95 | 96 | 208 | 205 | 229 | 158 | 147 | 588 | 515 | 234 | 230 | 278 | 766 | 497 | 349 | 369 | 530 | 170 | 149 | 452 |
| 1 / 112 . | 389 | 131 | 97 | 98 | 243 | 205 | 253 | 163 | 151 | 480 | 520 | 228 | 231 | 279 | 770 | 495 | 349 | 358 | 513 | 154 | 159 | 426 |
| 1 / 113 . | 385 | 132 | 98 | 98 | 237 | 216 | 238 | 166 | 150 | 532 | 547 | 217 | 232 | 288 | 785 | 494 | 344 | 360 | 513 | 148 | 155 | 444 |
| 1 / 114 . | 385 | 130 | 97 | 98 | 243 | 227 | 246 | 159 | 148 | 468 | 564 | 233 | 237 | 284 | 762 | 494 | 338 | 367 | 516 | 171 | 156 | 436 |
| 1 / 115 . | 377 | 132 | 97 | 97 | 258 | 233 | 239 | 168 | 150 | 562 | 552 | 227 | 231 | 280 | 767 | 493 | 339 | 362 | 518 | 160 | 159 | 460 |
| 1 / 116 . | 376 | 132 | 95 | 97 | 243 | 214 | 258 | 163 | 148 | 517 | 556 | 232 | 235 | 284 | 816 | 496 | 347 | 368 | 506 | 175 | 159 | 436 |
| 1 / 117 . | 388 | 128 | 97 | 97 | 240 | 217 | 238 | 161 | 148 | 527 | 568 | 218 | 226 | 283 | 786 | 491 | 330 | 363 | 514 | 174 | 152 | 433 |
| 1 / 118 . | 377 | 129 | 94 | 98 | 255 | 236 | 251 | 162 | 149 | 537 | 506 | 224 | 232 | 281 | 793 | 497 | 331 | 356 | 529 | 158 | 157 | 439 |
| 1 / 119 . | 377 | 131 | 96 | 97 | 225 | 230 | 256 | 157 | 149 | 502 | 552 | 233 | 233 | 291 | 734 | 495 | 345 | 363 | 522 | 153 | 155 | 441 |
| 1 / 120 . | 371 | 131 | 97 | 97 | 246 | 230 | 236 | 163 | 150 | 506 | 577 | 227 | 227 | 288 | 758 | 493 | 351 | 355 | 525 | 166 | 150 | 450 |
| Average | 377 | 131 | 101 | 94 | 237 | 227 | 260 | 164 | 150 | 529 | 551 | 228 | 237 | 289 | 795 | 483 | 350 | 373 | 521 | 163 | 154 | 456 |

Table b: survey of museum assemblage

| Accn No | Field No | Description | Composition | Room No |
|-------------|-----------|--|----------------|-------------------|
| 1930.13B.3 | 30-11-8 | glazed mudbrick, opaque yellowish glaze | glazed ceramic | H11 |
| 1930.14.1 | | glazed lion figurine, green glaze | glazed ceramic | |
| 1930.14.10 | | glazed offering stand | glazed ceramic | G50 |
| 1930.14.32 | | glazed lion figurine | glazed ceramic | |
| 1930.14.6 | | glazed socket, white glaze | glazed ceramic | |
| 1930.14.9 | | glazed object, patchy green glaze | glazed ceramic | |
| 1930.15.1 | | glazed vessel | glazed ceramic | |
| 1930.15.2 | 29-12-203 | glazed bowl | glazed ceramic | Grave 32 |
| 1930.15.4 | | glazed vessel dark green glaze in places | glazed ceramic | |
| 1930.15.5 | | glazed vessel, lustrous green glaze | glazed ceramic | G101 (grave) |
| 1930.15.6 | | glazed vessel, friable glaze layer | glazed ceramic | |
| 1930.15.7 | | glazed vessel, friable glaze layer | glazed ceramic | 430-2 |
| 1930.15.8 | 29-12-390 | glazed vessel, small green-glazed | glazed ceramic | |
| 1930.15.9 | | glazed vessel, turquoise-green glaze | glazed ceramic | |
| 1930.16.3 | | glazed vessel, blue glaze | glazed ceramic | Zigi 30 |
| 1930.16.4 | 28-11-418 | glazed vessel | glazed ceramic | S219 |
| 1930.46.3 | | glazed vessel fragment, lustre ware | glazed ceramic | |
| 1930.47.14 | | blue frit vessel fragment | frit | G29 |
| 1930.49.59 | | glazed vessel fragments | glazed ceramic | |
| 1930.49.60 | | glazed vessel fragment, green glaze | glazed ceramic | |
| 1930.52.07 | | glazed vessel fragment | glazed ceramic | W11 |
| 1930.52.08 | | glazed vessel fragment | glazed ceramic | H10 |
| 1930.52.1 | | 70 glazed vessel fragments most with room numbers | glazed ceramic | |
| 1930.52.1 | | two colourless vessel fragments | glass | |
| 1930.52.2 | | numerous glazed vessel fragments | glazed ceramic | |
| 1930.52.2 | | Figurine fragment | glass | |
| 1930.52.3 | | six glazed vessel fragments | glazed ceramic | |
| 1930.52.4 | | glazed vessel fragments | glazed ceramic | G63, L4, G32, H20 |
| 1930.52.5 | | glazed vessel fragments | glazed ceramic | |
| 1930.52.6 | | numerous glazed vessel fragments | glazed ceramic | |
| 1930.57.4 | 31-2-11 | faience vessel fragment | faience | G29 |
| 1930.5B.1 | | glazed lion fragment, red paint yellowish glaze | glazed ceramic | |
| 1930.5B.137 | | glazed lion fragment, red paint yellowish glaze | glazed ceramic | G50 |
| 1930.60.1 | 28-11-190 | Two beads | stone | S105 |
| 1930.60.10 | 31-2-122 | One inlaid oblong bead | glass | G53 |
| 1930.60.100 | 30-2-304 | One large spherical bead | | H16 |
| 1930.60.101 | 30-2-310 | 22 small beads; three blue; one ? Black | frit/faience | H15 |
| 1930.60.102 | 30-2-330 | Four spherical beads | ? | H6 |
| 1930.60.106 | 30-2-357 | Four beads | ? | G55 |
| 1930.60.109 | 30-2-361 | one white fragment | ? | H15 |
| 1930.60.111 | 30-2-405 | c36 various beads inc six blue f/fr | various | H14 |
| 1930.60.112 | 30-2-417 | 30 various beads inc: two ?inlaid; four blue f/fr; one yellow | various | H8 |
| 1930.60.113 | 30-2-420 | 36 various beads inc: three blue f/fr; one ?glass; two ?inlaid glass; one red f/fr | various | H18 |
| 1930.60.114 | 30-2-428 | 20 beads; inc 1 yellow f/fr; 2 blue f/fr | various | H15 |
| 1930.60.12 | | two stone beads one ?fragments of yellow glaze | stone | unknown |
| 1930.60.125 | 30-11-4 | One spherical bead | ? | H14 |
| 1930.60.126 | 30-1-86 | One spherical bead | ? | L4 |
| 1930.60.128 | 30-11-104 | One bead | ? | H42 |
| 1930.60.135 | 31-12-215 | Eight beads | ? | G50 |
| 1930.60.136 | 31-1-134 | One spherical bead ?inlaid | ? | Gr54 |
| 1930.60.137 | 31-3-14 | Five beads; one blue f/fr | ? | H14 |
| 1930.60.138 | 31-3-22 | 21 very small beads; inc 4 blue f/fr; 1 yellow f/fr; | frit/faience | H7 |
| 1930.60.139 | 28-11-205 | One very small blue bead | frit/faience | S107 |
| 1930.60.140 | 30-2-112 | 100s beads; various colours inc blue glass and yellow f/fr | various | G50 |
| 1930.60.143 | | Five beads; two ?glass; two white; one blue f/fr | various | unknown |

| | | | | |
|-------------|-----------|---|--------------|---------|
| 1930.60.144 | 30-2-406 | One striped bead | ? | H14 |
| 1930.60.148 | 28-12-589 | One fragment ?yellow ?glass bead | ?glass | S158 |
| 1930.60.17 | 30-12-259 | three beads, two frit/faience | various | H12 |
| 1930.60.2 | 28-11-444 | two modern beads | frit/faience | unknown |
| 1930.60.27 | 28-11-328 | One frit bead ?colour | frit | unknown |
| 1930.60.30 | 28-12-429 | six ?modern glass beads | glass | unknown |
| 1930.60.33 | 28-12-265 | frit bead ?colour | frit | S132 |
| 1930.60.35 | 28-12-348 | small ?glass bead | ? | S178 |
| 1930.60.36 | 28-12-433 | tiny blue frit bead | frit | K333 |
| 1930.60.37 | 28-12-531 | One glass/glazed bead | ?glass | P310 |
| 1930.60.38 | 28-12-559 | One glass/glazed bead | ?glass | unknown |
| 1930.60.39 | 30-2-39 | Eight frit beads blue/yellow | frit | G29 |
| 1930.60.4 | 28-12-240 | three black beads, two frit/faience | various | unknown |
| 1930.60.40 | 29-01-98- | inlaid bead | glass | unknown |
| 1930.60.404 | 30-2-341 | Four spherical beads | ? | H11 |
| 1930.60.405 | 30-2-346 | One large, five small beads ? Black ? polychrome | ? | G55 |
| 1930.60.41 | 29-1-205 | One spherical yellow bead ?glass/frit | ? | P416 |
| 1930.60.42 | 29-1-206 | One spherical ?glass bead | ?glass | U410 |
| 1930.60.43 | 29-1-366 | Small ?glass/frit bead | ?glass | N120 |
| 1930.60.44 | 29-1-366 | Small ?glass/frit bead ?yellow | ?glass | P349 |
| 1930.60.446 | | Two cylindrical beads; blue, ?polychrome | ?glass | unknown |
| 1930.60.45 | 29-1-368 | Small ?glass/frit bead | ?glass | P400 |
| 1930.60.47 | 29-2-103 | One small bead ?glass yellow | ?glass | P464 |
| 1930.60.48 | 29-3-3 | 17 frit/faience beads blue/white | frit | N120 |
| 1930.60.49 | 29-3-9 | Small cylindrical bead | ? | P464 |
| 1930.60.50 | 29-3-26 | One small blue bead | frit/faience | N120 |
| 1930.60.51 | 29-11-17 | One small bead | ? | B2 |
| 1930.60.53 | 29-12-7 | One round bead frit blue | frit | unknown |
| 1930.60.56 | 29-12-106 | two barrel beads; ?black | ? | Gr6 |
| 1930.60.57 | 29-12-107 | One small squarish bead | ? | Gr6 |
| 1930.60.58 | 29-12-111 | One small squarish bead | ? | Gr6 |
| 1930.60.61 | 29-12-119 | One spherical bead ?marbled | ? | Gr6 |
| 1930.60.62 | 29-12-138 | one small bead | ? | B30 |
| 1930.60.63 | 29-12-145 | Four tiny beads blue | frit/faience | F14 |
| 1930.60.66 | 29-12-243 | One large spherical bead | ? | unknown |
| 1930.60.67 | 29-12-274 | six very small beads | ? | F19 |
| 1930.60.69 | 29-12-292 | One spherical bead | ? | G24 |
| 1930.60.70 | 29-12-313 | two rough beads | ?glass | G26 |
| 1930.60.71 | 29-12-317 | fragment, small, ? yellow | ? | F30 |
| 1930.60.73 | 30-1-204 | Fragments | ?glass | G29 |
| 1930.60.75 | 30-3-66 | three very small beads blue | frit/faience | G41 |
| 1930.60.76 | 30-1-67 | Five tiny beads | ? | G29 |
| 1930.60.77 | 30-12-49 | One barrel bead | ? | M8 |
| 1930.60.79 | 30-1-92 | spherical bead | ? | C22 |
| 1930.60.80 | 30-1-114 | Small round bead | ? | H6 |
| 1930.60.82 | 30-1-136 | Two spacer beads, blue | frit/faience | C6 |
| 1930.60.83 | 30-1-216 | numerous beads; one yellow | ? | G29 |
| 1930.60.84 | 30-1-217 | numerous beads; 4 yellow f/fr | various | G29 |
| 1930.60.85 | 30-1-218 | 10 spherical beads | ? | G29 |
| 1930.60.86 | 30-2-38 | Seven very small beads | ? | G29 |
| 1930.60.88 | 30-2-50 | three large spherical beads | ? | G29 |
| 1930.60.89 | 30-2-70 | 11 various beads; 1 yellow f/fr | ? | G53 |
| 1930.60.90 | 30-2-95 | two light blue beads | frit/faience | G50 |
| 1930.60.91 | 30-2-103 | Numerous tiny beads; bl f/fr; 1red f/fr; 1 red ?glass | various | G50 |
| 1930.60.92 | 30-2-186 | One ?glazed bead | ? | H20 |
| 1930.60.95 | 30-2-227 | 21 beads; 4 blf/fr; 1 ?inlaid | various | F2 |
| 1930.60.98 | 30-2-296 | 14 beads; 2 blf/fr; 1?gl; 1 yf/fr; 1 inlaid/painted | various | C30 |

| | | | | |
|-------------|-----------|--|--------------|---------|
| 1930.61.1 | 28-11-7 | One melon bead | ? | House T |
| 1930.61.10 | 28-11-259 | One small melon bead, blue | frit/faience | (?)209 |
| 1930.61.100 | 30-2-297 | One double bead, blue | frit/faience | C30 |
| 1930.61.101 | 30-2-313 | two spacer beads | ? | H15 |
| 1930.61.102 | 30-2-324 | Four spacer beads, blue one white | frit/faience | G29 |
| 1930.61.104 | 30-2-353 | One spacer bead, blue | frit/faience | C29 |
| 1930.61.107 | 30-2-352 | One hubbed bead, light blue | frit/faience | C29 |
| 1930.61.108 | 30-2-364 | One spacer bead, b` | frit/faience | H12 |
| 1930.61.11 | 28-11-292 | One spacer bead, white | ? | S110 |
| 1930.61.110 | 30-2-410 | three melon beads, blue, white | frit/faience | H14 |
| 1930.61.111 | 30-2-411 | Two spacer beads, blue | frit/faience | H14 |
| 1930.61.112 | 30-2-419 | Six beads, blue, black | frit/faience | H8 |
| 1930.61.115 | 30-2-60 | Four spacer beads + fragments | ?glass | G53 |
| 1930.61.116 | 29-1-47 | One spacer bead | ?stone | G67 |
| 1930.61.117 | 30-2-217 | One white bead | ? | G29 |
| 1930.61.119 | 30-12-256 | one melon bead, light blue | frit/faience | G73 |
| 1930.61.12 | 28-11-320 | One spacer bead | ? | S110 |
| 1930.61.123 | | Five beads, one large hubbed bead blue/yellow ?glass; four f/fr | various | unknown |
| 1930.61.124 | | 109 beads inc: blue f/fr, one red f/fr | frit/faience | unknown |
| 1930.61.125 | | numerous beads inc blue f/fr | various | unknown |
| 1930.61.126 | 30-2-117 | 32 beads, black, blue, white | frit/faience | G50 |
| 1930.61.128 | 30-2-202 | three melon beads, blue, white | frit/faience | G29 |
| 1930.61.129 | 30-1-211 | Spacer bead fragments | ?glass | G29 |
| 1930.61.13 | 28-11-324 | One spacer bead, blue | frit/faience | S111 |
| 1930.61.130 | 30-2-338 | Six beads, various, black, blue, white | frit/faience | F2 |
| 1930.61.131 | 30-2-343 | Six beads, various, black, blue, white | frit/faience | H10 |
| 1930.61.132 | 30-2-422 | Six beads, various, black, blue, white, one yellow | frit/faience | H18 |
| 1930.61.133 | 29-1-296 | One spacer bead, light blue | frit/faience | unknown |
| 1930.61.135 | 29-11-205 | one spacer fragment | ? | Gr8 |
| 1930.61.136 | 30-2-69 | One melon bead | ? | G53 |
| 1930.61.144 | | various beads, stone/fr/shell: 1 yello f/fr, two white ?glass, five spacer | various | unknown |
| 1930.61.16 | 28-12-100 | One tiny dark blue bead | frit/faience | S156 |
| 1930.61.2 | 30-11-89 | One barrel bead, ?yellow | ? | (?)202 |
| 1930.61.26 | 29-1-19 | One spacer bead | ? | P322 |
| 1930.61.3 | 30-1-70 | One ?inlaid bead | ? | G29 |
| 1930.61.30 | 30-1-73 | One spacer bead | ?glass | G29 |
| 1930.61.33 | 29-1-335 | One tiny spherical bead, blue | frit/faience | P400 |
| 1930.61.35 | 29-1-367 | One spacer fragment | ? | K432 |
| 1930.61.36 | 29-1-369 | One spacer fragment, ?trailed decoration | ? | P309 |
| 1930.61.40 | 29-2-27 | One melon bead | ? | P360 |
| 1930.61.46 | 29-2-255 | one spacer bead | ? | K443 |
| 1930.61.47 | 29-2-323 | One hubbed bead, blue | frit/faience | P482 |
| 1930.61.48 | 29-2-325 | One small melon bead, blue | frit/faience | R96 |
| 1930.61.53 | 28-11-75 | One hubbed bead, blue (tiny) | frit/faience | unknown |
| 1930.61.55 | 29-11-140 | One spacer fragment, blue | frit/faience | unknown |
| 1930.61.56 | 29-11-152 | One spacer fragment, blue | frit/faience | B4 |
| 1930.61.57 | 29-11-158 | One spacer fragment | ? | B20 |
| 1930.61.58 | 29-11-82 | One spacer fragment, blue | frit/faience | unknown |
| 1930.61.65 | 29-12-312 | one flat bead | ? | G26 |
| 1930.61.66 | 29-12-316 | One small bead, blue | frit/faience | G37 |
| 1930.61.68 | 29-12-86 | One spacer fragment | ? | C18 |
| 1930.61.7 | 28-11-247 | One bead | ?glass | S111 |
| 1930.61.70 | 29-12-65 | One small melon bead | ? | Gr13 |
| 1930.61.71 | 30-1-98 | One small melon bead | ? | G28 |
| 1930.61.73 | 30-1-113 | One spacer bead, dark blue | frit/faience | F2 |
| 1930.61.74 | 30-1-163 | one large melon bead, blue | ? | G78 |
| 1930.61.77 | 30-1-208 | two beads | ? | G29 |

| | | | | |
|--------------|-----------|---|--------------|---------|
| 1930.61.78 | 30-1-212 | two spacer fragments | ? | G29 |
| 1930.61.79 | 30-1-213 | two spacer beads; one yellow; one ?glass | ?glass | G29 |
| 1930.61.8 | 28-11-252 | One spacer bead. Blue | frit/faience | S111 |
| 1930.61.81 | 30-2-36 | two hubbed beads,yellow | ? | G29 |
| 1930.61.82 | 30-2-54 | One melon bead | ? | G29 |
| 1930.61.83 | 30-2-58 | Seven spacer beads | ? | G53 |
| 1930.61.84 | 30-2-60 | two melon beads, blue | frit/faience | G53 |
| 1930.61.85 | 30-2-61 | Five spacer beads; four ?glass | ?glass | G53 |
| 1930.61.86 | 30-2-67 | Large melon bead, blue | frit/faience | G53 |
| 1930.61.87 | 30-2-76 | One spacer fragment | ? | G53 |
| 1930.61.88 | 30-2-91 | Numerous spacer beads | various | G50 |
| 1930.61.89 | 30-2-97 | Numerous spacer beads, blue | frit/faience | G50 |
| 1930.61.9 | 28-11-253 | One small melon bead, blue | frit/faience | S107 |
| 1930.61.90 | 30-2-102 | Numerous beads; blue, black, white | ? | G50 |
| 1930.61.91 | 30-2-104 | Numerous tiny beads; blue, black, red, yello | frit/faience | G50 |
| 1930.61.94 | 30-2-226 | Four small melon beads, one black, one blue | frit/faience | F2 |
| 1930.61.95 | 30-2-233 | One spacer bead, white | ? | F2 |
| 1930.61.96/7 | 30-2-286 | Two large melon beads, black, blue | frit/faience | H16 |
| 1930.61.98 | 30-2-292 | Two beads; melon/spacer, blue | frit/faience | C43 |
| 1930.61.99 | 30-2-295 | One spacer bead, blue | frit/faience | C4 |
| 1930.62.10 | 28-12-94 | One amulet | ?tc | unknown |
| 1930.62.101 | 30-2-407 | Numerous beads inc: 3 yellow ?glass, some blue, red | frit/faience | H14 |
| 1930.62.102 | 30-2-414 | three beads, blue f/fr, ?glass | various | G23 |
| 1930.62.103 | 30-2-416 | several beads inc: two large cylindrical glass, blue f/fr, yellow, f/fr | various | H8 |
| 1930.62.103 | | various beads, some ?inlaid | ? | unknown |
| 1930.62.104 | 30-2-42 | several beads: one ?glass inlaid, two blue f/fr, one yellow f/fr | various | G29 |
| 1930.62.105 | 30-2-429 | Eight cylindrical beads, two blue f/fr, two ?glass | various | H15 |
| 1930.62.106 | 30-3-19 | One cylindrical bead, ?blue | ?glass | H35 |
| 1930.62.107 | 30-1-72 | One cylindrical bead, ?blue | ?glass | G29 |
| 1930.62.108 | 30-12-170 | two beads, blue | frit/faience | L4 |
| 1930.62.109 | 30-2-365 | two melon beads, blue | frit/faience | H12 |
| 1930.62.109 | 31-1-146 | One tiny bead, white | frit/faience | G29 |
| 1930.62.110 | 31-2-16 | One cylindrical bead | ? | H5 |
| 1930.62.111 | 31-2-25 | One cylindrical bead | ?stone | G29 |
| 1930.62.112 | 31-2-30 | One ?bead | ? | G78 |
| 1930.62.113 | 31-2-45 | One cylindrical fragment | ? | L4 |
| 1930.62.115 | | Numerous tiny beads, white | ? | unknown |
| 1930.62.116 | 28-12-203 | One spacer fragment | ?glass | unknown |
| 1930.62.117 | 29-12-307 | Two cylindrical beads; white | ? | F22 |
| 1930.62.12 | 28-12-185 | One tiny bead, blue | frit/faience | (?)146 |
| 1930.62.13 | 28-12-205 | One large disc bead | ?stone | C51 |
| 1930.62.14 | 28-12-266 | one cylindrical bead | ? | (?)173 |
| 1930.62.16 | 28-12-426 | One large disc bead, blue | frit/faience | P310 |
| 1930.62.17 | 28-12-548 | One tiny bead, blue | frit/faience | P360 |
| 1930.62.18 | 29-11-42 | One tiny bead, blue | frit/faience | P387 |
| 1930.62.19 | 29-12-50 | One ?inlaid bead | ? | Gr24 |
| 1930.62.21 | 29-1-129 | one large bead | ? | unknown |
| 1930.62.22 | 29-1-131 | Nine cylindrical beads, blue+white | frit/faience | N383 |
| 1930.62.23 | 29-1-151 | One tiny bead, white | ? | (?)391 |
| 1930.62.25 | 29-1-306 | One tiny bead, blue | frit/faience | P401 |
| 1930.62.26 | 29-1-330 | One small bead, blue | frit/faience | P400 |
| 1930.62.27 | 29-1-87 | One large cylindrical bead | ? | P399 |
| 1930.62.29 | 29-1-469 | One tiny bead, blue | frit/faience | P341 |
| 1930.62.30 | 29-2-11 | one large cylindrical bead | ? | P309 |
| 1930.62.31 | 29-2-20 | One tiny bead, blue | frit/faience | L11/20 |
| 1930.62.32 | 29-2-110 | one barrel bead | ? | unknown |
| 1930.62.34 | 29-2-148 | one tiny bead, light blue | frit/faience | K453 |

| | | | | |
|------------|-----------|---|--------------|---------|
| 1930.62.36 | 29-2-254 | one cylindrical bead, ?burnt | ? | L11 |
| 1930.62.37 | 31-3-37 | One cylindrical bead | ?glass | P387 |
| 1930.62.38 | 29-1-53 | One cylindrical bead | ?glass | P351 |
| 1930.62.4 | 28-11-255 | One bead | ?glass | unknown |
| 1930.62.41 | 29-11-178 | one large cylindrical bead, blue | frit/faience | Gr8 |
| 1930.62.42 | 29-11-182 | One cylindrical bead, blue | ?glass | I2 |
| 1930.62.43 | 29-12-2 | One tiny bead, wluce | frit/faience | B2 |
| 1930.62.44 | 29-1-334 | One small bead, blue | frit/faience | P326 |
| 1930.62.45 | 29-12-98- | three tiny beads, blue | frit/faience | F1 |
| 1930.62.46 | 29-12-103 | One tiny bead, white | ? | F1 |
| 1930.62.48 | 29-12-133 | two beads | ?glass | Gr6 |
| 1930.62.49 | 29-12-185 | one barrel bead, white | ? | B33 |
| 1930.62.5 | 28-11-258 | Nine tiny beads, blue, yellow | frit/faience | S108 |
| 1930.62.50 | 29-12-192 | One cylindrical bead, white | ? | B36 |
| 1930.62.52 | 29-12-233 | One inlaid bead, blue | glass | C12 |
| 1930.62.54 | 29-12-275 | one cylindrical bead, blue | frit/faience | F19 |
| 1930.62.56 | 29-12-308 | One cylindrical bead + fragments, blue | frit/faience | F18 |
| 1930.62.59 | 29-12-365 | one cylindrical bead, blue | frit/faience | F24 |
| 1930.62.6 | 28-11-307 | One small disc bead | ? | unknown |
| 1930.62.60 | 30-1-6 | One spacer fragment, dark blue | frit/faience | F35 |
| 1930.62.61 | 28-11-34 | One tiny bead, blue | frit/faience | H2 |
| 1930.62.62 | 29-12-38 | One cylindrical bead, small, blue | frit/faience | G29 |
| 1930.62.63 | 29-12-56 | one large cylindrical bead | ? | Gr24 |
| 1930.62.65 | 30-3-62 | one cylindrical bead, ?painted | ? | G41 |
| 1930.62.67 | 30-1-107 | numerous tiny beads, yellow | ? | G32 |
| 1930.62.68 | 30-1-209 | Five beads, three ?inlaid glass, two blue f/fr | various | G29 |
| 1930.62.69 | 30-2-24 | One cylindrical bead | ? | B38 |
| 1930.62.70 | 30-2-32 | Two large cylindrical beads | ? | G29 |
| 1930.62.71 | 30-2-53 | Three large cylindrical beads | ? | G29 |
| 1930.62.72 | 30-2-34 | Five large cylindrical beads | ? | G29 |
| 1930.62.73 | 30-2-40 | 11 cylindrical beads blue, black | frit/faience | G29 |
| 1930.62.74 | 30-2-62 | six cylindrical beads, three ?glass | ?glass | G53 |
| 1930.62.75 | 30-2-65 | one cylindrical bead, blue | frit/faience | G53 |
| 1930.62.77 | 30-2-73 | three ?inlaid beads + frags | ? | G53 |
| 1930.62.78 | 30-2-74 | Numerous inlaid beads | ?glass | G53 |
| 1930.62.79 | 30-2-68 | Two ribbed beads, blue | frit/faience | G53 |
| 1930.62.79 | 30-2-75 | 17 various beads, blue, one black | frit/faience | G53 |
| 1930.62.8 | 28-11-506 | one bead | ?stone | L2 |
| 1930.62.80 | 30-2-84 | One bead, white | ? | G53 |
| 1930.62.81 | 30-2-100 | 262 beads mostly blue, few red | frit/faience | G50 |
| 1930.62.82 | 30-2-111 | Numerous square beads incl two yellow?glass | various | G50 |
| 1930.62.83 | | numerous beads, some red f/fr | various | unknown |
| 1930.62.84 | 30-2-114 | 350 beads incl: yellow ?glass | ?glass | G50 |
| 1930.62.85 | 30-2-140 | two double beads | ?glass | G50 |
| 1930.62.86 | 30-2-148 | one very large cylindrical bead | ? | H27 |
| 1930.62.87 | 30-2-176 | one cylindrical bead | ? | H33 |
| 1930.62.88 | 30-2-182 | one cylindrical bead tiny, blue | frit/faience | H40 |
| 1930.62.89 | 30-2-220 | one cylindrical bead | ? | G29 |
| 1930.62.9 | 29-12-58 | Three disc beads | ?stone | Gr24 |
| 1930.62.90 | 30-2-229 | 14 cylindrical beads: four blue f/fr, two black, two ?glass | various | F2 |
| 1930.62.92 | 30-2-273 | Sic squarish beads | ? | G57 |
| 1930.62.94 | 30-2-321 | One squarish bead | ? | C30 |
| 1930.62.95 | 30-2-326 | 10 beads, black, blue, red | ? | H7 |
| 1930.62.96 | 30-2-339 | One cylindrical bead, ?painted/inlaid | ? | F2 |
| 1930.62.97 | 30-2-340 | Five beads (four cylindrical) | ? | H11 |
| 1930.62.99 | 30-2-349 | three beads, blue, white | frit/faience | C28 |
| 1930.63.1 | 28-11-348 | One squarish bead | ? | unknown |

| | | | | |
|-------------|-----------|---|--------------|---------|
| 1930.63.11 | 29-11-120 | One flat bead, blue | frit/faience | Gr6 |
| 1930.63.13 | 29-12-59 | One eye bead | ?glass | Gr24 |
| 1930.63.15 | 29-12-124 | One flat bead, white | ?glass | C2 |
| 1930.63.16 | 29-12-121 | One cylindrical bed | ? | Gr6 |
| 1930.63.17 | 29-12-163 | One flat bead, blue | frit/faience | F2 |
| 1930.63.18 | 29-12-213 | one cylindrical bead | ?glass | Gr26 |
| 1930.63.19 | 29-12-254 | one cylindrical bead | ?glass | F26 |
| 1930.63.2 | 28-11-400 | One inlaid bead | ?glass | unknown |
| 1930.63.20 | 29-12-266 | One eye bead | ?glass | F30 |
| 1930.63.21 | 29-12-280 | Two beads | ? | G37 |
| 1930.63.22 | 29-12-347 | One eye bead | ?glass | B19 |
| 1930.63.23 | 30-1-20 | Three flat beads, blue, white | frit/faience | F2 |
| 1930.63.25 | 30-1-103 | One bead | ?stone | unknown |
| 1930.63.27 | 30-2-37 | Five flat beads, white, yellow | frit/faience | G29 |
| 1930.63.28 | 30-2-73 | one flat bead | frit/faience | G53 |
| 1930.63.29 | 30-2-47 | c12 eye beads | ?glass | G29 |
| 1930.63.3 | 28-12-183 | One flat bead, yellow | frit/faience | M2 |
| 1930.63.30 | 30-2-56 | One bead, blue | frit/faience | G29 |
| 1930.63.31 | 30-2-69 | Various beads incl: ?glass, f/fr, stone, blue, black, white | various | G53 |
| 1930.63.32 | 30-2-72 | 8 eye beads | ?glass | G53 |
| 1930.63.33 | 30-2-82 | One flat bead | ? | G53 |
| 1930.63.34 | 30-2-83 | two flat beads | ?glass | G53 |
| 1930.63.36 | 30-2-96 | 34 beads, incl: large cylindrical and fragments some ?burnt ?glass | various | G50 |
| 1930.63.37 | 30-2-99 | Numerous beads, incl eye beads | various | G50 |
| 1930.63.38 | 30-2-106 | Seven beads, inc rhomboid, yellow/blue?glass | ?glass | G50 |
| 1930.63.39 | 30-2-107 | Five beads, black | ? | G50 |
| 1930.63.4 | 28-12-202 | One flat bead, yellow | frit/faience | S130 |
| 1930.63.40 | 30-2-115 | 315 beads incl: ?yellow glass, ?inlaid glass | various | G50 |
| 1930.63.41 | 30-2-116 | 12 beads blue | frit/faience | G50 |
| 1930.63.42 | 30-2-120 | Five eye beads | ?glass | G50 |
| 1930.63.43 | 30-2-230 | Three inlaid beads | ?glass | F2 |
| 1930.63.44 | 30-2-285 | One flat bead, blue | frit/faience | H10 |
| 1930.63.45 | 30-2-299 | 7 beads, cylindrical one ?inlaid | ?glass | C30 |
| 1930.63.46 | 30-2-302 | one flat bead | ? | H7 |
| 1930.63.47 | 30-2-311 | Five cylindrical beads, one ?glass | ? | H15 |
| 1930.63.48 | 30-2-314 | One squarish bead | ?stone | H15 |
| 1930.63.49 | 30-2-344 | Three beads, one ?glass | ? | H10 |
| 1930.63.5 | 28-12-551 | One spherical bead, yellow | ?glass | K303 |
| 1930.63.50 | 30-2-367 | One flat bead, blue | frit/faience | G47 |
| 1930.63.51 | 30-2-406 | 20 various, some inlaid, ?glass | various | H14 |
| 1930.63.52 | 30-2-409 | Two eye beads | ?glass | H14 |
| 1930.63.53 | 30-2-418 | Nine beads incl inlaid and ?glass | ?glass | H8 |
| 1930.63.54 | 30-2-435 | One eye bead | ?glass | H15 |
| 1930.63.55 | 30-1-59 | One bead yellow glazed | ?faience | H5 |
| 1930.63.56 | 28-12-60 | One ?inlaid bead | ?glass | Gr24 |
| 1930.63.57 | 30-11-28 | One large cylindrical bead | ? | L4 |
| 1930.63.58 | 30-12-216 | Five barrel beads | ? | G50 |
| 1930.63.59 | 31-3-20 | 11 beads incl: ?glass, shell, stone, yellow f/fr | various | G32 |
| 1930.63.6 | 29-1-406 | One flat bead | ? | P313 |
| 1930.63.60 | | 31 various beads incl ?glass f/fr | various | unknown |
| 1930.63.61 | 30-2-113 | Various beads incl: ?glass, and very deteriorated yellow, pink, green | various | G50 |
| 1930.63.7 | 29-1-556 | One bead, white | ? | N120 |
| 1930.63.9 | 29-2-99 | One bead, white | ? | P445 |
| 1930.65.157 | 29-12-370 | one bead | ?stone | unknown |
| 1930.66.103 | 30-2-335 | two spherical beads | ? | C37 |
| 1930.66.14 | 30-1-44 | one bead | ?glass | Gr24 |
| 1930.66.15 | 29-2-44 | Numerous tiny beads | frit/faience | Gr24 |

| | | | | |
|------------|-----------|--|--------------|---------|
| 1930.66.18 | 30-12-51 | One bead yellow | ?faience | G67 |
| 1930.66.20 | 29-11-56 | Numerous tiny beads, ?some glazed | ? | W4 |
| 1930.66.21 | 29-11-57 | One spherical bead, blue | ? | B4 |
| 1930.66.27 | 29-12-204 | One spherical bead, blue | ? | Gr25 |
| 1930.66.28 | 29-12-205 | one spherical bead, white | ?glass | Gr25 |
| 1930.66.35 | 30-2-35 | Five large cylindrical beads | various | G29 |
| 1930.66.36 | 30-2-79 | One flat bead, blue | frit/faience | G53 |
| 1930.66.38 | 30-2-135 | Numerous tiny beads, blue, white, yellow | frit/faience | G29 |
| 1930.66.43 | 30-2-413 | Six beads | frit/faience | G23 |
| 1930.66.45 | 30-2-288 | three beads, blue f/fr, ?glass | various | C39 |
| 1930.66.49 | | Two eye beads | ?glass | unknown |
| 1930.66.57 | 31-1-90 | One spherical bead | ?clay | unknown |
| 1930.66.58 | 31-1-127 | two beads | ? | L4A |
| 1930.66.61 | 31-1-130 | One bead, blue, ?glazed | ? | L4A |
| 1930.66.63 | 31-2-20 | one large bead | ?stone | H7 |
| 1930.66.64 | 31-2-46 | one bead | ?stone | L4 |
| 1930.66.66 | | Seven beads incl eye beads, cylindrical, spherical and inlaid | ?glass | G50 |
| 1930.66.72 | | 37 various spherical beads, some inlaid | ? | unknown |
| 1930.66.73 | | Fragment, white | ?glass | unknown |
| 1930.66.84 | | Numerous small beads blue, one pink | frit/faience | unknown |
| 1930.66.85 | | 132 various spherical beads, some inlaid | ? | unknown |
| 1930.66.86 | | 339 various spherical beads | ? | unknown |
| 1930.66.88 | | 279 various spherical beads | ? | unknown |
| 1930.66.89 | | 137 various cylindrical beads, some glass, spherical blue f/fr beads used as inserts | various | unknown |
| 1930.66.90 | | Numerous cylindrical beads, most glass, some f/fr; some stone | various | G29 |
| 1930.66.99 | | Amulet, blue | frit/faience | unknown |
| 1930.67.10 | 29-1-122 | Five cylindrical beads | ? | N383 |
| 1930.67.11 | 29-1-123 | Two frog beads | frit/faience | N392 |
| 1930.67.12 | 29-1-150 | one fly bead, blue | frit/faience | (?)412 |
| 1930.67.13 | 29-2-19 | One bead, blue | frit/faience | P467 |
| 1930.67.14 | 30-1-42 | Three beads | ?glass | P470 |
| 1930.67.15 | 29-2-107 | Three beads, one yellow | ?glass | P470 |
| 1930.67.16 | 29-12-51 | One cylindrical bead, white | ? | Gr24 |
| 1930.67.17 | 29-11-149 | One incised fragment | ?stone | F8 |
| 1930.67.18 | 29-11-156 | Large fluted bead | ?glass | F8 |
| 1930.67.2 | 28-11-108 | one bead, white | ?glass | unknown |
| 1930.67.20 | 29-12-123 | Three small beads | ? | Gr6 |
| 1930.67.21 | 29-12-144 | one beads | ?stone | F14 |
| 1930.67.22 | 29-12-268 | One ?inlaid bead | ? | F19 |
| 1930.67.26 | 30-1-104 | One bead | ?glass | C26 |
| 1930.67.28 | 30-2-44 | One light blue bead, ?glazed | ?faience | G29 |
| 1930.67.30 | 30-2-86 | One frog? Bead | frit/faience | G53 |
| 1930.67.31 | 30-2-88 | Lion amulet? | ? | G50 |
| 1930.67.32 | 30-2-105 | two flat beads | frit/faience | G50 |
| 1930.67.33 | 30-2-123 | Two granulated beads, red, white | frit/faience | G50 |
| 1930.67.36 | 30-2-128 | One bird bead, white | ?glass | G50 |
| 1930.67.37 | 30-2-131 | One spacer bead, white | ? | G50 |
| 1930.67.38 | 30-2-136 | Two amulets | ?glass | G50 |
| 1930.67.4 | 28-11-430 | Two beads | ?stone | unknown |
| 1930.67.40 | 30-2-139 | Two beads | ? | G50 |
| 1930.67.42 | 30-2-141 | Three beads, white, yellow | frit/faience | G50 |
| 1930.67.43 | 30-2-142 | One bead, hexagonal | ? | G50 |
| 1930.67.44 | 30-2-144 | One eye bead | ?glass | G50 |
| 1930.67.45 | | Three pendant fragments, green/brown staining on exterior | ? | G50 |
| 1930.67.46 | 30-2-197 | two beads | ? | G50 |
| 1930.67.47 | 30-2-198 | two incised zoomorph? Beads | ? | G29 |
| 1930.67.49 | 30-2-223 | one fly bead | frit/faience | G29 |

| | | | | |
|------------|-----------|---|----------------|---------|
| 1930.67.5 | 28-12-225 | One spherical bead, white | ?glass | X147 |
| 1930.67.51 | 30-2-234 | One ?inlaid bead | ? | F2 |
| 1930.67.52 | 30-2-272 | Three cylindrical beads | ? | G57 |
| 1930.67.53 | | two beads, one yellow | frit/faience | unknown |
| 1930.67.54 | 30-2-281 | one hubbed bead | ?glass | H10 |
| 1930.67.55 | 30-2-283 | Four fluted beads | ? | H10 |
| 1930.67.56 | 30-2-284 | One rhomboidal bead | ?glass | H10 |
| 1930.67.57 | 30-2-294 | two beads, blue | frit/faience | H18 |
| 1930.67.58 | 30-2-301 | Three beads, one fluted | ?glass | H7 |
| 1930.67.59 | 30-2-312 | Three beads | frit/faience | H15 |
| 1930.67.6 | 28-12-510 | nine beads, eight blue f/fr; one white ?glass | various | P348 |
| 1930.67.60 | 30-2-331 | Three beads, blue, red, white | frit/faience | H6 |
| 1930.67.61 | 30-2-332 | Five beads inc one ?glass, white blue f/fr | various | H6 |
| 1930.67.62 | 30-2-334 | Five beads inc one ?glass | various | H14 |
| 1930.67.64 | 30-2-350 | Amulet | ? | C28 |
| 1930.67.65 | 30-2-359 | Five beads | ?glass | H10 |
| 1930.67.67 | 30-2-412 | Large fragment of plain sun disc pendant; heavy white weathering on exterior | glass | H14 |
| 1930.67.68 | 30-2-423 | One frog bead | ? | H18 |
| 1930.67.70 | 30-2-437 | One frog bead, blue | frit/faience | H15 |
| 1930.67.72 | 30-12-125 | One hubbed bead, blue | frit/faience | L4 |
| 1930.67.73 | 30-12-171 | One bead, ?burnt | ? | L4 |
| 1930.67.76 | 30-12-261 | Two beads | ? | G72 |
| 1930.67.77 | 30-12-262 | Three beads, one eye bead ?glass two blue f/fr | various | G29 |
| 1930.67.8 | 28-12-590 | Two fragments, blue | various | S158 |
| 1930.67.80 | 30-1-33 | amulet | ? | H12 |
| 1930.67.81 | | One ?form | ? | unknown |
| 1930.67.82 | 30-2-71 | Plain sun disc pendant fragments, white, chalky exterior, opaque turquoise at centre | glass | G53 |
| 1930.67.84 | 28-12-479 | Two beads, black thin.walled | ? | unknown |
| 1930.67.85 | 30-2-119 | Seven flat beads; fragments ?glass | various | G50 |
| 1930.67.86 | 30-2-148 | One double bead | ? | H27 |
| 1930.67.87 | | Nine beads/amulets, one ?glass unusual shape | various | unknown |
| 1930.67.88 | | 12 various beads inc: one ?glass, yellow f/fr | ? | unknown |
| 1930.67.89 | | One frog bead, blue | frit/faience | unknown |
| 1930.67.9 | 29-1-87 | two beads, brownish yellow | ? | P399 |
| 1930.67.90 | | Eye bead, three pendant fragments | glass | |
| 1930.67.90 | | Eye bead, three pendant fragments | glass | unknown |
| 1930.67.92 | | ? Glazed lid | glazed ceramic | |
| 1930.67.94 | | Plain sun disc pendant fragments, one greenish, one white exterior, turquoise at centre | glass | |
| 1930.67.95 | | Large plain sun disc pendant fragment, heavy weathering on exterior | glass | |
| 1930.68.1 | 29-12-112 | numerous beads | frit/faience | B25 |
| 1930.68.10 | | Numerous beads inc: inlaid ?glass; blue f/fr | various | Zigi 30 |
| 1930.68.11 | | Numerous small beads | ? | Zigi 30 |
| 1930.68.12 | | Various small beads | ? | G29 |
| 1930.68.15 | 30-2-3 | Various beads inc eye bead, ?yellow glass, spacer bead, inlaid cylindrical beads | various | G50 |
| 1930.68.16 | | Seven eye beads, ?burnt | ?glass | G50 |
| 1930.68.17 | | Various beads inc: small wrapped coarse frag; yellow bead ?comp | various | unknown |
| 1930.68.19 | | Numerous beads: blue f/fr, yellow ?comp; ?glass fragments | various | G50 |
| 1930.68.24 | | Seven beads, two ?glass | various | H18 |
| 1930.68.25 | | One melon bead | ? | H33 |
| 1930.68.28 | | Fragments | ? | unknown |
| 1930.68.30 | | Large eye bead | ?glass | unknown |
| 1930.68.7 | | One black bead, incised | ?stone | Shil 15 |
| 1930.68.73 | | Five beads, one banded | ? | H6 |
| 1930.68.9 | | Five beads; fragments ?glass | various | Shil 26 |

| | | | | |
|-------------|--------------------------------|--|----------------|---------|
| 1930.69.10 | | Numerous beads, blue + yellow f/fr; some glass fragments, some inlaid | various | unknown |
| 1930.69.12 | 30-1-12; 30-2-316; 30-2-358 | Six beads, five ?glass, one yellow ?glass | ?glass | H15/H10 |
| 1930.69.15 | | One ?painted bead | ?faience | unknown |
| 1930.69.16 | | One large bead, bright areas ?intrusive | ? | unknown |
| 1930.69.30 | | Moulded sun disc fragment; large fancy bead | glass | unknown |
| 1930.69.30 | | Moulded sun disc fragment; large fancy bead | glass | |
| 1930.69.39 | 28-12-? | Very numerous small fragments incl glass and some inlaid | various | F24 |
| 1930.69.40 | | one small bead | ? | unknown |
| 1930.69.41 | 30-12-258 | Six beads, two blue | frit/faience | G73 |
| 1930.69.42 | | Nine beads, one ?faience spacer | ? | unknown |
| 1930.69.43 | | One hubbed bead | ? | unknown |
| 1930.69.44 | | One sperical bead, large | ? | unknown |
| 1930.69.45 | | One female symbol | ?glass | |
| 1930.69.46 | | Three small melon beads | ? | unknown |
| 1930.69.47 | | One hubbed bead, blue | frit/faience | unknown |
| 1930.69.48 | | One bracelet frag | ? | |
| 1930.69.50 | | One amulet | ? | |
| 1930.69.51 | 29-11-141 | One amulet | ? | B20 |
| 1930.69.55 | 30-2-293 | Two small beads | ? | H18 |
| 1930.69.56 | 28-12-355 | One spherical bed | ? | (?)173 |
| 1930.69.57 | | One spherical bead | ?faience | unknown |
| 1930.69.58 | | Five beads, one fluted | ? | unknown |
| 1930.69.59 | | Six beads, one blue f/fr | various | unknown |
| 1930.69.60 | | Three beads | ? | unknown |
| 1930.69.61 | | One squarish bead | ? | unknown |
| 1930.69.62 | | Three beads, one yellow | ? | unknown |
| 1930.69.63 | 30-2-91 | Nine spacer beads, some ?glass | various | G50 |
| 1930.69.64 | | Several beads incl white spotted bead | ? | unknown |
| 1930.69.65 | | One bead, yellow | ?faience | unknown |
| 1930.69.66 | | Two flat beads, one ?glass | ?glass | unknown |
| 1930.69.67 | | Three fragments, | glass | unknown |
| 1930.69.68 | | One rhomboidal bead | ?glass | unknown |
| 1930.69.69 | 30-2-118 | Four fluted beads, one ?glass | various | G50 |
| 1930.69.79 | 31-2-120 | Eight beads: three ?glass, five inlaid, | ?glass | G67 |
| 1930.82..57 | 30-12-118 | Large eye bead | glass | H15 |
| 1930.82.1 | | Marbled vessel fragment, thin.walled, reddish.brown | ? | |
| 1930.82.10 | | Three vessel fragments, undecorated blue glass, black staining on one | glass | L22 |
| 1930.82.11 | | Pottery sherd with attached glass ?intrusive | glass/tc | |
| 1930.82.12 | | Colourless incised fragment ?intrusive | glass | H33 |
| 1930.82.13 | | Fluted decorated vessel fragment, white decoration, chalky exterior | glass | |
| 1930.82.14 | | Decorated vessel fragment, white/red decoration | glass | G50 |
| 1930.82.15 | | Several fragments decorated vessel(s); some yellow decoration; blue glass | glass | M79 |
| 1930.82.16 | | Undecorated vessel fragment, black staining on exterior, heavily pitted interior | glass | |
| 1930.82.17 | | Numerous fragments, undecorated blue glass, some with black staining on exterior | glass | L22 |
| 1930.82.18 | | Very large eye bead | ?glass | unknown |
| 1930.82.19 | 31-1-41 | glazed vessel , very small, white glaze | glazed ceramic | |
| 1930.82.21 | 28-11-12 | Colourless vessel fragments (late) | glass | M100 |
| 1930.82.23 | | Two fluted vessel fragments, white decorated | glass | L22 |
| 1930.82.24 | | Very large ?marbled fragments . heavily restored | ? | G29 |
| 1930.82.26 | | Mace/staff head - blue with yellow globules | glass | |
| 1930.82.3 | | Small marbled fragment red/yellow/white | ? | Zigi 33 |
| 1930.82.33 | | Greenish clear fragment | glass | |

| | | | | |
|------------|-----------|--|----------------|----------|
| 1930.82.34 | | Five thin colourless (greenish) fragments | glass | |
| 1930.82.38 | 29-12-135 | Two fragments, blue, one neck of bottle | glass | Grave 32 |
| 1930.82.39 | | Vessel fragments | glass | |
| 1930.82.4 | | Three decorated vessel fragments; yellow, white, red decoration, blue at core | glass | Shil 15 |
| 1930.82.41 | | Five colourless fragments | glass | |
| 1930.82.45 | | One colourless fragment ?faceted | glass | |
| 1930.82.46 | | One colourless fragment | glass | |
| 1930.82.47 | | Raw glass - translucent greenish numerous air bubbles | glass | |
| 1930.82.48 | | Plain sun disc pendant heavy exterior alteration, blue core | glass | H33 |
| 1930.82.49 | | ? Figurine | glass | |
| 1930.82.50 | | Raw glass fragment dark blue | glass | K62 |
| 1930.82.51 | | One fragment decorated, white/brown exterior | glass | G50 |
| 1930.82.52 | | One fragment decorated, white/brown exterior | glass | G50 |
| 1930.82.53 | | Decorated vessel fragment (bottle) set in clay matrix | glass | L8 |
| 1930.82.54 | | Raw glass fragment dark blue | glass | |
| 1930.82.55 | | Numerous small blue fragments undecorated | glass | R87/M100 |
| 1930.82.56 | | ?figurine | glass | G50 |
| 1930.82.58 | | Six small fragments | ?glass | L4 |
| 1930.82.6 | 28-12-306 | Colourless fragment ?intrusive | glass | unknown |
| 1930.82.61 | | Small decorated vessel fragments | glass | L9 |
| 1930.82.64 | | Figurine/amulet | glass | G29 |
| 1930.82.65 | | Nine fluted fragments white decoration ?restoration | glass | G29 |
| 1930.82.66 | | two fragments white/yellow decoration | glass | |
| 1930.82.67 | | Six vessel fragments white decoration | glass | |
| 1930.82.68 | | three fragments, very fine white/red decoration | glass | |
| 1930.82.69 | 30-2-333 | One fragment white decoration | glass | H14 |
| 1930.82.7 | | One small decorated vessel fragment, yellow spots on white and blue, blue core | glass | M100 |
| 1930.82.70 | | 16 fragments white decoration, some black staining, soil adhering to some surfaces | glass | G50 |
| 1930.82.71 | | Two fragments | glass | G50 |
| 1930.82.72 | | Seven fragments -white/red decoration appears uncleaned | glass | |
| 1930.82.73 | | Numerous fragments, more than one vessel restored in places "treated with A-A" | glass | G50 |
| 1930.82.74 | | Three fragments greenish tinted colourless | glass | |
| 1930.82.75 | | two fragments | ?glass | |
| 1930.82.9 | | Deteriorated glass flakes in ?soil matrix | glass | H35 |
| 1930.IC.10 | | wall nail, very thin greenish glaze | glazed ceramic | 206 |
| 1930.IC.13 | 30-12-99 | wall nail, green glaze | glazed ceramic | G50 |
| 1930.IC.16 | 30-1-152 | wall nail, very thin greenish glaze | glazed ceramic | H7 |
| 1930.IC.17 | 30-2-379 | wall nail, green glaze, metallic copper in places | glazed ceramic | G50 |
| 1930.IC.19 | 31-1-157 | wall nail, patchy greenish-white glaze | glazed ceramic | G50 |
| 1930.IC.20 | 30-1-149 | wall nail, very thin greenish glaze | glazed ceramic | G47 |
| 1930.IC.21 | 30-1-197 | wall nail, green glaze | glazed ceramic | G50 |
| 1930.IC.22 | 30-1-176 | wall nail, thick green glaze | glazed ceramic | H7 |
| 1930.IC.24 | | wall nail, green glaze | glazed ceramic | |
| 1930.IC.25 | 31-1-164 | wall nail, yellow and green glaze | glazed ceramic | G50 |
| 1930.IC.5 | 30-2-271 | wall nail, green glaze, chalky | glazed ceramic | G52 |
| 1930.IC.6 | 31-1-158 | wall nail, thick green glaze | glazed ceramic | G50 |
| 1930.IC.7 | 31-1-163 | wall nail, green glaze | glazed ceramic | G50 |
| 1930.IC.8 | 31-1-159 | wall nail, green glaze | glazed ceramic | G50 |
| 1930.IC.9 | 31-2-33- | wall nail, bulbous shape, little glaze | glazed ceramic | L4 |
| 1930.ID.1 | 28-11-80 | wall nail, restored fragments yellowish-green glaze | glazed ceramic | |
| 1930.ID.10 | 32-2-57 | wall nail fragments, patchy yellowish-green glaze | glazed ceramic | G50 |
| 1930.ID.13 | | wall nail, thick yellowish-green glaze | glazed ceramic | 348 |
| 1930.ID.14 | | wall nail, yellowish-green glaze | glazed ceramic | 344 |
| 1930.ID.16 | | wall nail, green glaze | glazed ceramic | H7 |
| 1930.ID.17 | | wall nail, thick yellowish-green glaze | glazed ceramic | |

| | | | | |
|-----------|-----------|--|-----------------------|---------|
| 1930.ID.3 | 31-1-157 | wall nail, thick glaze turquoise in places | glazed ceramic | G50 |
| 1930.ID.4 | 30-11-13 | wall nail, green glaze | glazed ceramic | H15 |
| 1930.ID.6 | 31-1-166 | wall nail, yellowish-green glaze | glazed ceramic | G50 |
| 1930.ID.7 | 31-3-38 | wall nail, yellowish-green glaze | glazed ceramic | H12 |
| 1930.ID.9 | 30-12-150 | wall nail, yellowish-green glaze | glazed ceramic | G50 |
| 1930.IH.2 | 30-11-100 | glazed object, whitish-green glaze | glazed ceramic | H11 |
| 1930.IH.4 | 30-12-220 | glazed wall decoration(?), whitish-green glaze | glazed ceramic | H11 |
| N25 | | Small marbled fragment red/yellow/white | marbelised faience | |
| N64 | | Blue pigment lump | frit | Shil 25 |

Table c: survey of finds notebooks

| Field No. | Description (notebook) | Material (notebook) | Accn No. | Room no. |
|-----------|---|---------------------|-------------|----------|
| 29-12-96 | ?glass ribbed bead | glass | | A5 |
| 29-12-360 | inlaid bead | composition | | B18 |
| 29-12-2 | blue bead | stone | 1930-62-43 | B2 |
| 29-11-17 | white spherical bead | composition | 1930-60-51 | B2 |
| 29-11-141 | yellow bead | composition | 1930-69-51 | B20 |
| 29-11-158 | spacer bead white | ?stone | 1930-61-57 | B20 |
| 29-11-158 | white spacer bead | stone | | B20 |
| 29-12-112 | group of beads, ribbed, fluted, light yellow spacer | composition | 1930-68-1 | B25 |
| 29-12-138 | light green bead | composition | 1930-60-62 | B30 |
| 29-12-185 | white bead | stone | 1930-62-49 | B33 |
| 29-12-192 | cylindrical bead | composition | 1930-62-50 | B36 |
| 30-2-24 | white bead | stone | 1930-62-69 | B38 |
| 29-11-57 | cylindrical bead | composition | 1930-66-21 | B4 |
| 29-11-152 | broken lapis bead | stone | 1930-61-56 | B4 |
| 29-11-70 | three ribbed glazed beads | composition | 1930-61-52 | B7 |
| 30-2-354 | two ribbed beads | composition | 1930-61-105 | C12 |
| 29-12-279 | blue/green cylindrical bead | stone | | C17 |
| 29-12-297 | white cylindrical bead | composition | | C19 |
| 29-12-331 | three flat and eight yellow beads | composition | | C19 |
| 29-12-124 | white bead | composition | 1930-63-15 | C2 |
| 30-1-92 | yellow spherical bead | composition | 1930-60-79 | C22 |
| 30-1-96 | black bead | stone | | C22 |
| 30-1-104 | white bead | composition | 1930-67-26 | C26 |
| 30-2-348 | decorated glass fragment | glass | | C28 |
| 30-2-349 | three cylindrical beads | composition | 1930-62-99 | C28 |
| 30-2-350 | white pendant | composition | 1930-67-64 | C28 |
| 30-2-351 | black/yellow bead | stone | | C29 |
| 30-2-353 | two blue spacer beads | composition | 1930-61-104 | C29 |
| 30-2-296 | 20 spherical beads yellow/blue/white | composition | 1930-60-98 | C30 |
| 30-2-297 | six ribbed beads | composition | 1930-61-100 | C30 |
| 30-2-298 | six cylindrical beads blue/white/black | composition | | C30 |
| 30-2-299 | four barrel beads | composition | 1930-63-45 | C30 |
| 30-2-321 | faceted bead | stone | 1930-62-94 | C30 |
| 30-2-335 | two yellow spherical beads | composition | 1930-66-103 | C37 |
| 30-2-336 | black spacer bead | composition | | C37 |
| 30-2-288 | four spherical/ribbed beads yellow/blue | composition | 1930-66-45 | C39 |
| 30-2-295 | blue spherical bead | composition | 1930-61-99 | C4 |
| 30-11-105 | white fluted bead | stone | | D15 |
| 30-11-123 | grey bead | stone | | D15 |
| 29-12-97 | light blue ribbed bead | composition | 1930-61-60 | F1 |
| 29-12-98 | three blue ribbed beads | composition | 1930-62-45 | F1 |
| 29-12-103 | white bead | stone | 1930-62-46 | F1 |
| 29-12-126 | six small blue frog beads | composition | | F1 |
| 29-12-154 | green-glazed pot | terracotta | | F10 |
| 29-12-86 | spacer bead | composition | | F11 |
| 29-12-144 | bead | composition | 1930-67-21 | F14 |
| 29-12-145 | four small blue beads | composition | 1930-60-63 | F14 |
| 29-12-183 | mother of pearl bead | stone | | F16 |
| 29-12-248 | ribbed translucent bead | stone | | F16 |
| 29-12-267 | spherical bead | composition | | F19 |
| 29-12-268 | spherical bead, painted | composition | 1930-67-22 | F19 |
| 29-12-269 | oblong white painted bead | composition | 1930-62-53 | F19 |
| 29-12-270 | frog bead | composition | 1930-67-23 | F19 |
| 29-12-271 | ribbed bead, light yellow | composition | | F19 |
| 29-12-273 | two incised blue/yellow beads | composition | | F19 |
| 29-12-274 | group of white beads | composition | 1930-60-67 | F19 |

| | | | | |
|-----------|---|-------------|-------------|-----|
| 29-12-275 | blue cylindrical bead | composition | 1930-62-54 | F19 |
| 30-1-56 | yellow/brown beads | composition | | F2 |
| 30-1-20 | flat circular bead, white | composition | 1930-63-23 | F2 |
| 29-12-163 | flat blue bead | composition | 1930-63-17 | F2 |
| 30-1-113 | spacer bead blue | composition | 1930-61-73 | F2 |
| 30-2-226 | 10 ribbed beads blue/white/black | composition | 1930-61-94 | F2 |
| 30-2-227 | 22 spherical beads blue/white/yellow | composition | 1930-60-95 | F2 |
| 30-2-228 | turquoise bead | stone | | F2 |
| 30-2-229 | 17 cylindrical beads yellow/blue/white | composition | 1930-62-90 | F2 |
| 30-2-230 | three painted barrel beads | composition | 1930-63-43 | F2 |
| 30-2-231 | lapis bead | stone | | F2 |
| 30-2-233 | white spacer bead | composition | 1930-61-95 | F2 |
| 30-2-234 | white spacer bead | composition | 1930-67-51 | F2 |
| 30-2-337 | five spherical beads yellow/blue | composition | | F2 |
| 30-2-338 | five spherical beads black/white/blue | composition | 1930-61-130 | F2 |
| 30-2-339 | five cylindrical beads blue/white | composition | 1930-62-96 | F2 |
| 29-12-239 | white bead | stone | | F24 |
| 29-12-240 | black bead | stone | | F24 |
| 29-12-290 | glazed vase | terracotta | | F24 |
| 29-12-365 | blue cylindrical bead | composition | 1930-62-59 | F24 |
| 29-12-226 | ribbed bead | composition | 1930-61-62 | F25 |
| 29-12-254 | white bead, dark paint | composition | 1930-63-19 | F26 |
| 29-12-278 | yellow spherical bead | composition | | F26 |
| 29-12-309 | white bead | stone | | F27 |
| 29-12-310 | white bead | stone | | F27 |
| 29-12-266 | button' | composition | 1930-63-20 | F30 |
| 29-12-317 | light yellow bead | composition | 1930-60-71 | F30 |
| 30-1-6 | two blue cylindrical beads | composition | | F35 |
| 30-1-19 | blue cylindrical bead | composition | 1930-62-60 | F35 |
| 29-12-358 | bird-like black bead | composition | | F37 |
| 29-11-148 | cylindrical lapis bead | stone | | F5 |
| 29-12-220 | black bead | stone | | F8 |
| 29-11-156 | greenish 'flower' bead | composition | | F8 |
| 29-3-212 | glass bead blue greenish painted | glass | 1930-67-18 | F8 |
| 30-1-78 | oblong bead | composition | | G14 |
| 29-12-348 | red bead | composition | 1930-60-72 | G14 |
| 30-1-40 | lapis bead | stone | | G18 |
| 29-12-292 | white bead | composition | 1930-62-55 | G24 |
| 29-12-312 | flat yellow bead fragment | composition | 1930-61-65 | G26 |
| 29-12-313 | two beads | composition | 1930-60-70 | G26 |
| 30-1-187 | fly bead | composition | 1930-67-27 | G26 |
| 30-1-98 | ribbed bead with green paint traces | composition | 1930-61-71 | G28 |
| 30-1-34 | spacer bead fragment | composition | | G29 |
| 30-1-35 | spacer bead fragment | composition | | G29 |
| 30-1-44 | blue cylindrical bead | composition | | G29 |
| 30-1-61 | brown bead | stone | | G29 |
| 30-1-64 | yellow/green painted bead | composition | | G29 |
| 30-1-65 | two cylindrical blue beads | composition | 1930-62-64 | G29 |
| 30-1-67 | two white cylindrical beads | composition | 1930-60-76 | G29 |
| 30-1-68 | blue ribbed bead | composition | 1930-61-69 | G29 |
| 30-1-70 | white ribbed bead | composition | 1930-61-3 | G29 |
| 30-1-72 | three blue beads | composition | 1930-62-107 | G29 |
| 30-1-73 | group of white beads | composition | 1930-61-30 | G29 |
| 30-1-86 | yellow bead | composition | 1930-60-126 | G29 |
| 31-3-18 | seven spherical paste beads; various faience/frit beads | various | | G29 |
| 29-12-276 | mouse'bead | composition | | G29 |
| 29-12-277 | inlaid bead | composition | | G29 |

| | | | | |
|-----------|---|-------------|---------------|-----|
| 30-1-102 | circular bead rings of black paint | composition | | G29 |
| 30-1-129 | green-glazed wall nail | terracotta | | G29 |
| 30-1-130 | green-glazed wall nail | terracotta | | G29 |
| 30-1-140 | green-glazed wall nail | terracotta | | G29 |
| 30-1-196 | green-glazed lion statue | terracotta | | G29 |
| 30-1-204 | frit cup blue | frit | 1930-60-73 | G29 |
| 30-1-205 | three blue ribbed beads | composition | 1930-61-124/7 | G29 |
| 30-1-206 | three hubbed blue beads | composition | 1930-61-75 | G29 |
| 30-1-207 | two hubbed blue beads | composition | 1930-61-137 | G29 |
| 30-1-208 | three ribbed beads, black, yellow, white | composition | 1930-61-77 | G29 |
| 30-1-209 | four blue cylindrical beads | composition | 1930-62-68 | G29 |
| 30-1-210 | two spacer bead, greenish white | composition | | G29 |
| 30-1-211 | group spacer fragments, greenish white | composition | 1930-61-129 | G29 |
| 30-1-212 | two spacer beads white | composition | 1930-61-78 | G29 |
| 30-1-213 | two spacer beads, blue/yellow | composition | 1930-61-79 | G29 |
| 30-1-214 | one blue spacer bead | composition | 1930-61-80 | G29 |
| 30-1-215 | one yellow spacer bead | composition | 1930-60-83 | G29 |
| 30-1-216 | 26 spherical beads white/yellow | composition | 1930-60-84 | G29 |
| 30-1-217 | 16 spherical beads white/yellow | composition | 1930-60-85 | G29 |
| 30-1-218 | 10 spherical beads white/yellow.grey | composition | 1930-97-77 | G29 |
| 30-12-262 | six beads spherical white; eye bead; spherical blue | not stated | | G29 |
| 30-2-135 | string of beads white/blue/yellow | composition | 1930-66-38 | G29 |
| 30-2-191 | four white frog beads | composition | | G29 |
| 30-2-198 | two 'mouse' beads | composition | 1930-67-47 | G29 |
| 30-2-199 | three white bird-shaped beads | composition | | G29 |
| 30-2-200 | two fly beads blue/white | composition | 1930-67-48 | G29 |
| 30-2-201 | two lion-headed beads black | composition | | G29 |
| 30-2-202 | three ribbed beads, blue, yellow, white | composition | 1930-61-128 | G29 |
| 30-2-210 | grey rectangular bead | stone | | G29 |
| 30-2-211 | circular black glass bead | glass | | G29 |
| 30-2-216 | white barrel bead | stone | | G29 |
| 30-2-218 | six ribbed beads white/black/blue | composition | | G29 |
| 30-2-219 | two blue spacer beads | composition | | G29 |
| 30-2-22 | ? Mace head | composition | | G29 |
| 30-2-220 | white cylindrical bead | composition | 1930-62-89 | G29 |
| 30-2-223 | teardrop-shaped white bead | composition | 1930-67-49 | G29 |
| 30-2-32 | two cylindrical black/white beads | composition | 1930-62-70 | G29 |
| 30-2-324 | four blue spacer beads | composition | 1930-61-102 | G29 |
| 30-2-33 | three white cylindrical beads | composition | | G29 |
| 30-2-34 | five cylindrical beads | composition | 1930-62-72 | G29 |
| 30-2-35 | five oblong greenish-white beads | composition | 1930-66-35 | G29 |
| 30-2-36 | two yellow beads | composition | 1930-61-81 | G29 |
| 30-2-37 | five flat yellow/white beads | composition | 1930-63-27 | G29 |
| 30-2-374 | glass staff head | glass | | G29 |
| 30-2-38 | six circular yellow/white beads | composition | 1930-60-86 | G29 |
| 30-2-39 | 16 spherical beads blue/white/yellow | composition | 1930-60-39 | G29 |
| 30-2-40 | 10 cylindrical beads blue/yellow/grey/black | composition | 1930-62-73 | G29 |
| 30-2-41 | 14 painted beads | composition | | G29 |
| 30-2-42 | flat blue pendant | composition | 1930-62-104 | G29 |
| 30-2-43 | flat disc bead, blue | composition | | G29 |
| 30-2-44 | light blue spherical bead | composition | 1930-67-28 | G29 |
| 30-2-440 | glazed boar head fragments | terracotta | | G29 |
| 30-2-45 | staff head | glass | | G29 |
| 30-2-46 | two white fly beads | composition | | G29 |
| 30-2-47 | 12 circular painted beads | composition | 1930-63-29 | G29 |
| 30-2-48 | female symbol amulet | composition | 1930-67-29 | G29 |
| 30-2-49 | spherical white and blue bead | composition | 1930-69-14 | G29 |

| | | | | |
|-------------|--|---------------|------------|-----|
| 30-2-50 | three spherical white beads | composition | 1930-60-88 | G29 |
| 30-2-51 | green/white plaque | composition | | G29 |
| 30-2-52 | oblong beads on bronze wire | composition | | G29 |
| 30-2-53 | black ribbed bead | composition | 1930-62-71 | G29 |
| 30-2-54 | yellow ribbed bead | composition | 1930-61-82 | G29 |
| 30-2-55 | white fly bead | composition | | G29 |
| 30-2-56 | blue disc bead | composition | 1930-63-30 | G29 |
| 31-2-11 | cup fragment | composition | | G29 |
| 30-1-75 | flat yellow bead | stone | | G32 |
| 30-1-76 | white cylindrical bead | stone | | G32 |
| 31-3-20 | various beads | various | 1930-63-59 | G32 |
| 30-1-100 | black/white cylindrical painted bead | composition | 1930-63-24 | G32 |
| 30-1-107 | group of light yellow beads | composition | 1930-62-67 | G32 |
| 30-12-114 | yellow bead | stone | | G32 |
| 29-12-357 | large white ribbed bead | composition | | G33 |
| 29-12-280 | two oblong beads, yellow | composition | 1930-63-21 | G37 |
| 29-12-316 | blue ribbed bead | composition | 1930-61-66 | G37 |
| 30-3-62 | barrel bead | composition | 1930-62-65 | G41 |
| 30-3-66 | quadilateral bead white/black | composition | 1930-60-75 | G41 |
| 30-1-88 | rectangular bead | stone | | G42 |
| 30-12-24 | white fluted bead | stone | | G47 |
| 30-1-149 | green-glazed wall nail | terracotta | | G47 |
| 30-1-150 | green-glazed jar | terracotta | | G47 |
| 30-1-151 | green-glazed wall nail | terracotta | | G47 |
| 30-2-367 | blue circular bead | composition | 1930-63-50 | G47 |
| 31-3-33 | various beads | various | | G50 |
| 30-11-60 | green-glazed wall nail | terracotta | | G50 |
| 30-12-71 | green-glazed wall nail | terracotta | | G50 |
| 30-12-97 | green-glazed wall nail | terracotta | | G50 |
| 30-12-99 | green-glazed wall nail | terracotta | | G50 |
| 31-3-12 | two beads | frit | | G50 |
| 31-3-15 | five beads | paste | | G50 |
| 31-3-16 | 275 beads | paste/faience | | G50 |
| 31-3-17 | 16 spherical paste beads; two eye beads; 12 spherical faience beads; two clay beads; 10 frit barrel beads; eight cylindrical paste/faience; 40 small cylindrical paste/faience | various | | G50 |
| 31-3-19 | various beads | faience/frit | | G50 |
| 31-3-21 | various beads | various | | G50 |
| 30-1-197 | green-glazed wall nail | terracotta | | G50 |
| 30-1-200 | yellow/red glazed lion | terracotta | | G50 |
| 30-1-202 | light green bead | composition | | G50 |
| 30-12-133 | glazed lions paw | terracotta | | G50 |
| 30-12-134 | glazed lions paw | terracotta | | G50 |
| 30-12-135 | green-glazed wall nail | terracotta | | G50 |
| 30-12-138 | glazed tripod | terracotta | | G50 |
| 30-12-150 | green-glazed wall nail | terracotta | | G50 |
| 30-12-152 | grey/black veined bead | stone | | G50 |
| 30-12-195 | two white beads | stone | | G50 |
| 30-12-205 | white rectangular bead | stone | | G50 |
| 30-12-207 | white bead | stone | | G50 |
| 30-12-213/4 | white bead | stone | | G50 |
| 30-12-215 | eight beads yellow/white | composition | | G50 |
| 30-12-216 | five beads white/yellow/grey | composition | 1930-63-58 | G50 |
| 30-12-217 | white ribbed bead | composition | | G50 |
| 30-12-222 | figurine fragment yellow/green glaze | terracotta | | G50 |
| 30-12-251 | glazed sheep head | terracotta | | G50 |
| 30-12-260 | 12 beads | paste/faience | | G50 |
| 30-2-100 | 400 blue cylindrical beads | composition | 1930-62-81 | G50 |

| | | | | |
|----------|---|-------------|-------------|-----|
| 30-2-101 | 450 ribbed beads black.white.grey | composition | | G50 |
| 30-2-102 | 65 hubbed beads | composition | 1930-61-90 | G50 |
| 30-2-103 | 850 spherical blue beads | composition | 1930-60-91 | G50 |
| 30-2-104 | 200 cylindrical beads black/white/blue/red/yellow | composition | 1930-61-91 | G50 |
| 30-2-105 | 4 flat rectangular beads | composition | 1930-67-32 | G50 |
| 30-2-106 | 25 rhomboidal beads blue/yellow/white/brown | composition | 1930-63-38 | G50 |
| 30-2-107 | 17 disc-shaped beads blue/white/black/yellow | composition | 1930-63-39 | G50 |
| 30-2-108 | seven fly beads yellow/white/blue | composition | | G50 |
| 30-2-109 | four fly beads white/blue | composition | | G50 |
| 30-2-110 | 13 triangular beads yellow/white/blue | composition | | G50 |
| 30-2-111 | 21 rectangular beads black/white/yellow/grey | composition | 1930-62-82 | G50 |
| 30-2-112 | 1060 circular beads white/yellow/green/grey | composition | 1930-60-140 | G50 |
| 30-2-113 | 428 cylindrical beads blue/white/yellow/black/green | composition | 1930-63-61 | G50 |
| 30-2-114 | 350 spherical beads yellow/white/greenish-white/black | composition | 1930-62-84 | G50 |
| 30-2-115 | 315 barrel beads blue/green/white/black/yellow | composition | 1930-63-40 | G50 |
| 30-2-116 | 25 barrel beads blue | composition | 1930-63-41 | G50 |
| 30-2-117 | 31 double ribbed beads black/white/blue | composition | 1930-61-126 | G50 |
| 30-2-118 | 13 barrel ribbed beads black | composition | 1930-69-69 | G50 |
| 30-2-119 | 15 rectangular white beads | composition | 1930-67-85 | G50 |
| 30-2-120 | five rectangular white/black painted beads | composition | 1930-63-42 | G50 |
| 30-2-121 | five frog beads blue | composition | | G50 |
| 30-2-122 | six frog beads , white | composition | | G50 |
| 30-2-123 | eight granulated beads - red/white | composition | 1930-67-33 | G50 |
| 30-2-124 | two lotus bud beads | ? | | G50 |
| 30-2-125 | two rams head amulets white | composition | 1930-67-34 | G50 |
| 30-2-126 | bull's head amulet black | composition | 1930-67-35 | G50 |
| 30-2-128 | two white bird-shaped beads | composition | 1930-67-36 | G50 |
| 30-2-129 | five lion head beads black | composition | 1930-67-41 | G50 |
| 30-2-130 | five 'mouse' beads, white | composition | | G50 |
| 30-2-131 | ribbed spacer bead, white | composition | 1930-67-37 | G50 |
| 30-2-132 | bull's head amulet white | composition | | G50 |
| 30-2-133 | white ribbed spacer bead | composition | | G50 |
| 30-2-134 | white ring-like bead | composition | | G50 |
| 30-2-136 | two female symbol amulets | composition | 1930-67-38 | G50 |
| 30-2-138 | white ribbed bead | composition | 1930-67-39 | G50 |
| 30-2-139 | two yellow pendants | composition | 1930-67-40 | G50 |
| 30-2-140 | two 'butterfly' beads | composition | 1930-62-85 | G50 |
| 30-2-141 | three beads yellow/white/black | composition | 1930-37-42 | G50 |
| 30-2-142 | white faceted barrel bead | composition | 1930-67-43 | G50 |
| 30-2-143 | white cross-hatched bead fragment | stone | 1930-66-39 | G50 |
| 30-2-144 | inlaid flower-shaped object | ? | 1930-67-44 | G50 |
| 30-2-145 | white human mask | | 1930-67-46 | G50 |
| 30-2-171 | three plain sun discs | glass | | G50 |
| 30-2-172 | decorated sun disc pendant | glass | | G50 |
| 30-2-173 | plain sun disc fragments | glass | | G50 |
| 30-2-174 | decorated spacer bead green/white | composition | | G50 |
| 30-2-190 | blue fly bead | composition | | G50 |
| 30-2-197 | two white beads | composition | | G50 |
| 30-2-375 | pipe bead yellow | composition | | G50 |
| 30-2-378 | green-glazed wall nail | terracotta | | G50 |
| 30-2-380 | glazed bird figurine | terracotta | | G50 |
| 30-2-381 | moulded glass plaque | glass | | G50 |
| 30-2-393 | spherical beads grey/black/white | stone | | G50 |
| 30-2-395 | three beads | stone | | G50 |
| 30-2-396 | black/white cylindrical painted bead | stone | | G50 |
| 30-2-397 | octagonal bead | stone | | G50 |
| 30-2-398 | black bead | stone | | G50 |

| | | | | |
|-----------|--|-------------|-------------------|---------|
| 30-2-399 | black rectangular bead | stone | | G50 |
| 30-2-400 | grey rectangular bead | stone | | G50 |
| 30-2-401 | black/yellow circular bead | stone | | G50 |
| 30-2-402 | greenish bead | stone | | G50 |
| 30-2-90 | 56 cylindrical beads greenish-white/white/grey + fragments | composition | 1930-61-88 | G50 |
| 30-2-91 | 62 spacer beads greenish-white/white/yellow/grey + fragments | composition | 1930-69-63 | G50 |
| 30-2-92 | 65 barrel beads greenish-white + fragments | composition | | G50 |
| 30-2-93 | 185 blue ribbed beads | composition | | G50 |
| 30-2-94 | 25 blue disc-shaped beads | composition | | G50 |
| 30-2-95 | seven blue spherical beads | composition | 1930-60-90 | G50 |
| 30-2-96 | 190 painted beads and fragments | composition | 1930-63-36 | G50 |
| 30-2-97 | 43 spacer beads | composition | 1930-61-89 | G50 |
| 30-2-98 | 1200 beads circular/spherical black/white/grey | composition | | G50 |
| 30-2-99 | 125 eye beads | composition | 1930-63-37 | G50 |
| 31-1-156 | green-glazed wall nail fragment | terracotta | | G50 |
| 31-1-157 | green-glazed wall nail | terracotta | | G50 |
| 31-1-158 | green-glazed wall nail | terracotta | | G50 |
| 31-1-159 | green-glazed wall nail | terracotta | | G50 |
| 31-1-160 | green-glazed wall nail | terracotta | | G50 |
| 31-1-161 | green-glazed wall nail | terracotta | | G50 |
| 31-1-162 | green-glazed wall nail | terracotta | | G50 |
| 31-1-163 | green-glazed wall nail | terracotta | | G50 |
| 31-1-164 | green-glazed wall nail | terracotta | | G50 |
| 31-1-165 | green-glazed wall nail | terracotta | | G50 |
| 31-1-166 | green-glazed wall nail | terracotta | | G50 |
| 31-1-167 | green-glazed wall nail | terracotta | | G50 |
| 31-1-168 | green-glazed wall nail | terracotta | | G50 |
| 31-2-117 | light grey bead | stone | | G50 |
| 31-2-74 | glass eye from statue | glass | | G50 |
| 31-3-13 | various beads | various | | G50/G29 |
| 30-2-170 | glass inlay plaque | glass/stone | 1930-82-20 | G52 |
| 30-2-192 | brown bead | stone | | G52 |
| 30-11-10 | glazed pot (glazed inside) | terracotta | | G53 |
| 31-3-23 | various beads | various | | G53 |
| 30-12-235 | white bead | stone | | G53 |
| 30-12-236 | translucent bead | stone | | G53 |
| 30-12-237 | green spherical bead | stone | | G53 |
| 30-2-57 | five blue spacer beads | composition | | G53 |
| 30-2-58 | seven white spacer beads | composition | 1930-61-83 | G53 |
| 30-2-59 | white ribbed spacer bead | composition | | G53 |
| 30-2-60 | group of greenish white spacer beads | composition | 1930-61-115 | G53 |
| 30-2-61 | group spacer fragments, greenish white | composition | 1930-61-85 | G53 |
| 30-2-62 | seven greenish white cylindrical beads | composition | 1930-62-74 | G53 |
| 30-2-63 | five greenish white cylindrical beads | composition | | G53 |
| 30-2-64 | 31 cylindrical beads white/green/grey | composition | | G53 |
| 30-2-65 | cylindrical bead (intact) | composition | 1930-62-75 | G53 |
| 30-2-66 | two blue ribbed beads | composition | | G53 |
| 30-2-67 | blue ribbed bead | composition | 1930-61-86 | G53 |
| 30-2-68 | blue ribbed beads | composition | 1930-62-79 | G53 |
| 30-2-69 | 32 barrel beads white/light grey | composition | 1930-61-136/63-31 | G53 |
| 30-2-70 | 32 spherical beads white/yellow | composition | 1930-60-89 | G53 |
| 30-2-70a | plain sun disc pendant | glass | | G53 |
| 30-2-71 | plain sun disc pendant fragments | glass | 1930-67-82 | G53 |
| 30-2-72 | 13 circular beads | glass | 1930-63-32 | G53 |
| 30-2-73 | Five painted beads | composition | 1930-62-77/63-28 | G53 |

| | | | | |
|-----------|---|---------------|-------------|-----|
| 30-2-74 | painted bead fragments | composition | 1930-62-78 | G53 |
| 30-2-75 | 17 cylindrical beads yellow/blue/white | composition | 1930-62-79 | G53 |
| 30-2-76 | two rectangular beads | composition | 1930-61-87 | G53 |
| 30-2-77 | green ribbed cone (inlaid bead) | composition | | G53 |
| 30-2-78 | circular plaque raised flower design | composition | | G53 |
| 30-2-79 | rectangular bead, blue | composition | 1930-66-36 | G53 |
| 30-2-80 | rhomboidal bead. Green | composition | | G53 |
| 30-2-81 | white hubbed bead | composition | | G53 |
| 30-2-82 | disc shaped bead | composition | 1930-63-33 | G53 |
| 30-2-83 | two flat circular beads | composition | 1930-63-34 | G53 |
| 30-2-84 | white triangular bead | composition | 1930-62-80 | G53 |
| 30-2-86 | frog bead, blue | composition | 1930-67-30 | G53 |
| 30-2-88 | complex 'head' bead fragment | composition | | G53 |
| 30-2-89 | black rectangular bead | stone | | G53 |
| 31-2-122 | three spherical beads/eight various beads | paste | 1930-60-10 | G53 |
| 30-1-146 | green-glazed jar | terracotta | | G54 |
| 31-1-134 | green spherical bead | | | G54 |
| 30-2-345 | Five painted beads | stone | | G55 |
| 30-2-346 | six circular beads | composition | 1930-60-405 | G55 |
| 30-2-356 | brown translucent spacer bead | stone | | G55 |
| 30-2-357 | four white spherical beads | composition | 1930-60-106 | G55 |
| 30-2-272 | seven white cylindrical beads | stone | 1930-67-52 | G57 |
| 29-11-92 | ribbed bead, yellow painted | ? | | G6 |
| 29-11-120 | blue flat bead | composition | | G6 |
| 29-11-120 | spherical lapis bead | stone | | G6 |
| 29-11-140 | broken lapis bead | stone | | G6 |
| 29-12-107 | greenish bead | stone | | G6 |
| 29-12-108 | grey bead | stone | | G6 |
| 30-3-85 | four black circular beads | composition | | G65 |
| 30-3-59 | silver nose ring with yellow beads | various | | G66 |
| 30-12-51 | white spacer bead | stone | 1930-66-18 | G67 |
| 31-2-120 | three beads/fragments | frit | 1930-69-79 | G67 |
| 30-12-151 | green-glazed jar | terracotta | | G73 |
| 30-12-219 | glazed wall nail | terracotta | | G73 |
| 30-12-256 | blue bead | faience | 1930-61-119 | G73 |
| 30-12-257 | white cylindrical bead | faience | | G73 |
| 30-12-258 | six beads | paste/faience | 1930-69-41 | G73 |
| 31-1-17 | dark blue bead | glass | | G74 |
| 30-1-163 | ribbed bead | composition | 1930-61-74 | G78 |
| 31-2-30 | white flat bead | composition | 1930-62-112 | G78 |
| 30-2-188 | white spherical bead | composition | | G9 |
| 30-1-145 | green-glazed wall nail | terracotta | | H10 |
| 30-1-169 | green-glazed wall nail | terracotta | | H10 |
| 30-1-172 | green-glazed figurine fragment | terracotta | | H10 |
| 30-1-195 | green-glazed figurine fragment | terracotta | | H10 |
| 30-2-281 | four hubbed beads | composition | 1930-67-54 | H10 |
| 30-2-282 | five spherical beads yellow/white | composition | 1930-60-97 | H10 |
| 30-2-283 | four painted barrel beads | composition | 1930-67-55 | H10 |
| 30-2-284 | rhomboidal bead, yellow and grey | composition | 1930-67-56 | H10 |
| 30-2-285 | blue disc shaped bead | composition | 1930-63-44 | H10 |
| 30-2-343 | 54 beads spherical/spacer/ribbed | composition | 1930-61-131 | H10 |
| 30-2-344 | five barrel beads black/white/yellow | composition | 1930-63-49 | H10 |
| 30-2-358 | four cylindrical beads blue/yellow | composition | | H10 |
| 30-2-359 | four circular beads white/yellow/black | composition | 1930-67-65 | H10 |
| 30-11-6 | glazed Ishtar figurine | terracotta | | H11 |
| 30-11-8 | glazed brick | terracotta | | H11 |
| 30-11-100 | green-glazed wall nail fragment | terracotta | | H11 |

| | | | | |
|-----------|---|---------------------|------------------------|-----|
| 30-1-171 | green-glazed wall nail | terracotta | | H11 |
| 30-12-220 | glazed wall plaque | terracotta | | H11 |
| 30-2-340 | five cylindrical beads black/white/yellow | composition | 1930-62-97 | H11 |
| 30-2-341 | four spherical beads | composition | 1930-60-404 | H11 |
| 30-2-342 | painted barrel bead | composition | 1930-62-98 | H11 |
| 31-3-37 | incised faience bead | faience | 1930-60-17 | H12 |
| 31-3-38 | green-glazed wall nail | terracotta | 1930-61-108 | H12 |
| 30-12-259 | three beads | paste/faience | 1930-62-109 | H12 |
| 30-2-364 | blue spacer bead | composition | | H12 |
| 30-2-365 | two ribbed beads black/blue | composition | | H12 |
| 30-2-279 | two circular/cylindrical beads | composition | | H13 |
| 30-11-3 | bead | composition | 1930-60-124 | H14 |
| 30-11-4 | decorated bead | composition | 1930-60-125 | H14 |
| 31-3-14 | five beads | paste/faience | | H14 |
| 30-2-309 | faience' plaque red/blue flower inlaid pattern | faience | | H14 |
| 30-2-333 | decorated glass fragments | glass | 1930-82-69 | H14 |
| 30-2-334 | five spherical beads | composition | 1930-67-62 | H14 |
| 30-2-405 | 50 spherical/circular beads yellow/white/blue | composition + stone | 1930-60-111 | H14 |
| 30-2-406 | 21 barrel beads greenish-white/white/blue/yellow | composition + stone | 1930-60-144/1930-63-51 | H14 |
| 30-2-407 | 23 cylindrical beads greenish-white/white/blue/yellow/black | composition + stone | 1930-62-101 | H14 |
| 30-2-409 | two black-banded circular beads | composition | 193063-52 | H14 |
| 30-2-410 | nine ribbed beads white/yellow/blue/black | composition | 1930-61-110 | H14 |
| 30-2-411 | two blue spacer beads | composition | 1930-61-111 | H14 |
| 30-2-412 | plain sun disc fragment | glass | 1930-67-67 | H14 |
| 30-11-13 | green-glazed wall nail | terracotta | | H15 |
| 30-12-115 | green-glazed wall nail | terracotta | | H15 |
| 30-2-310 | two spherical beads white/yellow/blue | composition | 1930-60-101 | H15 |
| 30-2-311 | six barrel beads white/blue/black | composition | 1930-63-47 | H15 |
| 30-2-312 | four ribbed beads blue/black/white | composition | 1930-67-59 | H15 |
| 30-2-313 | two spacer beads | composition | 1930-61-101 | H15 |
| 30-2-314 | three rectangular beads | composition | 1930-63-48 | H15 |
| 30-2-315 | two circular beads | composition | | H15 |
| 30-2-316 | seven cylindrical beads blue/white | composition | | H15 |
| 30-2-317 | white 'mouse' bead | composition | | H15 |
| 30-2-318 | marble bead | stone | | H15 |
| 30-2-360 | white ribbed bead | composition | | H15 |
| 30-2-361 | eight white spherical beads | composition | 1930-60-109 | H15 |
| 30-2-362 | blue hubbed bead | composition | | H15 |
| 30-2-363 | white cylindrical bead | composition | 1930-62-100 | H15 |
| 30-2-426 | decorated sun disc pendant | glass | | H15 |
| 30-2-427 | three hubbed beads | composition | | H15 |
| 30-2-428 | 22 spherical beads blue/white/yellow some painted | composition | 1930-60-114 | H15 |
| 30-2-429 | six cylindrical beads blue/white/greenish-white | composition | 1930-62-105 | H15 |
| 30-2-430 | seven ribbed beads blue/black/white | composition | 1930-61-114 | H15 |
| 30-2-431 | eight barrel beads white/greenish-white some painted | composition | | H15 |
| 30-2-432 | two white 'mouse' beads | composition | 1930-67-69 | H15 |
| 30-2-433 | two beads | stone | | H15 |
| 30-2-434 | yellow circular bead | stone | | H15 |
| 30-2-435 | inlay head circular | composition | 1930-63-54 | H15 |
| 30-2-437 | frog bead | composition | 1930-67-70 | H15 |
| 30-11-97 | green-glazed wall nail fragment | terracotta | | H16 |
| 30-2-286 | ribbed bead green/blue | composition | 1930-61-96/7 | H16 |
| 30-2-287 | decorated glass fragments | glass | | H16 |
| 30-2-304 | spherical bead | composition | 1930-60-100 | H16 |
| 30-2-293 | two spherical beads white/yellow | composition | 1930-69-55 | H18 |

| | | | | |
|-----------|--|-------------|-------------|-----|
| 30-2-294 | two blue spherical beads | composition | 1930-67-57 | H18 |
| 30-2-420 | 40 beads spherical/circular white/black/yellow/blue - some painted | composition | 1930-60-113 | H18 |
| 30-2-421 | 14 cylindrical beads blue/greenish-white/white some painted | composition | | H18 |
| 30-2-422 | seven ribbed beads and spacer beads blue/white/yellow | composition | 1930-61-132 | H18 |
| 30-2-423 | frog bead | composition | 1930-67-68 | H18 |
| 30-1-42 | blue bead | composition | 1930-67-14 | H2 |
| 30-1-90 | white bead | composition | 1930-60-78 | H2 |
| 30-2-186 | black banded spherical bead | composition | 1930-60-92 | H20 |
| 30-2-280 | white ribbed bead | composition | | H21 |
| 30-2-183 | white hubbed bead | composition | 1930-61-92 | H22 |
| 30-2-278 | cone shaped bead | stone | | H25 |
| 30-2-185 | marble bead | stone | | H33 |
| 30-3-19 | cylindrical bead | composition | 1930-62-106 | H35 |
| 30-3-23 | grey bead | stone | | H35 |
| 30-11-103 | greenish-white spherical bead | composition | | H38 |
| 30-3-10 | cylindrical bead | stone | | H39 |
| 30-2-182 | blue cylindrical bead | composition | 1930-62-88 | H40 |
| 30-11-104 | greenish-white spherical bead | composition | 1930-60-128 | H42 |
| 30-3-56 | bead | stone | | H43 |
| 30-3-79 | bead | stone | | H45 |
| 30-3-4 | painted barrel bead | composition | | H45 |
| 30-3-3 | black spacer bead | stone | | H47 |
| 30-1-59 | cylindrical greenish bead | composition | 1930-63-55 | H5 |
| 31-2-16 | greenish cylindrical bead | composition | 1930-62-110 | H5 |
| 30-3-22 | mottled bead | stone | | H50 |
| 30-2-8 | green-glazed wall nail | terracotta | | H50 |
| 30-1-54 | glazed wall nail | terracotta | | H6 |
| 30-1-106 | greenish white ribbed bead | composition | 1930-61-72 | H6 |
| 30-1-114 | white bead | composition | 1930-60-80 | H6 |
| 30-1-127 | green-glazed wall nail | terracotta | | H6 |
| 30-1-128 | green-glazed wall nail | terracotta | | H6 |
| 30-1-138 | white bead | composition | 1930-63-29 | H6 |
| 30-2-330 | four spherical beads | composition | 1930-60-102 | H6 |
| 30-2-331 | five cylindrical beads red/blue/white | composition | 1930-67-60 | H6 |
| 30-2-332 | six various beads | composition | 1930-67-61 | H6 |
| 30-2-382 | glazed ceramic fragment (wall plaque) | terracotta | | H6 |
| 31-1-6 | white spherical bead | stone | | H60 |
| 31-3-22 | various beads | various | 1930-60-138 | H7 |
| 30-1-141 | green-glazed wall nail | terracotta | | H7 |
| 30-1-144 | green-glazed wall nail | terracotta | | H7 |
| 30-1-152 | green-glazed wall nail | terracotta | | H7 |
| 30-1-153 | green-glazed wall nail | terracotta | | H7 |
| 30-1-175 | green-glazed wall nail | terracotta | | H7 |
| 30-1-176 | green-glazed wall nail | terracotta | | H7 |
| 30-2-300 | 161 small beads greenish-white/yellow (single string) | composition | | H7 |
| 30-2-301 | three barrel beads white/yellow | composition | 1930-67-58 | H7 |
| 30-2-302 | disc shaped bead | composition | 1930-63-46 | H7 |
| 30-2-303 | white bead | stone | | H7 |
| 30-2-325 | two white ribbed beads | composition | 1930-61-103 | H7 |
| 30-2-326 | 10 spherical beads blue/yellow | composition | 1930-62-95 | H7 |
| 30-2-327 | bead | stone | | H7 |
| 31-2-121 | three beads | faience | | H70 |
| 30-2-320 | marble bead | stone | | H8 |
| 30-2-415 | white ribbed spacer bead | composition | | H8 |
| 30-2-416 | 14 cylindrical beads white/yellow/grey | composition | 1930-62-103 | H8 |
| 30-2-417 | 31 beads spherical/circular white/yellow/blue | composition | 1930-60-112 | H8 |

| | | | | |
|------------|--|-------------|-------------|------|
| 30-2-418 | seven barrel beads yellow/black | composition | 1930-63-53 | H8 |
| 30-2-419 | eight ribbed beads blue/black/yellow | composition | 1930-61-112 | H8 |
| 29-11-182 | green bead | stone | 1930-62-42 | I2 |
| 30-11-85 | blue bead | stone | | I27 |
| 28-12-242 | three fluted beads | composition | 1930-61-19 | K193 |
| 28-12-551 | white bead | composition | 1930-63-5 | K303 |
| 28-12-418 | small fragment of painted glass "silver paint" | glass | | K314 |
| 27-28 | five beads | not stated | | K32 |
| 31-2-123 | four beads | paste | | K330 |
| 28-12-433 | tiny blue bead | composition | 1930-60-36 | K333 |
| 29-2-165 | light grey oblong bead | stone | | K342 |
| 29-1-357 | oblong bead | stone | | K346 |
| 27-28-3037 | plain white glass | glass | 1930-82-59 | K36 |
| 29-1-260 | glazed jar | terracotta | | K421 |
| 29-1-559 | beads | stone | | K425 |
| 29-1-367 | spacer bead | composition | 1930-61-35 | K432 |
| 29-2-255 | spacer bead | stone | 1930-61-46 | K443 |
| 29-2-148 | blue bead | composition | 1930-62-34 | K453 |
| 27-28 | one bead | not stated | | L1 |
| 30-1-24 | light yellow ribbed bead | composition | | L10 |
| 27-28 | three beads | not stated | | L10 |
| 28-11-61 | glazed jar neck | terracotta | | L101 |
| 28-11-158 | glazed wall nail | terracotta | | L101 |
| 28-12-261 | thin dark brown glass vessel, broken | glass | | L101 |
| 28-12-470 | glazed wall nail | terracotta | | L101 |
| 27-28 | 24 beads | not stated | | L11 |
| 27-28-3061 | glass inlay plaque | glass | | L11 |
| 27-28-3066 | glass animal figurine | glass | | L11 |
| 27-28 | three beads | not stated | | L12 |
| 29-12-233 | oblong black bead | stone | | L12 |
| 27-28 | eight beads | not stated | | L13 |
| 27-28 | eight beads | not stated | | L15 |
| 28-11-19 | red/brown bead | stone | | L20 |
| 27-28 | five beads | not stated | | L25 |
| 27-28-348 | glazed wall nail fragment | terracotta | | L2-8 |
| 27-28 | 95 beads, most paste | paste | | L29 |
| 29-11-14 | glazed wall nail | terracotta | | L3 |
| 29-11-15 | glazed wall nail | terracotta | | L3 |
| 27-28 | one bead | not stated | | L30 |
| 27-28 | four beads | not stated | | L4 |
| 27-28-3036 | six fragments plain white glass | glass | 1930-82-58 | L4 |
| 30-11-36 | two white beads | stone | | L4 |
| 30-11-43 | white bead | stone | | L4 |
| 30-11-89 | white spherical bead | composition | | L4 |
| 30-11-28 | bead | composition | 1930-63-57 | L4 |
| 30-11-124 | crucible' | terracotta | | L4 |
| 30-12-124 | blue rectangular bead | stone | | L4 |
| 30-12-125 | greenish bead | composition | 1930-67-72 | L4 |
| 30-12-170 | two beads black spiral pattern | composition | 1930-62-108 | L4 |
| 30-12-171 | black bead | composition | 1930-67-73 | L4 |
| 30-12-172 | white bead | stone | | L4 |
| 30-12-234 | white bead | stone | | L4 |
| 30-12-245 | circular bead | stone | | L4 |
| 31-2-45 | light yellow bead | stone | 1930-62-113 | L4 |
| 28-12-142 | black bead | stone | | L44 |
| 27-28 | three beads | not stated | | L44 |
| 31-1-127 | two beads | composition | 1930-66-58 | L4A |

| | | | | |
|-----------|--|------------------|-------------|---------------|
| 31-1-128 | lapis bead | stone | | L4A |
| 31-1-130 | spherical bead | composition | 1930-66-61 | L4A |
| 31-1-131 | black cylindrical bead | stone | | L4A |
| 27-28-340 | glazed wall nail fragment | terracotta | | L5 |
| 27-28-346 | glazed wall nail fragment | terracotta | | L5 |
| 27-28-345 | glazed wall nail fragment | terracotta | | L6 |
| 30-1-136 | yellow bead | composition | | L6 |
| 30-12-175 | white bead | stone | | L6 |
| 30-12-255 | greenish-white fluted bead | frit | 1930-61-118 | L6 |
| 27-28-341 | glazed wall nail fragment | terracotta | | L7 |
| 30-12-147 | dark translucent bead | stone | | L7 |
| 30-12-174 | light grey fluted bead | stone | | L7 |
| 27-28 | four beads | not stated | | L8 |
| 27-28-336 | glazed wall nail fragment | terracotta | | L8 |
| 27-28-337 | glazed wall nail fragment | terracotta | | L8 |
| 27-28-338 | glazed wall nail fragment | terracotta | | L8 |
| 27-28-342 | glazed wall nail fragment | terracotta | | L8 |
| 27-28-343 | glazed wall nail fragment | terracotta | | L8 |
| 27-28-344 | glazed wall nail fragment | terracotta | | L8 |
| 30-12-233 | circular ivory coloured bead | stone | | L8 |
| 27-28 | one bead | not stated | | L9 |
| 27-28 | one bead | not stated | | location lost |
| 28-11-77 | amber bead | stone | | M100 |
| 28-11-78 | grey stone bead | stone | | M100 |
| 28-11-4 | red stone bead | stone | | M100 |
| 28-11-23 | white alabaster bead | stone | | M100 |
| 28-11-114 | agate bead | stone | | M100 |
| 28-11-133 | grey double bead | stone | | M100 |
| 28-11-135 | pink bead | stone | | M100 |
| 28-11-178 | coral bead | coral | | M100 |
| 28-11-202 | white bead | stone | | M100 |
| 28-11-239 | white bead | stone | | M100 |
| 28-11-240 | brown translucent bead | stone | | M100 |
| 28-11-242 | decorated glass fragments (50 X 25mm) | glass | | M100 |
| 28-11-249 | brown translucent bead | stone | | M100 |
| 28-12-214 | black cylindrical bead fragment | composition | | M100 |
| 28-10-52 | round glass bead | glass | | M100 |
| 31-10-53 | decorated fragment, yellow decoration, moulded rim | glass | | M100 |
| 28-10-26 | octagonal bead | composition | | M100 |
| 28-11-12 | decorated fragments - many | glass | | M100 |
| 28-11-11 | marbled fragments | marbelized glass | | M100 |
| 29-11-4 | glazed bowl | terracotta | | M2 |
| 30-2-262 | white/yellow bead | stone | | M9 |
| 30-2-265 | yellow/black bead | stone | | M9 |
| 27-28 | two beads | not stated | | M90 |
| 28-11-177 | blue bead | stone | | M94 |
| 28-11-284 | white spherical bead | stone | | M94 |
| 28-11-332 | white bead | stone | | M94 |
| 28-11-484 | yellow glass, small fragment | glass | | M94 |
| 28-10-48 | broken red stone bead | stone | | N102 |
| 28-10-19 | spacer bead | composition | | N102 |
| 29-3-25 | white bead | stone | | N120 |
| 29-3-26 | blue spherical bead | composition | 1930-60-50 | N120 |
| 28-11-331 | white bead | stone | | N120 |
| 29-1-207 | white bead | composition | | N120 |
| 29-1-556 | white bead | composition | 1930-63-7 | N120 |
| 29-1-561 | beads | stone | | N120 |

| | | | | |
|-----------|---|-------------|-----------------|------|
| 28-12-552 | spacer bead | composition | | N336 |
| 28-12-578 | blue bead | composition | 1930-67-7 | N358 |
| 29-1-122 | four white cylindrical beads | composition | 1930-67-10 | N383 |
| 29-1-131 | group of oblong beads | composition | 1930-67-22 | N383 |
| 29-1-123 | two blue incised beads | composition | 1930-67-11 | N392 |
| 28-12-317 | lapis coloured bead | stone | | P302 |
| 28-12-318 | yellow bead | stone | | P302 |
| 28-12-344 | black bead | stone | | P302 |
| 29-1-369 | spacer bead | composition | 1930-61-36 | P309 |
| 28-12-422 | two black beads | stone | | P310 |
| 28-12-426 | flat blue bead | composition | 1930-62-16 | P310 |
| 28-12-531 | white bead | composition | 1930-60-37 | P310 |
| 28-12-574 | green ribbed bead | composition | 1930-61-23 | P310 |
| 28-12-368 | green-glazed vessel/jar | terracotta | | P311 |
| 29-1-406 | oblong flat bead | composition | 1930-63-6 | P313 |
| 29-1-19 | yellow spacer bead | composition | 1930-61-26 | P322 |
| 28-12-434 | black bead | stone | | P326 |
| 29-1-334 | oblong green bead | composition | 1930-62-44 | P326 |
| 28-12-457 | green-glazed pot | terracotta | | P329 |
| 29-1-147 | green bead | stone | | P334 |
| 28-12-480 | black glass fragment | glass | | P341 |
| 29-1-469 | blue bead | composition | 1930-62-29 | P341 |
| 28-12-510 | white and blue beads 110cm below ground level | composition | | P348 |
| 29-1-366 | yellow bead | composition | 1930-60-43 | P349 |
| 27-28 | three beads | not stated | | P35 |
| 29-1-53 | white 'fancy' bead | composition | 1930-62-38 | P351 |
| 29-1-73 | spacer bead | composition | | P351 |
| 28-12-508 | glass fragment lustre on surface | glass | | P356 |
| 28-12-548 | blue oblong bead | composition | 1930-62-17 | P360 |
| 29-2-27 | ribbed bead | composition | 1930-61-40 | P360 |
| 29-1-178 | greenish ribbed bead | composition | | P370 |
| 28-12-594 | ribbed bead | composition | 1930-61-134 | P371 |
| 29-1-475 | lapis rectangular bead | stone | | P375 |
| 29-1-476 | painted bead | composition | | P375 |
| 29-3-6 | cylindrical bead | stone | | P376 |
| 29-1-49 | blue ribbed bead | composition | | P382 |
| 29-1-23 | blue hubbed bead | composition | 1930-61-27 | P382 |
| 29-11-41 | blue glazed bead ribbed | composition | 1930-61-50 | P387 |
| 29-11-42 | cylindrical glazed bead | composition | 1930-62-18 | P387 |
| 29-1-47 | blue bead | composition | | P387 |
| 29-2-157 | ribbed white bead | composition | 1930-61-45 | P387 |
| 29-1-371 | spherical bead | stone | | P389 |
| 29-2-235 | black bead | stone | | P389 |
| 29-1-87 | two white beads | composition | 1930-62-27/67-9 | P399 |
| 29-2-240 | white cylindrical bead | composition | 1930-62-35 | P399 |
| 29-1-330 | oblong bead, blue | composition | 1930-62-26 | P400 |
| 29-1-335 | blue bead | composition | 1930-61-33 | P400 |
| 29-1-339 | bird-shaped bead | composition | | P400 |
| 29-1-351 | ribbed white bead | composition | 1930-61-34 | P400 |
| 29-1-368 | white bead | composition | 1930-60-45 | P400 |
| 29-1-298 | white bead | stone | | P401 |
| 29-1-306 | small double blue bead | composition | 1930-62-25 | P401 |
| 29-2-307 | blue ribbed bead | composition | | P407 |
| 29-1-205 | white bead | composition | | P416 |
| 29-3-32 | black bead | stone | | P430 |
| 29-2-99 | white bead | composition | 1930-63-9 | P445 |
| 29-1-479 | white ribbed bead | composition | 1930-61-37 | P446 |

| | | | | |
|-----------|--|-------------|-------------|------|
| 29-11-40 | blue bead | composition | 1930-61-49 | P458 |
| 29-2-103 | yellow bead | composition | 1930-60-47 | P464 |
| 29-2-39 | white ribbed bead | composition | 1930-61-41 | P467 |
| 29-2-5 | two ribbed white beads | composition | 1930-61-39 | P467 |
| 29-2-9 | yellow bead | composition | | P468 |
| 29-2-44 | three white beads | composition | | P470 |
| 29-2-104 | ribbed white bead | composition | 1930-61-43 | P470 |
| 29-2-105 | two black painted beads | composition | | P470 |
| 29-2-106 | yellow ribbed bead | composition | 1930-61-44 | P470 |
| 29-2-107 | three flat black beads | composition | 1930-67-15 | P470 |
| 29-2-43 | oblong blue bead | composition | 1930-63-8 | P470 |
| 29-2-46 | greenish ribbed bead | composition | 1930-61-42 | P470 |
| 29-2-98 | green oblong bead | stone | | P470 |
| 29-2-172 | light grey oblong bead | stone | | P473 |
| 29-2-323 | white bead | composition | 1930-61-47 | P482 |
| 28-11-394 | button' (amulet) | composition | | R125 |
| 27-28 | one bead | not stated | | R46 |
| 30-1-109 | yellow pendants | stone | | R46 |
| 27-28 | one bead | not stated | | R70 |
| 27-28 | one bead | not stated | | R80 |
| 27-28 | two beads | not stated | | R87 |
| 28-12-308 | ?blue glass flat bead | glass | | R88 |
| 27-28 | one bead | not stated | | R88 |
| 28-11-84 | dark grey bead | stone | | R95 |
| 28-11-85 | bead | stone | | R95 |
| 29-1-90 | dark green glass bead | glass | | R96 |
| 28-11-246 | white translucent bead | stone | | R96 |
| 29-2-325 | blue ribbed bead | composition | 1930-61-48 | R96 |
| 28-11-282 | flat white composition bead | composition | | S104 |
| 28-12-300 | fragments of painted glass - green, white, yellow | glass | | S104 |
| 28-12-314 | blue spacer bead | composition | 1930-61-21 | S104 |
| 28-11-57 | black stone bead | stone | | S105 |
| 28-11-22 | white alabaster bead | stone | | S105 |
| 28-11-139 | white alabaster bead | stone | | S105 |
| 28-11-190 | grey/white bead | stone | 1930-60-1 | S105 |
| 28-11-191 | red bead | stone | | S105 |
| 28-11-250 | blue bead | stone | | S105 |
| 28-11-83 | mottled red bead | stone | | S106 |
| 28-11-178 | fluted bead | composition | | S106 |
| 28-11-167 | white bead | stone | | S107 |
| 28-11-205 | blue bead | stone | 1930-60-139 | S107 |
| 28-11-253 | ribbed bead | composition | 1930-61-9 | S107 |
| 28-11-258 | nine composition beads (two fluted, two cylindrical/five flat (blue) | composition | 1930-62-5 | S108 |
| 28-11-456 | green-glazed vase | terracotta | | S108 |
| 28-11-292 | spacer bead fragment, white | composition | 1930-61-11 | S110 |
| 28-11-308 | amulet | composition | | S110 |
| 28-11-320 | three spacer beads | composition | 1930-61-12 | S110 |
| 28-11-247 | spacer bead | composition | 1930-61-7 | S111 |
| 28-11-252 | spacer bead, blue | composition | 1930-61-8 | S111 |
| 28-11-323 | two spacer beads, blue | composition | | S111 |
| 28-11-324 | fragments spacer bead, blue | composition | 1930-61-13 | S111 |
| 28-11-333 | black bead | stone | | S111 |
| 28-11-366 | blue spherical bead | composition | | S111 |
| 28-11-416 | group of beads: spacer, spherical, cylindrical one 'flower shaped' | composition | | S111 |
| 28-11-325 | fragment of large fluted bead | composition | | S112 |
| 28-12-27 | incised white bead | | 1930-61-25 | S123 |

| | | | | |
|-----------|---|-------------|------------|---------|
| 28-11-379 | white cylindrical bead | composition | | S124 |
| 28-11-418 | green-glazed vase | terracotta | | S129 |
| 28-11-463 | white spacer bead fragments | composition | | S130 |
| 28-12-202 | white flat bead | composition | 1930-63-4 | S130 |
| 28-11-464 | white incised bead | | | S132 |
| 28-11-489 | four black beads | stone | | S132 |
| 28-12-265 | one greenish white bead | composition | 1930-60-33 | S132 |
| 28-12-138 | greenish painted cylindrical bead | composition | | S153 |
| 28-12-93 | black bead | stone | | S154 |
| 28-12-471 | white bead | composition | 1930-61-22 | S155 |
| 28-12-100 | blue and white fluted beads | composition | 1930-61-16 | S156 |
| 28-12-146 | white flat bead | composition | | S156 |
| 28-12-483 | blue glass fragments | glass | | S157 |
| 28-12-589 | white bead | stone | | S158 |
| 28-12-590 | two beads | composition | | S158 |
| 28-12-99 | sheeps head | composition | | S164 |
| 28-12-349 | green-glazed pot fragment | terracotta | | S168 |
| 28-12-474 | lapis coloured bead | stone | | S175 |
| 28-12-348 | white bead | composition | | S178 |
| 28-12-292 | spacer fragment | composition | | S185 |
| 28-12-243 | white bead | composition | | S191 |
| 28-12-413 | five red beads | stone | | S319 |
| 28-12-414 | green bead | stone | | S319 |
| 28-12-415 | black bead | stone | | S319 |
| 29-1-232 | spacer bead blue | composition | | S319 |
| 29-1-67 | three white ribbed beads | composition | | S395 |
| 29-1-558 | white ribbed bead | composition | 1930-61-38 | S395 |
| 27-28 | two beads | not stated | | Shil 1 |
| 27-28 | 10 beads | not stated | | Shil 10 |
| 27-28 | one bead | not stated | | Shil 10 |
| 27-28 | one bead | not stated | | Shil 12 |
| 27-28 | 10 beads | not stated | | Shil 13 |
| 27-28 | seven beads | not stated | | Shil 14 |
| 27-28 | seven beads | not stated | | Shil 15 |
| 27-28 | 13 beads | not stated | | Shil 15 |
| 27-28-252 | decorated glass fragments | glass | | Shil 15 |
| 27-28 | two beads | not stated | | Shil 16 |
| 27-28 | 30 beads + 10 fragments (single string) fluted beads, three other beads | not stated | | Shil 18 |
| 27-28 | one bead | not stated | | Shil 22 |
| 27-28 | one bead or button | not stated | | Shil 23 |
| 27-28 | two beads | not stated | | Shil 24 |
| 27-28 | five beads, including composite eye bead (glass/metal) | various | | Shil 26 |
| 27-28 | seven beads | not stated | | Shil 27 |
| 27-28 | one bead | not stated | | Shil 28 |
| 27-28 | eight beads | not stated | | Shil 29 |
| 27-28 | one bead and three fragments | not stated | | Shil 45 |
| 27-28 | one bead | not stated | | Shil 55 |
| 27-28 | three beads | not stated | | Shil 6 |
| 27-28 | 32 beads | not stated | | Shil 7 |
| 27-28-251 | decorated glass fragments | glass | | Shil 7 |
| 27-28 | one bead | not stated | | Shil 8 |
| 27-28 | one bead | not stated | | Shil 9 |
| 29-1-45 | white bead | composition | | U374 |
| 29-1-206 | white bead | composition | | U410 |
| 28-12-56 | incised white bead | | 1930-61-14 | unknown |
| 28-12-108 | white fluted bead | composition | 1930-61-17 | unknown |
| 28-12-225 | white spacer bead ribbed | composition | | unknown |

| | | | | |
|-----------|----------------------------------|-------------|-------------|---------|
| 28-12-266 | greenish white bead fragment | composition | | unknown |
| 28-12-355 | alabaster bead | stone | | unknown |
| 28-11-34 | incised bead | composition | | unknown |
| 28-11-259 | ribbed bead | composition | | unknown |
| 28-11-289 | rhomboidal white ?glass bead | ?glass | | unknown |
| 28-11-289 | white bead | ?glass | | unknown |
| 28-12-221 | broken bead | composition | | unknown |
| 28-12-567 | glazed wall nail | terracotta | | unknown |
| 29-1-151 | small bead | composition | | unknown |
| 29-1-140 | triangular blue bead | composition | | unknown |
| 29-1-560 | beads | stone | | unknown |
| 30-1-33 | spacer bead fragment | composition | | unknown |
| 28-11-24 | broken glass bead, violet | glass | | unknown |
| 28-12-65 | incised white bead | | | unknown |
| 28-11-76 | blue stone bead | stone | | unknown |
| 28-11-79 | amber bead | stone | | unknown |
| 28-11-93 | blue bead | stone | | unknown |
| 28-12-10 | fragment yellow painted glass | glass | | unknown |
| 28-11-15 | black stone bead | stone | | unknown |
| 27-28 | four beads | not stated | | unknown |
| 27-28 | five beads | not stated | | unknown |
| 27-28 | nine beads | not stated | | unknown |
| 28-11-103 | blue bead | stone | | unknown |
| 28-11-104 | carnelian bead | stone | | unknown |
| 28-11-115 | translucent yellow bead | stone | | unknown |
| 28-11-119 | carnelian bead | stone | | unknown |
| 28-11-120 | amber bead | stone | | unknown |
| 28-11-129 | translucent bead | stone | | unknown |
| 28-11-130 | carnelian bead | stone | | unknown |
| 28-11-131 | blue bead | stone | | unknown |
| 28-11-138 | white bead | stone | | unknown |
| 28-11-378 | cubic bead, greenish | composition | | unknown |
| 28-11-399 | 14 beads red, blue, white | composition | | unknown |
| 28-11-400 | white and black bead | composition | | unknown |
| 28-11-491 | yellow ?red glass fragments | glass | | unknown |
| 28-12-203 | bead fragments | composition | | unknown |
| 29-12-370 | brown bead | composition | | unknown |
| 29-2-110 | white oblong bead | composition | | unknown |
| 27-28 | 73 beads | not stated | | unknown |
| 27-28-339 | glazed wall nail fragment | terracotta | | unknown |
| 27-28-347 | glazed wall nail fragment | terracotta | | unknown |
| 27-28-349 | glazed wall nail fragment | terracotta | | unknown |
| 27-28-611 | decorated glass fragment | glass | | unknown |
| 29-1-85 | glass bead red and white stripes | ?glass | | V404 |
| 29-1-? | white bead | stone | | V404 |
| 29-11-36 | white bead | stone | | W4 |
| 28-11-127 | blue bead | ?glass | | W5 |
| 31-1-19 | blue fluted bead | composition | 1930-61-121 | X11 |
| 27-28 | 246 beads and nine shells | not stated | | Zigi 30 |
| 27-28 | 28 beads | not stated | | Zigi 33 |
| 27-28 | seven beads | not stated | | Zigi 34 |
| 27-28-613 | blue/black glass fragment | glass | | Zigi 34 |
| 27-28 | three beads | not stated | | Zigi 35 |
| 27-28 | five beads | not stated | | Zigi 42 |
| 28-12-296 | fluted bead | composition | 1930-61-20 | |
| 29-12-347 | flat three-colour bead | composition | | |
| 29-12-197 | green-glazed pot | terracotta | | |

| | | | | |
|-----------|--|---------------|------------|--|
| 29-12-246 | ribbed bead | composition | 1930-61-63 | |
| 29-12-308 | blue cylindrical bead | composition | | |
| 29-12-141 | yellow oblong bead | composition | | |
| 29-12-307 | white cylindrical bead | stone | | |
| 30-2-413 | eight spherical/circular beads yellow/white | composition | | |
| 30-2-414 | four painted cylindrical beads black/blue | composition | | |
| 30-1-48 | glazed pot | terracotta | | |
| 29-12-299 | bead fragment, white with black spots | composition | | |
| 30-1-108 | oblong yellow bead | composition | | |
| 30-12-261 | two beads | paste/faience | | |
| 29-12-78 | light yellow paste bead | composition | 1930-60-55 | |
| 29-12-65 | white flat bead | composition | | |
| 29-11-168 | black bead | stone | | |
| 29-12-22 | glass bowl | glass | | |
| 29-12-34 | lapis bead | stone | | |
| 29-11-142 | black rectangular bead | stone | | |
| 29-12-50 | rectangular bead | composition | | |
| 29-12-51 | three small beads | | | |
| 29-12-56 | white paste bead | composition | | |
| 29-12-58 | three small white beads, traces of green paint | composition | | |
| 29-12-59 | black paste bead | composition | | |
| 29-12-61 | transparent glass bead | glass | | |
| 29-12-135 | glass vase light blue | glass | | |
| 29-12-201 | black painted bead | composition | | |
| 29-12-204 | black painted bead | composition | | |
| 29-12-205 | white bead | composition | | |
| 29-12-213 | blue bead | composition | | |
| 29-11-89 | dark glass vase | glass | | |
| 29-11-90 | ribbed glass bowl | glass | | |
| 29-12-106 | two beads | composition | | |
| 29-12-107 | greenish bead | composition | | |
| 29-12-110 | ribbed bead | composition | 1930-61-61 | |
| 29-12-111 | greenish bead | composition | | |
| 29-12-117 | three painted black beads | composition | 1930-60-60 | |
| 29-12-118 | two oblong black beads | composition | 1930-62-47 | |
| 29-12-119 | bead with bronze object | composition | | |
| 29-12-122 | yellow quadrilateral bead | composition | | |
| 29-12-123 | three greenish beads | composition | | |
| 29-12-133 | two light blue beads | composition | | |
| 29-12-69 | oblong bead | composition | | |
| 29-11-205 | spacer bead white | composition | | |
| 29-11-214 | greenish glass bowl | glass | | |
| 30-2-148 | cylindrical bead | composition | | |
| 30-2-240 | green-glazed wall nail | terracotta | | |
| 30-2-203 | black bead | stone | | |
| 28-11-7 | four fluted beads | composition | | |
| 31-2-118 | bead of human head | composition | | |
| 31-1-25 | green-glazed jar | terracotta | | |
| 29-11-82 | blue bead | composition | | |
| 29-1-98 | blue/green bead | composition | | |
| 29-12-7 | black bead | stone | | |
| 28-12-577 | ribbed bead | composition | 1930-61-24 | |
| 31-3-? | barrel bead | stone | | |
| 30-1-135 | opal bead | stone | | |

Table d: Stratum II Rooms affected by Late Cemetery (from Plan 39 and Plan 13 (Stratum II))

| Room No | Grave No. | Depth recorded for burial (cm) | Depth recorded for SII pavement (cm) |
|--------------------------|-----------|--------------------------------|--------------------------------------|
| F2 | GR92 | 322 | 281/320 |
| F2 | GR77 | 201 | 281/320 |
| F3 | GR10 | 325 | 307 |
| F6/F3 (wall) | GR4 | 406 | 284(F3) |
| F1/F2 (wall) | GR11 | 413 | 294 (F1) |
| F4/F6 (wall) | GR37 | 405 | 309 (F4) |
| F4/F6 (wall) | GR38 | 412 | 309 (F4) |
| F17 (wall) | GR25 | 396 | 313 (F17) |
| F23/F14 (wall) | GR24 | 434 | 340 (F23) |
| F23/F16 (wall) | GR30 | 425 | 310 (F16) |
| F1/F14/F32/F30 (walls) | GR45 | 337 | 285 (F14) |
| F30 | G47 | 341 | 219 |
| F16 | GR39 | 414 | 310 |
| F24 | GR46 | 326 | 316 |
| F11 | GR23 | 389 | 340 |
| F11/F7/F25 (walls) | GR40 | 401 | 389 (F11) |
| F11/F7/F25 (walls) | GR41 | 354 | 382 (F7) |
| F7 | GR7 | 402 | 382 |
| F7 | GR36 | | 382 |
| F7 | GR29 | 432 | 382 |
| F7 | GR8 | 408 | 382 |
| F7 | GR9 | 426 | 382 |
| F38 | GR6 | 312 | |
| F38 | GR84 | 278 | |
| G5/F7 (wall) | GR26 | 404 | |
| G4/G5 (wall) | GR5 | 365 | |
| G (adjacent to Street 1) | GR57 | 385 | |
| G (adjacent to Street 1) | GR58 | 399 | |
| G (adjacent to Street 1) | GR59 | 368 | |
| G (adjacent to Street 1) | GR56 | 544 | |
| G (adjacent to Street 1) | GR71 | 355 | |
| G64/Street 1 | GR62 | 217 | |
| G64/Street 1 | GR60 | 312 | |
| G64/G61 | GR70 | 240 | |
| G61 | GR102 | 212 | |
| G61 | GR103 | 208 | |
| B7 | GR | 433 | |
| B | GR13 | 407 | |
| G14 | GR51 | 409 | |
| G14 | GR50 | 410 | |
| G14 | GR65 | 398 | |
| G14 | GR64 | 382 | |
| G14 | GR68 | 354 | |
| G14 | GR69 | 355 | |
| G32 | GR75 | 307 | |
| G26 | GR33 | 322 | |
| G37 | GR44 | 261 | |
| G37(wall) | GR101 | 243 | |
| G57 (wall) | GR95 | 250 | |
| G57 (wall) | GR94 | 277 | |
| G54/G48 (Street 6) | GR97 | 371 | 313 (G54) |
| G24 (wall) | GR79 | 478 | |
| G21A | GR72 | 411 | |
| G21A (wall) | GR78 | 379 | |
| G6 | GR31 | 413 | 375 |
| G6 | GR34 | 378 | 375 |

| | | | |
|---------------------|-------|-----|-----|
| G6 | GR35 | 368 | 375 |
| G51/G29 (wall) | GR85 | 355 | |
| G29 | GR80 | 426 | 363 |
| G29 (wall) | GR88 | | |
| G29/G50 (wall) | GR91 | 463 | |
| G50 | GR93 | 360 | 366 |
| G50 | GR86 | 436 | 366 |
| G50 | GR90 | 406 | 366 |
| G30 (wall) | GR43 | 466 | 366 |
| G18 | GR49 | 485 | |
| G18 | GR48 | 469 | |
| G16 | GR15 | 415 | |
| G16 | GR16 | 463 | |
| G17/G30 | GR17 | | |
| G17/G30 | GR32 | 416 | |
| G18/B38/B23 (wall) | GR20 | 549 | |
| Street 8/C9 (wall) | GR22 | 465 | |
| B (?Stratum III) | GR13 | 407 | |
| Street 7/H4 | GR89 | 369 | |
| Street 8/H50 (wall) | GR104 | 378 | 396 |
| H10 | GR87 | 387 | |
| H10 | GR105 | 384 | |